Lowest Order Virtual Element Approximations for Unsteady Fluid Flow Problems

A thesis submitted

in partial fulfillment for the award of the degree of

Doctor of Philosophy

in

Mathematics

by

Nitesh Verma

Department of Mathematics

Indian Institute of Space Science and Technology

Thiruvananthapuram, India

March 2022

Certificate

This is to certify that the thesis titled ***Lowest Order Virtual Element Approximations for Unsteady Fluid Flow Problems*** submitted by Ms. **Nitesh Verma**, to the Indian Institute of Space Science and Technology, Thiruvananthapuram, in partial fulfillment for the award of the degree of **Doctor of Philosophy** in **Mathematics**, is a bona fide record of the original work carried out by her under my supervision. The contents of this report, in full or in parts, have not been submitted to any other Institute or University for the award of any degree or diploma.

Dr. Sarvesh Kumar
Research Supervisor
Associate Professor
Dept. of Mathematics

Prof. C V Anil Kumar
Head of the Department
Dept. of Mathematics

Place: Thiruvananthapuram
Date: March 2022

Declaration

I declare that this thesis titled ***Lowest Order Virtual Element Approximations for Unsteady Fluid Flow Problems*** submitted in partial fulfillment for the award of the degree of **Doctor of Philosophy** in **Mathematics** is a record of original work carried out by me under the supervision of **Dr. Sarvesh Kumar**, and has not formed the basis for the award of any degree, diploma, associateship, fellowship, or other titles in this or any other Institution or University of higher learning. In keeping with the ethical practice in reporting scientific information, due acknowledgments have been made wherever the findings of others have been cited.

Nitesh

Nitesh Verma
Research Scholar
Dept. of Mathematics
Student ID: SC16D027

Place: Thiruvananthapuram
Date: March 2022

This thesis is dedicated to my parents for their love, support and sacrifices.

Acknowledgements

Firstly I would like to express my sincere gratitude to my research supervisor, Dr. Sarvesh Kumar, for giving me the opportunity to work under his guidance. I am very thankful to him for his continuous support, motivation, and guidance throughout my Ph.D. research in molding me into a better researcher and also helping me to successfully complete this thesis work.

I am very grateful to all my doctoral committee members, Dr. P. Danumjaya (Associate Prof., Dept. of Mathematics, BITS Goa), Prof. Raju K. George (Dean R&D, Dean Students Welfare, IIST), Prof. K.S.S. Moosath (Dept. of Mathematics, IIST), Prof. Deepak Mishra (HOD, Dept. of Avionics, IIST), and Dr. E. Natarajan (Associate Prof., Dept. of Mathematics, IIST), for their valuable suggestions, guidance, and constructive criticisms in each phase of my research work, which helped me a lot in improving the quality of research outputs.

I am sincerely thankful to Dr. Ricardo Ruiz-Baier (Associate Prof., Monash University, Australia), Prof. Raimund Bürger (CI^{2}MA, Universidad de Concepción, Chile), and Dr. David Mora (Associate Prof., Universidad del Bío-Bío, Concepción, Chile) for their unconditional support throughout my research period, and also for giving me the opportunity to visit Chile for research collaboration. I am very thankful to Dr. Verónica Anaya (Associate Prof., Universidad del Bío-Bío, Chile), Dr. Iván Velásquez, and Dr. Bryan Gómez-Vargas for all their help during my visit to Chile. I also like to thank Mr. Alberth Silgado, Ms. Yolanda Vásquez, and members of CI^{2}MA and UBB for their warm welcome and friendly support.

I cannot express enough thanks to my colleagues, Dr. Aryadutt Oamjee, Dr. Arun D.I., Ms. Monisha Mohan, and Mr. K. Prabith for being there in all my ups and downs, and always encouraging and motivating me to reach heights in my life. Also, I would like to thank all my friends from IIST, especially, Mr. Jogendra Singh, Mr. Narendra Singh Yadav, Dr. Sweta Dey, Dr. M. Arrutselvi, Mr. K. Muhammed Shiyas, Mr. Janaki Raman B., Dr. Mahesh T.V., and Mr. V.S. Sajith, for all their support in both academic and non-academic, during these years, and also for all the wonderful memories we had as a student family. Furthermore, I express thanks to the friendly mathematics department staff members Mr. Kareem, Mr. Anish, Ms.

Nisha, and Ms. Poornima for all their help in technical and academic works, even during the pandemic.

I am thankful to God for giving me very supportive and loving parents, Smt. Sheela Devi and Shri Bhal Singh Nirania. Besides, I am extremely thankful to my younger brother, Mr. Shubham Nirania who has been a pillar and always encouraged me to achieve my dreams. Without them, this thesis would not have been possible.

Nitesh Verma

Abstract

Problems in continuum mechanics are a constant source of systems of partial differential equations (PDEs) which are often difficult to solve. Among contemporary numerical methods designed for these types of problems, virtual element methods (VEMs) constitute a recent family of discretization schemes constructed using polytopal meshes, that are proven to be robust under many different scenarios. In this thesis, we focus on the developments of VEMs for the approximation of certain types of non-stationary coupled fluid flow problems. More precisely, the type of equations that are considered herein includes transient Stokes, Navier-Stokes, Biot, and coupled advection-diffusion-reaction and poroelasticity equations, the latter system describing species interaction within fully saturated deformable porous media. Using classical regularity assumptions on the solutions to the continuous set of governing equations, we construct lowest-order virtual element discretizations for each of these problems. An appealing feature of the resulting schemes is that the discrete velocities are locally divergence-free for incompressible flow problems and that the constructed virtual element spaces satisfy the necessary inf-sup conditions which permit to establish unique solvability of the associated discrete problems and Céa estimates for the approximate solutions. For the time discretization, a classical backward Euler scheme is employed, and we rigorously derive the main properties of the semi- and fully-discrete schemes for all problems. Moreover, by introducing appropriately defined projection operators, optimal *a priori* error estimates are established in natural norms for all field variables that are natural unknowns in the specific formulation. Further, for each problem, several numerical experiments are presented. They serve to illustrate the performance of the proposed schemes and also to validate experimentally the theoretical rates of convergence predicted by the error analysis.

Contents

List of Figures

List of Tables

Abbreviations

PDEs	Partial Differential Equations
FEM	Finite Element Method
VEM	Virtual Element Method
VE	Virtual Element
DoF	Degree of freedom
ADR	Advection-Diffusion-Reaction
Dim	Dimension
MFDM	Mimetic Finite Difference Method

Chapter 1

Introduction

The basic objective of this thesis is to discuss and analyze lowest order virtual element methods (VEMs) for the approximation of evolutionary fluid flow problems: Stokes, Navier-Stokes, poroelasticity, and coupled advection-diffusion-reaction and poroelastic equations on polygonal meshes.

1.1 Physical motivation

Many physical problems in diverse scientific and engineering applications are described by the evolutionary partial differential equations (PDEs). These kinds of PDEs frequently occur in fluid dynamics and solid mechanics. Here we will focus on the problems only related to fluid dynamics, and the purpose of this thesis is to develop robust and efficient numerical techniques for seeking the numerical solution of fluid flow problems of certain types. The viscous incompressible fluid flow problem with a small Reynolds number is modeled by a well-known nonlinear equation known as the Navier-Stokes equation, named after the French engineer physicist Claude-Louis Navier and Anglo-Irish physicist mathematician George Gabriel Stokes [1]. It is well known that this problem has paramount importance in many phenomena of scientific and engineering interest. This problem is used to model the ocean currents, water flow in a pipe, and airflow around a wing and hence, helps in predicting the weather, extraction of oil, design of aircraft and cars, the design of power stations, the study of blood flow, analysis of pollution and many other things (see, for instance, [2, 3]). Moreover, some physical phenomenons are modeled by coupling with Navier-Stokes equation, for instance, coupled Navier-Stokes and Maxwell's equation to study magnetohydrodynamics [4]. After many decades of active research, the study (well-posedness and solution process) of this type of system is still attracting considerable attention from many scientists/researchers. In general, the nonlinear problems are challenging to deal with, therefore, it is advisable to work on the linear counterpart of these problems known as Stokes equations (linear incompressible flow problem). In other words, Stokes equation models a type of fluid flow problem where advective inertial forces are small compared to viscous forces, and fluid has a low Reynolds number (very small as compared to 1). This is a typical situation in flows where the fluid velocities are very slow, the viscosities are very large, or the length scales of the flow are very small. Such equations are used in the various valuable process in bioscience, industries, and nature such as understanding of lubrication, swimming of microorganisms, the flow of lava, and also occurs in paint, MEMS devices, and in the flow of viscous polymers generally. Because of these applications, the first two chapters of this thesis are devoted to the development of suitable numerical schemes for the approximation of transient Stokes and Navier-Stokes equations.

Next, we focus on the physical phenomenon related to the fluid flow problems describing the interaction between the fluid flow and solid structure (or porous medium). A porous medium or a porous material is a solid (often called matrix) permeated by an interconnected network of pores (voids) filled with a fluid (liquid or gas). Many natural substances such as rocks, soils, biological tissues, and manufactured materials such as foams and ceramics can be considered as porous media [5]. Porous media whose solid matrix is elastic and the fluid is viscous, is known as poroelastic. A poroelastic medium is characterized by its porosity, permeability, and properties of its constituents (solid matrix and fluid). The concept of a porous medium originally emerged in soil mechanics, particularly in the works of Karl von Terzaghi [6, 7] (known as the father of soil mechanics). However, a more general concept of a poroelastic medium, independent of its nature or application, is usually attributed to a Belgian-American engineer Maurice Anthony Biot. He developed the theory of dynamic poroelasticity (now known as Biot's theory), which gives a complete and general description of the mechanical behavior of a poroelastic medium [8]. The poroelastic medium is composed of a mixture of incompressible grains forming a linearly elastic skeleton and interstitial fluid. Biot's equations for the linear theory of poroelasticity are derived from equations of linear elasticity for the solid matrix, Navier–Stokes equations for the viscous fluid, and Darcy's law for the flow of fluid through the porous material. The deformation of the porous medium is governed by linear elasticity, and thus, the problem is also known as the linear poroelasticity problem. From an applicative point of view, it is crucial to design and analyze numerical methods that are robust with respect to variation of model parameters since this variation might be significant in many problems of practical relevance. For example, in the filtration of flow in soft tissue, the permeability is typically of the order of $10^{-15}\,\mathrm{m}^2$, whereas common ranges for the Lamé parameters characterizing the dilation response of the material reach values within the 10^7 KPa [9].

Another consideration is that in many applications, species interactions do not occur in complete isolation. The species are rather immersed or move within (and interact with) a fluid-solid continuum, and the chemical reactions between the species inevitably affect the motion of the fluid. In some circumstances, reciprocal effects might be substantially large, leading to local changes in the observed flow patterns [10]. More specifically, in the types of problems considered herein, it is assumed that the chemical reactions are occurring between the two species in a porous medium saturated with fluid. In biomechanics, real biological tissues are conformed by living cells, and volume changes due to cell birth and death onset velocity fields and local deformation, eventually driving domain growth [11]. Interconnectivity of the porous microstructure is sufficient to accommodate fluid flowing locally in this case. Therefore, we suppose that the local fluctuations of a species' concentration are important enough to affect the fluid flow. In turn, we adopt here a two-way active transport: the poromechanical deformations affect the transport of the chemical species through advection and also by means of a volume-dependent modification of the reaction terms, and the solutes' concentration generate active stress resulting in a distributed load depending linearly on the concentration gradients in the context of microscopic-macroscopic mechanobiology. The occupancy of the event with additional species interaction in the fluid flowing through the deformable or elastic porous medium is described by coupling between the advection-diffusion-reaction (ADR) and the poroelasticity equation. This problem is encountered in rock consolidation and fractures, swelling of coals and clay, polymer dissolution, moisture within photo-voltaic devices, and other related disciplines. Few applications are explored in [12], which include traumatic brain injury and calcium dynamics (not related to cell biomechanics).

We stress that due to the inherent complexity of the coupling structures (mentioned above) and the nonlinearity of the involved equations for these models, obtaining analytical solutions or even closed-form solutions will be very difficult, and also their numerical simulation in complicated scenarios (such as domains with diverse types of boundary and transmission conditions) remains far from trivial. The development of an accurate and efficient numerical technique for seeking solutions to fluid flow problems is still today a very active research area. This thesis also aims to develop a unified theoretical framework for the mathematical and numerical analysis of non-stationary fluid flow problems, and also other PDE-based models that appear in the coupling of fluid flow and transport problems.

1.2 Virtual element methods: applications and developments

The most challenging problem for the numerical analysis community is introducing a numerical method that solves PDEs approximately on the complex geometries. In many realistic situations, the domain on which PDEs have been defined consists of general type elements, and therefore, polygonal/polyhedral mesh (see [13]) is desirable. Also, the complex domain can be handled with ease since the hanging nodes are no longer an obstacle in polygonal meshes. This is possible because any element having hanging nodes are exploited as a new element with hanging nodes as its additional, or new vertices. Hence, local refinements can be performed on polygonal meshes using fewer elements, in contrast to the classical mesh refinement techniques with triangular meshes, which suffer from the fact that local refinement propagates into their neighboring regions. Also, mesh-free methods with the C^k approximations for solving the problem can be considered to deal with the complex domains; however, they do not interpolate the given data on nodes, and thus, imposing the boundary conditions becomes difficult.

At this juncture, we would like to shed some light on the development of some numerical schemes that employ polygonal mesh. The initial works on polygonal mesh began in the early '70s with the seminal works of Wachspress [14]. Since then, various approaches have been proposed, including polygonal finite element method (PFEM) [15], mimetic finite differences method (MFDM) [16], gradient discretization method (GDM) [17] and recently, VEMs [18], weak Galerkin method (WG) [19] and hybrid high order method (HHO) [20]. Mesh-free methods motivated PFEMs, which works for the convex polygonal meshes. However, PFEM requires the shape functions that consists of rational, logarithmic, and trigonometric functions, which makes the implementation more involved. Finally, VEM evolved as a natural consequence of new developments and interpretations of the MFDM in which the degrees of freedom (DoFs) are associated with local virtual element (VE) spaces. This idea would help in designing high-order VEMs in a simple way compared to MFDM when higher-order elements are used. The WG method generalizes the standard Galerkin method where classical derivatives and differential operators (e.g., gradient, divergence, curl, etc.) are replaced by weakly defined derivatives and weak forms on functions with discontinuity, whereas the HHO method is linked to the nonconforming counterpart of VEM.

In view of the applicability of VEM with polygonal meshes, VEMs are proven to be very impressive and have attracted the scientific community as far as a numerical approximation of PDEs on polygonal meshes is concerned. The local and global VE spaces that include polynomial and non-polynomial functions on each element were first introduced in [18], and convergence analysis (for diffusion problems) of the proposed VEM was also presented. Later, the detailed implementation/computational aspects of VEM were discussed in [21]. The presence of polynomial functions in the VE spaces helps in demonstrating the convergence rates of the proposed VE schemes. After a close inspection, it is observed that this scheme was inspired by the MFDM ([22]), which also aim to generalize finite element methods (FEMs) over the very general type of polygonal meshes and therefore, can be considered as an extension of FEMs on the polygonal mesh. In contrast with classical finite element (FE) schemes, VEM does not require explicit construction of the discrete basis functions, and one needs to define suitable DoFs to put the discrete formulation in the matrix form. This is very desirable while dealing with polygonal meshes and demanding more accurate solutions, i.e., higher-order approximations. In fact, the word "virtual" stands for the non-explicit behavior of the basis functions corresponding to the finite-dimensional spaces defined on each element (polygon) used in the discrete formulation, and only DoFs are required for computing the bilinear forms that appear in the discrete formulation. To define the discrete bilinear forms, the local bilinear forms can be decomposed into two terms: one with both the entries as polynomial projections and the other as just the residue (non-polynomial part). For approximating the non-polynomial part and also to ensure the stability of the discrete bilinear forms, one needs to add a suitable stabilization term. The proposed stabilization term must vanish whenever at least one of the entries is a polynomial in order to make the scheme consistent. Various stabilization terms are satisfying these demands, and the choice depends on the problems and its discrete formulation (for more details, we refer to [18, 23]). We remark that the convergence analysis of VEM can be carried out analogously to FEM by introducing projection of the discrete solution onto polynomials.

Other fundamental properties of VEM include: making use of non-polynomial basis functions over arbitrary polygonal/polyhedral meshes [13], the capability of handling the complicated geometries generally used in solid-mechanics and fluid dynamics through general meshes, and usage of approximation spaces containing the higher-degree polynomial with ease. In view of their computational efficiency, VEMs have been developed for various problems within a decade, and few of the basic works are on general elliptic [24, 25], parabolic [26] and semi-linear [27, 28] problems. In literature, there are few contributions that dealt with VE approximations for Stokes [29, 30, 31], Navier-Stokes [32, 33, 34, 35], Darcy and Brinkmann [36], and poroelasticity [37, 38, 39] equations. Based on the high demands, VEM emerged as an accurate and efficient numerical scheme on polygonal meshes for solving the PDEs, and its rapid growth of research studies can be seen in [40, 41, 42, 43, 44] and references therein. Further, these methods extended to approximate non-linear problems [45, 46], the three dimensional problems [47, 48, 49, 50] and coupled problems [51, 52]. These methods also applied to the discretization with degenerate elements [53, 54] which require only the mesh elements as a union of star-shaped polygons, hence convenient for very general discretization. The VE scheme is also developed for the problems related to fluid dynamics in [35, 36, 55, 56] but still, there are many areas of fluid flow problems which are yet to develop.

1.3 Related works and specific contributions

There are several numerical techniques proposed in the literature for the approximations of the evolutionary fluid flow problem and its related application-oriented problems. For instance, a wide range of research articles on these problems are seen through many schemes such as FEM [57], discontinuous Galerkin (DG) method [58, 59], stabilized FEM [60, 61], non-conforming FEM [62], MFDM [63], finite volume methods (FVMs) [64, 65] and so on. Below, in the context of VEM, we highlight our contributions and related work from the literature for investigating the problems mentioned in Section 1.1.

Incompressible flow problems

Considering the applications of unsteady Stokes problems, different numerical techniques have been proposed such as finite difference methods (FDMs) [57], FEMs

[66, 63, 67, 68], FVMs [69, 64], nonconforming methods [70, 71], DG methods [72] and so on. We stress that in some of these articles, convergence analysis was carried out with certain regularity assumptions on the continuous solutions; for instance, $\partial_t \boldsymbol{u} \in [H^3(\Omega)]^2$ was used for the establishment of optimal error estimates. However, *Heywood and Rannacher* clearly mentioned and explained in [68] that the high regularity of the continuous solution (such as, $\|\partial_t \boldsymbol{u}\|_{3,\Omega} < \infty$ when t is close to 0) cannot be achieved in the real sense (for more details, see [68, 73, 74, 75]). Therefore, the possible remedy is to look for lower-order spaces such as $\mathbb{P}_1 - \mathbb{P}_1, \mathbb{P}_1 - \mathbb{P}_0$; however, these may not satisfy the discrete inf-sup condition, and suitable stabilizers are required for circumventing the inf-sup condition. In [76, 77, 78, 61, 79, 80, 81], several stabilized, or penalized FEMs are proposed for the approximations of steady and unsteady Stokes equations. We remark that the addition of consistent stabilized methods have their own disadvantages when applied to transient problems, e.g., small-time steps will lead to instabilities in the pressure approximation, see [82]. A stabilized VE scheme for a nonstationary version of the Navier-Stokes problem was proposed with only numerical experiments in [55], while the convergence analysis of the proposed method was not addressed. The present contribution differs from the above proposed VEM for the Stokes problem in that we use a stable lowest order ($k = 1$), stabilizer-free VE scheme for the transient Stokes problem. We have employed lowest order VE spaces that are divergence-free, satisfy the inf-sup condition, and are regarded as a natural extension of the VE space defined in [29] for the approximation of transient Stokes equations. Moreover, we have established the optimal error estimates with minimal realistic regularity assumptions (see [81, 68]) on the continuous solutions.

Transient Navier-Stokes equations have remarkable applications in fluid mechanics and several numerical techniques such as FEMs [67, 63, 57, 66], FVMs [64, 61, 69], nonconforming FEMs [79, 71], DG methods [72] and references therein, were proposed for seeking numerical approximations to the problem in past decades. Similar to the Stokes problem, the major difficulty lies in choosing the appropriate stable pair of discrete spaces based on spatial discretization, for instance, these spaces must obey the inf-sup condition [67]. In this work, we analyze the lowest order VE spaces for velocity and pressure that obey the inf-sup condition (without adding any stabilization term), which is used to show the well-posedness of the discrete formulation and establish the optimal error estimates for velocity and pressure. In literature, there are few contributions that dealt with VE approximations for Stokes [29, 30, 31] and Navier-Stokes [32, 33, 34, 35] problems. However, in these articles, a restriction on choosing the approximation order, or the degree of involved polynomials (denoted generally by k) is strictly imposed for VE spaces associated with velocity and pressure in order to satisfy the required inf-sup condition by the discrete spaces. In other words, it is mandatory to choose $k \geq 2$ in order to obtain stable spaces, and $k = 1$ can not be taken due to unavailability of the inf-sup condition for these discrete spaces until a suitable stabilizer is added [30, 55]. We would like to remark that even the usage of higher-order approximations is expected to be computationally expensive in general. Considering these points, we aim here to approach the discrete spaces that have an approximation of order one and also satisfy the required inf-sup condition [83]. Therefore, the proposed scheme is considered computationally less expensive compared to the existing higher-order schemes in the context of VE approximations for fluid flow problems due to reduced local DoFs in the case of [83].

Biot's equation

A variety of numerical methods has been used to generate approximate solutions to Biot's consolidation problem. Modern examples include high-order FDM [84], FEM [85, 86], nonconforming method [87, 88], DG method [89, 58], FVM [65], WG method [90, 91], and combined/hybrid discretisation method [92]; we further point out [93, 94, 37] where the authors present a polygonal discretisation based on HHO methods and VEM. These schemes are constructed using different formulations of the governing equations, including primal and several mixed forms. There is an extensive body of literature on the robust numerical schemes using the different mixed formulations or weighted norms in [95, 96, 97, 98]. A coupled VEM-finite volume formulation for the Biot equations was proposed in [37]. Recently, VEM has also been developed in [99] with another three-field formulation (seen in [100]) for Biot's equation. For reducing the computational cost, the problem has been inspected using the stabilized FEMs with low order elements [101, 102].

It is well known from the literature that the standard Galerkin method produces unstable and oscillatory numerical behavior of the pore pressure for a certain range of material parameters (small c_0) and the stabilization of pore pressure oscillations has been a subject of extensive research. A well-accepted theory on the cause of this pressure instability was proposed by Phillips and Wheeler, for more details [85] and references therein. It was mentioned that if the constrained specific storage term is null ($c_0 = 0$), the permeability of the porous medium is very low, a small-time step is used. In addition, it was also examined that there exists a locking phenomenon when λ is large, or the Poisson ratio approaches 0.5. Due to the occurrence of locking, the solid skeleton behaves as an incompressible medium, i.e., the deformation is in a divergence-free state. To avoid the locking phenomenon, the three-field non-symmetric formulation of the Biot's problem (by introducing total volumetric stress as a new variable) was first studied in [103] which is robust for $\lambda \to \infty$. For the approximation of time-dependent poroelasticity, we have proposed locking free VEM based on three field formulation (referring to [103]), and prove the stability of the discrete schemes without employing Gronwall's inequality. Further, with the help of suitable projection operators, we derive the error estimates for our time-dependent problem in natural norms that are robust concerning the dilation modulus of the deformable porous structure (which tends to infinity as the Poisson ratio approaches 0.5), and of the specific storage coefficient (reaching very small values in some regimes).

Advection-diffusion-reaction in poroelastic media

The presence of chemical solutes in so-called active poroelastic materials locally modifies morphoelastic properties, and these processes can be homogenized to obtain macroscopic models of poroelasticity coupled with ADR equations, having numerous applications mentioned in the previous section. From the viewpoint of solvability analysis of PDEs and/or the theoretical aspects of FE discretizations, the relevant literature contains few works specifically targeting the coupling of diffusion in deformable porous media (see [104, 105, 34, 106, 107, 103, 108]). Recently, a system of multiple-network poroelasticity was studied in [96] with the mixed FE schemes and developed the stability analysis. As in [96, 103] (also in Chapter 4), we employ here the three-field formulation for the poroelastic part of the problem. However, we adopt in our model an additional two-way active transport: the poromechanical deformations affect the transport of the chemical species through advection, and also by means of a volume-dependent modification of the reaction terms; the solutes' concentration generates active stress resulting in a distributed load depending linearly on the concentration gradients. In [12], we have addressed this model, performed a linear stability analysis to identify suitable ranges for the key coupling parameters, and conducted a full set of numerical tests in 2D and 3D. Later, in [109], we have studied the coupled problem through the semidiscrete in-time formulation, and then Schauder fixed point theorem combined with Fredholm's alternative and standard theory of quasi-linear equations were applied to establish solvability of the introduced formulation.

In this thesis, the coupled system is set up in a mixed-primal structure, where the equations of poroelasticity have a mixed form using displacement, pressure, and a rescaled total pressure, and the ADR system is also set in a primal form, solving for the species' concentrations. The advantage of using this approach is that the stability results are independent of the Lamé constant of the solid, and this is particularly important to prevent the volumetric locking. By following [109], we propose a fully discrete scheme by employing backward Euler scheme for time discretization and VE discretization for space variable, and present convergence analysis for the proposed fully discrete formulation. In contrast with, e.g., [110, 111], the advecting velocity in this model was that of the solid (instead of the Darcy velocity), which is not a primary variable in our formulation, and in turn, gave an extra $1/(\Delta t)$ term by the use of backward Euler scheme, thus complicating the analysis of semi and fully discrete schemes. We further stress that the complexity in this analysis (which are not present in the earlier literature) was due to the advective coupling appearing in the ADR system of equations. Therefore, we have proceeded here with the advection term containing the displacement instead of velocity to focus on space approximation, and the analysis can be extended with advecting velocity in a similar fashion.

1.4 Preliminaries

In this section, we introduce some standard notations and basic notions from functional analysis to be used throughout the thesis. Let $\Omega \subset \mathbb{R}^2$ be a bounded, convex polygonal domain with Lipschitz boundary $\partial\Omega$. For $p \in [1, \infty)$, let $L^p(\Omega)$ denote the linear space of all (equivalence classes of) Lebesgue measurable functions ϕ, defined on Ω, that satisfy

$$\int_\Omega |\phi(x)|^p dx < \infty.$$

In this connection, the functions are considered to belong to the same equivalence class if they differ only on a set of measure zero. The space $L^p(\Omega)$, with $1 < p < \infty$, and equipped with the norm

$$\|\phi\|_{L^p(\Omega)} := \left(\int_\Omega |\phi(x)|^p dx \right)^{1/p}$$

is a Banach space. The space $L^\infty(\Omega)$ is the Banach space of all (equivalence classes of) Lebesgue measurable and essentially bounded functions, endowed with the norm

$$\|\phi\|_{L^\infty(\Omega)} := ess \sup_{x\in\Omega} |\phi(x)|.$$

It is well known that $L^2(\Omega)$ is a Hilbert space with respect to the inner product $(\cdot,\cdot)$ defined by

$$(\phi,\psi) := \int\limits_\Omega \phi(x)\psi(x)dx.$$

For $s \in \mathbb{N}$ and $p \in [1,\infty]$, the classical Sobolev space $W^{s,p}(\Omega)$ is defined as the linear space of all functions $\phi \in L^p(\Omega)$ having distributional derivatives $D^\alpha\phi \in L^p(\Omega)$ for all multi-indices α of order $|\alpha| \le s$, and is equipped with the norm

$$\|\phi\|_{W^{s,p}(\Omega)} = \|\phi\|_{s,p,\Omega} := \left(\sum_{|\alpha|\le s} \int\limits_\Omega |D^\alpha\phi(x)|^p dx\right)^{1/p}.$$

Furthermore, we introduce the semi-norm

$$|\phi|_{s,p,\Omega} := \left(\sum_{|\alpha|=s} \int\limits_\Omega |D^\alpha\phi(x)|^p dx\right)^{1/p}.$$

Analogously, for $p=\infty$,

$$\|\phi\|_{s,\infty,\Omega} := \max_{|\alpha|\le s} \|D^\alpha\phi\|_{L^\infty(\Omega)}.$$

The spaces $W^{s,p}(\Omega)$ are Banach spaces. For simplicity, we use the abbreviation $H^s(\Omega) := W^{s,2}(\Omega)$ and define $W^{0,p}(\Omega) := L^p(\Omega)$. We note that $H^s(\Omega)$ is a Hilbert space with respect to the inner product

$$(\phi,\psi)_{s,\Omega} := \sum_{|\alpha|\le s} \int\limits_\Omega D^\alpha\phi(x)D^\alpha\psi(x)dx, \quad \forall \phi,\psi \in H^s(\Omega),$$

and the induced norm

$$\|\phi\|_{s,\Omega} := \left(\sum_{|\alpha|\le s} \int\limits_\Omega |D^\alpha\phi(x)|^2 dx\right)^{1/2}.$$

The space $H_0^1(\Omega)$ is characterized by

$$H_0^1(\Omega) := \{\phi \in H^1(\Omega) : \phi = 0 \text{ on } \partial\Omega\}.$$

The space L_0^2 is the space of square-integrable functions with zero mean value, that is

$$L_0^2(\Omega) := \{q \in L^2(\Omega) : \int_\Omega q \; dx = 0\}.$$

Let T be a positive time that defines the time interval $I := (0, T]$, then for $p \in [1, \infty)$ and s a non-negative integer, we denote by $L^p(0, T; H^s(\Omega))$, the Banach (or Bochner-type) space of all L^p integrable vector valued functions $\phi(t) : I \longrightarrow H^s(\Omega)$ with the norm given by

$$\|\phi\|_{L^p(0,T;H^s(\Omega))} := \left(\int\limits_0^T \|\phi(t)\|_{s,\Omega}^p \, dt \right)^{1/p}.$$

Analogously, $L^\infty(0, T; H^s(\Omega))$ is the Banach space of all essentially bounded vector valued functions $\phi(t) : I \longrightarrow H^s(\Omega)$ endowed with the norm

$$\|\phi\|_{L^\infty(0,T;H^s(\Omega))} := ess \sup_{t \in I} \|\phi(t)\|_{s,\Omega}.$$

Next, we state few well known results that will be frequently used in the analysis.

- **Cauchy-Schwarz inequality.** If $\{a_i\}_{i=1}^N$ and $\{b_i\}_{i=1}^N$ are non-negative real numbers. Then

$$\left(\sum_{i=1}^N a_i b_i \right) \leq \left(\sum_{i=1}^N a_i^2 \right)^{1/2} \left(\sum_{i=1}^N b_i^2 \right)^{1/2}.$$

- **Hölder's inequality.** Let $\phi \in L^p(\Omega),\ \psi \in L^q(\Omega)$. Then for $1 \leq p, q < \infty$ with $\frac{1}{p} + \frac{1}{q} = 1$, we have

$$\left| \int\limits_\Omega \phi(x)\psi(x) dx \right| \leq \left(\int\limits_\Omega |\phi(x)|^p dx \right)^{1/p} \left(\int\limits_\Omega |\psi(x)|^q dx \right)^{1/q}.$$

- **Poincaré inequality.** Let $\Omega \subset \mathbb{R}^2$ be a bounded open subset. Then there exists a positive constant $C = C(\Omega)$, such that

$$\|\phi\|_{0,\Omega} \leq C|\phi|_{1,\Omega}, \quad \forall \phi \in H_0^1(\Omega).$$

- **Korn's inequality.** For all $\boldsymbol{v} \in [H^1(\Omega)]^2$, we have the inequality for some constant C,

$$\|\boldsymbol{v}\|_{1,\Omega} \leq C\|\boldsymbol{\varepsilon}(\boldsymbol{v})\|_{0,\Omega}.$$

- **Inf-sup condition.** We say that the well-defined bilinear form $b(\cdot,\cdot)$ defined on $\mathbf{V} \times Q$ satisfies the inf-sup condition if for each $q \in Q$ there exists a constant $\beta > 0$ such that

$$\sup_{(0 \neq)\boldsymbol{v} \in \mathbf{V}} \frac{b(\boldsymbol{v}, q)}{\|\boldsymbol{v}\|_{\mathbf{V}}} \geq \beta\|q\|_Q.$$

- **Young's inequality.** If a and b are non-negative real numbers, then for every $\varepsilon > 0$, the following inequality holds

$$ab \leq \frac{a^2}{2\varepsilon} + \frac{\varepsilon b^2}{2}.$$

- **Gronwall's inequality.** Let $g(t)$ and $h(t)$ be continuous functions with $h(t) \geq 0$ on interval $t_0 \leq t \leq t_0 + a$. If a continuous function $\phi(t)$ has the following property

$$\phi(t) \leq g(t) + \int_{t_0}^{t} \phi(s)h(s)ds, \quad t_0 \leq t \leq t_0 + a,$$

then

$$\phi(t) \leq g(t) + \int_{t_0}^{t} g(s)h(s)\exp\left(\int_{s}^{t} h(\tau)d\tau\right)ds, \quad t_0 \leq t \leq t_0 + a,$$

In particular, when $g(t) = C$ is a non-negative constant, then we have

$$\phi(t) \leq C\exp\left(\int_{t_0}^{t} h(s)ds\right), \quad t_0 \leq t \leq t_0 + a.$$

- **Discrete Gronwall's inequality.** Let $\Delta t, B$, and a^j, b^j, c^j, d^j for $j \geq 0$ be non-negative numbers such that

$$a^n + (\Delta t)\sum_{j=0}^{n} b^j \leq \Delta t \sum_{j=0}^{n} c^j a^j + \Delta t \sum_{j=0}^{n} d^j + B, \quad n \geq 0.$$

If $(\Delta t)c^j < 1$ for all j and $\gamma^j := (1 - \Delta t\ c^j)^{-1}$ for any j, then

$$a^n + (\Delta t)\sum_{j=0}^{n} b^j \leq \exp\left(\Delta t \sum_{j=0}^{n} \gamma^j c^j\right)\Big(\Delta t \sum_{j=0}^{n} d^j + B\Big), \quad n \geq 0.$$

Remark 1.1. *Throughout this thesis, the notation C is used to denote a generic positive constant which may take different values at different places. Also, the vector-valued functions are denoted with bold letters for clarity.*

1.5 Overview

As mentioned before, this thesis focused on developing new VEMs for approximating a class of unsteady fluid flow problems; in particular, we have performed a VE analysis for Stokes, Navier-Stokes, Biot's, and coupled poroelastic-ADR equations. For all these equations, we have shown the discrete problem is well-posed and derived the optimal error estimates. Moreover, numerical experiments are conducted at the end of each chapter in order to support the theoretical findings and judge the performance of the proposed methods. The content of this thesis is divided into six chapters and organized as follows.

Chapter 1 includes an enormous view of the thesis works and mentions some of the important applications of problems that we have considered in the thesis, and also the purpose of VEMs with polygonal meshes while dealing with fluid flow problems. An extensive literature of VEMs and their recent developments are also highlighted in this chapter. Also, we have specified the preliminaries for subsequent chapters.

In Chapter 2, we have proposed a new lowest order VE scheme to approximate the time-dependent Stokes problem. The discrete formulation (both semi and fully) is analyzed by newly introduced divergence-free local VE spaces. With the help of appropriate projection operators onto the polynomials and a new L^2 projector, optimal error estimates are derived with minimal regularity assumptions (without non-local compatibility conditions).

In Chapter 3, we have explored applications of VEMs that were introduced in Chapter 2 for the approximation of transient Navier-Stokes problems. By employing the backward Euler method for time discretization, a fully discrete scheme is presented and analyzed. Further, using the Sobolev embedding theorem, interpolation theorems, and Gronwall's inequality, the stability, and optimal error estimates are established for both semi and fully discrete schemes.

Chapter 4 is devoted to study VEM for non-stationary linear poroelasticity problem. Here, by following [103] we have proposed locking free (robust with respect to λ) three field VE formulation, and discuss the well-posedness of both semi and fully discrete schemes without using Gronwall's inequality. Moreover, optimal error estimates are derived for all three fields that appear in the formulation.

In Chapter 5, we aim to develop VEMs for the coupled poroelastic and ADR equations. By employing the lowest order VE spaces introduced in Chapter 4, and backward Euler scheme for time derivative, the fully discrete formulation is proposed and analyzed. We stress that the resultant discrete scheme is designed in such a manner that it is explicit (even linear) at each time level. The convergence rates are derived for both spatial and temporal discretization through suitable projection operators.

Finally, based on computational and theoretical observations made from Chapter 2 to Chapter 5, the core of this thesis is briefly discussed in Chapter 6. We have also highlighted the major contributions and critical assessments of each chapter in terms of its efficiency and accuracy. We close this chapter by mentioning a few relevant extensions of this thesis.

Chapter 2

Stokes equations

The Stokes equation describes a linear incompressible fluid flow problem which is governed by an initial-boundary value problem, in terms of the fluid flow velocity vector $\boldsymbol{u}(t) : \Omega \to \mathbb{R}^2$ and the scalar pressure field $p(t) : \Omega \to \mathbb{R}$ for all $t \in (0, T]$, satisfying

$$\partial_t \boldsymbol{u} - \mathbf{div}\big(\nu\ \boldsymbol{\nabla} \boldsymbol{u} - p\mathbf{I}\big) = \boldsymbol{f} \qquad \text{in } \Omega \times (0, T], \tag{2.0.1a}$$

$$\operatorname{div} \boldsymbol{u} = 0 \qquad \text{in } \Omega \times (0, T], \tag{2.0.1b}$$

$$\boldsymbol{u} = \mathbf{0} \qquad \text{on } \partial\Omega \times (0, T], \tag{2.0.1c}$$

$$\boldsymbol{u}(\cdot, 0) = \boldsymbol{u}_0 \qquad \text{on } \Omega \times \{0\}, \tag{2.0.1d}$$

where Ω is a bounded convex domain in $\mathbb{R}^2$, $\partial_t \boldsymbol{u}$ is the flow acceleration, $\nu \in \mathbb{R}$ (> 0) is the viscosity of the fluid, $\boldsymbol{u}_0(\boldsymbol{x})$ is the initial velocity, and $\boldsymbol{f}(\boldsymbol{x}, t)$ is the external body force.

This chapter studies VE approximations for the non-stationary incompressible flow problem (2.0.1) on polygonal meshes. The proposed discrete scheme is based on pressure-velocity formulations, and the spaces associated with velocity and pressure are designed such that they obey the discrete inf-sup (LBB) condition. The spatial discretization of velocity is based on conforming VE space that consists of piecewise linear polynomials as well as non-polynomial functions with normal components on the midpoint of mesh edges as a quadratic polynomial, and the pressure approximation relies on discontinuous piecewise constants. A backward Euler method is employed for time discretization. By introducing suitable energy and L^2 projection operators, optimal error estimates are established in H^1- and L^2- norms for both semi and fully discrete schemes under the minimum regularity assumptions on continuous solutions. Moreover, several numerical experiments are conducted to verify the obtained theoretical rate of convergence and examine the performance of the proposed scheme.

The novelty lies in establishing the optimal error estimates with minimal realistic regularity assumptions on the continuous solutions of the governing equation (presented in Lemma 2.1 of the current chapter, also see [81, 68] for more details). The convergence analysis presented here does not demand the boundedness for the higher-order derivatives of exact velocity $\boldsymbol{u}$, such as $\|\boldsymbol{u}\|_{3,\Omega}$ and $\|\partial_t \boldsymbol{u}\|_{1,\Omega}$. We stress that showing these terms are uniformly bounded is equivalent to verifying the global compatibility in terms of the initial condition and given load which may not be practical from the computational point of view (refer [68]). The convergence analysis is carried out with two projectors' help: first is the new L^2 projection P_h onto discrete VE space, and the other is the Stokes projection S_h (also see [39]). We have observed that the proposed fully discrete scheme performs well even with a small-time step through our numerical experiments, whereas stabilized or penalized FE schemes with lowest order approximations may not work well [82]. We stress that the analysis presented here can be extended to more applicable time-dependent problems, such as miscible displacement problems and coupled fluid-flow problems. We would like to pursue these studies shortly so that applications of the proposed scheme become more transparent. Moreover, this chapter can be considered as a bridging stone for the other model problems in fluid dynamics consisting of the transient Stokes problem.

The content of this chapter is organized as follows: In Section 2.1, we state the variational formulation, and the minimal regularity assumptions on the continuous solutions $\boldsymbol{u}$ and p. We also address here the well-posedness of weak formulation for the problem (2.0.1). By introducing local and global VE spaces, we propose the discrete formulations with space and time discretization in Section 2.2, and also discuss the well-posedness of both the schemes. The convergence analysis of the proposed schemes for the primary variables velocity $\boldsymbol{u}$ and pressure p is established with the suitable norms in Section 2.3. Several numerical investigations have been carried out in Section 2.4 to validate the theoretical results achieved in the current chapter.

2.1 Variational formulation and its wellposedness

We define the admissible spaces for velocity and pressure, respectively as

$$\mathbf{V} := [H_0^1(\Omega)]^2 \quad \text{and} \quad Q := L_0^2(\Omega).$$

Assume that the load function $\boldsymbol{f}, \partial_t \boldsymbol{f} \in \mathbf{L}^2(0,T;[H_0^1(\Omega)]^2)$ and initial condition $\boldsymbol{u}_0 \in [H^2(\Omega)]^2 \cap \mathbf{V}$ with $\operatorname{div} \boldsymbol{u}_0 = 0$, i.e.,

$$|\boldsymbol{u}_0|_{2,\Omega}^2 + \int_0^T (\|\boldsymbol{f}(s)\|_{1,\Omega}^2 + \|\partial_t \boldsymbol{f}(s)\|_{1,\Omega}^2)\,\mathrm{d}s \leq C.$$

Now, multiplying (2.0.1a) and (2.0.1b) with test functions $\boldsymbol{v} \in \mathbf{V}$ and $q \in Q$ respectively, and integrating by parts with boundary condition (2.0.1c) yields the following weak formulation corresponding to (2.0.1): For all $t > 0$, find $\boldsymbol{u}(t) \in \mathbf{V}$ and $p(t) \in Q$ such that

$$m(\partial_t \boldsymbol{u}, \boldsymbol{v}) + a(\boldsymbol{u}, \boldsymbol{v}) + b(\boldsymbol{v}, p) = F(\boldsymbol{v}) \qquad \forall \boldsymbol{v} \in \mathbf{V}, \tag{2.1.1a}$$

$$b(\boldsymbol{u}, q) = 0 \qquad \forall q \in Q, \tag{2.1.1b}$$

with initial condition (2.0.1d) $\boldsymbol{u}(\cdot, 0) = \boldsymbol{u}_0$ almost everywhere in Ω, and the bilinear forms defined as,

$$m(\boldsymbol{u}, \boldsymbol{v}) := \int_\Omega \boldsymbol{u} \cdot \boldsymbol{v}\; dx, \quad a(\boldsymbol{u}, \boldsymbol{v}) := \nu \int_\Omega \boldsymbol{\nabla} \boldsymbol{u} : \boldsymbol{\nabla} \boldsymbol{v}\; dx,$$
$$F(\boldsymbol{v}) := \int_\Omega \boldsymbol{f} \cdot \boldsymbol{v}\; dx, \quad b(\boldsymbol{v}, q) := -\int_\Omega \operatorname{div} \boldsymbol{v}\; q\; dx.$$

We note that these bilinear forms satisfies the following properties which will be used in the subsequent analysis.

- $m(\cdot,\cdot)$ is positive definite form:

$$m(\boldsymbol{v}, \boldsymbol{v}) = \|\boldsymbol{v}\|_{0,\Omega}^2 \quad \forall \boldsymbol{v} \in \mathbf{V}.$$

- $a(\cdot,\cdot)$ is coercive: using Poincare's inequality, we get

$$a(\boldsymbol{v}, \boldsymbol{v}) = \nu |\boldsymbol{v}|_{1,\Omega}^2 \geq C\; \nu \|\boldsymbol{v}\|_{1,\Omega}^2 \quad \forall \boldsymbol{v} \in \mathbf{V}.$$

- $b(\cdot,\cdot)$ satisfies the inf-sup condition: there exists $\beta > 0$ such that (see [67])

$$\sup_{\boldsymbol{v}(\neq 0)\in \mathbf{V}} \frac{b(\boldsymbol{v},q)}{\|\boldsymbol{v}\|_{1,\Omega}} \geq \beta \|q\|_{0,\Omega} \qquad \forall q \in Q.$$

- $a(\cdot,\cdot)$ is continuous: the Cauchy Schwarz inequality gives

$$a(\boldsymbol{u},\boldsymbol{v}) \leq C\|\boldsymbol{u}\|_{1,\Omega}\|\boldsymbol{v}\|_{1,\Omega} \quad \forall \boldsymbol{u},\boldsymbol{v} \in \mathbf{V}.$$

- $F(\cdot)$ is continuous: again the Cauchy-Schwarz inequality gives

$$F(\boldsymbol{v}) \leq C\|\boldsymbol{f}\|_{0,\Omega}\|\boldsymbol{v}\|_{1,\Omega} \quad \forall \boldsymbol{v} \in \mathbf{V}.$$

In view of the above mentioned stability results, it is easy to show that (2.1.1) has a unique solution $(\boldsymbol{u},p) \in \mathbf{V}\times Q$ and also satisfies the following bounds, for details we refer to [67].

$$\begin{aligned} \|\boldsymbol{u}(t)\|_{0,\Omega}^2 + \int_0^t \left(\nu\|\boldsymbol{\nabla}\boldsymbol{u}(s)\|_{0,\Omega}^2 + \|\partial_t\boldsymbol{u}(s)\|_{0,\Omega}^2 + \|p(s)\|_{0,\Omega}^2\right) \mathrm{d}s \\ \lesssim \|\boldsymbol{u}_0\|_{0,\Omega}^2 + \int_0^t \|\boldsymbol{f}(s)\|_{0,\Omega}^2 \,\mathrm{d}s. \end{aligned} \tag{2.1.2}$$

At this end, we emphasis that the continuous solution $(\boldsymbol{u},p)$ possess the following regularity estimates, refer [68, 60, 112] for proof.

Lemma 2.1. *Assume Ω is a smooth domain then for a given $\boldsymbol{f}$, the problem* (2.1.1) *has a unique solution $(\boldsymbol{u},p)$ and satisfies*

$$\sup_{0<t\leq T} (\|\partial_t\boldsymbol{u}\|_{0,\Omega}^2 + |\boldsymbol{u}|_{2,\Omega}^2 + \|p\|_{1,\Omega}^2) \leq C, \tag{2.1.3}$$

$$\sup_{0<t\leq T} \sigma(t)\|\partial_t\boldsymbol{u}\|_{1,\Omega}^2 + \int_0^T \sigma(t)(\|\partial_{tt}\boldsymbol{u}\|_{0,\Omega}^2 + \|\partial_t\boldsymbol{u}\|_{2,\Omega}^2 + \|\partial_t p\|_{1,\Omega}^2)\, dt \leq C, \tag{2.1.4}$$

where $\sigma(t) := \min\{1,t\}$.

The regularity assumption on the continuous solutions mentioned in the above lemma will be used in establishing the error estimates reported in Section 2.3.

2.2 Virtual element formulation

In this section, we propose the VE formulation and discuss its well-posedness. We proceed by introducing new VE spaces (associated with velocity and pressure fields) through defining the required projection operators onto piecewise polynomials.

2.2.1 Projection operators and virtual element spaces

Let $\{\mathcal{T}_h\}_{h>0}$ be the family of partitions of the closed domain $\bar{\Omega}$ into polygons K of diameter h_K, mesh size $h := \max_{K\in\mathcal{T}_h} h_K$ and boundary ∂K. Also, e denotes a generic edge of any element K; N_K^v stands for the total number of vertices in K, and $V_i,\ 1 \leq i \leq N_K^v$ represent any vertex in K. We denote the unit normal pointing outwards K by $\boldsymbol{n}_K$ with $\boldsymbol{n}_K^e := \boldsymbol{n}_K|_e$, a unit normal vector on edge e, and the unit tangent vector along edge e as $\boldsymbol{t}_K^e$ for all $e \in \partial K$. We also suppose that the polygonal mesh $\mathcal{T}_h$ satisfy the following assumptions (refer [32]):

- $(A1)$ Each K is open and simply connected (convex or concave) sets whose boundary ∂K is a non-intersecting poly-line consisting of a finite number of straight line segments;

- $(A2)$ For every h and every $K \in \mathcal{T}_h$, there exists $C_{\mathcal{T}} > 0$ such that the ratio between the shortest edge and h_K is larger than $C_{\mathcal{T}}$;

- $(A3)$ Each $K \in \mathcal{T}_h$ is star-shaped with respect to every point within a ball of radius $C_{\mathcal{T}} h_K$.

In what follows, we denote the norm and seminorm in local space $H^s(K),\ s > 0$ for any $K \in \mathcal{T}_h$ as $\|\cdot\|_{s,K}$ and $|\cdot|_{s,K}$ respectively. The space $\mathbb{P}_k(S)$ denotes the space of polynomials of degree $\leq k$ for any integer $k \geq 0$ and a subset S of $\mathbb{R}^2$; and $W^\perp$ as the orthogonal complement of any space W. Denoting the vector space for polynomial functions over $\mathbb{R}^2$ by $[\mathbb{P}_k(K)]^2$ then define a new polynomial vector space $\boldsymbol{\mathcal{G}}(K) \subseteq [\mathbb{P}_1(K)]^2$ as $\boldsymbol{\mathcal{G}}(K) := \nabla\mathbb{P}_2(K)$. We note that the orthogonal complement $\boldsymbol{\mathcal{G}}^\perp(K)$ has dimension 1 and generated by a vector function $\boldsymbol{g}^\perp := [\bar{y}, -\bar{x}]$ where $\bar{x}, \bar{y}$ are scaled functions in polygon K.

Before proceeding to define the VE spaces, the prerequisites are mentioned for further analysis. The energy operator $\boldsymbol{\Pi}_K^{\boldsymbol{\nabla}} : [H^1(K)]^2 \to [\mathbb{P}_1(K)]^2$ is defined as,

$$(\boldsymbol{\nabla}(\boldsymbol{\Pi}_K^{\boldsymbol{\nabla}}\boldsymbol{v} - \boldsymbol{v}), \boldsymbol{\nabla}\boldsymbol{p}_1)_{0,K} = 0, \quad P^{0,K}(\boldsymbol{\Pi}_K^{\boldsymbol{\nabla}}\boldsymbol{v} - \boldsymbol{v}) = 0 \quad \forall\ \boldsymbol{p}_1 \in [\mathbb{P}_1(K)]^2, \boldsymbol{v} \in [H^1(K)]^2,$$

where $P^{0,K}\boldsymbol{v} := \frac{1}{N_K^v}\sum_{i=1}^{N_K^v} \boldsymbol{v}(V_i)$ take care of the projection onto constants.

The local space $\mathcal{B}(\partial K)$ on the boundary ∂K is

$$\mathcal{B}(\partial K) := \{\boldsymbol{v} \in [C^0(\partial K)]^2 : \boldsymbol{v}|_e \cdot \boldsymbol{n}_K^e \in \mathbb{P}_2(e), \boldsymbol{v}|_e \cdot \boldsymbol{t}_K^e \in \mathbb{P}_1(e) \quad \forall e \in \partial K\}.$$

Then we recall the local space from [29] on each element K given as

$$\mathbf{W}_h(K) := \{\boldsymbol{v}_h \in [H^1(K)]^2 \cap \mathcal{B}(\partial K) : \begin{cases} (-\boldsymbol{\Delta}\boldsymbol{v}_h + \nabla s)|_K = \mathbf{0}, \\ \operatorname{div} \boldsymbol{v}_h|_K = c_d \in \mathbb{P}_0(K) \end{cases} \quad \text{for some } s \in L^2(K)\},$$

for $c_d := \frac{1}{|K|}(\int_{\partial K} \boldsymbol{v}_h \cdot \boldsymbol{n}_K \, \mathrm{d}s)$. The well-defined space $\mathbf{W}_h(K)$ has dimension $3N_K^v$. We can note that the local space $\mathbf{W}_h(K)$ is motivated from the Bernardi-Raugel FE space $\mathbf{V}_{\text{fem}}$ [67, 29], and $[\mathbb{P}_1(K)]^2$ is subset of $\mathbf{V}_{\text{fem}}$ as well as $\mathbf{W}_h(K)$. The DoFs for local space $\mathbf{W}_h(K)$ are: for any $\boldsymbol{v}_h \in \mathbf{W}_h(K)$,

- (D_v1) the value of $\boldsymbol{v}_h$ at the vertices of element K;
- (D_v2) the moments of normal component of $\boldsymbol{v}_h$ on each edge on ∂K, that is,

$$\int_e \boldsymbol{v}_h \cdot \boldsymbol{n}_K^e \, \mathrm{d}s \qquad \forall e \in \partial K.$$

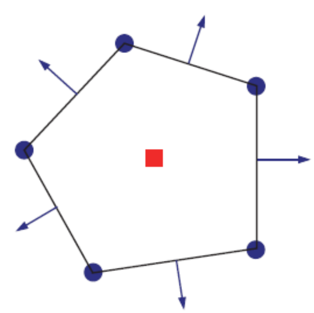

Figure 2.1: DoFs for velocity(with blue dot and normal moment), and pressure (red square)

Lemma 2.2. *The DoFs for the local space $\mathbf{W}_h(K)$ are $(D_v1) - (D_v2)$.*

Proof. The number of functionals $(D_v1) - (D_v2)$ are $3N_K^v$, which is also equal to the dimension of local space $\mathbf{W}_h(K)$. Suppose that $\boldsymbol{v}_h \in \mathbf{W}_h(K)$ and its value on $(D_v1)-(D_v2)$ vanishes then we show that $\boldsymbol{v}_h$ vanishes in K. The components $\boldsymbol{v}_h|_e \cdot \boldsymbol{t}_K^e$,

$\boldsymbol{v}_h|_e \cdot \boldsymbol{n}_K^e$ are polynomials, and it can be computed exactly through quadrature rules and DoFs which implies that $\boldsymbol{v}_h|_e \cdot \boldsymbol{n}_K^e$ and $\boldsymbol{v}_h|_e \cdot \boldsymbol{t}_K^e$ vanishes on all edges $e \in \partial K$ giving $\boldsymbol{v}_h|_e = 0$ on each $e \in \partial K$. Also, $\boldsymbol{v}_h|_e \cdot \boldsymbol{n}_K^e = 0$ implies $\operatorname{div} \boldsymbol{v}_h$ vanishes trivially in K. Using integration by parts and $\boldsymbol{v}_h = \mathbf{0}$ on ∂K, we obtain

$$|\boldsymbol{v}_h|_{1,K}^2 = -\int_K (\boldsymbol{\Delta} \boldsymbol{v}_h) \cdot \boldsymbol{v}_h + \int_{\partial K} ((\boldsymbol{\nabla} \boldsymbol{v}_h) \boldsymbol{n}_K) \cdot \boldsymbol{v}_h = -\int_K (\boldsymbol{\Delta} \boldsymbol{v}_h) \cdot \boldsymbol{v}_h.$$

Note that $(-\boldsymbol{\Delta} \boldsymbol{v}_h + \nabla s)|_K = 0$ for some $s \in L^2(K)$. Again applying integration by parts leads to

$$|\boldsymbol{v}_h|_{1,K}^2 = -\int_K \nabla s \cdot \boldsymbol{v}_h = \int_K \operatorname{div} \boldsymbol{v}_h \; s - \int_{\partial K} s \; (\boldsymbol{v}_h \cdot \boldsymbol{n}_K).$$

The semi-norm of $\boldsymbol{v}_h$ in K is zero with $\boldsymbol{v}_h = \mathbf{0}$ on ∂K then Poincaré inequality imply $\boldsymbol{v}_h = \mathbf{0}$ in K. $\square$

Remark 2.1. *The VE space $\mathbf{W}_h(K)$, introduced in [29], can be used here, however, this leads to a suboptimal convergence result for velocity in the L^2- norm. Hence, for deriving optimal L^2 error estimates, we define a modified version of space $\mathbf{W}_h(K)$ whose idea was first introduced in [24] for elliptic problem, and in [36, 32] for stationary Brinkmann and Navier-Stokes problems.*

We proceed by defining the required local L^2-projection $\mathbf{\Pi}_K^{\mathbf{0}} : [L^2(K)]^2 \to [\mathbb{P}_1(K)]^2$ as

$$(\mathbf{\Pi}_K^{\mathbf{0}} \boldsymbol{v} - \boldsymbol{v}, \boldsymbol{p}_1)_{0,K} = 0, \quad \forall \boldsymbol{p}_1 \in [\mathbb{P}_1(K)]^2.$$

This operator will help us in defining the discrete bilinear form that will appear in the discrete formulation. The term $(\boldsymbol{v}_h, \boldsymbol{p}_1)_{0,K}$ is not computable $\forall \boldsymbol{v}_h \in \mathbf{W}_h(K)$, and this motivate us to follow [32] (considered with $k \geq 2$) to define a modified VE space to make it calculable. First, we define the extended supplementary space $\tilde{\mathbf{V}}_h$ element-wise as

$$\tilde{\mathbf{V}}_h(K) := \{\boldsymbol{v}_h \in [H^1(K)]^2 \cap \mathcal{B}(\partial K) : \begin{cases} (-\boldsymbol{\Delta} \boldsymbol{v}_h + \nabla s)|_K \in \boldsymbol{\mathcal{G}}^{\perp}(K) \\ \operatorname{div} \boldsymbol{v}_h|_K = c_d \in \mathbb{P}_0(K), \end{cases} \quad \text{for some } s \in L^2(K)\}.$$

The dimension of space $\tilde{\mathbf{V}}_h(K)$ is $3N_K^v + 1$.

Lemma 2.3. *The DoFs for the local discrete space $\tilde{\mathbf{V}}_h(K)$ are: (D_v1), (D_v2), and*

- (D_v3) *the moment* $\int_K \boldsymbol{v}_h \cdot \boldsymbol{g}^\perp \, dx$ *with* $\boldsymbol{g}^\perp \in \boldsymbol{\mathcal{G}}^\perp(K)$.

Proof. The number of functionals in $(D_v1) - (D_v3)$ are $3N_K^v + 1$, and same as the dimension of the local space $\tilde{\mathbf{V}}_h(K)$. Suppose $\boldsymbol{v}_h \in \tilde{\mathbf{V}}_h(K)$ and its value on $(D_v1) - (D_v3)$ vanishes then from proof of Lemma 2.2, $\boldsymbol{v}_h|_e = 0$ on each $e \in \partial K$ and $\operatorname{div} \boldsymbol{v}_h = 0$ in K. Note that $-\boldsymbol{\Delta v}_h + \nabla s = \boldsymbol{g}^\perp$ for $\boldsymbol{g}^\perp \in \boldsymbol{\mathcal{G}}^\perp(K)$. Then, use of (D_v3) implies

$$|\boldsymbol{v}_h|^2_{1,K} = \int_K (\boldsymbol{g}^\perp - \nabla s) \cdot \boldsymbol{v}_h = \int_K \operatorname{div} \boldsymbol{v}_h \; s - \int_{\partial K} s \; (\boldsymbol{v}_h \cdot \boldsymbol{n}_K).$$

Hence, the Poincaré inequality yields $\boldsymbol{v}_h = \mathbf{0}$. $\square$

Now we define the local VE spaces $\mathbf{V}_h(K)$ and $Q_h(K)$ associated with the velocity $\boldsymbol{u}$ and pressure p, respectively as follows,

$$\mathbf{V}_h(K) := \{\boldsymbol{v}_h|_K \in \tilde{\mathbf{V}}_h(K) : (\boldsymbol{\Pi}_K^{\boldsymbol{\nabla}} \boldsymbol{v}_h - \boldsymbol{v}_h, \boldsymbol{g}^\perp)_{0,K} = 0 \text{ for } \boldsymbol{g}^\perp \in \boldsymbol{\mathcal{G}}^\perp(K)\},$$

$$\text{and} \qquad Q_h(K) := \mathbb{P}_0(K).$$

The degree of freedom for $Q_h(K)$ is

- (D_q) value of q_h at any point in K.

Lemma 2.4. *The DoFs for the local discrete space* $\mathbf{V}_h(K)$ *are same as that for local space* $\mathbf{W}_h(K)$*, that is* $(D_v1) - (D_v2)$.

Proof. The dimension of local VE space $\mathbf{V}_h(K)$ is equal to dimension of $\tilde{\mathbf{V}}_h(K)$ minus one (due to restriction in the local space). This gives the dimension of local VE space $\mathbf{V}_h(K)$ is same as the number of DoFs for $\mathbf{W}_h(K)$. Assuming that the values of $\boldsymbol{v}_h$ at vertices and the moment $\int_e (\boldsymbol{v}_h \cdot \boldsymbol{n}_e^K) \, \mathrm{d}s$ vanishes for $\boldsymbol{v}_h \in \mathbf{V}_h(K)$. Recalling the proof of Lemma 2.3, we get $\boldsymbol{v}_h|_e = \mathbf{0}$ for all $e \in \partial K$. Also, the projection $\boldsymbol{\Pi}_K^{\boldsymbol{\nabla}} \boldsymbol{v}_h = 0$ since it is computed exactly from (D_v1)-(D_v2). Then $(\boldsymbol{v}_h, \boldsymbol{g}^\perp)_{0,K} = (\boldsymbol{\Pi}_K^{\boldsymbol{\nabla}} \boldsymbol{v}_h, \boldsymbol{g}^\perp)_{0,K} = 0$ for $\boldsymbol{v}_h \in \mathbf{V}_h(K)$. Noting that $\mathbf{V}_h(K) \subset \tilde{\mathbf{V}}_h(K)$ gives $\boldsymbol{v}_h \in \tilde{\mathbf{V}}_h(K)$ and values of $\boldsymbol{v}_h$ vanishes at (D_v1)-(D_v3) then the use of Lemma 2.3 conclude $\boldsymbol{v}_h$ vanishes in K. $\square$

Next, we define the global finite-dimensional VE spaces as follows,

$$\mathbf{V}_h := \{\boldsymbol{v}_h \in \mathbf{V} : \boldsymbol{v}_h|_K \in \mathbf{V}_h(K) \quad \forall K \in \mathcal{T}_h\},$$
$$Q_h := \{q_h \in Q : q_h|_K \in Q_h(K) \quad \forall K \in \mathcal{T}_h\}.$$

It can be clearly seen that the DoFs for the global discrete space $\mathbf{V}_h$ are:

- the values of $\boldsymbol{v}_h$ at the internal vertices of each $K \in \mathcal{T}_h$;
- the moments of $\boldsymbol{v}_h \cdot \boldsymbol{n}_K^e$, that is $\int_e (\boldsymbol{v} \cdot \boldsymbol{n}_K^e)\, \mathrm{d}s$ for each internal edge e on ∂K, $K \in \mathcal{T}_h$.

The DoFs for Q_h are

- the values of $q_h \in Q_h$ at any point in K for each $K \in \mathcal{T}_h$.

Let N_K^V and N_K^Q denotes the dimension of local spaces $\mathbf{V}_h(K)$ and $Q_h(K)$, respectively; And N^V and N^Q as the dimension of $\mathbf{V}_h$ and Q_h, respectively. The notation $\mathrm{dof}_r(s)$ stands for the $r-$th degree of a given function s.

2.2.2 VE formulation and well-posedness analysis

On each element K and for $\boldsymbol{u}_h, \boldsymbol{v}_h \in \mathbf{V}_h(K)$ and $q_h \in Q_h(K)$, we define the following local bilinear forms,

$$\begin{aligned} m_h^K(\boldsymbol{u}_h, \boldsymbol{v}_h) &:= m^K(\boldsymbol{\Pi}_K^{\mathbf{0}} \boldsymbol{u}_h, \boldsymbol{\Pi}_K^{\mathbf{0}} \boldsymbol{v}_h) + S^{0,K}((\boldsymbol{u}_h - \boldsymbol{\Pi}_K^{\mathbf{0}} \boldsymbol{u}_h), (\boldsymbol{v}_h - \boldsymbol{\Pi}_K^{\mathbf{0}} \boldsymbol{v}_h)), \\ a_h^K(\boldsymbol{u}_h, \boldsymbol{v}_h) &:= a^K(\boldsymbol{\Pi}_K^{\boldsymbol{\nabla}} \boldsymbol{u}_h, \boldsymbol{\Pi}_K^{\boldsymbol{\nabla}} \boldsymbol{v}_h) + \nu S^{\nabla,K}(\boldsymbol{u}_h - \boldsymbol{\Pi}_K^{\boldsymbol{\nabla}} \boldsymbol{u}_h, (\boldsymbol{u}_h - \boldsymbol{\Pi}_K^{\boldsymbol{\nabla}} \boldsymbol{v}_h), \end{aligned}$$

where

$$m^K(\boldsymbol{u}_h, \boldsymbol{v}_h) := \int_K \boldsymbol{u}_h \cdot \boldsymbol{v}_h \; dx, \quad a^K(\boldsymbol{u}_h, \boldsymbol{v}_h) := \nu \int_K \boldsymbol{\nabla} \boldsymbol{u}_h : \boldsymbol{\nabla} \boldsymbol{v}_h \; dx,$$

and the local stabilization forms $S^{0,K}(\cdot,\cdot)$ and $S^{\nabla,K}(\cdot,\cdot)$ are defined as (see [24, 30]):

$$\begin{aligned} S^{0,K}(\boldsymbol{u}, \boldsymbol{v}) &:= \gamma_K^0 \mathrm{area}(K) \sum_{i,j=1}^{N_K^V} \mathrm{dof}_i(\boldsymbol{u}) \mathrm{dof}_j(\boldsymbol{v}), && \forall \boldsymbol{u}, \boldsymbol{v} \in \mathrm{Ker}(\boldsymbol{\Pi}_K^{\mathbf{0}}), \\ S^{\nabla,K}(\boldsymbol{u}, \boldsymbol{v}) &:= \alpha_K^{\nabla} \sum_{i,j=1}^{N_K^V} \mathrm{dof}_i(\boldsymbol{u}) \mathrm{dof}_j(\boldsymbol{v}), && \forall \boldsymbol{u}, \boldsymbol{v} \in \mathrm{Ker}(\boldsymbol{\Pi}_K^{\boldsymbol{\nabla}}), \end{aligned}$$

where γ_K^0 and α_K^{∇} are some positive constants independent of h_K. In our numerical tests, we have taken $\gamma_K^0 = 1$ and $\alpha_K^{\nabla} = 1$. Let $\boldsymbol{\Phi}_i, i = 1, 2 \cdots N_K^V$ are the canonical basis functions for the virtual space $\mathbf{V}_h(K)$ defined as:

$$\mathrm{dof}_i(\boldsymbol{\Phi}_j) = \delta_{ij}.$$

Then under the assumption $(A2)$, it is easy to see that $a^K(\mathbf{\Phi}_i, \mathbf{\Phi}_i) \simeq 1$ and $m^K(\mathbf{\Phi}_i, \mathbf{\Phi}_i) \simeq \text{area}(K)$. Therefore, the local stabilization terms $S^{0,K}(\cdot,\cdot)$ and $S^{\nabla,K}(\cdot,\cdot)$ satisfies the following, see also [18].

$$
\begin{aligned}
\gamma_* m^K(\boldsymbol{v}_h, \boldsymbol{v}_h) \leq S^{0,K}(\boldsymbol{v}_h, \boldsymbol{v}_h) \leq \gamma^* m^K(\boldsymbol{v}_h, \boldsymbol{v}_h) \quad \forall \boldsymbol{v}_h \in \operatorname{Ker}(\mathbf{\Pi}_K^{\mathbf{0}}), \\
\alpha_* a^K(\boldsymbol{v}_h, \boldsymbol{v}_h) \leq S^{\nabla,K}(\boldsymbol{v}_h, \boldsymbol{v}_h) \leq \alpha^* a^K(\boldsymbol{v}_h, \boldsymbol{v}_h) \quad \forall \boldsymbol{v}_h \in \operatorname{Ker}(\mathbf{\Pi}_K^{\boldsymbol{\nabla}}),
\end{aligned}
\tag{2.2.1}
$$

where $\gamma_*, \gamma^*, \alpha_*, \alpha^* > 0$ are constants independent of diameter h_K. Thus, the following holds for each $K \in \mathcal{T}_h$,

- Stability: There exists positive constants $C_\gamma, C^\gamma, C_\alpha, C^\alpha$, independent of h_K, such that $\forall \boldsymbol{v}_h \in \mathbf{V}_h(K)$,

$$
\begin{aligned}
C_\gamma m^K(\boldsymbol{v}_h, \boldsymbol{v}_h) \leq m_h^K(\boldsymbol{v}_h, \boldsymbol{v}_h) \leq C^\gamma m^K(\boldsymbol{v}_h, \boldsymbol{v}_h), \\
C_\alpha a^K(\boldsymbol{v}_h, \boldsymbol{v}_h) \leq a_h^K(\boldsymbol{v}_h, \boldsymbol{v}_h) \leq C^\alpha a^K(\boldsymbol{v}_h, \boldsymbol{v}_h).
\end{aligned}
\tag{2.2.2}
$$

- Consistency: For all $\boldsymbol{p}_1 \in [\mathbb{P}_1(K)]^2$ and $\boldsymbol{v}_h \in \mathbf{V}_h(K)$,

$$
\begin{aligned}
m_h^K(\boldsymbol{p}_1, \boldsymbol{v}_h) = m^K(\boldsymbol{p}_1, \mathbf{\Pi}_K^{\mathbf{0}} \boldsymbol{v}_h) = m^K(\boldsymbol{p}_1, \boldsymbol{v}_h), \\
a_h^K(\boldsymbol{p}_1, \boldsymbol{v}_h) = a^K(\boldsymbol{p}_1, \mathbf{\Pi}_K^{\boldsymbol{\nabla}} \boldsymbol{v}_h) = a^K(\boldsymbol{p}_1, \boldsymbol{v}_h).
\end{aligned}
\tag{2.2.3}
$$

The load function is locally defined as,

$$
F_h^K(\boldsymbol{v}_h) := (\boldsymbol{f}_h, \boldsymbol{v}_h)_{0,K} \quad \text{with } \boldsymbol{f}_h|_K := \mathbf{\Pi}_K^{\mathbf{0}} \boldsymbol{f}.
$$

Now considering the above defined local forms and local bilinear form

$$
b^K(\boldsymbol{v}, q) := -\int_K \operatorname{div} \boldsymbol{v}\, q \,\mathrm{d}x,
$$

then the global discrete bilinear forms for all $\boldsymbol{u}_h, \boldsymbol{v}_h \in \mathbf{V}_h$ and $q_h \in Q_h$ are defined as follows,

$$
\begin{gathered}
m_h(\boldsymbol{u}_h, \boldsymbol{v}_h) := \sum_{K \in \mathcal{T}_h} m_h^K(\boldsymbol{u}_h, \boldsymbol{v}_h), \quad b(\boldsymbol{v}_h, q_h) := \sum_{K \in \mathcal{T}_h} b^K(\boldsymbol{v}_h, q_h), \\
a_h(\boldsymbol{u}_h, \boldsymbol{v}_h) := \sum_{K \in \mathcal{T}_h} a_h^K(\boldsymbol{u}_h, \boldsymbol{v}_h),
\end{gathered}
$$

and the load term as

$$F_h(\boldsymbol{v}_h) := \sum_{K\in\mathcal{T}_h} F_h^K(\boldsymbol{v}_h).$$

With the help of above defined discrete bilinear forms, we define semi-discrete formulation corresponding to the weak form (2.1.1a)-(2.1.1b) as: For each $t \in (0,T]$, find $\boldsymbol{u}_h(t) \in \mathbf{V}_h$ and $p_h(t) \in Q_h$ such that

$$m_h(\partial_t \boldsymbol{u}_h, \boldsymbol{v}_h) + a_h(\boldsymbol{u}_h, \boldsymbol{v}_h) + b(\boldsymbol{v}_h, p_h) = F_h(\boldsymbol{v}_h) \qquad \forall \boldsymbol{v}_h \in \mathbf{V}_h, \tag{2.2.4a}$$

$$b(\boldsymbol{u}_h, q_h) = 0 \qquad \forall q_h \in Q_h, \tag{2.2.4b}$$

with $\boldsymbol{u}_h(0)$ as an appropriate approximation of the initial velocity $\boldsymbol{u}_0$, defined later in Section 2.3. In view of the stability properties of $S^{0,K}(\cdot,\cdot)$ and $S^{\nabla,K}(\cdot,\cdot)$ given in (3.2.1), we have

- $m_h(\cdot,\cdot)$ is continuous:

$$m_h(\boldsymbol{u}_h, \boldsymbol{v}_h) \lesssim C\|\boldsymbol{u}_h\|_{0,\Omega}\|\boldsymbol{v}_h\|_{0,\Omega} \quad \forall \boldsymbol{u}_h, \boldsymbol{v}_h \in \mathbf{V}_h.$$

- $a_h(\cdot,\cdot)$ is coercive: For all $\boldsymbol{v}_h \in \mathbf{V}_h$, we get

$$\begin{aligned} a_h(\boldsymbol{v}_h, \boldsymbol{v}_h) &= \sum_{K\in\mathcal{T}_h} \Big(a^K(\boldsymbol{\Pi}_K^{\boldsymbol{\nabla}}\boldsymbol{v}_h, \boldsymbol{\Pi}_K^{\boldsymbol{\nabla}}\boldsymbol{v}_h) + S^{\nabla,K}((\mathbf{I}-\boldsymbol{\Pi}_K^{\boldsymbol{\nabla}})\boldsymbol{v}_h, (\mathbf{I}-\boldsymbol{\Pi}_K^{\boldsymbol{\nabla}})\boldsymbol{v}_h) \Big) \\ &\geq \nu \sum_{K\in\mathcal{T}_h} \Big(\|\boldsymbol{\Pi}_K^{\boldsymbol{\nabla}}\boldsymbol{v}_h\|_{1,K}^2 + \alpha_* \|(\mathbf{I}-\boldsymbol{\Pi}_K^{\boldsymbol{\nabla}})\boldsymbol{v}_h\|_{1,K}^2 \Big) \geq C\ \nu \|\boldsymbol{v}_h\|_{1,\Omega}^2. \end{aligned}$$

- $a_h(\cdot,\cdot)$ is continuous:

$$a_h(\boldsymbol{u}_h, \boldsymbol{v}_h) \leq C\nu\|\boldsymbol{u}_h\|_{1,\Omega}\|\boldsymbol{v}_h\|_{1,\Omega} \quad \forall \boldsymbol{u}_h, \boldsymbol{v}_h \in \mathbf{V}_h.$$

- $F_h(\cdot)$ is continuous:

$$F_h(\boldsymbol{v}_h) \leq \sum_{K\in\mathcal{T}_h} \|\boldsymbol{\Pi}_K^{\mathbf{0}}\boldsymbol{f}\|_{0,K}\|\boldsymbol{v}_h\|_{0,K} \leq C\|\boldsymbol{f}\|_{0,\Omega}\|\boldsymbol{v}_h\|_{1,\Omega} \quad \forall \boldsymbol{v}_h \in \mathbf{V}_h.$$

Lemma 2.5. *Assume that the bilinear form $b(\cdot,\cdot)$ satisfies discrete inf-sup condition on $\mathbf{V}_h \times Q_h$ then the semi-discrete problem (2.2.4) has a unique solution $\boldsymbol{u}_h \in \mathbf{V}_h$ for* *given* $\boldsymbol{u}_h(0)$ *and satisfies (for all* $t \in [0,T]$*),*

$$\begin{aligned}\|\boldsymbol{u}_h(t)\|_{1,\Omega}^2 + \int_0^t (\nu\|\boldsymbol{u}_h(s)\|_{1,\Omega}^2 + \|\partial_t \boldsymbol{u}_h(s)\|_{0,\Omega}^2 + \|p_h(s)\|_{0,\Omega}^2)\, ds \\ \lesssim \|\boldsymbol{u}_h(0)\|_{1,\Omega}^2 + \int_0^t \|\boldsymbol{f}(s)\|_{0,\Omega}^2\, ds.\end{aligned} \tag{2.2.5}$$

Proof. The properties of the discrete bilinear forms $a_h(\cdot,\cdot), b(\cdot,\cdot)$, discrete linear functional $F_h(\cdot)$ and the well-known theorems from ordinary differential equations implies that the semi-discrete problem (2.2.4) has a unique solution, see also [68]. Taking $\boldsymbol{v}_h = \boldsymbol{u}_h$ in (2.2.4a) gives

$$\frac{1}{2}\frac{d}{dt}\|\boldsymbol{u}_h\|_{0,\Omega}^2 + \nu\|\boldsymbol{u}_h\|_{1,\Omega}^2 \leq C\|\boldsymbol{f}\|_{0,\Omega}\|\boldsymbol{u}_h\|_{0,\Omega}.$$

Employing the Young's inequality and then integrating from 0 to t imply

$$\|\boldsymbol{u}_h(t)\|_{0,\Omega}^2 + \nu\int_0^t \|\boldsymbol{u}_h(s)\|_{1,\Omega}^2\, \mathrm{d}s \lesssim \|\boldsymbol{u}_h(0)\|_{0,\Omega}^2 + \int_0^t \|\boldsymbol{f}(s)\|_{0,\Omega}^2\, \mathrm{d}s.$$

Again considering (2.2.4a) with $\boldsymbol{v}_h = \partial_t \boldsymbol{u}_h$ and in similar manner, we get

$$\nu\|\boldsymbol{u}_h(t)\|_{1,\Omega}^2 + \int_0^t \|\partial_t \boldsymbol{u}_h(s)\|_{0,\Omega}^2\, \mathrm{d}s \lesssim \nu\|\boldsymbol{u}_h(0)\|_{1,\Omega}^2 + \int_0^t \|\boldsymbol{f}(s)\|_{0,\Omega}^2\, \mathrm{d}s.$$

Thus the above bounds and discrete inf-sup condition lead to (2.2.5). $\square$

Below, we state the well known stability results for the solution of the problem (2.2.4) in terms of $\sigma(t)$.

Lemma 2.6. *The discrete solution* $(\boldsymbol{u}_h(t), p_h(t)) \in \mathbf{V}_h \times Q_h$ *of the problem* (2.2.4a)-(2.2.4b) *satisfies*

$$\sup_{0<t\leq T}(\|\partial_t \boldsymbol{u}_h\|_{0,\Omega}^2 + \|\boldsymbol{u}_h\|_{2,\Omega}^2 + \|p_h\|_{1,\Omega}^2) \leq C, \tag{2.2.6}$$

$$\sup_{0<t\leq T}\sigma(t)\|\partial_t \boldsymbol{u}_h\|_{1,\Omega}^2 + \int_0^T \sigma(t)(\|\partial_{tt}\boldsymbol{u}_h\|_{0,\Omega}^2 + \|\partial_t \boldsymbol{u}_h\|_{2,\Omega}^2 + \|\partial_t p_h\|_{1,\Omega}^2)\, dt \leq C. \tag{2.2.7}$$

The proof of this lemma based on the properties of bilinear forms and integration by parts. Therefore, we skip the proof here, and refer to [112, 60, 81] and the references within.

2.2.3 Fully-discrete scheme

For the approximation of time derivative, we employ the backward Euler scheme by considering its simplicity and unconditional stability, and in this connection, we discretize the time interval $[0, T]$ into the discrete points t_n/subinterval $[t_{n-1}, t_n]$, where $t_n = n\Delta t$ for $n = 1, \dots, N$ and $\Delta t = \frac{T}{N}$. We define δ_t as an approximation of time derivative at time t_n for any discrete function g_h^n as

$$\delta_t g_h^n := \frac{g_h^n - g_h^{n-1}}{\Delta t}.$$

In order to avoid the ambiguity in notations, the solution of semi-discrete scheme and fully discrete scheme at time $t = t_n$, will be denoted by $\boldsymbol{u}_h(t_n)$ and $\boldsymbol{u}_h^n$, respectively.

With above notation, the fully discretize scheme corresponding to the continuous formulation (2.1.1a)-(2.1.1b) read as: Given initial conditions $\boldsymbol{u}_h^0 := \boldsymbol{u}_h(0)$, find $\boldsymbol{u}_h^n \in \mathbf{V}_h, p_h^n \in Q_h$ for each $n = 1, \dots, N$ such that

$$m_h(\delta_t \boldsymbol{u}_h^n, \boldsymbol{v}_h) + a_h(\boldsymbol{u}_h^n, \boldsymbol{v}_h) + b(\boldsymbol{v}_h, p_h^n) = F_h^n(\boldsymbol{v}_h) \qquad \forall \boldsymbol{v}_h \in \mathbf{V}_h, \tag{2.2.8a}$$

$$b(\boldsymbol{u}_h^n, q_h) = 0 \qquad \forall q_h \in Q_h. \tag{2.2.8b}$$

Since $\mathbf{V}_h$ and Q_h are finite-dimensional spaces, (2.2.8) can be considered as a system of $N^V + N^Q$ linear algebraic equations in $N^V + N^Q$ unknowns for each n. Taking $\boldsymbol{v}_h = \boldsymbol{u}_h^n$, $q_h = p_h^n$, $\boldsymbol{f} = \mathbf{0}$ and $\boldsymbol{u}_h(0) = \mathbf{0}$ in (2.2.8), and using the stability properties of $m_h(\cdot, \cdot)$ and $a_h(\cdot, \cdot)$ given in (2.2.2) together with discrete inf-sup condition of $b(\cdot, \cdot)$ implies $\boldsymbol{u}_h^n = \mathbf{0}$ and $p_h^n = 0$, which in turn, assure the uniqueness of the solution of (2.2.8). Now again using the structure of linear system, uniqueness implies existence.

Moreover, the solution $\boldsymbol{u}_h^n \in \mathbf{V}_h$ and $p_h^n \in Q_h$ of (2.2.8) are bounded as follows,

$$\begin{aligned} \max_{1 \le j \le n} \|\boldsymbol{u}_h^j\|_{1,\Omega}^2 + \sum_{j=1}^{n} (\nu \|\boldsymbol{u}_h^j\|_{1,\Omega}^2 + \|\delta_t \boldsymbol{u}_h^j\|_{0,\Omega}^2 + \|p_h^j\|_{0,\Omega}^2) \\ \le C\big(\|\boldsymbol{u}_h(0)\|_{1,\Omega}^2 + \sum_{j=1}^{n} \|\boldsymbol{f}^j\|_{0,\Omega}^2\big). \end{aligned} \tag{2.2.9}$$

2.3 Convergence analysis

In this section, we develop the error estimates for both semi-discrete and fully discrete schemes with minimal realistic regularity assumptions on the continuous solution that are specifically mentioned in Lemma 2.1 and 2.6. With the help of two projection operators: L^2 projection P_h onto discrete space $\mathbf{V}_h$, and the Stokes projection S_h, we derive the error estimates of velocity in H^1 and L^2 norms, and for pressure in L^2 norm. We stress that, in general, higher-order regularity is needed for establishing the optimal error estimates; however, we derive these estimates with minimum regularity assumptions, and therefore this can be considered as one of the main contributions of this chapter. We start with the following auxiliary results used frequently in our subsequent analysis.

Lemma 2.7. *Let $\boldsymbol{u}_\pi \in [\mathbb{P}_1(K)]^2$ be the polynomial approximation of $\boldsymbol{u}$. Under the regularity assumption on the polygonal mesh (mentioned in Section 2.2), there exists a positive constant C independent of h such that (see [113, 18])*

$$\sum_{K\in\mathcal{T}_h} (\|\boldsymbol{u}-\boldsymbol{u}_\pi\|_{0,K} + h_K\ |\boldsymbol{u}-\boldsymbol{u}_\pi|_{1,K}) \leq Ch^2|\boldsymbol{u}|_{2,\Omega}. \tag{2.3.1}$$

Lemma 2.8. *For each $\boldsymbol{u} \in \mathbf{V} \cap [H^{s+1}(\Omega)]^2$ with $0 \leq s \leq 1$ and under the regularity assumption on the polygonal mesh (mentioned in Section 2.2), there exist an interpolant $\boldsymbol{u}_I \in \mathbf{V}_h$ satisfying*

$$\|\boldsymbol{u}-\boldsymbol{u}_I\|_{0,\Omega} + h\ |\boldsymbol{u}-\boldsymbol{u}_I|_{1,\Omega} \leq Ch^{s+1}|\boldsymbol{u}|_{s+1,\Omega}. \tag{2.3.2}$$

Proof. By introducing a piecewise linear Clément interpolant $\boldsymbol{u}_c \in [H^1(\Omega)]^2$ of $\boldsymbol{u}$ defined on sub-triangulation (formed by joining the vertices of polygon K with its barycentre) of the polygon K and proceeding analogously to the proof of Proposition 4.2 given in [30], it is easy to see that there exists an interpolant $\boldsymbol{w}_I \in \mathbf{W}_h$ through combining on each K such that

$$\|\boldsymbol{u}-\boldsymbol{w}_I\|_{0,\Omega} + h\ |\boldsymbol{u}-\boldsymbol{w}_I|_{1,\Omega} \leq Ch^{s+1}|\boldsymbol{u}|_{s+1,\Omega}.$$

Now using the estimates of $\boldsymbol{w}_I \in \mathbf{W}_h$, we establish the interpolant estimates for the modified space $\mathbf{V}_h$ by following [32]. For this purpose, we define interpolant $\boldsymbol{u}_I \in \mathbf{V}_h$ locally on each element K as $\mathrm{dof}_i(\boldsymbol{u}_I) = \mathrm{dof}_i(\boldsymbol{w}_I)$, $1 \leq i \leq 3\, N_K^v$. Since the spaces $\mathbf{W}_h(K)$ and $\mathbf{V}_h(K)$ are same on the boundary of K containing piecewise linear along the edge and piecewise quadratic along the normal component at mid point on each edge. Thus, $\boldsymbol{u}_I = \boldsymbol{w}_I$ on ∂K. By definition of local spaces, we get $\mathrm{div}(\boldsymbol{u}_I - \boldsymbol{w}_I) = 0$ in each K and also, the computation through DoFs yields $\boldsymbol{\Pi}_K^{\boldsymbol{\nabla}}\boldsymbol{u}_I = \boldsymbol{\Pi}_K^{\boldsymbol{\nabla}}\boldsymbol{w}_I$.

Again, in view of definition of local space $\mathbf{V}_h(K)$, we have $-\boldsymbol{\Delta u}_I - \nabla s_2 = \boldsymbol{g}^{\perp}$ for some $s_2 \in L^2_0(K)$, $\boldsymbol{g}^{\perp} \in \mathcal{G}^{\perp}(K)$. Now define $\boldsymbol{z}_h := \boldsymbol{u}_I - \boldsymbol{w}_I$. Note that from the definition of $\mathbf{V}_h(K)$ and for $\boldsymbol{h}^{\perp} \in \mathcal{G}^{\perp}(K)$, we have

$$\int_K \boldsymbol{z}_h \cdot \boldsymbol{h}^{\perp} = \int_K (\boldsymbol{\Pi}^{\boldsymbol{\nabla}}_K \boldsymbol{u}_I - \boldsymbol{w}_I) \cdot \boldsymbol{h}^{\perp} = \int_K (\boldsymbol{\Pi}^{\boldsymbol{\nabla}}_K \boldsymbol{w}_I - \boldsymbol{w}_I) \cdot \boldsymbol{h}^{\perp}. \tag{2.3.3}$$

Hence, $\boldsymbol{z}_h \in [H^1(K)]^2$ solve the problem: find $(\boldsymbol{z}_h, \hat{s}, \boldsymbol{g}^{\perp}) \in [H^1_0(K)]^2 \times L^2_0(K) \times \boldsymbol{\mathcal{G}}^{\perp}(K)$ such that for all $(\boldsymbol{w}, q, \boldsymbol{h}^{\perp}) \in [H^1_0(K)]^2 \times L^2_0(K) \times \boldsymbol{\mathcal{G}}^{\perp}(K)$,

$$\begin{aligned} a^K(\boldsymbol{z}_h, \boldsymbol{w}) + b^K(\boldsymbol{w}, \hat{s}) + c^K(\boldsymbol{w}, \boldsymbol{g}^{\perp}) &= 0, \\ b^K(\boldsymbol{z}_h, q) &= 0, \\ c^K(\boldsymbol{z}_h, \boldsymbol{h}^{\perp}) &= (\boldsymbol{\Pi}^{\boldsymbol{\nabla}}_K \boldsymbol{w}_I - \boldsymbol{w}_I, \boldsymbol{h}^{\perp})_{0,K}, \end{aligned} \tag{2.3.4}$$

where the bilinear form $c^K(\boldsymbol{z}_h, \boldsymbol{h}^{\perp}) := \int_K \boldsymbol{z}_h \cdot \boldsymbol{h}^{\perp} \,\mathrm{d}x$. By defining a scaled norm on $\boldsymbol{\mathcal{G}}^{\perp}(K)$, it has been shown in [32] that $b^K(\cdot,\cdot) + c^K(\cdot,\cdot)$ satisfies the inf-sup condition on each K, and hence an appeal to general saddle point formulations will guarantee the well-posedness of (2.3.4) on each K. Therefore, using the stability of the solution of Stokes problem, zero mean value of $(\boldsymbol{\Pi}^{\boldsymbol{\nabla}}_K \boldsymbol{w}_I - \boldsymbol{w}_I)$ and stability property of $\boldsymbol{\Pi}^{\boldsymbol{\nabla}}_K$ with respect to $|\cdot|_{1,K}$, i.e., $|\boldsymbol{\Pi}^{\boldsymbol{\nabla}}_K \boldsymbol{v}|_{1,K} \leq C|\boldsymbol{v}|_{1,K} \, \forall \boldsymbol{v} \in \mathbf{V}$, we infer that (see Theorem 4.1 in [32] for more details)

$$\begin{aligned} |\boldsymbol{z}_h|_{1,K} &\leq C|\boldsymbol{\Pi}^{\boldsymbol{\nabla}}_K \boldsymbol{w}_I - \boldsymbol{w}_I|_{1,K} \leq |(\mathbf{I} - \boldsymbol{\Pi}^{\boldsymbol{\nabla}}_K)(\boldsymbol{w}_I - \boldsymbol{u})|_{1,K} + |(\mathbf{I} - \boldsymbol{\Pi}^{\boldsymbol{\nabla}}_K)\boldsymbol{u}|_{1,K} \\ &\leq C h^s_K |\boldsymbol{u}|_{s+1,K}. \end{aligned}$$

Using the scaled Poincaré inequality for the L^2 estimate of $\boldsymbol{z}_h \in [H^1_0(K)]^2$, we achieve the required result (2.3.2) with an application of triangle's inequality. $\square$

Lemma 2.9. *The bilinear form $b(\cdot,\cdot)$ satisfies the discrete inf-sup condition on $\mathbf{V}_h \times Q_h$, that is, there exists a $\beta_h > 0$ such that*

$$\sup_{(0\neq)\boldsymbol{v}_h \in \mathbf{V}_h} \frac{b(\boldsymbol{v}_h, q_h)}{\|\boldsymbol{v}_h\|_{1,\Omega}} \geq \beta_h \|q_h\|_{0,\Omega} \qquad \forall q_h \in Q_h. \tag{2.3.5}$$

Proof. The discrete inf-sup condition on spaces $\mathbf{W}_h$ and Q_h has been established in [22], and the proof is essentially based on the DoFs for the space $\mathbf{W}_h$ as well as the estimates of interpolant operator in $\mathbf{W}_h$. Also, the DoFs of the modified space $\mathbf{V}_h$ and original space $\mathbf{W}_h$ are same, we only provide a sketch of the proof of

(2.3.5). First considering the interpolant $\boldsymbol{v}_I$ defined in Lemma 2.8, we define operator $\pi_h : \mathbf{V} \longrightarrow \mathbf{V}_h$ by using the DoFs of $\mathbf{V}_h$ as follows,

$$\begin{aligned} \pi_h \boldsymbol{v}(V_i) &= \boldsymbol{v}_I(V_i) \quad \forall \text{ vertices } V_i \text{ in } \mathcal{T}_h \\ \int_e \pi_h \boldsymbol{v} \cdot \boldsymbol{n}_K^e &= \int_e \boldsymbol{v} \cdot \boldsymbol{n}_K^e \quad \forall e \in \partial K,\ K \in \mathcal{T}_h. \end{aligned} \tag{2.3.6}$$

Since $q_h \in \mathbb{P}_0(K)$, an application of Gauss divergence theorem and (2.3.6) on each element K, immediately gives

$$b(\pi_h \boldsymbol{v} - \boldsymbol{v}, q_h) = 0 \quad \forall \boldsymbol{v} \in \mathbf{V} \text{ and } q_h \in Q_h. \tag{2.3.7}$$

Moreover, using the similar arguments used in the proof of Lemma 4.3 of [22] together with Lemma 2.8, it is not hard to see that (see also [43, 30])

$$\|\pi_h \boldsymbol{v}\|_{1,\Omega} \leq C \|\boldsymbol{v}\|_{1,\Omega}. \tag{2.3.8}$$

Since continuous inf-sup conditions holds for the space $\mathbf{V}$ and Q, the condition (2.3.7) and bound (2.3.8) concludes the proof of (2.3.5) by recalling the standard Fortin's trick. □

Defining the continuous kernel space $\mathbf{X}$ and discrete kernel space $\mathbf{X}_h$ as,

$$\begin{aligned} \mathbf{X} &:= \{\boldsymbol{v} \in \mathbf{V} : b(\boldsymbol{v}, q) = 0 \ \forall q \in Q\} = \{\boldsymbol{v} \in \mathbf{V} : \operatorname{div} \boldsymbol{v} = 0\}, \\ \mathbf{X}_h &:= \{\boldsymbol{v}_h \in \mathbf{V}_h : b(\boldsymbol{v}_h, q_h) = 0 \ \forall q_h \in Q_h\} = \{\boldsymbol{v}_h \in \mathbf{V}_h : \operatorname{div} \boldsymbol{v}_h = 0\}. \end{aligned}$$

We note that for a given $\boldsymbol{v} \in \mathbf{X}$, we have the following approximation property for the space $\mathbf{X}_h$ as a consequence of the discrete inf-sup condition given in Lemma 2.9 (see [63] and also [32]):

$$\inf_{\boldsymbol{z}_h \in \mathbf{X}_h \setminus \{0\}} \|\boldsymbol{v} - \boldsymbol{z}_h\|_{1,\Omega} \leq \inf_{\boldsymbol{v}_h \in \mathbf{V}_h \setminus \{0\}} \|\boldsymbol{v} - \boldsymbol{v}_h\|_{1,\Omega}. \tag{2.3.9}$$

Now, for given $\boldsymbol{u}, p$ (solutions of the continuous problem (2.1.1)), we define the classical Stokes projection $S_h(\boldsymbol{u}, p) := (S_h^{\boldsymbol{u}} \boldsymbol{u}, S_h^p p) \in \mathbf{V}_h \times Q_h$ (see [63] and [67]) that satisfies

$$a_h(S_h^{\boldsymbol{u}} \boldsymbol{u}, \boldsymbol{v}_h) + b(\boldsymbol{v}_h, S_h^p p) = a(\boldsymbol{u}, \boldsymbol{v}_h) + b(\boldsymbol{v}_h, p) \qquad \forall \boldsymbol{v}_h \in \mathbf{V}_h, \tag{2.3.10a}$$

$$b(S_h^{\boldsymbol{u}}\boldsymbol{u}, q_h) = b(\boldsymbol{u}, q_h) \qquad \forall q_h \in Q_h. \tag{2.3.10b}$$

Note that use of (2.3.10b) and (2.1.1b) implies $b(S_h^{\boldsymbol{u}}\boldsymbol{u}, q_h) = 0$ for all $q_h \in Q_h$ and thus, $\operatorname{div} S_h^{\boldsymbol{u}}\boldsymbol{u} = 0$ and $S_h^{\boldsymbol{u}}\boldsymbol{u} \in \mathbf{X}_h$.

Below, we derive estimates of the Stokes projection S_h by using the properties of discrete bilinear forms and duality arguments for the L^2 estimates.

Lemma 2.10. *Let* $(\boldsymbol{u}, p) \in \mathbf{V} \times Q$ *be the solution of the continuous problem* (2.1.1) *and* $(S_h^{\boldsymbol{u}}\boldsymbol{u}, S_h^p p) \in \mathbf{V}_h \times Q_h$ *satisfies* (2.3.10)*, then there exists a positive constant* C *independent of* h *such that*

$$\|\boldsymbol{u} - S_h^{\boldsymbol{u}}\boldsymbol{u}\|_{0,\Omega} + h(|\boldsymbol{u} - S_h^{\boldsymbol{u}}\boldsymbol{u}|_{1,\Omega} + \|p - S_h^p p\|_{0,\Omega}) \leq Ch^2(|\boldsymbol{u}|_{2,\Omega} + |p|_{1,\Omega}). \tag{2.3.11}$$

Proof. Let $\boldsymbol{w}_h = (\boldsymbol{v}_h - S_h^{\boldsymbol{u}}\boldsymbol{u})$ for any $\boldsymbol{v}_h \in \mathbf{X}_h$ then $\operatorname{div} \boldsymbol{w}_h = 0$. The following yields by using stability and consistency of $a_h(\cdot,\cdot)$, and Lemma 2.7,

$$\begin{aligned}
C|\boldsymbol{w}_h|_{1,\Omega}^2 \leq a_h(\boldsymbol{w}_h, \boldsymbol{w}_h) &= a_h(\boldsymbol{v}_h, \boldsymbol{w}_h) - a_h(S_h^{\boldsymbol{u}}\boldsymbol{u}, \boldsymbol{w}_h) \\
&= \sum_{K \in \mathcal{T}_h} \left(a_h^K(\boldsymbol{v}_h - \boldsymbol{u}_\pi, \boldsymbol{w}_h) - a^K(\boldsymbol{u} - \boldsymbol{u}_\pi, \boldsymbol{w}_h)\right) \\
&\leq C\,\left(h\,|\boldsymbol{u}|_{2,\Omega} + |\boldsymbol{u} - \boldsymbol{v}_h|_{1,\Omega}\right)|\boldsymbol{w}_h|_{1,\Omega}.
\end{aligned}$$

The triangle's inequality, taking infimum over $\boldsymbol{v}_h \in X_h$ then use of inequality (2.3.9) and the application of Lemma 2.8 gives

$$\begin{aligned}
|\boldsymbol{u} - S_h^{\boldsymbol{u}}\boldsymbol{u}|_{1,\Omega} &\leq C\,\left(h\,|\boldsymbol{u}|_{2,\Omega} + \inf_{\boldsymbol{v}_h \in \mathbf{X}_h} |\boldsymbol{u} - \boldsymbol{v}_h|_{1,\Omega}\right) \\
&\leq C\,\left(h\,|\boldsymbol{u}|_{2,\Omega} + \inf_{\boldsymbol{v}_h \in \mathbf{V}_h} |\boldsymbol{u} - \boldsymbol{v}_h|_{1,\Omega}\right) \leq C\,h\,|\boldsymbol{u}|_{2,\Omega}.
\end{aligned} \tag{2.3.12}$$

For pressure estimates, take any $q_h \in Q_h$ then the discrete inf-sup condition gives

$$\beta_h\|q_h - S_h^p p\|_{0,\Omega} \leq \sup_{\boldsymbol{v}_h \in \mathbf{V}_h \setminus \{0\}} \frac{b(\boldsymbol{v}_h, q_h - S_h^p p)}{|\boldsymbol{v}_h|_{1,\Omega}}.$$

Using (2.1.1), (2.2.4), and (2.3.1) for $\boldsymbol{v}_h \in \mathbf{V}_h$, we arrive at

$$\begin{aligned}
b(\boldsymbol{v}_h, q_h - S_h^p p) &= b(\boldsymbol{v}_h, q_h - p) + b(\boldsymbol{v}_h, p - S_h^p p) \\
&= b(\boldsymbol{v}_h, q_h - p) + (a_h(S_h^{\boldsymbol{u}}\boldsymbol{u}, \boldsymbol{v}_h) - a(\boldsymbol{u}, \boldsymbol{v}_h))
\end{aligned}$$

$$= b(\boldsymbol{v}_h, q_h - p) + \sum_{K\in\mathcal{T}_h} (a_h^K(S_h^{\boldsymbol{u}}\boldsymbol{u} - \boldsymbol{u}_\pi, \boldsymbol{v}_h) - a^K(\boldsymbol{u} - \boldsymbol{u}_\pi, \boldsymbol{v}_h))$$
$$\leq C\ (\|p - q_h\|_{0,\Omega} + h|\boldsymbol{u}|_{2,\Omega})|\boldsymbol{v}_h|_{1,\Omega}.$$

Again the best approximation properties of Q_h and triangle inequality gives

$$\|p - S_h^p p\|_{0,\Omega} \leq Ch(|\boldsymbol{u}|_{2,\Omega} + |p|_{1,\Omega}). \tag{2.3.13}$$

Next we use the duality arguments in order to achieve the L^2 estimates for velocity. For given $\mathbf{g} \in [L^2(\Omega)]^2$, find $(\boldsymbol{\varphi}, \zeta) \in \mathbf{V} \times Q$ such that

$$\begin{aligned} a(\boldsymbol{\varphi}, \boldsymbol{v}) + b(\boldsymbol{v}, \zeta) &= (\mathbf{g}, \boldsymbol{v}) \quad \forall\ \boldsymbol{v} \in \mathbf{V}, \\ b(\boldsymbol{\varphi}, q) &= \ 0 \qquad\quad \forall\ q \in Q. \end{aligned} \tag{2.3.14}$$

Since the domain Ω is convex, the regularity theory of Stokes problem yield that the solution $\boldsymbol{\varphi}$ and ζ of (2.3.14) satisfy

$$|\boldsymbol{\varphi}|_{2,\Omega} + |\zeta|_{1,\Omega} \leq C\|\mathbf{g}\|_{0,\Omega}. \tag{2.3.15}$$

Taking $\boldsymbol{v} = \mathbf{g} := \boldsymbol{u} - S_h^{\boldsymbol{u}}\boldsymbol{u}$ in (2.3.14), then the Stokes projection (2.3.10), interpolant $\boldsymbol{\varphi}_I \in \mathbf{V}_h$, consistency of $a_h(\cdot,\cdot)$ from (2.2.3) and use of (2.3.14) for $q = S_h^p p - p$ gives

$$\begin{aligned} \|\boldsymbol{u} - S_h^{\boldsymbol{u}}\boldsymbol{u}\|_{0,\Omega}^2 &= a(\boldsymbol{u} - S_h^{\boldsymbol{u}}\boldsymbol{u}, \boldsymbol{\varphi}) + b(\boldsymbol{u} - S_h^{\boldsymbol{u}}\boldsymbol{u}, \zeta) \\ &= a(\boldsymbol{u} - S_h^{\boldsymbol{u}}\boldsymbol{u}, \boldsymbol{\varphi} - \boldsymbol{\varphi}_I) + b(\boldsymbol{u} - S_h^{\boldsymbol{u}}\boldsymbol{u}, \zeta - q_h) + a(\boldsymbol{u} - S_h^{\boldsymbol{u}}\boldsymbol{u}, \boldsymbol{\varphi}_I) \\ &= a(\boldsymbol{u} - S_h^{\boldsymbol{u}}\boldsymbol{u}, \boldsymbol{\varphi} - \boldsymbol{\varphi}_I) + b(\boldsymbol{u} - S_h^{\boldsymbol{u}}\boldsymbol{u}, \zeta - q_h) + b(\boldsymbol{\varphi} - \boldsymbol{\varphi}_I, S_h^p p - p) \\ &\quad + \sum_{K\in\mathcal{T}_h} \big(a_h^K(S_h^{\boldsymbol{u}}\boldsymbol{u} - \boldsymbol{u}_\pi, \boldsymbol{\varphi}_I - \boldsymbol{\varphi}_\pi) - a^K(S_h^{\boldsymbol{u}}\boldsymbol{u} - \boldsymbol{u}_\pi, \boldsymbol{\varphi}_I - \boldsymbol{\varphi}_\pi)\big). \end{aligned}$$

Using continuity of $a(\cdot,\cdot)$, $a_h(\cdot,\cdot)$ and $b(\cdot,\cdot)$, together with Lemma 2.7, 2.8, estimates (2.3.12), (2.3.13), and the best approximation of ζ, we easily obtain

$$\begin{aligned} &a(\boldsymbol{u} - S_h^{\boldsymbol{u}}\boldsymbol{u}, \boldsymbol{\varphi} - \boldsymbol{\varphi}_I) + b(\boldsymbol{u} - S_h^{\boldsymbol{u}}\boldsymbol{u}, \zeta - q_h) + b(\boldsymbol{\varphi} - \boldsymbol{\varphi}_I, S_h^p p - p) \\ &\qquad + \sum_{K\in\mathcal{T}_h} \big(a_h^K(S_h^{\boldsymbol{u}}\boldsymbol{u} - \boldsymbol{u}_\pi, \boldsymbol{\varphi}_I - \boldsymbol{\varphi}_\pi) - a^K(S_h^{\boldsymbol{u}}\boldsymbol{u} - \boldsymbol{u}_\pi, \boldsymbol{\varphi}_I - \boldsymbol{\varphi}_\pi)\big) \\ &\leq Ch^2\big(|\boldsymbol{u}|_{2,\Omega} + |p|_{1,\Omega}\big)(|\boldsymbol{\varphi}|_{2,\Omega} + |\zeta|_{1,\Omega}). \end{aligned}$$

Finally the bound (2.3.15) concludes the estimates (2.3.11). □

Next we define the L^2 projection P_h: $[L^2(\Omega)]^2 \to \mathbf{V}_h$ such that

$$m_h(P_h\boldsymbol{v}, \boldsymbol{v}_h) = m(\boldsymbol{v}, \boldsymbol{v}_h) \quad \forall \boldsymbol{v}_h \in \mathbf{V}_h, \tag{2.3.16}$$

which has the following estimates.

Lemma 2.11. *There exists a constant C independent of h such that*

$$\|\boldsymbol{v} - P_h\boldsymbol{v}\|_{0,\Omega} \leq Ch^2|\boldsymbol{v}|_{2,\Omega}. \tag{2.3.17}$$

Proof. We can write $\boldsymbol{v} - P_h\boldsymbol{v} = (\boldsymbol{v} - \boldsymbol{v}_I) + (\boldsymbol{v}_I - P_h\boldsymbol{v})$ and then denote $\delta_h = P_h\boldsymbol{v} - \boldsymbol{v}_I$. Thus, an application of stability and consistency of $m_h(\cdot,\cdot)$ together with (2.3.1) and (2.3.16) yields

$$\begin{aligned} C\|P_h\boldsymbol{v} - \boldsymbol{v}_I\|^2_{0,\Omega} &\leq m(\boldsymbol{v}, \delta_h) - m_h(\boldsymbol{v}_I, \delta_h) \\ &= \sum_{K\in\mathcal{T}_h} \Big(m^K(\boldsymbol{v} - \boldsymbol{v}_\pi, \delta_h) - m_h^K(\boldsymbol{v}_I - \boldsymbol{v}_\pi, \delta_h) \Big) \leq Ch^2|\boldsymbol{v}|_{2,\Omega}\|\delta_h\|_{0,\Omega}. \end{aligned}$$

A use of triangle's inequality and the estimates given in (2.3.2) gives the L^2 estimates. □

2.3.1 H^1 estimate for velocity

We begin by introducing $\eta_h(t) := (P_h\boldsymbol{u} - \boldsymbol{u}_h)(t)$ and $\theta_h(t) := (S_h^{\boldsymbol{u}}\boldsymbol{u} - \boldsymbol{u}_h)(t)$, and prove the following lemma that plays a crucial role in establishing the optimal error estimates for the velocity in H^1- norm which will be given by our main Theorem 2.1.

Lemma 2.12. *Let $\boldsymbol{u}(t)$ and $\boldsymbol{u}_h(t)$ be the solution of* (2.1.1) *and* (2.2.4) *respectively for each $t \in (0, T]$, then there exists a positive constant C independent of h such that*

$$\begin{aligned} &\|(\boldsymbol{u} - \boldsymbol{u}_h)(t)\|^2_{0,\Omega} + \nu \int_0^t |(\boldsymbol{u} - \boldsymbol{u}_h)(s)|^2_{1,\Omega}\, ds \\ &\quad \leq Ch^2 \left(1 + |\boldsymbol{u}_0|^2_{2,\Omega} + \int_0^t |\boldsymbol{f}(s)|^2_{1,\Omega}\, ds \right). \end{aligned} \tag{2.3.18}$$

Proof. Writing the error equation in terms of η_h with the use of (2.3.16), (2.2.4a) and (2.1.1a) gives

$$\begin{aligned} m_h(\partial_t\eta_h, \boldsymbol{v}_h) + a_h(\eta_h, \boldsymbol{v}_h) =& (F - F_h)(\boldsymbol{v}_h) + (a_h(P_h\boldsymbol{u}, \boldsymbol{v}_h) - a(\boldsymbol{u}, \boldsymbol{v}_h)) \\ & - b(\boldsymbol{v}_h, p - p_h). \end{aligned} \tag{2.3.19}$$

Taking $\boldsymbol{v}_h = \theta_h$ in (2.3.19) and from (2.3.10b) and (2.2.4b), we note that

$$b(\theta_h, q_h) = 0 \qquad \forall q_h \in Q_h, \tag{2.3.20}$$

then using (2.3.10a), we get

$$\begin{aligned} m_h(\partial_t \eta_h, \theta_h) + a_h(\eta_h, \theta_h) &= (a_h(P_h\boldsymbol{u}, \theta_h) - a(\boldsymbol{u}, \theta_h)) + (F - F_h)(\theta_h) - b(\theta_h, p - S_h^p p) \\ &= a_h(\eta_h - \theta_h, \theta_h) + (F - F_h)(\theta_h). \end{aligned}$$

From (2.3.16), we obtain

$$\begin{aligned} m_h(\partial_t \eta_h, \eta_h) + a_h(\theta_h, \theta_h) &= m_h(\partial_t \eta_h, \eta_h - \theta_h) + (F - F_h)(\theta_h) \\ &= \big(m(\partial_t \boldsymbol{u}, \eta_h - \theta_h) - m_h(\partial_t \boldsymbol{u}_h, \eta_h - \theta_h)\big) \\ &\quad + (F - F_h)(\theta_h). \end{aligned} \tag{2.3.21}$$

The bounds of $m_h(\cdot,\cdot)$, $a_h(\cdot,\cdot)$ along with the polynomial approximation $\boldsymbol{u}_\pi$, consistency of $a_h(\cdot,\cdot)$ in (2.3.21), and a use of Poincaré and Young's inequalities infer that

$$\begin{aligned} \frac{1}{2}\frac{d}{dt}\|\eta_h\|_{0,\Omega}^2 + \nu|\theta_h|_{1,\Omega}^2 &\lesssim m_h(\partial_t \eta_h, \eta_h) + a_h(\theta_h, \theta_h) \\ &\leq Ch^2((\|\partial_t \boldsymbol{u}\|_{0,\Omega} + \|\partial_t \boldsymbol{u}_h\|_{0,\Omega})|\boldsymbol{u}|_{2,\Omega} + |\boldsymbol{f}|_{1,\Omega}^2) + \frac{\nu}{2}\,|\theta_h|_{1,\Omega}^2. \end{aligned}$$

Integrating from 0 to t, and using the bounds (2.1.3) and (2.2.6) implies

$$\|\eta_h(t)\|_{0,\Omega}^2 + \nu \int_0^t |\theta_h(s)|_{1,\Omega}^2 \,\mathrm{d}s \leq \|\eta_h(0)\|_{0,\Omega}^2 + Ch^2\left(1 + \int_0^t |\boldsymbol{f}(s)|_{1,\Omega}^2 \,\mathrm{d}s\right).$$

Choose $\boldsymbol{u}_h(0) = P_h\boldsymbol{u}(0)$ then triangle inequality together with Lemma 2.11 and Lemma 2.10 implies (2.3.18). □

Theorem 2.1. *Let $\boldsymbol{u}(t)$ and $\boldsymbol{u}_h(t)$ be the solutions of continuous problem* (2.1.1) *and semi-discrete problem* (2.2.4) *respectively for each $t \in (0, T]$. Then, there exists a positive constant C independent of h such that*

$$\begin{aligned} \sigma(t)|(\boldsymbol{u} - \boldsymbol{u}_h)(t)|_{1,\Omega}^2 &+ \int_0^t \sigma(s)\|\partial_t(\boldsymbol{u} - \boldsymbol{u}_h)(s)\|_{0,\Omega}^2 \\ &\leq Ch^2\Big(1 + |\boldsymbol{u}_0|_{2,\Omega}^2 + \int_0^t (1 + \sigma(s)\ h^2)|\boldsymbol{f}(s)|_{1,\Omega}^2\, ds\Big). \end{aligned} \tag{2.3.22}$$

Proof. Writing the error equation in terms of θ_h using equations (2.1.1a), (2.2.4a) and (2.3.10a), we get

$$\begin{aligned} m_h(\partial_t\theta_h, \boldsymbol{v}_h) + a_h(\theta_h, \boldsymbol{v}_h) &= (m_h(\partial_t S_h\boldsymbol{u}, \boldsymbol{v}_h) - m(\partial_t\boldsymbol{u}, \boldsymbol{v}_h)) \\ &\quad + (F - F_h)(\boldsymbol{v}_h) + b(v_h, p_h - S_h^p p). \end{aligned} \tag{2.3.23}$$

Taking the test function $\boldsymbol{v}_h = \partial_t\theta_h$ in (2.3.23) then the stability of bilinear forms $m_h(\cdot,\cdot)$, $a_h(\cdot,\cdot)$, equation (2.3.20) and consistency of $m_h(\cdot,\cdot)$ gives

$$\begin{aligned} \|\partial_t\theta_h\|_{0,\Omega}^2 + \frac{\nu}{2}\frac{d}{dt}|\theta_h|_{1,\Omega}^2 &\lesssim m_h(\partial_t\theta_h, \partial_t\theta_h) + a_h(\theta_h, \partial_t\theta_h) \\ &= (m_h(\partial_t S_h^{\boldsymbol{u}}\boldsymbol{u}, \partial_t\theta_h) - m(\partial_t\boldsymbol{u}, \partial_t\theta_h)) + (F - F_h)(\partial_t\theta_h) \\ &= \sum_{K\in\mathcal{T}_h} (m_h^K(\partial_t(S_h^{\boldsymbol{u}}\boldsymbol{u} - \boldsymbol{\Pi}_K^{\boldsymbol{0}}\boldsymbol{u}), \partial_t\theta_h) - m^K(\partial_t(\mathbf{I} - \boldsymbol{\Pi}_K^{\boldsymbol{0}})\boldsymbol{u}, \partial_t\theta_h)) \\ &\qquad + (F - F_h)(\partial_t\theta_h) \\ &\leq Ch^4(|\partial_t\boldsymbol{u}|_{2,\Omega}^2 + |\partial_t p|_{1,\Omega}^2 + |\boldsymbol{f}|_{1,\Omega}^2) + \frac{1}{2}\|\partial_t\theta_h\|_{0,\Omega}^2. \end{aligned}$$

Multiplying by $\sigma(t)$, we arrive at

$$\sigma(t)\|\partial_t\theta_h\|_{0,\Omega}^2 + \nu\frac{d}{dt}\Big(\sigma(t)|\theta_h|_{1,\Omega}^2\Big) \leq \nu|\theta_h|_{1,\Omega}^2 + C\sigma(t)h^4(|\partial_t\boldsymbol{u}|_{2,\Omega}^2 + |\partial_t p|_{1,\Omega}^2 + |\boldsymbol{f}|_{1,\Omega}^2).$$

Integrating now from 0 to t and use of bounds (2.1.4) imply

$$\begin{aligned} &\nu\ \sigma(t)|\theta_h(t)|_{1,\Omega}^2 + \int_0^t \sigma(s)\|\partial_t\theta_h(s)\|_{0,\Omega}^2\,\mathrm{d}s \\ &\qquad \leq Ch^4 + \int_0^t \big(\nu|\theta_h(s)|_{1,\Omega}^2 + Ch^4\sigma(s)|\boldsymbol{f}(s)|_{1,\Omega}^2\big)\,\mathrm{d}s. \end{aligned} \tag{2.3.24}$$

An application of triangle's inequality and Lemma 2.12 give the bound for second term on right hand side of (2.3.24) as,

$$\nu\int_0^t |\theta_h(s)|_{1,\Omega}^2\,\mathrm{d}s \leq \|\eta_h(0)\|_{0,\Omega}^2 + Ch^2\left(1 + \int_0^t |\boldsymbol{f}(s)|_{1,\Omega}^2\,\mathrm{d}s\right).$$

Therefore, the use of bounds (2.3.11) and (2.3.24) yield the required bound (2.3.22). $\square$

2.3.2 L^2 estimate for pressure and velocity

We start by proving the two essential results given below in Lemmas 2.13 and 2.14 which will be helpful in deriving optimal error estimates for pressure and velocity in the L^2 norm with minimum regularity.

Lemma 2.13. *Let* $\boldsymbol{u}$ *and* $\boldsymbol{u}_h$ *are the solutions of continuous problem* (2.1.1) *and semi-discrete problem* (2.2.4), *respectively. Then, we have*

$$\begin{aligned}\sigma^2(t)\|\partial_t(\boldsymbol{u}-\boldsymbol{u}_h)(t)\|^2_{0,\Omega} &+ \nu\int_0^t \sigma^2(s)|\partial_t(\boldsymbol{u}-\boldsymbol{u}_h)(s)|^2_{1,\Omega}\,ds \\ &\le Ch^2\Big(1+|\boldsymbol{u}_0|^2_{2,\Omega}+\int_0^t \big((1+\sigma(s)\ h^2)|\boldsymbol{f}(s)|^2_{1,\Omega}+\sigma^2(s)|\partial_t\boldsymbol{f}(s)|^2_{1,\Omega}\big)\,ds\Big).\end{aligned} \tag{2.3.25}$$

where C *is a positive constant independent of* h.

Proof. Differentiating the error equation (2.3.19) with respect to time and taking $\boldsymbol{v}_h = \partial_t\theta_h$, we obtain (similar to (2.3.21))

$$\begin{aligned}m_h(\partial_{tt}\eta_h,\partial_t\eta_h)+a_h(\partial_t\theta_h,\partial_t\theta_h) = \big(m(\partial_{tt}\boldsymbol{u},\partial_t(\eta_h-\theta_h)) - m_h(\partial_{tt}\boldsymbol{u}_h,\partial_t(\eta_h-\theta_h))\big) \\ + (\partial_t\boldsymbol{f}-\partial_t\boldsymbol{f}_h,\partial_t\theta_h).\end{aligned}$$

The stability of the discrete bilinear forms and (2.3.20) implies

$$\begin{aligned}\frac{1}{2}\frac{d}{dt}\|\partial_t\eta_h\|^2_{0,\Omega} &+ \nu|\partial_t\theta_h|^2_{1,\Omega} \\ &\le Ch|\partial_t\boldsymbol{f}|_{1,\Omega}\|\partial_t\theta_h\|_{0,\Omega}+Ch^2(\|\partial_{tt}\boldsymbol{u}\|_{0,\Omega}+\|\partial_{tt}\boldsymbol{u}_h\|_{0,\Omega})|\partial_t\boldsymbol{u}|_{2,\Omega} \\ &\le Ch^2(|\partial_t\boldsymbol{f}|^2_{1,\Omega}+|\partial_t\boldsymbol{u}|^2_{2,\Omega}+\|\partial_{tt}\boldsymbol{u}\|^2_{0,\Omega}+\|\partial_{tt}\boldsymbol{u}_h\|^2_{0,\Omega})+\frac{\nu}{2}|\partial_t\theta_h|^2_{1,\Omega}.\end{aligned}$$

Multiplying the above bound with $\sigma^2(t)$ to get

$$\begin{aligned}\frac{d}{dt}\big(\sigma^2(t)\|\partial_t\eta_h\|^2_{0,\Omega}\big) &+ \nu\,\sigma^2(t)|\partial_t\theta_h|^2_{1,\Omega} \\ &\le \sigma(t)\|\partial_t\eta_h\|^2_{0,\Omega}+Ch^2\sigma^2(t)\big(|\partial_t\boldsymbol{f}|^2_{1,\Omega}+|\partial_t\boldsymbol{u}|^2_{2,\Omega}+\|\partial_{tt}\boldsymbol{u}\|^2_{0,\Omega}+\|\partial_{tt}\boldsymbol{u}_h\|^2_{0,\Omega}\big).\end{aligned}$$

Integrating the above equation for time from 0 to t then using Theorem 2.1 together with regularity results from Lemma 2.1 and 2.6, and the triangle's inequality to deduce the desired result (2.3.25). □

Lemma 2.14. *The solutions $\boldsymbol{u}$ and $\boldsymbol{u}_h$ of (2.1.1) and (2.2.4) satisfies*

$$\int_0^T \|(\boldsymbol{u}-\boldsymbol{u}_h)(t)\|_{0,\Omega}^2 \; dt \leq Ch^4\Big(1+|\boldsymbol{u}_0|_{2,\Omega}^2+\int_0^T |\boldsymbol{f}(s)|_{1,\Omega}^2 \, ds\Big),$$

where C is positive constant independent of h.

Proof. We consider the following backward in time dual problem: Find $\boldsymbol{\phi}(t) \in \mathbf{V}$ and $\psi(t) \in Q$ for each $t \in (0, T]$ such that

$$m(\boldsymbol{v}, \partial_t \boldsymbol{\phi}) - a(\boldsymbol{v}, \boldsymbol{\phi}) - b(\boldsymbol{v}, \psi) = (\boldsymbol{u}-\boldsymbol{u}_h, \boldsymbol{v}) \qquad \forall \boldsymbol{v} \in \mathbf{V}, \tag{2.3.26a}$$

$$b(\boldsymbol{\phi}, q) = 0 \qquad \forall q \in Q. \tag{2.3.26b}$$

with $\boldsymbol{\phi}(T) = 0$ a.e. in Ω. We note that the problem (2.3.26) has a unique solution $(\boldsymbol{\phi}, \psi) \in \mathbf{V} \times Q$ and satisfies (see [112] for more details)

$$\begin{aligned}\max_{0\leq t\leq T} |\boldsymbol{\phi}(t)|_{1,\Omega}^2 + \int_0^T (|\boldsymbol{\phi}(t)|_{2,\Omega}^2 + \|\psi(t)\|_{1,\Omega}^2 + \|\partial_t \boldsymbol{\phi}(t)\|_{0,\Omega}^2)\,\mathrm{d}t \\ \leq C\int_0^T \|(\boldsymbol{u}-\boldsymbol{u}_h)(t)\|_{0,\Omega}^2\,\mathrm{d}t.\end{aligned} \tag{2.3.27}$$

Taking $\boldsymbol{v} = \boldsymbol{u} - \boldsymbol{u}_h$ in (2.3.26a) gives

$$\|\boldsymbol{u}-\boldsymbol{u}_h\|_{0,\Omega}^2 = m(\boldsymbol{u}-\boldsymbol{u}_h, \partial_t\boldsymbol{\phi}) - a(\boldsymbol{u}-\boldsymbol{u}_h, \boldsymbol{\phi}) - b(\boldsymbol{u}-\boldsymbol{u}_h, \psi).$$

The use of interpolants $\boldsymbol{\phi}_I$ and ψ_I give

$$\begin{aligned}\|\boldsymbol{u}-\boldsymbol{u}_h\|_{0,\Omega}^2 = \frac{d}{dt}m(\boldsymbol{u}-\boldsymbol{u}_h, \boldsymbol{\phi}) - \Big(&m(\partial_t(\boldsymbol{u}-\boldsymbol{u}_h), \boldsymbol{\phi}) + a(\boldsymbol{u}-\boldsymbol{u}_h, \boldsymbol{\phi}-\boldsymbol{\phi}_I) \\ &+ b(\boldsymbol{u}-\boldsymbol{u}_h, \psi-\psi_I) + a(\boldsymbol{u}-\boldsymbol{u}_h, \boldsymbol{\phi}_I) + b(\boldsymbol{u}-\boldsymbol{u}_h, \psi_I)\Big).\end{aligned}$$

The equations (2.1.1b), (2.2.4b) gives $b(\boldsymbol{u}-\boldsymbol{u}_h, q_h) = 0$, for all $q_h \in Q_h$ as $\mathbf{V}_h \subset \mathbf{V}$. Then the use of the equations (2.1.1) and (2.2.4) leads to

$$\begin{aligned}\|\boldsymbol{u}-\boldsymbol{u}_h\|_{0,\Omega}^2 &= \frac{d}{dt}m(\boldsymbol{u}-\boldsymbol{u}_h, \boldsymbol{\phi}) - \Big(m(\partial_t(\boldsymbol{u}-\boldsymbol{u}_h), \boldsymbol{\phi}-\boldsymbol{\phi}_I) + m(\partial_t\boldsymbol{u}, \boldsymbol{\phi}_I) \\ &\qquad + a(\boldsymbol{u}-\boldsymbol{u}_h, \boldsymbol{\phi}-\boldsymbol{\phi}_I) + b(\boldsymbol{u}-\boldsymbol{u}_h, \psi-\psi_I) + a(\boldsymbol{u}, \boldsymbol{\phi}_I)\Big) \\ &\qquad + (m(\partial_t\boldsymbol{u}_h, \boldsymbol{\phi}_I) + a(\boldsymbol{u}_h, \boldsymbol{\phi}_I)) \\ &= \frac{d}{dt}m(\boldsymbol{u}-\boldsymbol{u}_h, \boldsymbol{\phi}) - (F-F_h)(\boldsymbol{\phi}_I) - \Big(m(\partial_t(\boldsymbol{u}-\boldsymbol{u}_h), \boldsymbol{\phi}-\boldsymbol{\phi}_I)\end{aligned}$$

$$
\begin{aligned}
&+ a(\boldsymbol{u}-\boldsymbol{u}_h,\boldsymbol{\phi}-\boldsymbol{\phi}_I) + b(\boldsymbol{u}-\boldsymbol{u}_h,\psi-\psi_I)\Big)\\
&+ (m(\partial_t\boldsymbol{u}_h,\boldsymbol{\phi}_I) - m_h(\partial_t\boldsymbol{u}_h,\boldsymbol{\phi}_I))\\
&+ (a(\boldsymbol{u}_h,\boldsymbol{\phi}_I) - a_h(\boldsymbol{u}_h,\boldsymbol{\phi}_I)).
\end{aligned}
$$

Integrating in time from 0 to T and use of $\phi(T)=0$, we end up with

$$
\begin{aligned}
\|E_{\boldsymbol{u}}\|_{0,\Omega}^2 &:= \int_0^T \|(\boldsymbol{u}-\boldsymbol{u}_h)(s)\|_{0,\Omega}^2\,\mathrm{d}s\\
&= -\underbrace{m((\boldsymbol{u}-\boldsymbol{u}_h)(0),\boldsymbol{\phi}(0))}_{:=T_1} - \underbrace{\int_0^T m(\partial_t(\boldsymbol{u}-\boldsymbol{u}_h),\boldsymbol{\phi}-\boldsymbol{\phi}_I)\,\mathrm{d}s}_{:=T_2}\\
&\quad -\underbrace{\int_0^T (a(\boldsymbol{u}-\boldsymbol{u}_h,\boldsymbol{\phi}-\boldsymbol{\phi}_I) + b(\boldsymbol{u}-\boldsymbol{u}_h,\psi-\psi_I) + (F-F_h)(\boldsymbol{\phi}_I))\,\mathrm{d}s}_{:=T_3}\\
&\quad +\underbrace{\int_0^T \Big(((m(\partial_t\boldsymbol{u}_h,\boldsymbol{\phi}_I) - m_h(\partial_t\boldsymbol{u}_h,\boldsymbol{\phi}_I)) + (a(\boldsymbol{u}_h,\boldsymbol{\phi}_I) - a_h(\boldsymbol{u}_h,\boldsymbol{\phi}_I))\Big)\,\mathrm{d}s}_{:=T_4}.
\end{aligned}
$$

Take $\boldsymbol{u}_h(0) = S_h^{\boldsymbol{u}}\boldsymbol{u}_0$ in term T_1 and regularity (2.3.27) implies

$$
T_1 \le Ch^2|\boldsymbol{u}_0|_{2,\Omega}\|\boldsymbol{\phi}(0)\|_{0,\Omega} \le Ch^2|\boldsymbol{u}_0|_{2,\Omega}\ \|E_{\boldsymbol{u}}\|_{0,\Omega}.
$$

Use of Cauchy-Schwarz and triangle's inequalities along with the bounds (2.1.3) and (2.2.6), an application of Lemma 2.8 and regularity result (2.3.27) gives

$$
\begin{aligned}
T_2 &\le C\int_0^T (\|\partial_t\boldsymbol{u}\|_{0,\Omega} + \|\partial_t\boldsymbol{u}_h\|_{0,\Omega})\|\boldsymbol{\phi}-\boldsymbol{\phi}_I\|_{0,\Omega}\,\mathrm{d}s \le Ch^2\Big(\int_0^T |\boldsymbol{\phi}(s)|_{2,\Omega}^2\,\mathrm{d}s\Big)^{1/2}\\
&\le C\ h^2\|E_{\boldsymbol{u}}\|_{0,\Omega}.
\end{aligned}
$$

Use of Cauchy-Schwarz inequality, (2.3.18), interpolant estimates for $\boldsymbol{\phi}$ and ψ, (2.1.2), (2.1.3) and (2.3.27) implies

$$
\begin{aligned}
T_3 &\le C\Big(\int_0^T |(\boldsymbol{u}-\boldsymbol{u}_h)(s)|_{1,\Omega}^2\,\mathrm{d}s\Big)^{1/2}\Big(\int_0^T (|(\boldsymbol{\phi}-\boldsymbol{\phi}_I)(s)|_{1,\Omega}^2 + \|(\psi-\psi_I)(s)\|_{0,\Omega}^2)\,\mathrm{d}s\Big)^{1/2}\\
&\qquad + Ch^2\int_0^T |\boldsymbol{f}(s)|_{1,\Omega}|\boldsymbol{\phi}(s)|_{1,\Omega}\,\mathrm{d}s\\
&\le Ch^2\left(1 + |\boldsymbol{u}_0|_{2,\Omega}^2 + \int_0^T |\boldsymbol{f}(s)|_{1,\Omega}^2\,\mathrm{d}s\right)^{1/2}\|E_{\boldsymbol{u}}\|_{0,\Omega}.
\end{aligned}
$$

Employing the consistency of bilinear forms $m_h(\cdot,\cdot)$, $a_h(\cdot,\cdot)$ together with Cauchy-Schwarz inequality, (2.3.18), (2.1.3), (2.2.5) and (2.3.27), we easily obtain

$$\begin{aligned}T_4 = \sum_{K\in\mathcal{T}_h}\int_0^T \Big(& m^K(\partial_t\boldsymbol{u}_h, \boldsymbol{\phi}_I - \Pi_K^0\boldsymbol{\phi}) - m_h^K(\partial_t\boldsymbol{u}_h, \boldsymbol{\phi}_I - \Pi_K^0\boldsymbol{\phi}) \\ &+ a^K(\boldsymbol{u}_h - \Pi_K^0\boldsymbol{u}, \boldsymbol{\phi}_I - \Pi_K^0\boldsymbol{\phi}) - a_h^K(\boldsymbol{u}_h - \Pi_K^0\boldsymbol{u}, \boldsymbol{\phi}_I - \Pi_K^0\boldsymbol{\phi})\Big)\,\mathrm{d}s \\ \le C\, h^2 &\left(1 + |\boldsymbol{u}_0|_{2,\Omega}^2 + \int_0^T |\boldsymbol{f}(s)|_{1,\Omega}^2\,\mathrm{d}s\right)^{1/2} \|E_{\boldsymbol{u}}\|_{0,\Omega}.\end{aligned}$$

Now combining the bounds of T_i, we complete the rest of the proof. □

Above results enable us to prove the L^2 estimates for pressure and velocity. First we develop the estimates for pressure and then proceed for velocity.

Theorem 2.2. *Let p and p_h be the solutions of* (2.1.1) *and* (2.2.4)*. Then there exists a positive constant C independent of h such that*

$$\sigma^2(t)\|(p-p_h)(t)\|_{0,\Omega}^2 \le Ch^2\left(1+\sigma^2(t)|\boldsymbol{f}|_{1,\Omega}^2\right).$$

Proof. Split the pressure error in terms of Stokes projection as

$$p - p_h = (p - S_h^p p) + (S_h^p p - p_h).$$

The inf-sup condition $b(\cdot,\cdot)$ on $\mathbf{V}_h$ gives

$$\beta_h\|S_h^p p - p_h\|_{0,\Omega} \le \sup_{\boldsymbol{v}_h\in\mathbf{V}_h\setminus\{0\}} \frac{b(\boldsymbol{v}_h, S_h^p p - p_h)}{|\boldsymbol{v}_h|_{1,\Omega}}, \tag{2.3.28}$$

where (2.1.1) and (2.2.4) gives

$$\begin{aligned}b(\boldsymbol{v}_h, S_h^p p - p_h) &= b(\boldsymbol{v}_h, S_h^p p - p) + b(\boldsymbol{v}_h, p - p_h) \\ &= b(\boldsymbol{v}_h, S_h^p p - p) + (F - F_h)(\boldsymbol{v}_h) + (m_h(\partial_t\boldsymbol{u}_h, \boldsymbol{v}_h) - m(\partial_t\boldsymbol{u}, \boldsymbol{v}_h)) \\ &\quad + (a_h(\boldsymbol{u}_h, \boldsymbol{v}_h) - a(\boldsymbol{u}, \boldsymbol{v}_h)).\end{aligned}$$

In view of the definitions of L^2 projection P_h (given in (2.3.16)) and Stokes projection $S_h^{\boldsymbol{u}}$ (given in (2.3.10)) together with their estimates (2.3.17) and (2.3.11), we infer that

$$b(\boldsymbol{v}_h, S_h^p p - p_h) = b(\boldsymbol{v}_h, S_h^p p - p) + (F - F_h)(\boldsymbol{v}_h) + m_h(\partial_t\boldsymbol{u}_h - \partial_t P_h\boldsymbol{u}, \boldsymbol{v}_h)$$

$$
\begin{aligned}
&+ (a_h(\boldsymbol{u}_h - S_h^{\boldsymbol{u}}\boldsymbol{u}, \boldsymbol{v}_h) - a(\boldsymbol{u} - S_h^{\boldsymbol{u}}\boldsymbol{u}, \boldsymbol{v}_h)) \\
\le\, & Ch(|p|_{1,\Omega} + |\boldsymbol{u}|_{2,\Omega} + |\boldsymbol{f}|_{1,\Omega})\|\boldsymbol{v}_h\|_{1,\Omega} \\
&+ (|\boldsymbol{u} - \boldsymbol{u}_h|_{1,\Omega} + |\boldsymbol{u} - S_h^{\boldsymbol{u}}\boldsymbol{u}|_{1,\Omega})|\boldsymbol{v}_h|_{1,\Omega} \\
&+ (\|\partial_t \boldsymbol{u} - \partial_t \boldsymbol{u}_h\|_{0,\Omega} + \|\partial_t \boldsymbol{u} - \partial_t P_h \boldsymbol{u}\|_{0,\Omega})\|\boldsymbol{v}_h\|_{0,\Omega}. \qquad (2.3.29)
\end{aligned}
$$

Multiply the inequality (2.3.29) with $\sigma(t)$, using Lemma 2.13 and (2.3.28) to arrive at

$$
\begin{aligned}
\sigma(t)\|(S_h^p p - p_h)(t)\|_{0,\Omega} &\le Ch\big(1 + \sigma(t)\big(|\boldsymbol{u}|_{2,\Omega} + |p|_{1,\Omega} + |\boldsymbol{f}|_{1,\Omega} + |\partial_t \boldsymbol{u}|_{2,\Omega} + |\partial_t p|_{1,\Omega}\big)\big) \\
&\le Ch(1 + \sigma(t)|\boldsymbol{f}|_{1,\Omega}).
\end{aligned}
$$

Finally, the triangle's inequality, use of (2.3.11), and above bound yields the required estimate. □

Theorem 2.3. *Let $\boldsymbol{u}$ and $\boldsymbol{u}_h$ be solutions of* (2.1.1) *and* (2.2.4)*, respectively. Then there exists a positive constant independent of h such that*

$$
\sigma(t)\|(\boldsymbol{u} - \boldsymbol{u}_h)(t)\|_{0,\Omega}^2 \le Ch^4\Big(1 + |\boldsymbol{u}_0|_{2,\Omega}^2 + \int_0^T (1 + \sigma(s))|\boldsymbol{f}(s)|_{1,\Omega}^2\, ds\Big). \qquad (2.3.30)
$$

Proof. Consider the error equation (2.3.23) in terms of the Stokes projection; and taking $\boldsymbol{v}_h = \theta_h$ with use of property (2.3.20) implies

$$
m_h(\partial_t \theta_h, \theta_h) + a_h(\theta_h, \theta_h) = (m_h(\partial_t S_h^{\boldsymbol{u}}\boldsymbol{u} - \partial_t P_h \boldsymbol{u}, \theta_h)) + (F - F_h)(\theta_h).
$$

Using (2.3.16) then the Cauchy-Schwarz and Young's inequalities together with the estimates of projection P_h (2.3.17) and (2.3.11) implies

$$
\begin{aligned}
\frac{1}{2}\frac{d}{dt}\|\theta_h\|_{0,\Omega}^2 + \nu|\theta_h|_{1,\Omega}^2 &\le (m_h(\partial_t S_h^{\boldsymbol{u}}\boldsymbol{u} - \partial_t P_h, \theta_h)) + (F - F_h)(\theta_h) \\
&\le Ch^4\big(|\partial_t \boldsymbol{u}|_{2,\Omega}^2 + |\partial_t p|_{1,\Omega}^2 + |\boldsymbol{f}|_{1,\Omega}^2\big) + \frac{1}{2}\|\theta_h\|_{0,\Omega}^2.
\end{aligned}
$$

Multiply with $\sigma(t)$ and get

$$
\begin{aligned}
&\frac{d}{dt}\big(\sigma(t)\|\theta_h\|_{0,\Omega}^2\big) + \nu\, \sigma(t)|\theta_h|_{1,\Omega}^2 \\
&\quad \le C\Big((1 + \sigma(t))\|\theta_h\|_{0,\Omega}^2 + \sigma(t)\ h^4(|\boldsymbol{f}|_{1,\Omega}^2 + |\partial_t \boldsymbol{u}|_{2,\Omega}^2 + |\partial_t p|_{1,\Omega}^2)\Big).
\end{aligned}
$$

Integrating the above bound from 0 to t and then the use of Lemma 2.14 and the regularity assumption (2.1.4) implies

$$\sigma(t)\|\theta_h(t)\|_{0,\Omega}^2 \,\mathrm{d}s \leq Ch^4\Big(1+|\boldsymbol{u}_0|_{2,\Omega}^2+\int_0^T (1+\sigma(s))|\boldsymbol{f}(s)|_{1,\Omega}^2 \,\mathrm{d}s\Big). \tag{2.3.31}$$

Thus the estimate (2.3.30) can be obtained from (2.3.11) and (2.3.31) with the help of triangle's inequality. □

2.3.3 Fully discrete error analysis

Following analogously to the semi-discrete scheme, in this section, we estimate the error that occurred through time discretization, i.e., by employing the backward Euler scheme for the approximation of time derivative. We proceed to collect the ingredients required to establish the convergence results stated in the main theorem (Theorem 2.4). Let Z be a Hilbert space, then for any function $\vartheta \in H^1(t_{n-1}, t_n; Z)$, we have the following integral formula,

$$\vartheta(t_n) - \frac{1}{\Delta t}\int_{t_{n-1}}^{t_n} \vartheta(s)\,\mathrm{d}s = \frac{1}{\Delta t}\int_{t_{n-1}}^{t_n} (s-t_{n-1})\partial_t\vartheta(s)\,\mathrm{d}s. \tag{2.3.32}$$

Integrating the equation (2.2.4a) from t_{n-1} to t_n, we have

$$\begin{aligned} m_h\Big(\delta_t\boldsymbol{u}_h(t_n), \boldsymbol{v}_h\Big) + \frac{1}{\Delta t}\int_{t_{n-1}}^{t_n} \big(a_h(\boldsymbol{u}_h(s), \boldsymbol{v}_h) + b(\boldsymbol{v}_h, p_h(s))\big)\,\mathrm{d}s& \\ = \frac{1}{\Delta t}\int_{t_{n-1}}^{t_n} (\boldsymbol{f}_h(s), \boldsymbol{v}_h)\,\mathrm{d}s;& \end{aligned} \tag{2.3.33}$$

And differentiating the equation (2.2.4a) with respect to time respectively gives

$$m_h(\partial_{tt}\boldsymbol{u}_h, \boldsymbol{v}_h) + a_h(\partial_t\boldsymbol{u}_h, \boldsymbol{v}_h) + b(\boldsymbol{v}_h, \partial_t p_h) = (\partial_t\boldsymbol{f}_h, \boldsymbol{v}_h). \tag{2.3.34}$$

Using the integral formula (2.3.32) and equation (2.3.34), we can rewrite the equation (2.3.33) as

$$\begin{aligned} m_h(\delta_t\boldsymbol{u}_h(t_n), \boldsymbol{v}_h) + a_h(\boldsymbol{u}_h(t_n), \boldsymbol{v}_h) + b(\boldsymbol{v}_h, p_h(t_n))& \\ = F_h^n(\boldsymbol{v}_h) - \frac{1}{\Delta t}\int_{t_{n-1}}^{t_n} (s-t_{n-1})m_h(\partial_{tt}\boldsymbol{u}_h(s), \boldsymbol{v}_h)\,\mathrm{d}s.& \end{aligned} \tag{2.3.35}$$

Denote the errors in time for velocity and pressure as $\boldsymbol{e}_{\boldsymbol{u}}^n = \boldsymbol{u}_h(t_n) - \boldsymbol{u}_h^n$ and $e_p^n = p_h(t_n) - p_h^n$, respectively then the error equation for time discretisation by subtracting (2.2.8) from (2.3.35) given as

$$\begin{aligned} m_h(\delta_t \boldsymbol{e}_{\boldsymbol{u}}^n, \boldsymbol{v}_h) + a_h(\boldsymbol{e}_{\boldsymbol{u}}^n, \boldsymbol{v}_h) + b(\boldsymbol{v}_h, e_p^n) \\ = -\frac{1}{\Delta t}\int_{t_{n-1}}^{t_n} (s - t_{n-1}) m_h(\partial_{tt}\boldsymbol{u}_h(s), \boldsymbol{v}_h)\,\mathrm{d}s. \end{aligned} \tag{2.3.36}$$

We would require the duality arguments (constructing the dual problem corresponding to (2.2.8)) for obtaining the desired L^2 estimates for velocity and pressure. We begin with introducing the dual problem as: For a given $\boldsymbol{z}_h^n \in \mathbf{V}_h$, find $(\boldsymbol{\phi}_h^{n-1}, \psi_h^{n-1}) \in \mathbf{V}_h \times Q_h$ such that

$$m_h(\boldsymbol{v}_h, \delta_t \boldsymbol{\phi}_h^n) - a_h(\boldsymbol{v}_h, \boldsymbol{\phi}_h^{n-1}) - b(\boldsymbol{v}_h, \psi_h^{n-1}) = (\boldsymbol{z}_h^n, \boldsymbol{v}_h) \qquad \forall \boldsymbol{v}_h \in \mathbf{V}_h, \tag{2.3.37a}$$

$$b(\boldsymbol{\phi}_h^{n-1}, q_h) = 0 \qquad \forall q_h \in Q_h. \tag{2.3.37b}$$

The above problem has a unique solution $(\boldsymbol{\phi}_h^{n-1}, \psi_h^{n-1}) \in \mathbf{V}_h \times Q_h$ and the solution satisfies (see [76])

$$\max_{1\le j\le N} |\boldsymbol{\phi}_h^j|_{1,\Omega}^2 \ + \ (\Delta t)\sum_{j=1}^{n-1}\left(\|\delta_t \boldsymbol{\phi}_h^j\|_{0,\Omega}^2 + \|\psi_h^j\|_{0,\Omega}^2\right) \ \le \ C\ (\Delta t)\sum_{j=1}^{n}\|\boldsymbol{z}_h^j\|_{0,\Omega}^2. \tag{2.3.38}$$

At this end, we prove the following results which will be used in deriving the optimal convergence rate.

Lemma 2.15. *Let $(\boldsymbol{u}_h(t_n), p_h(t_n)) \in \mathbf{V}_h \times Q_h$ and $(\boldsymbol{u}_h^n, p_h^n) \in \mathbf{V}_h \times Q_h$ be the solutions of semi-discrete problem* (2.2.4) *and fully discrete problem* (2.2.8) *respectively for each $n = 1, \ldots, N$. Then we have*

$$(\Delta t)\sum_{j=1}^{n}\|\boldsymbol{e}_{\boldsymbol{u}}^j\|_{0,\Omega}^2 \le C\ \Delta t^2, \tag{2.3.39}$$

where C is positive constant independent of the mesh parameters h and Δt.

Proof. Taking $\boldsymbol{v}_h = \boldsymbol{e}_{\boldsymbol{u}}^n$ in (2.3.37a) with $\boldsymbol{z}_h^n = \boldsymbol{e}_{\boldsymbol{u}}^n$ and also, $b(\boldsymbol{e}_{\boldsymbol{u}}^n, \psi_h^{n-1}) = 0$ from equations (2.2.8b) and (2.2.4b) gives

$$\|\boldsymbol{e}_{\boldsymbol{u}}^n\|_{0,\Omega}^2 = m_h(\boldsymbol{e}_{\boldsymbol{u}}^n, \delta_t \boldsymbol{\phi}_h^n) - a_h(\boldsymbol{e}_{\boldsymbol{u}}^n, \boldsymbol{\phi}_h^{n-1}). \tag{2.3.40}$$

Taking $\boldsymbol{v}_h = \boldsymbol{\phi}_h^{n-1}$ in (2.3.36); and $b(\boldsymbol{\phi}_h^{n-1}, e_p^n) = 0$ using (2.3.37b) yields

$$\begin{aligned} m_h(\delta_t \boldsymbol{e}_{\boldsymbol{u}}^n, \boldsymbol{\phi}_h^{n-1}) &+ a_h(\boldsymbol{e}_{\boldsymbol{u}}^n, \boldsymbol{\phi}_h^{n-1}) \\ &= -\frac{1}{\Delta t} \int_{t_{n-1}}^{t_n} (s - t_{n-1}) m_h(\partial_{tt} \boldsymbol{u}_h(s), \boldsymbol{\phi}_h^{n-1})\, \mathrm{d}s. \end{aligned} \tag{2.3.41}$$

Adding (2.3.40) and (2.3.41) then multiplying the resultant equation with Δt implies

$$\Delta t\, \|\boldsymbol{e}_{\boldsymbol{u}}^n\|_{0,\Omega}^2 = m_h(\boldsymbol{e}_{\boldsymbol{u}}^n, \boldsymbol{\phi}_h^n) - m_h(\boldsymbol{e}_{\boldsymbol{u}}^{n-1}, \boldsymbol{\phi}_h^{n-1}) + \int_{t_{n-1}}^{t_n} (s - t_{n-1}) m_h(\partial_{tt} \boldsymbol{u}_h(s), \boldsymbol{\phi}_h^{n-1})\, \mathrm{d}s.$$

Summing over n then using $\boldsymbol{e}_{\boldsymbol{u}}^0 = \boldsymbol{0}$, $\boldsymbol{\phi}_h^n = \boldsymbol{0}$ and the Cauchy Schwarz inequality gives

$$\begin{aligned} \Delta t \sum_{j=1}^n \|\boldsymbol{e}_{\boldsymbol{u}}^j\|_{0,\Omega}^2 &\leq C \sum_{j=1}^n \Big(\int_{t_{j-1}}^{t_j} (s - t_{j-1}) \|\partial_{tt} \boldsymbol{u}_h(s)\|_{0,\Omega}\, \mathrm{d}s \Big) \|\boldsymbol{\phi}_h^{j-1}\|_{0,\Omega} \\ &\leq C \sum_{j=1}^n \Big(\int_{t_{j-1}}^{t_j} \sigma(s) \|\partial_{tt} \boldsymbol{u}_h(s)\|_{0,\Omega}^2\, \mathrm{d}s \Big)^{1/2} \Big(\Delta t \int_{t_{j-1}}^{t_j} 1\, \mathrm{d}s \Big)^{1/2} \|\boldsymbol{\phi}_h^{j-1}\|_{0,\Omega} \\ &\leq C \Big((\Delta t) \int_0^{t_n} \sigma(s) \|\partial_{tt} \boldsymbol{u}_h(s)\|_{0,\Omega}^2\, \mathrm{d}s \Big)^{1/2} \Big((\Delta t) \sum_{j=1}^n \|\boldsymbol{\phi}_h^{j-1}\|_{0,\Omega}^2 \Big)^{1/2}. \end{aligned}$$

Then we obtain (2.3.39) from the bound (2.3.38) for each j and regularity result (2.1.4). □

Lemma 2.16. *Let $\boldsymbol{u}_h(t_n)$ and $\boldsymbol{u}_h^n$ be the solutions of the semi-discrete problem (2.2.4) and fully-discrete problem (2.2.8) respectively. Then there exists a positive constant C independent of the mesh parameters h and Δt such that*

$$\sigma(t_n) \|\boldsymbol{e}_{\boldsymbol{u}}^n\|_{0,\Omega}^2 + (\Delta t) \sum_{j=1}^n \big(\sigma(t_j) |\boldsymbol{e}_{\boldsymbol{u}}^j|_{1,\Omega}^2 \big) \leq C\ \Delta t^2. \tag{2.3.42}$$

Proof. Taking the test function $\boldsymbol{v}_h = \boldsymbol{e}_{\boldsymbol{u}}^n$ in (2.3.36) and using the stability of the bilinear forms $m_h(\cdot,\cdot), a_h(\cdot,\cdot)$ to infer

$$\frac{1}{2(\Delta t)} \Big(\|\boldsymbol{e}_{\boldsymbol{u}}^n\|_{0,\Omega}^2 - \|\boldsymbol{e}_{\boldsymbol{u}}^{n-1}\|_{0,\Omega}^2 \Big) + \nu |\boldsymbol{e}_{\boldsymbol{u}}^n|_{1,\Omega}^2 \lesssim \Big| -\frac{1}{\Delta t} \int_{t_{n-1}}^{t_n} (s - t_{n-1}) m_h(\partial_{tt} \boldsymbol{u}_h(s), \boldsymbol{e}_{\boldsymbol{u}}^n)\, \mathrm{d}s \Big|.$$

Using the Cauchy Schwarz and Young inequalities, we obtain

$$\frac{1}{\Delta t}\Big(\|\boldsymbol{e}_{\boldsymbol{u}}^n\|_{0,\Omega}^2 - \|\boldsymbol{e}_{\boldsymbol{u}}^{n-1}\|_{0,\Omega}^2\Big) + \nu|\boldsymbol{e}_{\boldsymbol{u}}^n|_{1,\Omega}^2 \le C\int_{t_{n-1}}^{t_n}(s-t_{n-1})\|\partial_{tt}\boldsymbol{u}_h(s)\|_{0,\Omega}^2\,\mathrm{d}s. \quad (2.3.43)$$

Multiply equation (2.3.43) with $(\sigma(t_n)\ \Delta t)$ and using $\sigma(t_n) \le \sigma(t_{n-1}) + \Delta t$ gives

$$\begin{aligned}\sigma(t_n)\|\boldsymbol{e}_{\boldsymbol{u}}^n\|_{0,\Omega}^2 - \sigma(t_{n-1})\|\boldsymbol{e}_{\boldsymbol{u}}^{n-1}\|_{0,\Omega}^2 + \nu\ \sigma(t_n)\ \Delta t\ |\boldsymbol{e}_{\boldsymbol{u}}^n|_{1,\Omega}^2&\\ \le \Delta t\|\boldsymbol{e}_{\boldsymbol{u}}^{n-1}\|_{0,\Omega}^2 + C\ \Delta t\int_{t_{n-1}}^{t_n}\sigma(s)\|\partial_{tt}\boldsymbol{u}_h(s)\|_{0,\Omega}^2\,\mathrm{d}s.&\end{aligned}$$

Summation over n leads to

$$\begin{aligned}\sigma(t_n)\|\boldsymbol{e}_{\boldsymbol{u}}^n\|_{0,\Omega}^2 + \nu\ \Delta t\sum_{j=1}^{n}\sigma(t_j)\ |\boldsymbol{e}_{\boldsymbol{u}}^j|_{1,\Omega}^2&\\ \le \Delta t\sum_{j=1}^{n}\|\boldsymbol{e}_{\boldsymbol{u}}^{j-1}\|_{0,\Omega}^2 + C\ \Delta t\int_{0}^{t_n}\sigma(s)\|\partial_{tt}\boldsymbol{u}_h(s)\|_{0,\Omega}^2\,\mathrm{d}s.&\end{aligned}$$

Thus the bound (2.3.39) given by previous lemma concludes the final result (2.3.42).

□

Lemma 2.17. *Let* $(\boldsymbol{u}_h, p_h) \in \mathbf{V}_h \times Q_h$ *and* $(\boldsymbol{u}_h^n, p_h^n) \in \mathbf{V}_h \times Q_h$ *be the solutions of the semi-discrete problem* (2.2.4) *and fully-discrete problem* (2.2.8) *respectively. Then the following holds*

$$\sigma(t_n)\|e_p^n\|_{0,\Omega} \le C\ \Delta t, \quad (2.3.44)$$

where C *is positive constant independent of the mesh parameters* h *and* Δt.

Proof. Consider the error equation (2.3.36), that is,

$$b(\boldsymbol{v}_h, e_p^n) = -\Big(m_h(\delta_t\boldsymbol{e}_{\boldsymbol{u}}^n, \boldsymbol{v}_h) + a_h(\boldsymbol{e}_{\boldsymbol{u}}^n, \boldsymbol{v}_h) + \frac{1}{\Delta t}\int_{t_{n-1}}^{t_n}(s-t_{n-1})m_h(\partial_{tt}\boldsymbol{u}_h(s), \boldsymbol{v}_h)\,\mathrm{d}s\Big).$$

Using discrete inf-sup condition of bilinear form $b(\cdot,\cdot)$ and multiplying with $\sigma(t_n)$ gives

$$\sigma(t_n)\|e_p^n\|_{0,\Omega}^2 \le C\sigma(t_n)\big(\|\delta_t\boldsymbol{e}_{\boldsymbol{u}}^n\|_{0,\Omega}^2 + \nu|\boldsymbol{e}_{\boldsymbol{u}}^n|_{1,\Omega}^2 + \int_{t_{n-1}}^{t_n}\sigma(s)\|\partial_{tt}\boldsymbol{u}_h(s)\|_{0,\Omega}^2\,\mathrm{d}s\big).$$

Summing over n followed with multiplying by Δt gives

$$\Delta t \sum_{j=1}^{n} \sigma(t_j)\|e_p^n\|_{0,\Omega}^2 \leq C\big(\Delta t \sum_{j=1}^{n} \sigma(t_j)\|\delta_t \boldsymbol{e}_{\boldsymbol{u}}^j\|_{0,\Omega}^2 + \nu \Delta t \sum_{j=1}^{n} \sigma(t_j)|\boldsymbol{e}_{\boldsymbol{u}}^j|_{1,\Omega}^2 + \Delta t^2 \int_0^{t_n} \sigma(s)\|\partial_{tt}\boldsymbol{u}_h(s)\|_{0,\Omega}^2 \,\mathrm{d}s\big). \tag{2.3.45}$$

We require here the estimates for term $(\Delta t)\sum_{j=1}^{n}\sigma(t_j)\|\delta_t \boldsymbol{e}_{\boldsymbol{u}}^n\|_{0,\Omega}^2$. Take $\boldsymbol{v}_h = \delta_t \boldsymbol{e}_{\boldsymbol{u}}^n$ in (2.3.36) and using the similar steps as followed in the proof of Lemma 2.16 leads to

$$\frac{\nu}{\Delta t}\Big(\|\nabla \boldsymbol{e}_{\boldsymbol{u}}^n\|_{0,\Omega}^2 - \|\nabla \boldsymbol{e}_{\boldsymbol{u}}^{n-1}\|_{0,\Omega}^2\Big) + \|\delta_t \boldsymbol{e}_{\boldsymbol{u}}^n\|_{0,\Omega}^2 \leq C \int_{t_{n-1}}^{t_n} (s - t_{n-1})\|\partial_{tt}\boldsymbol{u}_h(s)\|_{0,\Omega}^2 \,\mathrm{d}s.$$

Multiplying with $\sigma(t_n)$ and summing over n gives

$$(\Delta t)\sum_{j=1}^{n}\sigma(t_j)\|\delta_t \boldsymbol{e}_{\boldsymbol{u}}^n\|_{0,\Omega}^2 \leq C\Delta t^2. \tag{2.3.46}$$

Use of the bounds (2.3.46) and (2.3.42) in (2.3.45) implies (2.3.44). $\square$

Finally, an application of the triangle's inequality together with Theorems 2.1, 2.2 and 2.3, Lemmas 2.16 and 2.17 enable us to state the following main theorem.

Theorem 2.4. *Let $(\boldsymbol{u}(t_n), p(t_n)) \in \mathbf{V} \times Q$ and $(\boldsymbol{u}_h^n, p_h^n) \in \mathbf{V}_h \times Q_h$ be the solutions of the continuous problem* (2.1.1) *and fully discrete problem* (2.2.8) *respectively at time t_n for each $n = 1, \ldots, N$. Then there exists a positive constant C, independent of the mesh parameters h and Δt, such that*

$$\sigma(t_n)\|\boldsymbol{u}(t_n) - \boldsymbol{u}_h^n\|_{0,\Omega}^2 \leq C(h^4 + \Delta t^2),$$
$$\sigma^2(t_n)\|p(t_n) - p_h^n\|_{0,\Omega}^2 \leq C(h^2 + \Delta t^2).$$

Remark 2.2. *We stress that the convergence analysis can be easily extended to other divergences free and higher-order VE methods, i.e., $k \geq 2$ introduced in [30, 32]. However, in that case, one would require a higher regularity assumption on the continuous solution. Moreover, stabilized methods would also demand higher regularity on the continuous solution for achieving the optimal rate of convergence, for instance, it is seen in [114] that the lowest order approximation ($\mathbb{P}_1-\mathbb{P}_0$) with stabilization technique will require $\boldsymbol{u}_{ttt} \in \mathbf{L}^\infty(0,T;[L^2(\Omega)]^2)$ for deriving the error estimates.*

2.4 Numerical experiments

In this section, we present our numerical experiments to confirm the theoretical rate of convergence for pressure and velocity established in Section 2.3. In order to judge the computational efficiency and performance of the proposed VE discretization (applied for spatial variable), we have considered three different kinds of meshes: Distorted square $\mathcal{D}_h$, distorted hexagonal mesh $\mathcal{W}_h$ and non-convex mesh $\mathcal{N}_h$ in the square domain Ω_S demonstrated respectively in figures 2.2(a)- 2.2(c) (for more details, see [30]). For the time discretization, we have employed the backward Euler method, and report the convergence in time as well as spatial variables. In contrast with consistently stabilized methods, we have inferred through numerical tests that the present scheme yield stable pressure even with small time step. Moreover, we also perform the proposed scheme on the lid-driven cavity problem to see the real computational advantages of the proposed scheme. All the computations are done using MATLAB.

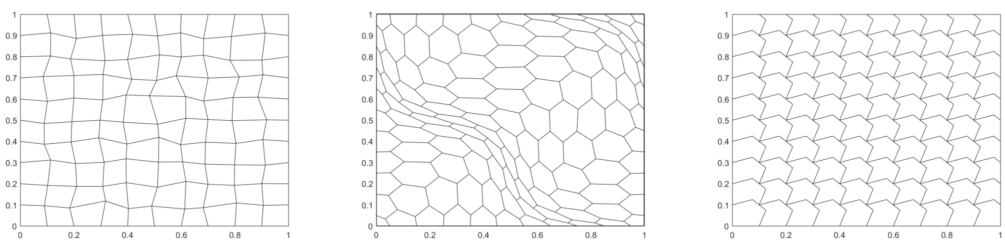

(a) (b) (c)

Figure 2.2: Samples of meshes employed for the numerical tests: (a) Concave mesh $\mathcal{N}_h$, (b) Distorted hexagonal $\mathcal{H}_h$, and (c) Distorted quadilateral $\mathcal{D}_h$ mesh.

The spatial error associated with velocity and pressure while refining the mesh are defined as:

$$E_0(\boldsymbol{u}) := \Big(\sum_{K \in \mathcal{T}_h} \|\boldsymbol{u}(T) - \boldsymbol{\Pi}_K^{\boldsymbol{0}} \boldsymbol{u}_h^N\|_{0,K}^2 \Big)^{1/2}, \quad E_1(\boldsymbol{u}) := \Big(\sum_{K \in \mathcal{T}_h} \|\boldsymbol{\nabla}(\boldsymbol{u}(T) - \boldsymbol{\Pi}_K^{\boldsymbol{\nabla}} \boldsymbol{u}_h^N)\|_{0,K}^2 \Big)^{1/2},$$
$$\text{and} \qquad E(p) := \sum_{K \in \mathcal{T}_h} \|p(T) - p_h^N\|_{0,K},$$

and the corresponding computed rate of convergence are given by

$$r_1(\boldsymbol{u}) = \frac{log(E_1(\boldsymbol{u})/\tilde{E}_1(\boldsymbol{u}))}{log(h/\tilde{h})}, \quad r_0(\boldsymbol{u}) = \frac{log(E_0(\boldsymbol{u})/\tilde{E}_0(\boldsymbol{u}))}{log(h/\tilde{h})}, \quad r(p) = \frac{log(E(p)/\tilde{E}(p))}{log(h/\tilde{h})}$$

where $E_1(\boldsymbol{u}), E_0(\boldsymbol{u}), E(p)$ and $\tilde{E}_1(\boldsymbol{u}), \tilde{E}_0(\boldsymbol{u}), \tilde{E}(p)$ are errors for the mesh size h and a finer mesh size $\tilde{h}$, respectively.

2.4.1 Convergence in space over a square domain

Over a domain $\Omega_S := (0,1)^2$, we consider the following problem motiviated by [29] for which we have analytical solution. Construct the load function $\boldsymbol{f}(\boldsymbol{x}, t)$ so that the exact velocity of the fluid flow and pressure are given as

$$
\begin{aligned}
p(\boldsymbol{x}, t) &= t\Big(xy^2 - \frac{1}{6}\Big), \\
\boldsymbol{u}(\boldsymbol{x}, t) &= t \begin{bmatrix} -cos(2\pi x) sin(2\pi y) + sin(2\pi y) \\ sin(2\pi x) cos(2\pi y) - sin(2\pi x) \end{bmatrix}.
\end{aligned}
$$

Now by fixing the time step $\Delta t = 0.001$ and final time $T = 1$, we report numerical convergence rate for non-convex mesh in the Table 2.1. Moreover, the computed order of convergence for all three meshes in Fig. 2.2 are depicted through log-log plot in Figure 2.3. From the Table 2.1 and Figure 2.3, we note that the computed rate of convergence for three different meshes are in agreement with theoretical rate of convergence.

Ndof	h^{-1}	$E_0(\boldsymbol{u})$	$r_0(\boldsymbol{u})$	$E_1(\boldsymbol{u})$	$r_1(\boldsymbol{u})$	$E(p)$	$r(p)$
218	4	0.2632	-	4.0577	-	0.3420	-
983	8	0.0583	2.18	2.0275	1.00	0.1968	0.80
4163	16	0.0161	1.86	1.0179	0.99	0.0658	1.60
17123	32	0.0051	1.66	0.5092	1.00	0.0196	1.75
69443	64	0.0012	2.06	0.2544	1.00	0.0061	1.70

Table 2.1: Computed errors and rate of convergence with varying mesh size h.

2.4.2 Convergence in time

To present the time convergence, we take given force $\boldsymbol{f}$ so that the exact velocity and pressure solutions are

$$
\begin{aligned}
\boldsymbol{u}(\boldsymbol{x}, t) &= (1 + t^5 + \exp^{-t/10} + \sin t) \begin{bmatrix} \sin(\pi x - 0.7) \sin(\pi y + 0.2) \\ \cos(\pi x - 0.7) \cos(\pi y + 0.2) \end{bmatrix}, \\
p(\boldsymbol{x}, t) &= (1 + t^5 + \exp^{-t/10} + \sin t)\Big(\sin(x)\cos(y) + (\cos(1) - 1)\sin(1)\Big),
\end{aligned}
$$

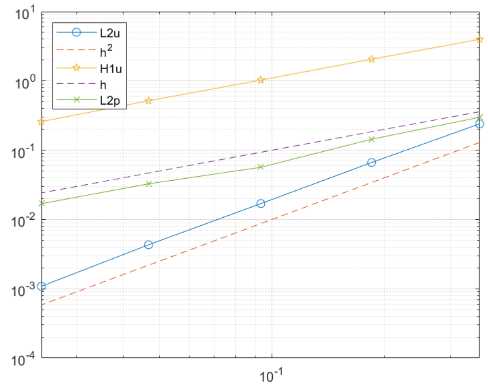

(a)

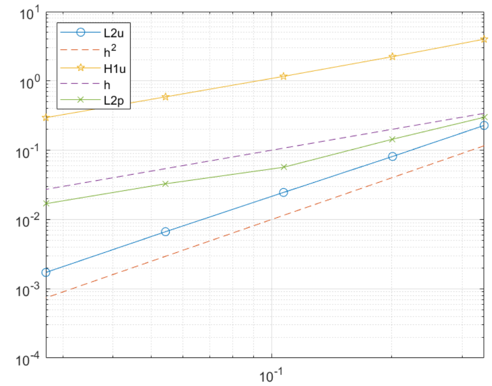

(b)

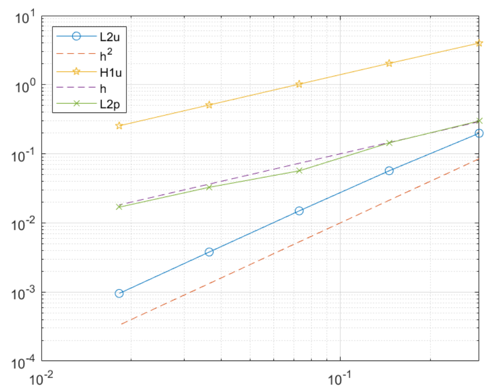

(c)

Figure 2.3: Convergence in space for three different meshes: (a) Non-convex, (b) Distorted Hexagonal, and (c) Distorted square mesh.

with viscosity $\nu = 1$ on domain Ω_S. In this example, we have considered here the nonhomogeneous boundary condition for velocity and given non-zero initial velocity $\boldsymbol{u}_0$ (calculated from exact velocity solution at $t = 0$) as

$$\boldsymbol{u}_0 = 2[\sin(\pi x - 0.7)\sin(\pi y + 0.2); \cos(\pi x - 0.7)\cos(\pi y + 0.2)].$$

The mesh size for the space discretization is $h = 0.01$ and time step $\Delta t = 2^{1-k}/10, k = 1, 2, 3, 4$ and final time $t_{\text{final}} = 1$. The computed rate of convergence at the final time $T = 1$ for velocity and pressure in $E_0(\boldsymbol{u})$ and $E(p)$ norms, respectively are given in Table 2.2, and we note that the computed rate of convergence matches with the theoretical rate of convergence in time.

Δt	$E_0(\boldsymbol{u})$	$r_0(\boldsymbol{u})$	$E(p)$	$r(p)$
0.1	0.00261	-	0.1401	-
0.05	0.001383	0.92	0.0739	0.94
0.025	7.256e-04	0.93	0.0392	0.97
0.0125	3.979e-04	0.87	0.0232	0.96

Table 2.2: Computed errors and rate of convergence with respect to time.

2.4.3 Lid-driven Cavity problem

Considering the applications of classical lid driven cavity problem, in literature, there are several numerical techniques used and tested for the approximation of this problem. For simplicity, here also we have considered the square domain Ω_S. In general, in this type of problems, there is no external force on the domain, that is, $\boldsymbol{f} = 0$ on Ω_S, and Dirichlet boundary condition for velocity, $\boldsymbol{u} = [1, 0]$ on top lid (which is $\{(x, y) \in \Omega : y = 1,\ 0 \leq x \leq 1\}$) and $\boldsymbol{u}$ vanishes on the rest of the boundary $\partial\Omega_S$, is employed. The distorted quadrilateral mesh $\mathcal{D}_h$ with viscosity $\nu = 1$, mesh size $h = 1/64$ and time step $\Delta t = 0.01$ is considered to compute the pressure and velocity which is shown in Fig. 2.4 and Fig. 2.5, respectively.

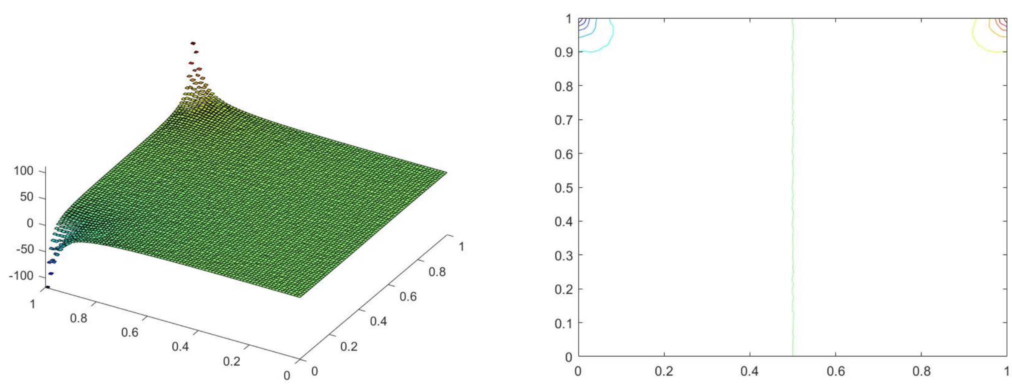

(a) (b)

Figure 2.4: Approximate solution of Cavity problem (a) pore pressure and (b) pressure contour.

It is clear from the Fig. 2.4(a) and Fig. 2.5(a) that the approximate pressure and velocity solution doesn't show any oscillations, and there is one vortex in upper-middle part of the cavity in Fig. 2.5(b). Moreover, the pressure singularity can be seen at the corners of the top lid in Fig. 2.4(b) as expected for this test.

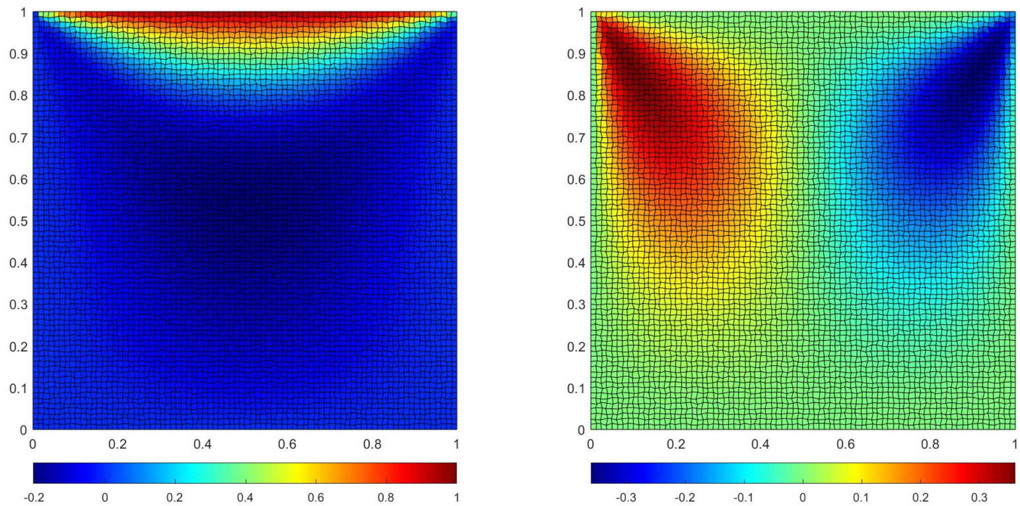

(a)

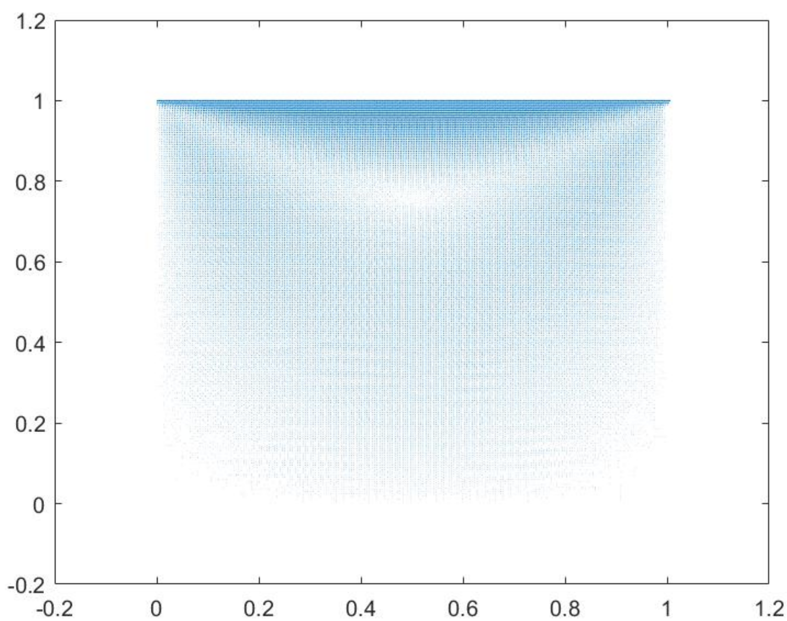

(b)

Figure 2.5: Approximate solution of Cavity problem (a) velocity components, (b) velocity vector.

Chapter 3

Navier-Stokes equations

In this chapter, we have extended the VE analysis proposed in Chapter 2 for the approximation of the non-stationary Navier-Stokes equation with emphasis on both theoretical and computational aspects. Here, we intended to propose the semi-discrete scheme (based on spatial discretization with VE method) and fully discrete scheme (employing the Euler-Backward scheme for time discretization), and also discuss and analyze their well-posedness. With the help of certain projection operators, error estimates are established in suitable norms for both semi and fully-discretized schemes. Moreover, several numerical experiments are conducted to verify the theoretical convergence rate and to observe the computational efficiency of the proposed schemes.

As far as VE approximations of transient Navier-Stokes are concerned, there are only very few VEM-based contributions available in the literature; for instance, see [55] in which stabilized VEM is discussed. We stress that in [55] only discrete formulation and its corresponding algorithm were presented for conducting the numerical experiments. However, theoretical convergence/error estimates of the proposed scheme were not established. Therefore, this work can be considered a first attempt that addresses both convergence analysis and implementation aspects of VEMs for non-stationary Navier-Stokes equations. We believe that the proposed analysis can be extended to more application-oriented problems consisting of time-dependent Navier-Stokes problems on polygonal meshes.

The content of this chapter is arranged in the following manner. We have introduced the governing equation and discussed its weak/variational formulation in Section 3.1. Next, we deal with VE formulation and well-posedness of both semi and fully discrete schemes in Section 3.2. With the help of Stokes and L^2 projection operators in Section 3.3, an optimal *a priori* error estimates for velocity and pressure in H^1 and L^2-norms are established. Lastly, we have reported numerical experiments in Section 3.4 to validate the theoretical convergence rates obtained in Section 3.3.

3.1 Governing equations and their variational formulation

We consider the following incompressible fluid flow problem in a domain $\Omega \subset \mathbb{R}^2$: For all $t \in (0, T]$ and $\boldsymbol{x} \in \Omega$, find the flow velocity $\boldsymbol{u}(\boldsymbol{x}, t)$ and the pore pressure $p(\boldsymbol{x}, t)$ such that

$$\partial_t \boldsymbol{u} - \mathbf{div}\big(\nu\, \boldsymbol{\nabla} \boldsymbol{u} - p\mathbf{I}\big) + (\boldsymbol{\nabla} \boldsymbol{u})\boldsymbol{u} = \boldsymbol{f} \qquad \text{in } \Omega \times (0, T], \tag{3.1.1a}$$

$$\operatorname{div} \boldsymbol{u} = 0 \qquad \text{in } \Omega \times (0, T], \tag{3.1.1b}$$

$$\boldsymbol{u} = \mathbf{0} \qquad \text{on } \partial\Omega \times (0, T], \tag{3.1.1c}$$

$$\boldsymbol{u}(\cdot, 0) = \boldsymbol{u}_0 \qquad \text{on } \Omega \times \{0\}, \tag{3.1.1d}$$

where ν is the viscosity of the fluid, $\boldsymbol{u}_0(\boldsymbol{x})$ is the initial velocity and $\boldsymbol{f}(\boldsymbol{x}, t)$ is the given body force.

Let $\mathbf{V} := [H_0^1(\Omega)]^2$ and $Q := L_0^2(\Omega)$ be the admissible spaces for velocity and pressure, respectively. We also assume that the load function $\boldsymbol{f} \in [L^2(\Omega)]^2$ and initial condition $\boldsymbol{u}_0 \in \mathbf{V}$. Multiplying the adequate test functions $\boldsymbol{v} \in \mathbf{V}$ and $q \in Q$ to the equations (3.1.1a) and (3.1.1b) respectively, with initial-boundary conditions (3.1.1c)-(3.1.1d), the weak formulation states: Find $\boldsymbol{u}(t) \in \mathbf{V}$, $p(t) \in Q$ such that, for all $t \in [0, T]$,

$$\begin{aligned} m(\partial_t \boldsymbol{u}, \boldsymbol{v}) + a(\boldsymbol{u}, \boldsymbol{v}) + \tilde{c}(\boldsymbol{u}; \boldsymbol{u}, \boldsymbol{v}) + b(\boldsymbol{v}, p) &= F(\boldsymbol{v}) \qquad && \forall \boldsymbol{v} \in \mathbf{V}, \\ b(\boldsymbol{u}, q) &= \ \ 0 && \forall q \in Q, \end{aligned} \tag{3.1.2}$$

where the bilinear forms are defined as

$$m(\boldsymbol{u}, \boldsymbol{v}) := \int_\Omega \boldsymbol{u} \cdot \boldsymbol{v}\; dx, \quad a(\boldsymbol{u}, \boldsymbol{v}) := \nu \int_\Omega \boldsymbol{\nabla} \boldsymbol{u} : \boldsymbol{\nabla} \boldsymbol{v}\; dx, \quad F(\boldsymbol{v}) := \int_\Omega \boldsymbol{f} \cdot \boldsymbol{v}\; dx,$$

$$\tilde{c}(\boldsymbol{w}; \boldsymbol{u}, \boldsymbol{v}) := \int_\Omega (\boldsymbol{\nabla} \boldsymbol{u}\, \boldsymbol{w}) \cdot \boldsymbol{v}\; dx = \sum_{i,j=1}^{2} \left(\frac{\partial \boldsymbol{u}_i}{\partial x_j} \boldsymbol{w}_j \right) \boldsymbol{v}_i, \quad b(\boldsymbol{v}, q) := -\int_\Omega \operatorname{div} \boldsymbol{v}\; q\; dx.$$

Note that the above bilinear forms are satisfying the following properties.

- $m(\cdot,\cdot)$ is a positive definite form:

$$m(\boldsymbol{v},\boldsymbol{v}) = \|\boldsymbol{v}\|_{0,\Omega}^2 \quad \forall \boldsymbol{v} \in \mathbf{V}.$$

- $a(\cdot,\cdot)$ is coercive:

$$a(\boldsymbol{v},\boldsymbol{v}) = \nu|\boldsymbol{v}|_{1,\Omega}^2 \geq C\ \nu\|\boldsymbol{v}\|_{1,\Omega}^2 \quad \forall \boldsymbol{v} \in \mathbf{V}. \qquad \text{(Poincaré inequality)}$$

- $b(\cdot,\cdot)$ satisfies the inf-sup condition: there exists $\beta > 0$ such that [67, 63]

$$\sup_{\boldsymbol{v}\in\mathbf{V}\setminus\{0\}} \frac{b(\boldsymbol{v},q)}{\|\boldsymbol{v}\|_{1,\Omega}} \geq \beta\|q\|_{0,\Omega} \qquad \forall q \in Q.$$

- $a(\cdot,\cdot)$ is continuous:

$$a(\boldsymbol{u},\boldsymbol{v}) \leq C\|\boldsymbol{u}\|_{1,\Omega}\|\boldsymbol{v}\|_{1,\Omega} \quad \forall \boldsymbol{u},\boldsymbol{v} \in \mathbf{V}. \qquad \text{(Cauchy Schwarz inequality)}$$

- $F(\cdot)$ is continuous:

$$F(\boldsymbol{v}) \leq C\|\boldsymbol{f}\|_{0,\Omega}\|\boldsymbol{v}\|_{0,\Omega} \leq C_P\|\boldsymbol{f}\|_{0,\Omega}\|\nabla\boldsymbol{v}\|_{0,\Omega} \quad \forall \boldsymbol{v} \in \mathbf{V}.$$

- $\tilde{c}(\cdot;\cdot,\cdot)$ is continuous: $\forall \boldsymbol{u},\boldsymbol{v},\boldsymbol{w} \in \mathbf{V}$,

$$\begin{aligned}
\tilde{c}(\boldsymbol{w};\boldsymbol{u},\boldsymbol{v}) &\leq \sum_{i,j=1}^{2} \left\|\frac{\partial \boldsymbol{u}_i}{\partial \boldsymbol{x}_j}\right\|_{0,\Omega} \|\boldsymbol{w}_j\boldsymbol{v}_i\|_{0,\Omega} \quad \text{(Cauchy Schwarz inequality)} \\
&\leq \sum_{i,j=1}^{2} \left\|\frac{\partial \boldsymbol{u}_i}{\partial \boldsymbol{x}_j}\right\|_{0,\Omega} \|\boldsymbol{w}_j\|_{L^4(\Omega)} \|\boldsymbol{v}_i\|_{L^4(\Omega)} \qquad \text{(Hölder's inequality)} \\
&\lesssim \|\boldsymbol{u}\|_{1,\Omega}\|\boldsymbol{w}\|_{1,\Omega}\|\boldsymbol{v}\|_{1,\Omega}. \ \text{(Sobolev embedding theorem:}H^1(\Omega) \subset L^4(\Omega))
\end{aligned}$$

- $\tilde{c}(\boldsymbol{u};\cdot,\cdot)$ is skew-symmetric bilinear form on the kernel space $\mathbf{X}$, where

$$\mathbf{X} := \{\boldsymbol{v} \in \mathbf{V} : b(\boldsymbol{v},q) = 0\ \forall q \in Q\} = \{\boldsymbol{v} \in \mathbf{V} : \operatorname{div}\boldsymbol{v} = 0\}. \qquad (\operatorname{div}\mathbf{V} \subset Q)$$

For all $\boldsymbol{u} \in \mathbf{X},\ \boldsymbol{v}, \boldsymbol{w} \in \mathbf{V}$, we have

$$\tilde{c}(\boldsymbol{u}; \boldsymbol{v}, \boldsymbol{w}) = -\sum_{i,j=1}^{2} \int_{\Omega} \left(\left(\boldsymbol{v}_i \frac{\partial \boldsymbol{u}_j}{\partial \boldsymbol{x}_j} \right) \boldsymbol{w}_i + \boldsymbol{v}_i \left(\boldsymbol{u}_j \frac{\partial \boldsymbol{w}_i}{\partial \boldsymbol{x}_j} \right) \right) \quad \text{(Integration by parts)}$$
$$= -\int_{\Omega} \operatorname{div} \boldsymbol{u}(\boldsymbol{v} \cdot \boldsymbol{w}) - \int_{\Omega} (\boldsymbol{\nabla} \boldsymbol{w} \boldsymbol{u}) \cdot \boldsymbol{v} = -\tilde{c}(\boldsymbol{u}; \boldsymbol{w}, \boldsymbol{v}).$$

Next, we introduce a new skew-symmetric trilinear form $c(\cdot;\cdot,\cdot)$ by modifying the natural trilinear form $\tilde{c}(\cdot;\cdot,\cdot)$ as follows.

$$c(\boldsymbol{u}; \boldsymbol{v}, \boldsymbol{w}) := \frac{1}{2} \left(\tilde{c}(\boldsymbol{u}; \boldsymbol{v}, \boldsymbol{w}) - \tilde{c}(\boldsymbol{u}; \boldsymbol{w}, \boldsymbol{v}) \right) \quad \forall \boldsymbol{u}, \boldsymbol{v}, \boldsymbol{w} \in \mathbf{V}.$$

It is clear from the definition that $c(\boldsymbol{u}; \boldsymbol{w}, \boldsymbol{w}) = 0$ for all $\boldsymbol{u}, \boldsymbol{w} \in \mathbf{V}$, and also trilinear form $c(\cdot;\cdot,\cdot)$ is continuous. Thus, the weak formulation (3.1.2) can be rewritten as: find $\boldsymbol{u}(t) \in \mathbf{V}$ and $p(t) \in Q$ such that

$$m(\partial_t \boldsymbol{u}, \boldsymbol{v}) + a(\boldsymbol{u}, \boldsymbol{v}) + c(\boldsymbol{u}; \boldsymbol{u}, \boldsymbol{v}) + b(\boldsymbol{v}, p) = F(\boldsymbol{v}) \qquad \forall \boldsymbol{v} \in \mathbf{V}, \tag{3.1.3a}$$
$$b(\boldsymbol{u}, q) = 0 \qquad \forall q \in Q. \tag{3.1.3b}$$

The well-posedness of the problem (3.1.3) follows from the coercivity and continuity of the bilinear form $a(\cdot,\cdot)$, inf-sup condition of bilinear form $b(\cdot,\cdot)$ along with the skew-symmetricity of the bilinear form $c(\boldsymbol{u};\cdot,\cdot)$ (for more details, see [67]). In addition, the solution $\boldsymbol{u} \in \mathbf{V}$ of problem (3.1.3) satisfies

$$\|\boldsymbol{u}(t)\|_{0,\Omega}^2 + \nu \int_0^t |\boldsymbol{u}(s)|_{1,\Omega}^2 \,\mathrm{d}s \lesssim \|\boldsymbol{u}(0)\|_{0,\Omega}^2 + \frac{1}{\nu} \int_0^t \|\boldsymbol{f}(s)\|_{0,\Omega}^2 \,\mathrm{d}s. \tag{3.1.4}$$

Thus, we obtain the bound (3.1.4) by the usage of Young's inequality.

3.2 Virtual element formulation and its well-posedness

In this section, by introducing the stable pair of local and global discrete spaces associated with velocity and pressure, we propose the VE formulation corresponding to weak formulation (3.1.3). Here, we present both semi and fully discrete schemes, and address the existence of a unique VE solution.

3.2.1 Discrete spaces and their degrees of freedom

In this section, we propose the VE formulation and discuss its well-posedness by defining the required projection operators and VE spaces associated with velocity and pressure. We evoke the discretization assumptions and the local VE spaces from the previous chapter to define the discrete formulation. Recalling the discrete spaces from Section 2.2 of Chapter 2, the required local virtual spaces $\mathbf{V}_h(K)$ and $Q_h(K)$ on each element K associated with the velocity $\boldsymbol{u}$ and pressure p, respectively are defined as follows.

$$\mathbf{V}_h(K) := \Big\{\boldsymbol{v}_h \in [H^1(K)]^2 \cap \mathcal{B}(\partial K) : \begin{cases} -\boldsymbol{\Delta}\boldsymbol{v}_h + \nabla s \in \boldsymbol{\mathcal{G}}^{\perp}(K) & \text{for some } s \in L^2(K), \\ \operatorname{div} \boldsymbol{v}_h|_K = c_d \in \mathbb{P}_0(K) \end{cases}$$
$$(\boldsymbol{\Pi}_K^{\boldsymbol{\nabla}}\boldsymbol{v}_h - \boldsymbol{v}_h, \boldsymbol{g}^{\perp})_{0,K} = 0 \quad \forall \boldsymbol{g}^{\perp} \in \boldsymbol{\mathcal{G}}^{\perp}(K)\Big\},$$

$$Q_h(K) := \mathbb{P}_0(K),$$

where $c_d := \frac{1}{|K|}(\int_{\partial K} \boldsymbol{v}_h \cdot \boldsymbol{n}_K \, \mathrm{d}s)$, and the boundary space as

$$\mathcal{B}(\partial K) := \{\boldsymbol{v}_h \in [C^0(\partial K)]^2 : \boldsymbol{v}_h|_e \cdot \boldsymbol{t}_K^e \in \mathbb{P}_1(e), \boldsymbol{v}_h|_e \cdot \boldsymbol{n}_K^e \in \mathbb{P}_2(e) \; \forall e \in \partial K\}.$$

Remark 3.1. *For the analysis purpose we can opt the space $\mathbf{W}_h(K)$ (introduced in [29], and mentioned in Chapter 2) instead of $\mathbf{V}_h(K)$. However, employment of $\mathbf{W}_h(K)$ lead to sub-optimal error estimates for velocity and pressure.*

For any $\boldsymbol{v}_h \in \mathbf{V}_h(K)$, the DoFs for the space $\mathbf{V}_h(K)$ (see [83]) are

- (D_v1) the value of $\boldsymbol{v}_h$ at the vertices of element K;
- (D_v2) the edge moments of $\boldsymbol{v}_h$ along the unit outward normal of K, that is,

$$\int_e \boldsymbol{v}_h \cdot \boldsymbol{n}_K^e \quad \forall e \in \partial K.$$

From definition, we have the dimension of $\mathbf{V}_h(K)$ is equal to $3N_K^v$. The DoFs for space $Q_h(K)$ is

- (D_q) the value of function q_h at any point in K.

Based on the local spaces, we define the global finite-dimensional VE spaces as follows,

$$\mathbf{V}_h := \{\boldsymbol{v}_h \in \mathbf{V} : \boldsymbol{v}_h|_K \in \mathbf{V}_h(K) \quad \forall K \in \mathcal{T}_h\},$$
$$Q_h := \{q_h \in Q : q_h|_K \in Q_h(K) \quad \forall K \in \mathcal{T}_h\}.$$

In view of the definition of $\mathbf{V}_h$, it is immediate to see that following are the DoFs for the global discrete space $\mathbf{V}_h$,

- Values at all the interior vertices on each polygon $K \in \mathcal{T}_h$;
- And edge moments along the unit outward normal of K on each interior edge $e \in \partial K$ for all $K \in \mathcal{T}_h$.

The DoFs for Q_h are the values of function $q_h \in Q_h$ at any point in K for each $K \in \mathcal{T}_h$.

Now, to define the computable discrete formulation, we introduce another local tensor L^2-projection $\boldsymbol{\Pi}^{\mathbf{0},0}_K : [L^2(K)]^{2\times 2} \to [\mathbb{P}_0(K)]^{2\times 2}$ as,

$$(\boldsymbol{\Pi}^{\mathbf{0},0}_K \boldsymbol{\nabla} \boldsymbol{v} - \boldsymbol{\nabla} \boldsymbol{v}, \boldsymbol{p})_{0,K} = 0 \qquad \forall \boldsymbol{p} \in [\mathbb{P}_0(K)]^{2\times 2},\ \boldsymbol{v} \in [H^1(\Omega)]^2.$$

For any $\boldsymbol{u}_h, \boldsymbol{v}_h, \boldsymbol{w}_h \in \mathbf{V}_h(K)$ and $q_h \in Q_h(K)$, we define the local discrete forms on each element K through local projection operators (presented above and in Chapter 2) as follows.

$$m_h^K(\boldsymbol{u}_h, \boldsymbol{v}_h) := m^K(\boldsymbol{\Pi}^{\mathbf{0}}_K \boldsymbol{u}_h, \boldsymbol{\Pi}^{\mathbf{0}}_K \boldsymbol{v}_h) + S^{0,K}((\boldsymbol{u}_h - \boldsymbol{\Pi}^{\mathbf{0}}_K \boldsymbol{u}_h), (\boldsymbol{v}_h - \boldsymbol{\Pi}^{\mathbf{0}}_K \boldsymbol{v}_h)),$$
$$a_h^K(\boldsymbol{u}_h, \boldsymbol{v}_h) := a^K(\boldsymbol{\Pi}^{\boldsymbol{\nabla}}_K \boldsymbol{u}_h, \boldsymbol{\Pi}^{\boldsymbol{\nabla}}_K \boldsymbol{v}_h) + \nu\ S^{\nabla,K}((\mathbf{I} - \boldsymbol{\Pi}^{\boldsymbol{\nabla}}_K) \boldsymbol{u}_h, (\mathbf{I} - \boldsymbol{\Pi}^{\boldsymbol{\nabla}}_K) \boldsymbol{v}_h),$$
$$\tilde{c}_h^K(\boldsymbol{w}_h; \boldsymbol{u}_h, \boldsymbol{v}_h) := ((\boldsymbol{\Pi}^{\mathbf{0},0}_K \boldsymbol{\nabla} \boldsymbol{u}_h)\ \boldsymbol{\Pi}^{\mathbf{0}}_K \boldsymbol{w}_h, \boldsymbol{\Pi}^{\mathbf{0}}_K \boldsymbol{v}_h)_{0,K},$$
$$F_h^K(\boldsymbol{v}_h) := (\boldsymbol{\Pi}^{\mathbf{0}}_K \boldsymbol{f}, \boldsymbol{v}_h)_{0,K}, \quad b^K(\boldsymbol{v}_h, q_h) := -(\operatorname{div} \boldsymbol{v}_h, q_h)_{0,K},$$

where the local bilinear forms are the restrictions of the continuous forms on each element K, that is

$$m^K(\boldsymbol{u}_h, \boldsymbol{v}_h) := m(\boldsymbol{u}_h, \boldsymbol{v}_h)|_K, \quad a^K(\boldsymbol{u}_h, \boldsymbol{v}_h) := a(\boldsymbol{u}_h, \boldsymbol{v}_h)|_K.$$

And the stabilization terms $S^{0,K}(\cdot,\cdot)$ and $S^{\nabla,K}(\cdot,\cdot)$ are defined as, see [24]

$$S^{0,K}(\boldsymbol{u}_h, \boldsymbol{v}_h) := \operatorname{area}(K) \sum_{i,j=1}^{N^V} \operatorname{dof}_i(\boldsymbol{u}_h) \operatorname{dof}_j(\boldsymbol{v}_h), \qquad \forall \boldsymbol{u}_h, \boldsymbol{v}_h \in \operatorname{Ker}(\boldsymbol{\Pi}^{\mathbf{0}}_K),$$

$$S^{\nabla,K}(\boldsymbol{u}_h,\boldsymbol{v}_h) := \sum_{i,j=1}^{N^V} \mathrm{dof}_i(\boldsymbol{u}_h)\mathrm{dof}_j(\boldsymbol{v}_h), \qquad \forall \boldsymbol{u}_h,\boldsymbol{v}_h \in \mathrm{Ker}(\boldsymbol{\Pi}_K^{\boldsymbol{\nabla}}),$$

by denoting N^V and N^Q as the dimension of spaces $\mathbf{V}_h$ and Q_h, respectively.

We note that the classical stabilizer terms $S^{0,K}(\cdot,\cdot)$ and $S^{\nabla,K}(\cdot,\cdot)$ satisfy the following stability with respect to the continuous bilinear forms [30],

$$\begin{aligned} \zeta_* m^K(\boldsymbol{u}_h,\boldsymbol{v}_h) \le S^{0,K}(\boldsymbol{u}_h,\boldsymbol{v}_h) \le \zeta^* m^K(\boldsymbol{u}_h,\boldsymbol{v}_h) \quad \forall \boldsymbol{u}_h,\boldsymbol{v}_h \in \mathrm{Ker}(\boldsymbol{\Pi}_K^{\mathbf{0}}), \\ \alpha_* a^K(\boldsymbol{u}_h,\boldsymbol{v}_h) \le S^{\nabla,K}(\boldsymbol{u}_h,\boldsymbol{v}_h) \le \alpha^* a^K(\boldsymbol{u}_h,\boldsymbol{v}_h) \quad \forall \boldsymbol{u}_h,\boldsymbol{v}_h \in \mathrm{Ker}(\boldsymbol{\Pi}_K^{\boldsymbol{\nabla}}), \end{aligned} \tag{3.2.1}$$

where $\zeta_*,\zeta^*,\alpha_*,\alpha^* > 0$ are constants independent of diameter h_K of polygon K. Now considering the above defined local forms, we set the global discrete bilinear and trilinear forms for all $\boldsymbol{u}_h,\boldsymbol{v}_h \in \mathbf{V}_h$ and $q_h \in Q_h$ are simply set as sum over each polygon K as simply the sum over each polygon K,

$$\begin{aligned} m_h(\boldsymbol{u}_h,\boldsymbol{v}_h) &:= \sum_{K\in\mathcal{T}_h} m_h^K(\boldsymbol{u}_h,\boldsymbol{v}_h), \quad b(\boldsymbol{v}_h,q_h) := \sum_{K\in\mathcal{T}_h} b^K(\boldsymbol{v}_h,q_h), \\ a_h(\boldsymbol{u}_h,\boldsymbol{v}_h) &:= \sum_{K\in\mathcal{T}_h} a_h^K(\boldsymbol{u}_h,\boldsymbol{v}_h), \quad c_h(\boldsymbol{u}_h;\boldsymbol{u}_h,\boldsymbol{v}_h) := \sum_{K\in\mathcal{T}_h} c_h^K(\boldsymbol{u}_h;\boldsymbol{u}_h,\boldsymbol{v}_h) \end{aligned}$$

and the load term as

$$F_h(\boldsymbol{v}_h) := \sum_{K\in\mathcal{T}_h} F_h^K(\boldsymbol{v}_h).$$

Now we are in position to define our semi discrete VE formulation corresponding to the weak form (3.1.3) as: find $\boldsymbol{u}_h(t) \in \mathbf{V}_h$ and $p_h(t) \in Q_h$ for each $t \in (0,T]$ such that

$$m_h(\partial_t\boldsymbol{u}_h,\boldsymbol{v}_h) + a_h(\boldsymbol{u}_h,\boldsymbol{v}_h) + c_h(\boldsymbol{u}_h;\boldsymbol{u}_h,\boldsymbol{v}_h) + b(\boldsymbol{v}_h,p_h) = F_h(\boldsymbol{v}_h) \quad \forall \boldsymbol{v}_h \in \mathbf{V}_h, \tag{3.2.2a}$$

$$b(\boldsymbol{u}_h,q_h) = 0 \qquad \forall q_h \in Q_h, \tag{3.2.2b}$$

with given initial condition $\boldsymbol{u}_h(0)$ considered as an approximation of $\boldsymbol{u}_0$ chosen appropriately in derivation of the error analysis, and the discrete trilinear form $c_h(\cdot;\cdot,\cdot)$ is defined from $\tilde{c}_h(\cdot;\cdot,\cdot)$, analogous to the continuous trilinear form $c(\cdot,\cdot,\cdot)$.

The stability properties of $S^{0,K}(\cdot,\cdot)$ and $S^{\nabla,K}(\cdot,\cdot)$ given in (3.2.1) yields

- $m_h(\cdot,\cdot)$ is positive definite form: for all $\boldsymbol{v}_h \in \mathbf{V}_h$,

$$m_h(\boldsymbol{v}_h,\boldsymbol{v}_h) \geq \nu \sum_{K\in\mathcal{T}_h} \left(\|\mathbf{\Pi}_K^{\mathbf{0}}\boldsymbol{v}_h\|_{0,K}^2 + \zeta_* \|(\mathbf{I}-\mathbf{\Pi}_K^{\mathbf{0}})\boldsymbol{v}_h\|_{0,K}^2 \right) \geq \hat{C}_* \, \|\boldsymbol{v}_h\|_{0,\Omega}^2,$$

  where $\hat{C}_* := \min\{1,\zeta_*\}$.

- $a_h(\cdot,\cdot)$ is coercive: for all $\boldsymbol{v}_h \in \mathbf{V}_h$,

$$a_h(\boldsymbol{v}_h,\boldsymbol{v}_h) \geq \nu \sum_{K\in\mathcal{T}_h} \left(\|\mathbf{\Pi}_K^{\boldsymbol{\nabla}}\boldsymbol{v}_h\|_{1,K}^2 + \alpha_* \|(\mathbf{I}-\mathbf{\Pi}_K^{\boldsymbol{\nabla}})\boldsymbol{v}_h\|_{1,K}^2 \right) \geq C_*\nu \, \|\boldsymbol{v}_h\|_{1,\Omega}^2,$$

  where $C_* := \min\{1,\alpha_*\}$.

- $a_h(\cdot,\cdot)$ is continuous: for all $\boldsymbol{u}_h,\boldsymbol{v}_h \in \mathbf{V}_h$ (again by use of stability for $S^{\nabla,K}(\cdot,\cdot)$),

$$a_h(\boldsymbol{u}_h,\boldsymbol{v}_h) \leq C^* \; \nu \; \|\boldsymbol{u}_h\|_{1,\Omega}\|\boldsymbol{v}_h\|_{1,\Omega},$$

  where $C^* := \max\{1,\alpha^*\}$.

- $b(\cdot,\cdot)$ satisfies inf-sup condition on $\mathbf{V}_h \times Q_h$: there exists a $\beta_h > 0$ such that (see [83])

$$\sup_{\boldsymbol{v}_h\in\mathbf{V}_h\setminus\{0\}} \frac{b(\boldsymbol{v}_h,q_h)}{\|\boldsymbol{v}_h\|_1} \geq \beta_h\|q_h\|_0, \qquad \forall q_h \in Q_h.$$

- $F_h(\cdot)$ is continuous: for all $\boldsymbol{v}_h \in \mathbf{V}_h$,

$$F_h(\boldsymbol{v}_h) \leq \sum_{K\in\mathcal{T}_h} \|\mathbf{\Pi}_K^{\mathbf{0}}\boldsymbol{f}\|_{0,K}\|\boldsymbol{v}_h\|_{0,K} \leq \|\boldsymbol{f}\|_{0,\Omega}\|\boldsymbol{v}_h\|_{0,\Omega}.$$

Now, we generate the following result to show the continuity of the trilinear form $c_h(\cdot;\cdot,\cdot)$.

Lemma 3.1. *The projection operator $\mathbf{\Pi}_K^{\mathbf{0}}$ is bounded with respect to the L^s- norm with $s \geq 2$, that is,*

$$\|\mathbf{\Pi}_K^{\mathbf{0}}\boldsymbol{v}\|_{0,s,K} \leq C\|\boldsymbol{v}\|_{0,s,K} \quad \forall \boldsymbol{v} \in [L^s(K)]^2 \text{ and } K \in \mathcal{T}_h,$$

where C is independent of mesh size h.

Proof. The use of inverse estimates for polynomials (see [113, 32]) yields

$$\|\mathbf{\Pi}_K^{\mathbf{0}}\boldsymbol{v}\|_{0,s,K} \leq Ch^{2\left(\frac{1}{s}-\frac{1}{2}\right)}\|\mathbf{\Pi}_K^{\mathbf{0}}\boldsymbol{v}\|_{0,K}.$$

In view of the definition of $\mathbf{\Pi}_K^{\mathbf{0}}$, we have $\|\mathbf{\Pi}_K^{\mathbf{0}}\boldsymbol{v}\|_{0,K} \leq \|\boldsymbol{v}\|_{0,K}$. Now, the Hölder's inequality together with mesh regularity assumptions yields

$$\|\mathbf{\Pi}_K^{\mathbf{0}}\boldsymbol{v}\|_{0,s,K} \leq Ch^{2\left(\frac{1}{s}-\frac{1}{2}\right)}|K|^{\left(\frac{1}{2}-\frac{1}{s}\right)}\|\boldsymbol{v}\|_{0,s,K} \leq C\|\boldsymbol{v}\|_{0,s,K}.$$

□

- $c_h(\cdot;\cdot,\cdot)$ is continuous: for all $\boldsymbol{u}_h, \boldsymbol{v}_h, \boldsymbol{w}_h \in \mathbf{V}_h$ (use of Lemma 3.1 and the continuity of trilinear form $c(\cdot;\cdot,\cdot)$, refer [32]),

$$\begin{aligned} c_h(\boldsymbol{u}_h;\boldsymbol{v}_h,\boldsymbol{w}_h) &= \sum_{K\in\mathcal{T}_h}\frac{1}{2}\Big(((\mathbf{\Pi}_K^{\mathbf{0},0}\boldsymbol{\nabla}\boldsymbol{v}_h)\ \mathbf{\Pi}_K^{\mathbf{0}}\boldsymbol{u}_h, \mathbf{\Pi}_K^{\mathbf{0}}\boldsymbol{w}_h)_{0,K} \\ &\qquad - ((\mathbf{\Pi}_K^{\mathbf{0},0}\boldsymbol{\nabla}\boldsymbol{w}_h)\ \mathbf{\Pi}_K^{\mathbf{0}}\boldsymbol{u}_h, \mathbf{\Pi}_K^{\mathbf{0}}\boldsymbol{v}_h)_{0,K}\Big) \\ &\leq C\|\boldsymbol{u}_h\|_{1,\Omega}\|\boldsymbol{w}_h\|_{1,\Omega}\|\boldsymbol{v}_h\|_{1,\Omega}. \end{aligned}$$

Now, we produce the result below on the existence of unique solution of problem (3.2.2) and stability of the solution.

Lemma 3.2. *The semi-discrete problem* (3.2.2) *has a unique solution* $\boldsymbol{u}_h(t) \in \mathbf{V}_h$ *all* $t \in [0,T]$ *and given* $\boldsymbol{u}_h(0)$ *and satisfies,*

$$\|\boldsymbol{u}_h(t)\|_{0,\Omega}^2 + \nu\int_0^t |\boldsymbol{u}_h(s)|_{1,\Omega}^2\,ds \leq C\Big(\|\boldsymbol{u}_h(0)\|_{0,\Omega}^2 + \int_0^t \|\boldsymbol{f}(s)\|_{0,\Omega}^2\,ds\Big), \tag{3.2.3}$$

where the constant C *is independent of mesh size* h.

Proof. The properties of the discrete bilinear forms $a_h(\cdot,\cdot)$, $m_h(\cdot,\cdot)$ and $b(\cdot,\cdot)$, discrete trilinear form $c_h(\cdot;\cdot,\cdot)$, and discrete linear functional $F_h(\cdot)$ with the well-known wellposedness results from [57] implies that the semi-discrete problem (3.2.2) has a unique solution, see also [68]. Taking $\boldsymbol{v}_h = \boldsymbol{u}_h$ in (3.2.2a) gives

$$\frac{1}{2}\frac{d}{dt}\|\boldsymbol{u}_h\|_{0,\Omega}^2 + \nu|\boldsymbol{u}_h|_{1,\Omega}^2 \leq C\|\boldsymbol{f}\|_{0,\Omega}\|\boldsymbol{u}_h\|_{0,\Omega}.$$

Employing the Poincaré and Young's inequalities, then integrating from 0 to t lead to (3.2.3). □

3.2.2 Fully discrete scheme

The time interval $[0,T]$ is decomposed into subintervals $I_n := [t_{n-1}, t_n]$, where $t_n = n\Delta t$ for $n = 1, \dots, N$ and $\Delta t = \frac{T}{N}$. For the time discretization, we employ the backward Euler scheme, i.e, the approximation of the time derivative at t_n for any generic function g_h is defined as follows.

$$\delta_t g_h^n := \frac{g_h^n - g_h^{n-1}}{\Delta t}.$$

For the consistency in the notations, the solution of semi-discrete scheme and fully discrete scheme at time $t = t_n$, will be denoted by $\boldsymbol{u}_h(t_n)$ and $\boldsymbol{u}_h^n$, respectively. The fully discrete VE scheme corresponding to the continuous formulation (3.1.3) read as: Given initial conditions $\boldsymbol{u}_h^0 := \boldsymbol{u}_h(0)$, find $\boldsymbol{u}_h^n \in \mathbf{V}_h, p_h^n \in Q_h$ for each $n = 1, \dots, N$ such that

$$m_h(\delta_t \boldsymbol{u}_h^n, \boldsymbol{v}_h) + a_h(\boldsymbol{u}_h^n, \boldsymbol{v}_h) + c_h(\boldsymbol{u}_h^n; \boldsymbol{u}_h^n, \boldsymbol{v}_h) + b(\boldsymbol{v}_h, p_h^n) = F_h^n(\boldsymbol{v}_h) \quad \forall \boldsymbol{v}_h \in \mathbf{V}_h, \tag{3.2.4a}$$

$$b(\boldsymbol{u}_h^n, q_h) = 0 \qquad \forall q_h \in Q_h. \tag{3.2.4b}$$

The following lemma provide us the well-posedness of the above fully discrete scheme.

Lemma 3.3. *There exists a unique solution $\boldsymbol{u}_h^n \in \mathbf{V}_h$, $p_h^n \in Q_h$ of the problem* (3.2.4) *and also satisfies the following bound,*

$$\max_{1 \le j \le n} \|\boldsymbol{u}_h^j\|_{0,\Omega}^2 + \nu \Delta t \sum_{j=1}^{n} |\boldsymbol{u}_h^j|_{1,\Omega}^2 \le C\big(\|\boldsymbol{u}_h(0)\|_{0,\Omega}^2 + \Delta t \sum_{j=1}^{n} \|\boldsymbol{f}^j\|_{0,\Omega}^2\big), \tag{3.2.5}$$

where C is a positive constant and independent of h, Δt.

Proof. Taking $\boldsymbol{v}_h = \boldsymbol{u}_h^n, q_h = p_h^n$ in (3.2.4) then the coercivity of $a_h(\cdot;\cdot)$, skew-symmetry of $c_h(\boldsymbol{u}_h; \cdot, \cdot)$ and continuity of $F_h^n(\cdot)$, and use of Young's inequality give

$$\begin{aligned} \frac{1}{2}(\|\boldsymbol{u}_h^n\|_{0,\Omega}^2 - \|\boldsymbol{u}_h^{n-1}\|_{0,\Omega}^2) + \nu \Delta t |\boldsymbol{u}_h^n|_{1,\Omega}^2 &\le C\Delta t \ \|\boldsymbol{f}^n\|_{0,\Omega} \|\boldsymbol{u}_h^n\|_{0,\Omega} \\ &\le C\Delta t \ \|\boldsymbol{f}^n\|_{0,\Omega}^2 + \frac{\nu \Delta t}{2} |\boldsymbol{u}_h^n|_{1,\Omega}^2. \end{aligned}$$

Summing the bound above over n leads to (3.2.5). Now, the existence and uniqueness can be obtained from the stability result (3.2.5) and thus, the well-posedness of discrete scheme corresponding to the steady Navier-Stokes equation, refer [30, 33, 115]. $\square$

3.3 Convergence analysis

With the help of a projection named as Stokes projection (introduced in this section by (3.3.8)), we establish convergence results for both semi-discrete and fully discrete schemes. We derive the optimal error estimates for velocity in the H^1- norm, and for pressure in the L^2- norm under some regularity assumptions. We begin with collecting the preliminary results for the subsequent analysis.

Lemma 3.4. *The trilinear form $c_h(\cdot;\cdot,\cdot)$ satisfy the following bound:*

$$c_h(\boldsymbol{u};\boldsymbol{v},\boldsymbol{w}) \le C\|\boldsymbol{u}\|_{0,\Omega}^{1/2}\|\nabla\boldsymbol{u}\|_{0,\Omega}^{1/2}\|\nabla\boldsymbol{v}\|_{0,\Omega}\|\nabla\boldsymbol{w}\|_{0,\Omega} \quad \forall \boldsymbol{u},\boldsymbol{v},\boldsymbol{w}\in\mathbf{V}, \tag{3.3.1}$$

where C is independent of h.

Proof. Let $p_1 = 2,\ q_1 = 3,\ r_1 = 6$ then repeated application of generalized version of Hölder's inequality with $\frac{1}{p_1}+\frac{1}{q_1}+\frac{1}{r_1}=1$ along with Lemma 3.1 implies that

$$\begin{aligned}
\tilde{c}_h(\boldsymbol{u};\boldsymbol{v},\boldsymbol{w}) &\le \sum_{i,j=1}^{2}\sum_{K\in\mathcal{T}_h}\left\|\boldsymbol{\Pi}_K^{\mathbf{0},0}\frac{\partial \boldsymbol{v}_i}{\partial x_j}\right\|_{L^2(K)}\left\|\boldsymbol{\Pi}_K^{\mathbf{0}}\boldsymbol{u}_j\right\|_{L^3(K)}\left\|\boldsymbol{\Pi}_K^{\mathbf{0}}\boldsymbol{w}_i\right\|_{L^6(K)}\\
&\le \sum_{i,j=1}^{2}\left(\sum_{K\in\mathcal{T}_h}\left\|\boldsymbol{\Pi}_K^{\mathbf{0},0}\frac{\partial \boldsymbol{v}_i}{\partial x_j}\right\|_{L^2(K)}^2\right)^{\frac{1}{2}}\left(\sum_{K\in\mathcal{T}_h}\left\|\boldsymbol{\Pi}_K^{\mathbf{0}}\boldsymbol{u}_j\right\|_{L^3(K)}^3\right)^{\frac{1}{3}}\\
&\qquad\times\left(\sum_{K\in\mathcal{T}_h}\left\|\boldsymbol{\Pi}_K^{\mathbf{0}}\boldsymbol{w}_i\right\|_{L^6(K)}^6\right)^{\frac{1}{6}}\\
&\le C\sum_{i,j=1}^{2}\left\|\frac{\partial \boldsymbol{v}_i}{\partial x_j}\right\|_{0,\Omega}\|\boldsymbol{u}_j\|_{0,3,\Omega}\,\|\boldsymbol{w}_i\|_{0,6,\Omega}\,.
\end{aligned}$$

Employing the Sobolev embedding $W^{m,p}(\Omega)\subset L^q(\Omega)$, $mp<2$ and $1\le q\le\frac{2p}{2-mp}$ (see [116]) with choice of $p=2,\ q=3,\ m=1/2$. Also, use of embedding $W^{m,p}(\Omega)\subset L^q(\Omega)$, $q\in[1,\infty)$ for $mp=2$ and taking $p=2$, $m=1$, we arrive at

$$\tilde{c}_h(\boldsymbol{u};\boldsymbol{v},\boldsymbol{w}) \le C\sum_{i,j=1}^{2}\left\|\frac{\partial \boldsymbol{v}_i}{\partial x_j}\right\|_{0,\Omega}\|\boldsymbol{u}_j\|_{\frac{1}{2},2,\Omega}\,\|\boldsymbol{w}_i\|_{1,\Omega}\,. \tag{3.3.2}$$

The interpolation estimates (see [116, Theorem 4.17] on page 79), that is, for all $\boldsymbol{v} \in W^{m,p}(\Omega)$, $1 \le j \le m$, gives

$$\|\boldsymbol{v}\|_{W^{j,p}(\Omega)} \le C\|\boldsymbol{v}\|^{j/m}_{W^{m,p}(\Omega)}\|\boldsymbol{v}\|^{(m-j)/m}_{L^p(\Omega)}. \tag{3.3.3}$$

The choice of $j = 1/2$, $m = 1$, $p = 2$ in (3.3.3) and using Poincaré inequality, we get

$$\|\boldsymbol{v}\|_{W^{1/2,2}(\Omega)} \le C\|\boldsymbol{v}\|^{1/2}_{W^{1,2}(\Omega)}\|\boldsymbol{v}\|^{1/2}_{0,\Omega} \le C_P\|\nabla\boldsymbol{v}\|^{1/2}_{0,\Omega}\|\boldsymbol{v}\|^{1/2}_{0,\Omega}.$$

Thus, the use of above bound in (3.3.2) leads to

$$\tilde{c}_h(\boldsymbol{u};\boldsymbol{v},\boldsymbol{w}) \le C\,\|\nabla\boldsymbol{v}\|_{0,\Omega}\,\|\nabla\boldsymbol{u}\|^{1/2}_{0,\Omega}\|\boldsymbol{u}\|^{1/2}_{0,\Omega}\|\nabla\boldsymbol{w}\|_{0,\Omega}.$$

Proceeding analogously to this way, we can derive the same bounds for the second term $\tilde{c}_h(\boldsymbol{u};\boldsymbol{w},\boldsymbol{v})$ and hence, conclude the bound (3.3.1). □

Lemma 3.5. *Let $\boldsymbol{u}_\pi \in [\mathbb{P}_1(K)]^2$ be the polynomial approximation of $\boldsymbol{u}$ on each $K \in \mathcal{T}_h$. Under the regularity assumption on the polygonal mesh $\mathcal{T}_h$ (mentioned in Section 3.2), there exists a positive constant C independent of h such that (see [113, 18])*

$$\sum_{K\in\mathcal{T}_h}(\|\boldsymbol{u}-\boldsymbol{u}_\pi\|_{0,K} + h\,|\boldsymbol{u}-\boldsymbol{u}_\pi|_{1,K}) \le Ch^2|\boldsymbol{u}|_{2,\Omega}. \tag{3.3.4}$$

Lemma 3.6. *For each $\boldsymbol{u} \in \mathbf{V} \cap [H^{r+1}(\Omega)]^2$ with $0 \le r \le 1$ and under the regularity assumption on the polygonal mesh (mentioned in Section 3.2), there exist an interpolant $\boldsymbol{u}_I \in \mathbf{V}_h$ satisfying (see [83])*

$$\|\boldsymbol{u}-\boldsymbol{u}_I\|_{0,\Omega} + h_K\,|\boldsymbol{u}-\boldsymbol{u}_I|_{1,\Omega} \le Ch^{r+1}|\boldsymbol{u}|_{r+1,\Omega}. \tag{3.3.5}$$

Lemma 3.7. *The bilinear form $b(\cdot,\cdot)$ satisfies the discrete inf-sup condition on $\mathbf{V}_h \times Q_h$, that is, there exists a $\beta_h > 0$ such that (see [83])*

$$\sup_{\boldsymbol{v}_h\in\mathbf{V}_h\setminus\{0\}}\frac{b(\boldsymbol{v}_h,q_h)}{\|\boldsymbol{v}_h\|_{1,\Omega}} \ge \beta_h\|q_h\|_{0,\Omega} \qquad \forall q_h \in Q_h. \tag{3.3.6}$$

For the proof of Lemma 3.6 and 3.7, we refer to [83] and references therein.

Defining the discrete kernel space $\mathbf{X}_h$ with use of the fact that $\operatorname{div}\mathbf{V}_h \subset Q_h$, as

$$\mathbf{X}_h := \{\boldsymbol{v}_h \in \mathbf{V}_h : b(\boldsymbol{v}_h, q_h) = 0 \ \ \forall q_h \in Q_h\} = \{\boldsymbol{v}_h \in \mathbf{V}_h : \operatorname{div}\boldsymbol{v}_h = 0\}.$$

For a given $\boldsymbol{v} \in \mathbf{X}$, we have the following approximation property for the discrete space $\mathbf{X}_h$ as a consequence of the discrete inf-sup condition from Lemma 3.7 (see in [63, 32]):

$$\inf_{\boldsymbol{z}_h \in \mathbf{X}_h \setminus \{0\}} \|\boldsymbol{v} - \boldsymbol{z}_h\|_1 \leq \inf_{\boldsymbol{v}_h \in \mathbf{V}_h \setminus \{0\}} \|\boldsymbol{v} - \boldsymbol{v}_h\|_1. \tag{3.3.7}$$

Next, we define the classical Stokes projection $S_h(\boldsymbol{u}, p) := (S_h^{\boldsymbol{u}}\boldsymbol{u}, S_h^p p) \in \mathbf{V}_h \times Q_h$ as a solution of the following equation (see also [63] and [67]).

$$a_h(S_h^{\boldsymbol{u}}\boldsymbol{u}, \boldsymbol{v}_h) + b(\boldsymbol{v}_h, S_h^p p) = a(\boldsymbol{u}, \boldsymbol{v}_h) + b(\boldsymbol{v}_h, p) \qquad \forall \boldsymbol{v}_h \in \mathbf{V}_h, \tag{3.3.8a}$$

$$b(S_h^{\boldsymbol{u}}\boldsymbol{u}, q_h) = b(\boldsymbol{u}, q_h) \qquad \forall q_h \in Q_h. \tag{3.3.8b}$$

Choosing $\boldsymbol{v}_h = S_h^{\boldsymbol{u}}\boldsymbol{u}$ in (3.3.8) and using coercivity of the discrete bilinear form $a_h(\cdot, \cdot)$, we have

$$\|\nabla S_h^{\boldsymbol{u}}\boldsymbol{u}\|_{0,\Omega} + \|S_h^p p\|_{0,\Omega} \leq C(\|\nabla \boldsymbol{u}\|_{0,\Omega} + \|p\|_{0,\Omega}). \tag{3.3.9}$$

By definition of $S_h^{\boldsymbol{u}}$ in (3.3.8b) and use of (3.1.3b) implies $b(S_h^{\boldsymbol{u}}\boldsymbol{u}, q_h) = 0$ for all $q_h \in Q_h$ and thus $S_h^{\boldsymbol{u}}\boldsymbol{u} \in \mathbf{X}_h$. Then as seen in Chapter 2 the following error estimates of the operator S_h can be easily derived by using the properties of the bilinear forms $a_h(\cdot, \cdot)$, $b(\cdot, \cdot)$, Lemma 3.5 and 3.6, and appealing to the duality arguments (refer [83]).

Lemma 3.8. *Let* $(\boldsymbol{u}, p) \in \mathbf{V} \times Q$ *be the solution of the continuous problem* (3.1.3) *and* $(S_h^{\boldsymbol{u}}\boldsymbol{u}, S_h^p p) \in \mathbf{V}_h \times Q_h$ *satisfies the equation* (3.3.8) *then there exists a positive constant* C*, independent of* h*, such that*

$$\|\boldsymbol{u} - S_h^{\boldsymbol{u}}\boldsymbol{u}\|_{0,\Omega} + h(|\boldsymbol{u} - S_h^{\boldsymbol{u}}\boldsymbol{u}|_{1,\Omega} + \|p - S_h^p p\|_{0,\Omega}) \leq Ch^2(|\boldsymbol{u}|_{2,\Omega} + |p|_{1,\Omega}). \tag{3.3.10}$$

In the following lemma, we estimate the error between the trilinear forms $c(\cdot;\cdot,\cdot)$ and $c_h(\cdot;\cdot,\cdot)$. The main ideas of the following lemma are borrowed from [32].

Lemma 3.9. *For all* $\boldsymbol{u} \in [H^2(\Omega)]^2 \cap \mathbf{V}$ *and* $\boldsymbol{v}_h \in \mathbf{V}_h$*, the following holds.*

$$|c(\boldsymbol{u}; \boldsymbol{u}, \boldsymbol{v}_h) - c_h(\boldsymbol{u}; \boldsymbol{u}, \boldsymbol{v}_h)| \leq Ch|\boldsymbol{u}|_{2,\Omega}\|\nabla \boldsymbol{u}\|_{0,\Omega}\|\nabla \boldsymbol{v}_h\|_{0,\Omega}, \tag{3.3.11}$$

where C is independent of h.

Proof. We begin with splitting the skew-symmetric terms into simpler trilinear forms $\tilde{c}(\cdot;\cdot,\cdot)$ and $\tilde{c}_h(\cdot;\cdot,\cdot)$ in the following manner.

$$\begin{aligned} c(\boldsymbol{u};\boldsymbol{u},\boldsymbol{v}_h) - c_h(\boldsymbol{u};\boldsymbol{u},\boldsymbol{v}_h) &= \frac{1}{2}\Big(\big(\tilde{c}(\boldsymbol{u};\boldsymbol{u},\boldsymbol{v}_h) - \tilde{c}_h(\boldsymbol{u};\boldsymbol{u},\boldsymbol{v}_h)\big) \\ &\quad + \big(\tilde{c}(\boldsymbol{u};\boldsymbol{v}_h,\boldsymbol{u}) - \tilde{c}_h(\boldsymbol{u};\boldsymbol{v}_h,\boldsymbol{u})\big)\Big) \\ &:= \frac{1}{2}\sum_{i=1}^{2}\mathcal{C}_i(\boldsymbol{v}_h). \end{aligned}$$

We proceed to estimate $\mathcal{C}_i, i=1,2$. An application of generalized Hölder's inequality, Lemma 3.1, Sobolev embedding $W^{r,4}(\Omega) \subset H^{r+1}(\Omega)$, $r \geq 0$ and estimates of projections $\boldsymbol{\Pi}_K^{\mathbf{0}}$, $\boldsymbol{\Pi}_K^{\mathbf{0},0}$ gives

$$\begin{aligned} \mathcal{C}_1(\boldsymbol{v}_h) &= \sum_K \sum_{i,j=1}^{2} \int_K \Big(\frac{\partial \boldsymbol{u}_i}{\partial \boldsymbol{x}_j}\boldsymbol{u}_j\ (\boldsymbol{v}_{h,i} - \boldsymbol{\Pi}_K^{\mathbf{0}}\boldsymbol{v}_{h,i}) + \frac{\partial \boldsymbol{u}_i}{\partial \boldsymbol{x}_j}(\boldsymbol{u}_j - \boldsymbol{\Pi}_K^{\mathbf{0}}\boldsymbol{u}_j)\ \boldsymbol{\Pi}_K^{\mathbf{0}}\boldsymbol{v}_{h,i} \\ &\qquad - \Big((\mathbf{I} - \boldsymbol{\Pi}_K^{\mathbf{0},0})\frac{\partial \boldsymbol{u}_i}{\partial \boldsymbol{x}_j}\Big)\boldsymbol{\Pi}_K^{\mathbf{0}}\boldsymbol{u}_j\ \boldsymbol{\Pi}_K^{\mathbf{0}}\boldsymbol{v}_{h,i}\Big) \\ &\leq \sum_K \sum_{i,j=1}^{2} \Bigg(\left\|\frac{\partial \boldsymbol{u}_i}{\partial \boldsymbol{x}_j}\right\|_{L^4(K)} \|\boldsymbol{u}_j\|_{L^4(K)} \|\boldsymbol{v}_{h,i} - \boldsymbol{\Pi}_K^{\mathbf{0}}\boldsymbol{v}_{h,i}\|_{L^2(K)} \\ &\qquad + \left\|\frac{\partial \boldsymbol{u}_i}{\partial \boldsymbol{x}_j}\right\|_{L^4(K)} \|(\mathbf{I} - \boldsymbol{\Pi}_K^{\mathbf{0}})\boldsymbol{u}_j\|_{L^2(K)} \|\boldsymbol{\Pi}_K^{\mathbf{0}}\boldsymbol{v}_{h,i}\|_{L^4(K)} \\ &\qquad + \|\boldsymbol{u}_j\|_{L^4(K)} \left\|(\mathbf{I} - \boldsymbol{\Pi}_K^{\mathbf{0},0})\frac{\partial \boldsymbol{u}_i}{\partial \boldsymbol{x}_j}\right\|_{L^4(K)} \|\boldsymbol{\Pi}_K^{\mathbf{0}}\boldsymbol{v}_{h,i}\|_{L^2(K)}\Bigg) \\ &\leq Ch\, |\boldsymbol{u}|_{2,\Omega} \|\nabla \boldsymbol{u}\|_{0,\Omega} \|\nabla \boldsymbol{v}_h\|_{0,\Omega}. \end{aligned}$$

Proceeding in the similar fashion, we can easily obtain the following bounds for $\mathcal{C}_2(\boldsymbol{v}_h)$.

$$\mathcal{C}_2(\boldsymbol{v}_h) \leq Ch|\boldsymbol{u}|_{2,\Omega}\|\nabla \boldsymbol{u}\|_{0,\Omega}\|\nabla \boldsymbol{v}_h\|_{0,\Omega}.$$

Collecting all the bounds of $\mathcal{C}_i(\boldsymbol{v}_h), i=1,2$, we finally obtain the bound (3.3.11). $\square$

3.3.1 Estimates for semi-discrete scheme

We collect all the derived/recalled results to state the estimates below.

Theorem 3.1. *Let $(\boldsymbol{u}(t), p(t)) \in \mathbf{V} \times Q$ and $(\boldsymbol{u}_h(t), p_h(t)) \in \mathbf{V}_h \times Q_h$ be the solutions of continuous problem (3.1.3) and discrete problem (3.2.2) respectively for each $t \in (0, T]$. Assuming the additional regularity $\boldsymbol{u} \in [H^2(\Omega)]^2 \cap \mathbf{V}$ and $p \in H^1(\Omega) \cap Q$, then there exists a positive constant C independent of h such that*

$$\nu \|\boldsymbol{u} - \boldsymbol{u}_h\|^2_{\mathbf{L}^2([H^1(\Omega)]^2)} + \|p - p_h\|^2_{L^2(L^2(\Omega))} \leq C\, h^2. \tag{3.3.12}$$

Proof. Split the error as $(\boldsymbol{u} - \boldsymbol{u}_h)(t) := \boldsymbol{e}_I(t) + \boldsymbol{e}_A(t)$, where $\boldsymbol{e}_I(t) := (\boldsymbol{u} - S_h^{\boldsymbol{u}}\boldsymbol{u})(t)$ and $\boldsymbol{e}_A(t) := (S_h^{\boldsymbol{u}}\boldsymbol{u} - \boldsymbol{u}_h)(t)$. Now since the estimates for $\boldsymbol{e}_I(t)$ are known from Lemma 3.8, we proceed to establish the estimates for term $\boldsymbol{e}_A(t)$.

The error equation with the help of Stokes projection (3.3.8), weak form (3.1.3b) and semi-discrete form (3.2.2b) in terms of $\boldsymbol{e}_A$ is given as

$$\begin{aligned} m_h(\partial_t \boldsymbol{e}_A, \boldsymbol{v}_h) + a_h(\boldsymbol{e}_A, \boldsymbol{v}_h) = (F - F_h)(\boldsymbol{v}_h) + b(\boldsymbol{v}_h, p_h - S_h^p p) \\ - \big(m(\partial_t \boldsymbol{u}, \boldsymbol{v}_h) - m_h(\partial_t S_h^{\boldsymbol{u}}\boldsymbol{u}, \boldsymbol{v}_h)\big) \\ - \big(c(\boldsymbol{u}; \boldsymbol{u}, \boldsymbol{v}_h) - c_h(\boldsymbol{u}_h; \boldsymbol{u}_h, \boldsymbol{v}_h)\big). \end{aligned} \tag{3.3.13}$$

From equations (3.3.8), (3.1.3b) and (3.2.2b), we have for all $q_h \in Q_h$,

$$b(\boldsymbol{e}_A, q_h) = b(\boldsymbol{u} - \boldsymbol{u}_h, q_h) = 0. \tag{3.3.14}$$

Using (3.3.8) and taking $\boldsymbol{v}_h = \boldsymbol{e}_A$ in (3.3.13) together with (3.3.14) implies

$$\begin{aligned} m_h(\partial_t \boldsymbol{e}_A, \boldsymbol{e}_A) + a_h(\boldsymbol{e}_A, \boldsymbol{e}_A) = \underbrace{(F - F_h)(\boldsymbol{e}_A)}_{:=T_1} - \underbrace{\big(m(\partial_t \boldsymbol{u}, \boldsymbol{e}_A) - m_h(\partial_t S_h^{\boldsymbol{u}}\boldsymbol{u}, \boldsymbol{e}_A)\big)}_{:=T_2} \\ - \underbrace{\big(c(\boldsymbol{u}; \boldsymbol{u}, \boldsymbol{e}_A) - c_h(\boldsymbol{u}_h; \boldsymbol{u}_h, \boldsymbol{e}_A)\big)}_{:=T_3}. \end{aligned} \tag{3.3.15}$$

The Cauchy Schwarz inequality, estimate of the projection $\mathbf{\Pi}_K^{\mathbf{0}}$ and Poincaré inequality infer that

$$|T_1| \leq \|\boldsymbol{f} - \boldsymbol{f}_h\|_{0,\Omega} \|\boldsymbol{e}_A\|_{0,\Omega} \leq Ch|\boldsymbol{f}|_{1,\Omega} \|\nabla \boldsymbol{e}_A\|_{0,\Omega}.$$

The consistency of $m_h(\cdot, \cdot)$, use of Cauchy–Schwarz and triangle inequalities, repeated application of estimate for projection $\mathbf{\Pi}_K^{\mathbf{0}}$, and estimate (3.3.10) together with Poincaré inequality enable

$$
\begin{aligned}
T_2 &= \sum_{K\in\mathcal{T}_h} m^K(\partial_t(\mathbf{I}-\boldsymbol{\Pi}_K^{\mathbf{0}})\boldsymbol{u},\boldsymbol{e}_A) - m_h^K(\partial_t(S_h^{\boldsymbol{u}}\boldsymbol{u}-\boldsymbol{\Pi}_K^{\mathbf{0}}\boldsymbol{u}),\boldsymbol{e}_A)\\
&\leq \Big(\sum_{K\in\mathcal{T}_h}(\|\partial_t(\mathbf{I}-\boldsymbol{\Pi}_K^{\mathbf{0}})\boldsymbol{u}\|_{0,K} + \|\partial_t(S_h^{\boldsymbol{u}}\boldsymbol{u}-\boldsymbol{\Pi}_K^{\mathbf{0}}\boldsymbol{u})\|_{0,K})\Big)\|\boldsymbol{e}_A\|_{0,\Omega}\\
&\leq C\,h|\partial_t\boldsymbol{u}|_{1,\Omega}\|\nabla\boldsymbol{e}_A\|_{0,\Omega}.
\end{aligned}
$$

The estimates for term T_3 is quite involved and we proceed by separating the terms as

$$
T_3 = (c(\boldsymbol{u};\boldsymbol{u},\boldsymbol{e}_A) - c_h(\boldsymbol{u};\boldsymbol{u},\boldsymbol{e}_A)) + (c_h(\boldsymbol{u};\boldsymbol{u},\boldsymbol{e}_A) - c_h(\boldsymbol{u}_h;\boldsymbol{u}_h,\boldsymbol{e}_A)) := \sum_{i=1}^{2} T_{3,i}.
$$

The consequence of Lemma 3.9 gives

$$
T_{3,1} \leq C\,h|\boldsymbol{u}|_{2,\Omega}\|\nabla\boldsymbol{u}\|_{0,\Omega}\|\nabla\boldsymbol{e}_A\|_{0,\Omega}.
$$

For $T_{3,2}$, we employ Lemma 3.4, estimate of Stokes projection (3.3.10), stability bound of Stokes projection (3.3.9), continuity of trilinear form $c_h(\cdot,\cdot,\cdot)$, Poincaré inequality and bound (3.1.4) to obtain

$$
\begin{aligned}
T_{3,2} &= c_h(\boldsymbol{u};\boldsymbol{u}-\boldsymbol{u}_h,\boldsymbol{e}_A) + c_h(\boldsymbol{u}-\boldsymbol{u}_h;\boldsymbol{u}_h,\boldsymbol{e}_A)\\
&= c_h(\boldsymbol{u};\boldsymbol{e}_I,\boldsymbol{e}_A) + c_h(u;\boldsymbol{e}_A,\boldsymbol{e}_A) + c_h(\boldsymbol{e}_I;\boldsymbol{u}_h,\boldsymbol{e}_A) + c_h(\boldsymbol{e}_A;\boldsymbol{u}_h,\boldsymbol{e}_A)\\
&= c_h(\boldsymbol{u};\boldsymbol{e}_I,\boldsymbol{e}_A) + c_h(\boldsymbol{e}_I;\boldsymbol{u},\boldsymbol{e}_A) - c_h(\boldsymbol{e}_I;\boldsymbol{e}_I,\boldsymbol{e}_A) + c_h(\boldsymbol{e}_A;\boldsymbol{u},\boldsymbol{e}_A)\\
&\quad + c_h(\boldsymbol{e}_A;\boldsymbol{e}_A,\boldsymbol{e}_A) - c_h(\boldsymbol{e}_A;\boldsymbol{e}_I,\boldsymbol{e}_A)\\
&\leq Ch\|\nabla\boldsymbol{u}\|_{0,\Omega}(|\boldsymbol{u}|_{2,\Omega}+|p|_{1,\Omega})\|\nabla\boldsymbol{e}_A\|_{0,\Omega} + h^2(|\boldsymbol{u}|_{2,\Omega}+|p|_{1,\Omega})^2\|\nabla\boldsymbol{e}_A\|_{0,\Omega}\\
&\quad + \Big(\|\nabla\boldsymbol{u}\|_{0,\Omega}+\|p\|_{0,\Omega}\Big)\|\boldsymbol{e}_A\|_{0,\Omega}^{\frac{1}{2}}\|\nabla\boldsymbol{e}_A\|_{0,\Omega}^{\frac{3}{2}}.
\end{aligned}
$$

Collecting the bounds of $T_{3,i}$, $i=1,2$ and use of Young's inequality, we finally obtain the following bound for T_3.

$$
\begin{aligned}
T_3 &\leq Ch\Big((|\boldsymbol{u}|_{2,\Omega}+|p|_{1,\Omega})(\|\nabla\boldsymbol{u}\|_{0,\Omega}+h|\boldsymbol{u}|_{2,\Omega}+h|p|_{1,\Omega})\Big)\|\nabla\boldsymbol{e}_A\|_{0,\Omega}\\
&\qquad + \Big(\|\nabla\boldsymbol{u}\|_{0,\Omega}+\|p\|_{0,\Omega}\Big)\|\boldsymbol{e}_A\|_{0,\Omega}^{\frac{1}{2}}\|\nabla\boldsymbol{e}_A\|_{0,\Omega}^{\frac{3}{2}}\\
&\leq C\Big(\|\nabla\boldsymbol{u}\|_{0,\Omega}+\|p\|_{0,\Omega}\Big)^2\|\nabla\boldsymbol{e}_A\|_{0,\Omega}\|\boldsymbol{e}_A\|_{0,\Omega} + \frac{\nu}{4}\|\nabla\boldsymbol{e}_A\|_{0,\Omega}^2
\end{aligned}
$$

$$\leq C\Big(\|\nabla \boldsymbol{u}\|_{0,\Omega}+\|p\|_{0,\Omega}\Big)^4\|\boldsymbol{e}_A\|_{0,\Omega}^2+\frac{\nu}{2}\|\nabla \boldsymbol{e}_A\|_{0,\Omega}^2. \tag{3.3.16}$$

On substituting the bounds of T_1, T_2 and T_3 in (3.3.15) and applying the Young's inequality, we arrive at

$$\frac{1}{2}\frac{d}{dt}\|\boldsymbol{e}_A\|_{0,\Omega}^2+\frac{\nu}{2}\|\nabla \boldsymbol{e}_A\|_{0,\Omega}^2\leq C\Big(h^2+\Big(\|\nabla \boldsymbol{u}\|_{0,\Omega}+\|p\|_{0,\Omega}\Big)^4\|\boldsymbol{e}_A\|_{0,\Omega}^2\Big).$$

Now integrating over time from 0 to t then taking $\boldsymbol{u}_h(0):=\boldsymbol{u}_I(0)$, we get

$$\begin{aligned}\|\boldsymbol{e}_A(t)\|_{0,\Omega}^2+\nu\int_0^t\|\nabla \boldsymbol{e}_A(s)\|_{0,\Omega}^2\,\mathrm{d}s&\leq\|\boldsymbol{e}_A(0)\|_{0,\Omega}^2\\ +C\Big(h^2+\int_0^t\Big(\|\nabla \boldsymbol{u}(s)\|_{0,\Omega}+\|p(s)\|_{0,\Omega}\Big)^4\|\boldsymbol{e}_A(s)\|_{0,\Omega}^2\,\mathrm{d}s\Big).\end{aligned}$$

An application of Gronwall's lemma together with the additional regularities of $\boldsymbol{u}$ and p yields

$$\|\boldsymbol{e}_A(t)\|_{0,\Omega}^2+\nu\int_0^t\|\nabla \boldsymbol{e}_A(s)\|_{0,\Omega}^2\,\mathrm{d}s\leq Ch^2. \tag{3.3.17}$$

For pressure estimates, we split the error again in terms of Stokes projection as: $(p-p_h)(t)=(p-S_h^p p)(t)+(S_h^p p-p_h)(t):=e_S(t)+e_Q(t)$, and then proceed to derive estimate for $e_Q(t)$.

Now, an application of discrete inf-sup condition from Lemma 3.7 implies

$$\beta_h\|e_Q\|_{0,\Omega}\leq\sup_{\boldsymbol{v}_h\in\mathbf{V}_h\setminus\{0\}}\frac{b(\boldsymbol{v}_h,e_Q)}{\|\boldsymbol{v}_h\|_{1,\Omega}}. \tag{3.3.18}$$

From equations (3.1.3), (3.2.2) and (3.3.8), we get

$$\begin{aligned}b(\boldsymbol{v}_h,e_Q)&=a_h(\boldsymbol{e}_A,\boldsymbol{v}_h)+(\boldsymbol{f}-\boldsymbol{f}_h,\boldsymbol{v}_h)+\big(m_h(\partial_t\boldsymbol{u}_h,\boldsymbol{v}_h)-m(\partial_t\boldsymbol{u},\boldsymbol{v}_h)\big)\\&\quad+\big(c_h(\boldsymbol{u}_h;\boldsymbol{u}_h,\boldsymbol{v}_h)-c(\boldsymbol{u};\boldsymbol{u},\boldsymbol{v}_h)\big).\end{aligned}$$

The inequality (3.3.18) and integration from 0 to t implies

$$\begin{aligned}\int_0^t\|e_Q(s)\|_{0,\Omega}^2\,\mathrm{d}s\leq C\int_0^t\Big(&\|\boldsymbol{e}_A(s)\|_{1,\Omega}^2+\|(\boldsymbol{f}-\boldsymbol{f}_h)(s)\|_{0,\Omega}^2\\&+\|\partial_t(\boldsymbol{u}-\boldsymbol{u}_h)(s)\|_{0,\Omega}^2+\|\partial_t(\boldsymbol{u}-\boldsymbol{\Pi}_K^{\mathbf{0}}\boldsymbol{u})(s)\|_{0,\Omega}^2\end{aligned}$$

$$+\frac{1}{\|\boldsymbol{v}_h\|_{1,\Omega}^2}\Big(c_h(\boldsymbol{u}_h;\boldsymbol{u}_h,\boldsymbol{v}_h)-c(\boldsymbol{u};\boldsymbol{u},\boldsymbol{v}_h)\Big)^2\Big)\,\mathrm{d}s. \quad (3.3.19)$$

The following bound for $\partial_t \boldsymbol{e}_A$ is achieved by differentiating the error equation (3.3.13) with respect to time, choosing $\boldsymbol{v}_h = \partial_t \boldsymbol{e}_A$ and then imitating the proof of (3.3.17) analogously to obtain,

$$\|\partial_t \boldsymbol{e}_A\|_{0,\Omega}^2 + \nu \int_0^t \|\nabla(\partial_t \boldsymbol{e}_A)(s)\|_{0,\Omega}^2\, ds \leq Ch^2. \quad (3.3.20)$$

Use of triangle's inequality, bound of T_3 (3.3.16), estimate (3.3.20) and bound (3.3.19) with estimate from Lemma 3.8, the desired result follows. □

3.3.2 Estimates for fully-discrete scheme

Following analogously to the semi-discrete scheme in this section, we provide a sketch of the proof estimating the total error occurred through time discretization (by employing the backward Euler scheme) and space discretization. We introduce the following discrete l^2-norm for any bounded function $v(t) \in H^m(\Omega)$ on interval $[0,T]$ as

$$\|v\|_{l^2(H^m(\Omega))}^2 = \|v\|_{l^2(0,T;H^m(\Omega))}^2 := \sum_{i=1}^{N} (\Delta t)\|v(t_i)\|_{H^m(\Omega)}^2, \quad t_i = i\ \Delta t.$$

Theorem 3.2. *Let $(\boldsymbol{u}^n, p^n) \in \mathbf{V} \times Q$ and $(\boldsymbol{u}_h^n, p_h^n) \in \mathbf{V}_h \times Q_h$ be the solutions of the continuous problem* (3.1.3) *and fully discrete problem* (3.2.4)*, respectively for each $n = 1, \ldots, N$. Assuming the additional regularity that $\boldsymbol{u} \in [H^2(\Omega)]^2 \cap \mathbf{V}$ and $p \in H^1(\Omega) \cap Q$ then,*

$$\nu\|\boldsymbol{u} - \boldsymbol{u}_h\|_{\boldsymbol{l}^2([H^1(\Omega)]^2)}^2 + \|p - p_h\|_{l^2(L^2(\Omega))}^2 \leq C(h^2 + \Delta t^2), \quad (3.3.21)$$

for constant C independent of h.

Proof. Decompose the error as: $\boldsymbol{u}^n - \boldsymbol{u}_h^n = E_I^n + E_A^n$, where

$$E_I^n := \boldsymbol{u}^n - S_h^{\boldsymbol{u}}\boldsymbol{u}^n \quad \text{and} \quad E_A^n := S_h^{\boldsymbol{u}}\boldsymbol{u}^n - \boldsymbol{u}_h^n.$$

Using the estimates of Stokes projection in Lemma 3.8 at each time t_n, one obtains

$$\|E_I^n\|_{0,\Omega} + h\|\nabla E_I^n\|_{1,\Omega} \leq Ch^2(|\boldsymbol{u}^n|_{2,\Omega} + |p^n|_{1,\Omega}).$$

We proceed to obtain the estimates E_A^n. The following error equation in terms of E_A^n can be easily written with the help of Stokes projection (3.3.8), weak form (3.1.3) and fully discrete form (3.2.4).

$$\begin{aligned} m_h(\delta_t E_A^n, \boldsymbol{v}_h) + a_h(E_A^n, \boldsymbol{v}_h) = &(F^n - F_h^n)(\boldsymbol{v}_h) + b(\boldsymbol{v}_h, p_h^n - S_h^p p^n) \\ &+ \big(a_h(S_h^{\boldsymbol{u}}\boldsymbol{u}^n, \boldsymbol{v}_h) - a(\boldsymbol{u}^n, \boldsymbol{v}_h)\big) \\ &+ (m_h(\delta_t(S_h^{\boldsymbol{u}}\boldsymbol{u}^n), \boldsymbol{v}_h) - m(\partial_t \boldsymbol{u}^n, \boldsymbol{v}_h)) \\ &+ (c(\boldsymbol{u}^n; \boldsymbol{u}^n, \boldsymbol{v}_h) - c_h(\boldsymbol{u}_h^n; \boldsymbol{u}_h^n, \boldsymbol{v}_h)). \end{aligned} \tag{3.3.22}$$

Choosing $\boldsymbol{v}_h = E_A^n$, and using coercivity of $m_h(\cdot,\cdot)$ and $a_h(\cdot,\cdot)$, we infer that

$$\begin{aligned} &\frac{1}{2\Delta t}\big(\|E_A^n\|_{0,\Omega}^2 - \|E_A^{n-1}\|_{0,\Omega}^2\big) + \nu\|\nabla E_A^n\|_{0,\Omega}^2 \\ &\lesssim (m_h(\delta_t(S_h^{\boldsymbol{u}}\boldsymbol{u}^n), E_A^n) - m(\partial_t \boldsymbol{u}^n, E_A^n)) + (F^n - F_h^n)(E_A^n) \\ &\quad + \big(a_h(S_h^{\boldsymbol{u}}\boldsymbol{u}^n, E_A^n) - a(\boldsymbol{u}^n, E_A^n)\big) + (c(\boldsymbol{u}^n; \boldsymbol{u}^n, E_A^n) - c_h(\boldsymbol{u}_h^n; \boldsymbol{u}_h^n, E_A^n)). \end{aligned}$$

Multiplying the above inequality with Δt and then summing over n gives

$$\begin{aligned} &\frac{1}{2}\big(\|E_A^n\|_{0,\Omega}^2 - \|E_A^0\|_{0,\Omega}^2\big) + \nu\Delta t\sum_{j=1}^{n}\|\nabla E_A^j\|_{0,\Omega}^2 \\ &\lesssim \sum_{j=1}^{n}\Big(m_h\left(S_h^{\boldsymbol{u}}\boldsymbol{u}^j - S_h^{\boldsymbol{u}}\boldsymbol{u}^{j-1}, E_A^j\right) - (\Delta t)m(\partial_t \boldsymbol{u}^j, E_A^j)\Big) \\ &\quad + (\Delta t)\sum_{j=1}^{n}(F^j - F_h^j)(E_A^j) + (\Delta t)\sum_{j=1}^{n}\big(a_h(S_h^{\boldsymbol{u}}\boldsymbol{u}^j, E_A^j) - a(\boldsymbol{u}^j, E_A^j)\big) \\ &\quad + (\Delta t)\sum_{j=1}^{n}(c(\boldsymbol{u}^j; \boldsymbol{u}^j, E_A^j) - c_h(\boldsymbol{u}_h^j; \boldsymbol{u}_h^j, E_A^j)) := \sum_{i=1}^{4} G_i. \end{aligned} \tag{3.3.23}$$

Use of the polynomial approximation $\boldsymbol{\Pi}_K^{\mathbf{0}}\boldsymbol{u}$, Cauchy-Schwarz inequality and Taylor's expansion for any continuous function $f(t)$ is

$$f^j - f^{j-1} = (\Delta t)\partial_t f^j + \int_{t_{j-1}}^{t_j}(s - t_{j-1})\partial_{tt} f(s)\,\mathrm{d}s,$$

and thus implies

$$
\begin{aligned}
G_1 = \sum_{j=1}^{n} \Big(&\sum_{K\in\mathcal{T}_h} m_h^K((S_h^{\boldsymbol{u}}\boldsymbol{u}^j - S_h^{\boldsymbol{u}}\boldsymbol{u}^{j-1}) - \boldsymbol{\Pi}_K^{\mathbf{0}}(\boldsymbol{u}^j - \boldsymbol{u}^{j-1}), E_A^j) \\
&+ m^K(\boldsymbol{\Pi}_K^{\mathbf{0}}(\boldsymbol{u}^j - \boldsymbol{u}^{j-1}) - (\Delta t)\partial_t \boldsymbol{u}(t_j), E_A^j)\Big) \\
\le C \sum_{j=1}^{n} &\left(h|\boldsymbol{u}^j - \boldsymbol{u}^{j-1}|_{1,\Omega} + \left\|(\boldsymbol{u}^j - \boldsymbol{u}^{j-1}) - (\Delta t)\partial_t \boldsymbol{u}^j\right\|_{0,\Omega}\right) \|E_A^j\|_{0,\Omega} \\
\le C \sum_{j=1}^{n} &\left(h \left((\Delta t) \int_{t_{j-1}}^{t_j} |\partial_t \boldsymbol{u}(s)|_{1,\Omega}^2 \,\mathrm{d}s \right)^{1/2} \right. \\
&\left. + \Delta t \left((\Delta t) \int_{t_{j-1}}^{t_j} \|\partial_{tt} \boldsymbol{u}(s)\|_{0,\Omega}^2 \,\mathrm{d}s \right)^{1/2} \right) \left((\Delta t)\ \|E_A^j\|_{0,\Omega}^2 \right)^{1/2} \\
\le C(\Delta t)^{1/2} &\big(h\|\partial_t \boldsymbol{u}\|_{\mathbf{L}^2([H^1(\Omega)]^2)} + (\Delta t)\|\partial_{tt}\boldsymbol{u}\|_{\mathbf{L}^2([L^2(\Omega)]^2)}\big)\|E_A\|_{\boldsymbol{l}^2([L^2(\Omega)]^2)}.
\end{aligned}
$$

The bounds for other terms, i.e., $G_i, i = 2,3,4$ can be easily obtained as we have estimated the terms $T_i, 1 \le 3$ in the proof of Theorem 3.1. Now collecting all the bounds of G_i in (3.3.23), we conclude that

$$
\begin{aligned}
\sum_{i=2}^{4} G_i \lesssim{}& (h + \Delta t)\|E_A\|_{\boldsymbol{l}^2([H^1(\Omega)]^2)} \\
&+ \left((\Delta t) \sum_{j=1}^{n} \left(h(|\boldsymbol{u}^j|_{2,\Omega} + h|p^j|_{1,\Omega}) + \|\nabla \boldsymbol{u}(t_j)\|_{0,\Omega} \right) \right. \\
&\left. \times \|E_A^j\|_{0,\Omega}^{\frac{1}{2}} \|\nabla E_A^j\|_{0,\Omega}^{\frac{1}{2}} \right) \|E_A\|_{\boldsymbol{l}^2([H^1(\Omega)]^2)}.
\end{aligned}
$$

Choosing $\boldsymbol{u}_h^0 := \boldsymbol{u}_I^0$ and employing the Young's inequality, we finally arrive at

$$
\begin{aligned}
&\frac{1}{2}\|E_A^n\|_{0,\Omega}^2 + \frac{\nu}{2}\ \|E_A\|_{\boldsymbol{l}^2([H^1(\Omega)]^2)}^2 \\
&\quad \lesssim h^2 + \Delta t^2 + \Delta t \sum_{j=1}^{n} \left(h(|\boldsymbol{u}^j|_{2,\Omega} + h|p^j|_{1,\Omega}) + \|\nabla \boldsymbol{u}^j\|_{0,\Omega} \right)^4 \|E_A^j\|_{0,\Omega}^2.
\end{aligned}
$$

Now an application of the triangle's inequality and discrete Gronwall's lemma [75] concludes (3.3.21).

Proceeding analogously to the semi-discrete case, the estimates for pressure can be easily obtained by writing the error equations in terms of $E_Q^n := S_h^p p^n - p_h^n$ and

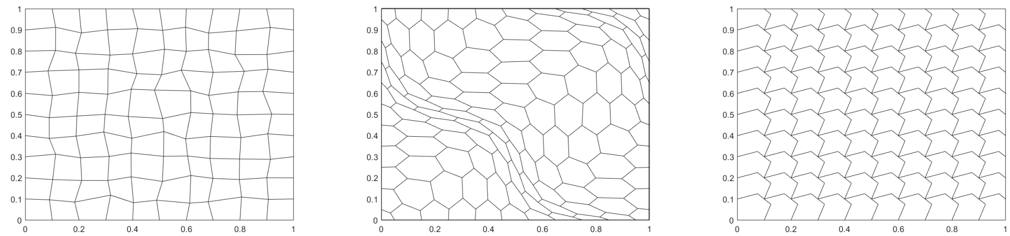

(a) (b) (c)

Figure 3.1: Samples of (a) Distorted square, (b) Distorted hexagonal, and (c) Non-convex meshes employed for the numerical tests in this section.

employing the inf-sup condition together with the properties of discrete forms $a_h(\cdot,\cdot)$, $b_h(\cdot,\cdot)$ and $c_h(\cdot;\cdot,\cdot)$ (also refer to [117, 115, 76]). □

3.4 Numerical tests

In this section, we illustrate the numerical verification of the theoretical rate of convergence of the proposed method. In order to see the computational efficiency of the VE methods used for space discretizations, we have considered here three different meshes: distorted square, distorted hexagonal, and non-convex mesh (see Fig. 3.1). After employing the backward Euler method (for time discretization) and the proposed VEMs, the resultant non-linear system of equations is solved by Newton's method. We compute the error for velocity and pressure in the following norms.

$$E_1(\boldsymbol{u}) := \Big(\sum_{K\in\mathcal{T}_h} \|\boldsymbol{\nabla}(\boldsymbol{u}-\boldsymbol{\Pi}_K^{\boldsymbol{\nabla}}\boldsymbol{u}_h)\|_{0,K}^2\Big)^{\frac{1}{2}},\ E_0(\boldsymbol{u}) := \Big(\sum_{K\in\mathcal{T}_h} \|\boldsymbol{u}-\boldsymbol{\Pi}_K^{\boldsymbol{0}}\boldsymbol{u}_h\|_{0,K}^2\Big)^{\frac{1}{2}}$$

$$\text{and} \qquad E_0(p) := \Big(\sum_{K\in\mathcal{T}_h} \|p-p_h\|_{0,K}^2\Big)^{\frac{1}{2}}.$$

For assessing the experimental convergence of the proposed scheme applied to (3.1.1) defined over domain $\Omega = (0,1)^2$, we consider the exact velocity of the fluid flow and pressure as follows.

$$p = t\Big(x^3y^3 - \frac{1}{16}\Big),$$

Ndof	h^{-1}	$E_1(\boldsymbol{u})$	$r_1(\boldsymbol{u})$	$E_0(\boldsymbol{u})$	$r_0(\boldsymbol{u})$	$E_0(p)$	$r_0(p)$
222	4	0.0108080	-	0.0024850	-	0.0295061	-
842	8	0.0060613	0.83	0.0010103	1.30	0.0174711	0.76
3282	16	0.0031157	0.96	0.0003372	1.58	0.0092992	0.91
12962	32	0.0015168	1.04	0.0000972	1.79	0.0047183	0.98
51522	64	0.0007375	1.04	0.0000260	1.90	0.0023658	1.00

Table 3.1: Errors and convergence rates r for fluid velocity and pressure.

$$\boldsymbol{u} = t^2 \begin{bmatrix} x^2(1-x)^4y^2(1-y)(3-5y) \\ -2x(1-x)^3(1-3x)y^3(1-y)^2 \end{bmatrix}.$$

Then the load function $\boldsymbol{f}$ is enforced from the equation (3.1.1). Moreover, we have taken viscosity $\nu = 1$, time step $\Delta t = 0.01$ and final time $T = 1$. The Table 3.1 displays the computed order of convergence (r) for velocity and pressure in the estimated errors $E_1(\boldsymbol{u})$, $E_0(\boldsymbol{u})$ and $E_0(p)$.

The computed order of convergence for all three meshes are reported in Fig. 3.2. From Table 3.1 and Figure 3.2, we observe that the computed and theoretical rate of convergence are in good agreement irrespective of the mesh type.

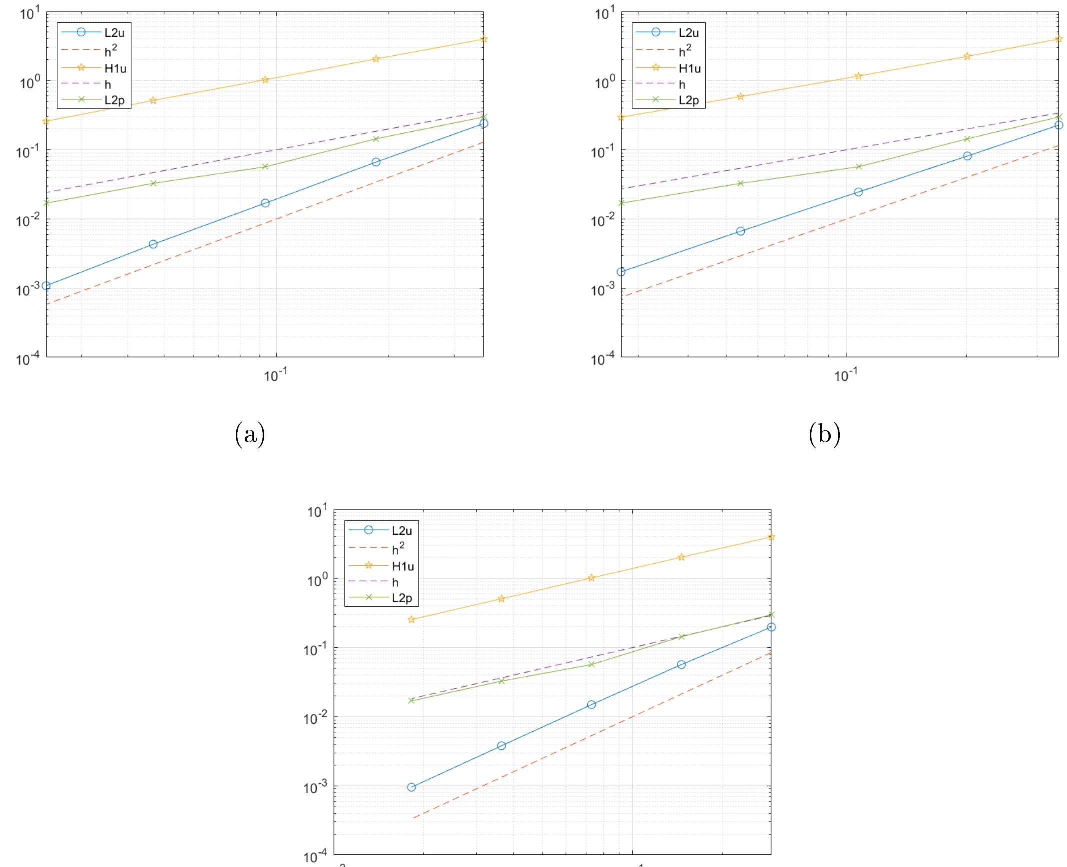

(a)

(b)

(c)

Figure 3.2: Convergence in space for three different meshes: (a) Distorted square, (b) Distorted Hexagonal, and (c) Non-convex mesh.

Chapter 4

Poroelasticity equations

In this chapter, by following [103], we propose a VE formulation for the numerical approximation of the transient linear poroelasticity problem. VE spaces proposed for displacement and total pressure form a stable pair, and these can be regarded as a generalization of the Bernardi-Raugel finite elements (piecewise linear elements enriched with bubbles normal to the faces for the displacement components, and piecewise constant approximations for total pressure, see, e.g., [67]). On the other hand, no compatibility between the spaces for total pressure and fluid pressure is needed. Therefore for the fluid pressure, we employ the enhanced VE space from [118, 25, 26], which allows us to construct a suitable projector onto piecewise linear functions. All this is restricted, for sake of simplicity, to the lowest-order 2D case, but one could extend the analysis to higher polynomial degrees and the 3D case, for instance, considering the discrete inf-sup stable pair from [30] for the Stokes problem. The main difficulties in our analysis lie in the definition of an adequate projection operator that allows treating the time-dependent problem. To handle this issue, we have combined Stokes-like and elliptic operators that constitute the new map here named poroelastic projector. We derive stability for semi-discrete and fully-discrete approximations and establish the optimal convergence of the VE scheme in the natural norms. These bounds turn to be robust with respect to the dilation modulus of the deformable porous structure (which tends to infinity as the Poisson ratio approaches 0.5) and of the specific storage coefficient (reaching very small values in some regimes), and therefore the method is considered locking-free. A further advantage of the proposed virtual discretization is that it combines primal and mixed VE spaces. In addition, this work can be seen as a stepping stone in the study of more complex coupled problems, including interface poroelastic phenomena and multiphysics (see, for instance, [119, 120, 109]).

We have arranged the contents of this chapter as follows. Section 4.1 is devoted to the definition of linear poroelasticity problem, and it also contains the precise definition of the continuous weak formulation using three fields and presents a few preliminary results needed in the semi-discrete analysis as well. In Section 4.2, we introduce the VE approximation in semi-discrete form. We specify the VE spaces, identify the degrees of freedom, and derive appropriate estimates for the discrete bilinear forms. The *a priori* error analysis has been derived in Section 4.3, with the help of the newly introduced poroelastic projection operator. The implementation of this problem on different families of polygonal meshes is then discussed in Section 4.4, where we confirm the theoretical rates of convergence and produce some applicative tests to gain insight into the behavior of the model problem.

4.1 Governing equations and their variational formulations

4.1.1 Strong form

A deformable porous medium is assumed to occupy the domain Ω, where Ω is an open and bounded set in $\mathbb{R}^2$ (simply for sake of notational convenience) with a Lipschitz continuous boundary $\partial\Omega$. The mathematical description of this interaction between deformation and flow can be placed in the context of the classical Biot problem, written as follows (see for instance, the exposition in [121]). In the absence of gravitational forces, and for a given body load $\boldsymbol{b}(t) : \Omega \to \mathbb{R}^2$ and a volumetric source or sink $\ell(t) : \Omega \to \mathbb{R}$, one seeks, for each time $t \in (0, T]$, the vector of displacements of the porous skeleton, $\boldsymbol{u}^s(t) : \Omega \to \mathbb{R}^2$, and the pore pressure of the fluid, $p(t) : \Omega \to \mathbb{R}$, satisfying the mass conservation of the fluid content and momentum balance equations

$$\left.\begin{aligned} \partial_t(c_0 p^f + \alpha \operatorname{div} \boldsymbol{u}^s) - \frac{1}{\eta} \operatorname{div}\big(\kappa(\boldsymbol{x})\nabla p\big) = \ell \\ -\operatorname{\mathbf{div}}\big(\lambda(\operatorname{div} \boldsymbol{u}^s)\mathbf{I} + 2\mu\boldsymbol{\varepsilon}(\boldsymbol{u}^s) - \alpha p^f \mathbf{I}\big) = \rho \boldsymbol{b} \end{aligned}\right\} \quad \text{in } \Omega \times (0, T],$$

where $\kappa(\boldsymbol{x})$ is the hydraulic conductivity of the porous medium (the mobility matrix, possibly anisotropic), ρ is the density of solid material, η is the constant viscosity of the interstitial fluid, c_0 is the constrained specific storage coefficient (typically small and representing the amount of fluid that can be injected during an increase of pressure maintaining a constant bulk volume), α is the Biot-Willis consolidation parameter (typically close to one), and μ and λ are the shear and dilation moduli associated with the constitutive law of the solid structure. The total stress

$$\boldsymbol{\sigma} = \lambda(\operatorname{div}\boldsymbol{u}^s)\mathbf{I} + 2\mu\boldsymbol{\varepsilon}(\boldsymbol{u}^s) - \alpha p^f\mathbf{I},$$

includes a contribution from the effective mechanical stress of a Hookean elastic material, $\boldsymbol{\sigma}_{\text{eff}} = \lambda(\operatorname{div}\boldsymbol{u}^s)\mathbf{I} + 2\mu\boldsymbol{\varepsilon}(\boldsymbol{u}^s)$, and the non-viscous fluid stress represented only by the pressure scaled with α. As in [95, 103], we consider here the volumetric part of the total stress ψ, hereafter called *total pressure*, as one of the primary variables. This property allows us to rewrite the time-dependent problem as

$$\left.\begin{aligned} -\mathbf{div}\big(2\mu\boldsymbol{\varepsilon}(\boldsymbol{u}^s) - \psi\mathbf{I}\big) &= \rho\boldsymbol{b} \\ \left(c_0 + \frac{\alpha^2}{\lambda}\right)\partial_t p^f - \frac{\alpha}{\lambda}\partial_t\psi - \frac{1}{\eta}\operatorname{div}(\kappa\nabla p^f) &= \ell \\ \psi - \alpha p^f + \lambda\operatorname{div}\boldsymbol{u}^s &= 0 \end{aligned}\right\} \quad \text{in } \Omega\times(0,T], \tag{4.1.1}$$

which we endow with appropriate initial data

$$p^f(0) = p^{f,0}, \quad \boldsymbol{u}^s(0) = \boldsymbol{u}^{s,0} \quad \text{in } \Omega\times\{0\},$$

(which, in turn, can be used to set the initial condition for the total pressure $\psi(0)$), and mixed-type boundary conditions in the following manner

$$\boldsymbol{u}^s = \mathbf{0} \quad \text{and} \quad \frac{\kappa}{\eta}\nabla p^f\cdot\boldsymbol{n} = 0 \qquad \text{on } \Gamma\times(0,T], \tag{4.1.2a}$$

$$\big(2\mu\boldsymbol{\varepsilon}(\boldsymbol{u}^s) - \psi\,\mathbf{I}\big)\boldsymbol{n} = \mathbf{0} \quad \text{and} \quad p^f = 0 \qquad \text{on } \Sigma\times(0,T], \tag{4.1.2b}$$

where the boundary $\partial\Omega = \Gamma\cup\Sigma$ is disjointly split into Γ and Σ where we prescribe clamped boundaries and zero fluid normal fluxes; and zero (total) traction together with constant fluid pressure, respectively. Homogeneity of the boundary conditions is only assumed to simplify the exposition of the analysis.

4.1.2 Weak formulation

In order to obtain a weak form (in space) for (4.1.1), we define the function spaces

$$\mathbf{V} := [H^1_\Gamma(\Omega)]^2,\ Q := H^1_\Sigma(\Omega),\ Z := L^2(\Omega).$$

Multiplying (4.1.1) by adequate test functions, integrating by parts (in space) whenever appropriate, and using the boundary conditions (4.1.2), leads to the following variational problem: For a given $t > 0$, find $\boldsymbol{u}^s(t) \in \mathbf{V}$, $p^f(t) \in Q$ and $\psi(t) \in Z$ such that

$$a_1(\boldsymbol{u}^s, \boldsymbol{v}^s) + b_1(\boldsymbol{v}^s, \psi) = F(\boldsymbol{v}^s) \quad \forall \boldsymbol{v}^s \in \mathbf{V}, \tag{4.1.3a}$$

$$\tilde{a}_2(\partial_t p^f, q^f) + a_2(p^f, q^f) - b_2(q^f, \partial_t \psi) = G(q^f) \quad \forall q^f \in Q, \tag{4.1.3b}$$

$$b_1(\boldsymbol{u}^s, \phi) + b_2(p^f, \phi) - a_3(\psi, \phi) = 0 \quad \forall \phi \in Z, \tag{4.1.3c}$$

where the bilinear forms $a_1 : \mathbf{V} \times \mathbf{V} \to \mathbb{R}$, $a_2 : Q \times Q \to \mathbb{R}$, $a_3 : Z \times Z \to \mathbb{R}$, $b_1 : \mathbf{V} \times Z \to \mathbb{R}$, $b_2 : Q \times Z \to \mathbb{R}$, and linear functionals $F : \mathbf{V} \to \mathbb{R}$, $G : Q \to \mathbb{R}$, are given by the following expressions:

$$\begin{aligned}
&a_1(\boldsymbol{u}^s, \boldsymbol{v}^s) := 2\mu \int_\Omega \boldsymbol{\varepsilon}(\boldsymbol{u}^s) : \boldsymbol{\varepsilon}(\boldsymbol{v}^s), \quad b_1(\boldsymbol{v}^s, \phi) := -\int_\Omega \phi \operatorname{div} \boldsymbol{v}^s,\\
&F(\boldsymbol{v}^s) := \int_\Omega \rho \boldsymbol{b} \cdot \boldsymbol{v}^s, \quad G(q^f) := \int_\Omega \ell\, q^f, \quad \tilde{a}_2(p^f, q^f) := \left(c_0 + \frac{\alpha^2}{\lambda}\right) \int_\Omega p^f q^f,\\
&a_2(p^f, q^f) := \frac{1}{\eta} \int_\Omega \kappa \nabla p^f \cdot \nabla q^f, \quad b_2(p^f, \phi) := \frac{\alpha}{\lambda} \int_\Omega p^f \phi, \quad a_3(\psi, \phi) := \frac{1}{\lambda} \int_\Omega \psi\phi.
\end{aligned} \tag{4.1.4}$$

4.1.3 Properties of the bilinear forms and linear functionals

We now list the continuity, coercivity, and inf-sup conditions for the variational forms in (4.1.4). These are employed in [103] to derive the well-posedness of the stationary form of (4.1.1).

First we have the bounds

$$a_1(\boldsymbol{u}^s, \boldsymbol{v}^s) \leq 2\mu \|\boldsymbol{\varepsilon}(\boldsymbol{u}^s)\|_{0,\Omega} \|\boldsymbol{\varepsilon}(\boldsymbol{v}^s)\|_{0,\Omega} \leq C \|\boldsymbol{u}^s\|_{1,\Omega} \|\boldsymbol{v}^s\|_{1,\Omega} \qquad \text{for all } \boldsymbol{u}^s, \boldsymbol{v}^s \in \mathbf{V},$$

$$b_1(\boldsymbol{v}^s, \phi) \leq \|\operatorname{div} \boldsymbol{v}^s\|_{0,\Omega} \|\phi\|_{0,\Omega} \leq C \|\boldsymbol{v}^s\|_{1,\Omega} \|\phi\|_{0,\Omega} \qquad \text{for all } \boldsymbol{v}^s \in \mathbf{V} \text{ and } \phi \in Z,$$

$$a_2(p^f, q^f) \leq \frac{\kappa_{\max}}{\eta} |p^f|_{1,\Omega} |q^f|_{1,\Omega} \leq \frac{\kappa_{\max}}{\eta} \|p^f\|_{1,\Omega} \|q^f\|_{1,\Omega} \qquad \text{for all } p^f, q^f \in Q,$$

$$b_2(q^f,\phi) \leq \frac{\alpha}{\lambda}\|q^f\|_{0,\Omega}\|\phi\|_{0,\Omega}, \quad a_3(\psi,\phi) \leq \frac{1}{\lambda}\|\psi\|_{0,\Omega}\|\phi\|_{0,\Omega} \qquad \text{for all } q^f \in Q \text{ and } \psi,\phi \in Z,$$
$$F(\boldsymbol{v}^s) \leq \rho\|\boldsymbol{b}\|_{0,\Omega}\|\boldsymbol{v}^s\|_{0,\Omega}, \quad G(q^f) \leq \|\ell\|_{0,\Omega}\|q^f\|_{0,\Omega} \qquad \text{for all } \boldsymbol{v}^s \in \mathbf{V} \text{ and } q^f \in Q,$$

along with the coercivity of the diagonal bilinear forms, i.e.,

$$\begin{aligned}
a_1(\boldsymbol{v}^s,\boldsymbol{v}^s) &= 2\mu\|\boldsymbol{\varepsilon}(\boldsymbol{v}^s)\|_{0,\Omega}^2 \geq C\|\boldsymbol{v}^s\|_{1,\Omega}^2 && \text{for all } \boldsymbol{v}^s \in \mathbf{V},\\
a_2(q^f,q^f) &\geq \frac{\kappa_{\min}}{\eta}\|q^f\|_{1,\Omega}^2 && \text{for all } q^f \in Q,\\
a_3(\phi,\phi) &= \frac{1}{\lambda}\|\phi\|_{0,\Omega}^2 && \text{for all } \phi \in Z,
\end{aligned}$$

and the following inf-sup condition: there exists a constant $\beta > 0$ such that

$$\sup_{\boldsymbol{v}^s \in \mathbf{V}\setminus\{0\}} \frac{b_1(\boldsymbol{v}^s,\phi)}{\|\boldsymbol{v}^s\|_{1,\Omega}} \geq \beta\|\phi\|_{0,\Omega} \quad \text{for all } \phi \in Z.$$

The solvability of the continuous problem is not the focus here, and we refer to [121] for the corresponding well-posedness and regularity results.

4.2 Virtual element approximation

4.2.1 Discrete spaces and degrees of freedom

In this section we construct a VEM associated with (4.1.3). We start denoting by $\{\mathcal{T}_h\}_h$ a sequence of partitions of the domain Ω into general polygons K (open and simply connected sets whose boundary ∂K is a non-intersecting poly-line consisting of a finite number of straight-line segments) having diameter h_K, and define as mesh size $h := \max_{K\in\mathcal{T}_h} h_K$. By N_K^v we denote the number of vertices in the polygon K, N_K^e stands for the number of edges on ∂K, and e is a generic edge of $\mathcal{T}_h$. For all $e \in \partial K$, we denote by $\boldsymbol{n}_K^e$ the unit normal pointing outwards K and by $\boldsymbol{t}_K^e$ the unit tangent vector along e on K, and V_i represents the i^{th} vertex of the polygon K. As in [18], and mentioned in Chapter 2, we assume regularity of the polygonal meshes $\mathcal{T}_h$.

Denoting by $\mathbb{P}_k(K)$ the space of polynomials of degree up to k, defined locally on $K \in \mathcal{T}_h$, we proceed to characterize the scalar energy projection operator Π_K^{∇} :

$H^1(K) \to \mathbb{P}_1(K)$ by the relations

$$\big(\nabla(\Pi_K^{\nabla} q - q), \nabla r\big)_{0,K} = 0, \qquad P_K^0(\Pi_K^{\nabla} q - q) = 0, \tag{4.2.1}$$

valid for all $q \in H^1(K)$ and $r \in \mathbb{P}_1(K)$, and where $(\cdot,\cdot)_{0,K}$ denotes the L^2-product on K, and

$$P_K^0(q) := \int_{\partial K} q \,\mathrm{d}s.$$

If we now denote by $\mathcal{M}_k(K)$ the space of monomials of degree up to k, defined locally on $K \in \mathcal{T}_h$, we can define, on each polygon $K \in \mathcal{T}_h$, the local VE spaces for displacement, fluid pressure, and total pressure, as

$$\begin{aligned}
\mathbf{V}_h(K) &:= \left\{ \boldsymbol{v}_h \in [H^1(K)]^2 \cap \mathcal{B}(\partial K) : \begin{cases} (-\Delta \boldsymbol{v}_h - \nabla s)|_K = \mathbf{0}, \\ \operatorname{div} \boldsymbol{v}_h = c_d \in \mathbb{P}_0(K) \end{cases} \text{for some } s \in L^2(K) \right\}, \\
Q_h(K) &:= \big\{ q_h \in H^1(K) \cap C^0(\partial K) : \; q_h|_e \in \mathbb{P}_1(e) \; \forall e \in \partial K, \; \Delta q_h|_K \in \mathbb{P}_1(K), \\
&\qquad\qquad (\Pi_K^{\nabla} q_h - q_h, m_\alpha)_{0,K} = 0 \; \forall m_\alpha \in \mathcal{M}_1(K) \big\}, \\
Z_h(K) &:= \mathbb{P}_0(K),
\end{aligned} \tag{4.2.2}$$

where we define

$$\mathcal{B}(\partial K) := \big\{ \boldsymbol{v}_h \in [C^0(\partial K)]^2 : \boldsymbol{v}_h|_e \cdot \boldsymbol{t}_K^e \in \mathbb{P}_1(e), \boldsymbol{v}_h|_e \cdot \boldsymbol{n}_K^e \in \mathbb{P}_2(e) \quad \forall e \in \partial K \big\}.$$

It is clear from the above definitions that the dimension of $\mathbf{V}_h(K)$ is $3N_K^e$, the dimension of $Q_h(K)$ is N_K^v, and that of $Z_h(K)$ is one. Note that the VE space of degree $k = 1$, introduced in [24], has been utilized here for the approximation of fluid pressure. This facilitates the computation of L^2-projection onto the space of polynomials of degree up to 1 (which are required to define the zero-order discrete bilinear form on $Q_h(K)$). Next, and in order to take advantage of the features of VEM discretizations (for instance, estimation for the terms of discrete formulation without explicit computation of basis functions), we need to specify the degrees of freedom associated with (4.2.2). These entities will consist of discrete functionals of the type (taking as an example the space for total pressure)

$$(D_i) : Z_{h|K} \to \mathbb{R}; \qquad Z_{h|K} \ni \phi \mapsto D_i(\phi),$$

and we start with the degrees of freedom for the local displacement space $\mathbf{V}_h(K)$:

- (D_v1) the values of a discrete displacement $\boldsymbol{v}_h$ at vertices of the element;
- (D_v2) the normal displacement $\boldsymbol{v}_h \cdot \boldsymbol{n}_K^e$ at the mid-point of each edge $e \in \partial K$.

Then we precise the degrees of freedom for the local fluid pressure space $Q_h(K)$:

- (D_q) the values of q_h at vertices of the polygonal element.

And similarly, the degree of freedom for the local total pressure space $Z_h(K)$:

- (D_z) the value of ϕ_h over K.

It has been proven elsewhere (see e.g. [24, 29, 18]) that these degrees of freedom are unisolvent in their respective spaces.

We also define global counterparts of the local VE spaces as follows:

$$
\begin{aligned}
\mathbf{V}_h &:= \{\boldsymbol{v}_h \in \mathbf{V} : \boldsymbol{v}_h|_K \in \mathbf{V}_h(K)\ \forall K \in \mathcal{T}_h\}, \\
Q_h &:= \{q_h \in Q : q_h|_K \in Q_h(K)\ \forall K \in \mathcal{T}_h\}, \\
Z_h &:= \{\phi_h \in Z : \phi_h|_K \in Z_h(K)\ \forall K \in \mathcal{T}_h\}.
\end{aligned}
$$

In addition, we denote by N^V the number of degrees of freedom for $\mathbf{V}_h$, by N^Q the number of degrees of freedom for Q_h, and by $\mathrm{dof}_r(s)$ the r-th degree of a given function s.

4.2.2 Virtual element formulation

For all $\boldsymbol{u}_h^s, \boldsymbol{v}_h^s \in \mathbf{V}_h(K)$ and $p_h^f, q_h^f \in Q_h(K)$ we now define the local discrete bilinear forms

$$
\begin{aligned}
a_1^h(\boldsymbol{u}_h^s, \boldsymbol{v}_h^s)|_K &:= a_1^K(\boldsymbol{\Pi}_K^{\boldsymbol{\varepsilon}} \boldsymbol{u}_h^s, \boldsymbol{\Pi}_K^{\boldsymbol{\varepsilon}} \boldsymbol{v}_h^s) + S_1^K\big((\mathbf{I} - \boldsymbol{\Pi}_K^{\boldsymbol{\varepsilon}})\boldsymbol{u}_h^s, (\mathbf{I} - \boldsymbol{\Pi}_K^{\boldsymbol{\varepsilon}})\boldsymbol{v}_h^s\big), \\
a_2^h(p_h^f, q_h^f)|_K &:= a_2^K(\Pi_K^{\nabla} p_h^f, \Pi_K^{\nabla} q_h^f) + S_2^K\big((I - \Pi_K^{\nabla})p_h^f, (I - \Pi_K^{\nabla})q_h^f\big), \\
\tilde{a}_2^h(p_h^f, q_h^f)|_K &:= \tilde{a}_2^K(\Pi_K^0 p_h^f, \Pi_K^0 q_h^f) + S_0^K\big((I - \Pi_K^0)p_h^f, (I - \Pi_K^0)q_h^f\big),
\end{aligned}
$$

where the stabilization of the bilinear forms $S_1^K(\cdot,\cdot), S_2^K(\cdot,\cdot), S_0^K(\cdot,\cdot)$ acting on the kernel of their respective operators $\boldsymbol{\Pi}_K^{\boldsymbol{\varepsilon}}$, Π_K^{∇}, Π_K^0, is defined as

$$
S_1^K(\boldsymbol{u}_h^s, \boldsymbol{v}_h^s) := \sigma_1^K \sum_{l=1}^{N^V} \mathrm{dof}_l(\boldsymbol{u}_h^s)\mathrm{dof}_l(\boldsymbol{v}_h^s), \quad \boldsymbol{u}_h^s, \boldsymbol{v}_h^s \in \ker(\boldsymbol{\Pi}_K^{\boldsymbol{\varepsilon}});
$$

$$S_2^K(p_h^f, q_h^f) := \sigma_2^K \sum_{l=1}^{N^Q} \mathrm{dof}_l(p_h^f)\mathrm{dof}_l(q_h^f), \quad p_h^f, q_h^f \in \ker(\Pi_K^\nabla);$$

$$S_0^K(p_h^f, q_h^f) := \sigma_0^K \mathrm{area}(K) \sum_{l=1}^{N^Q} \mathrm{dof}_l(p_h^f)\mathrm{dof}_l(q_h^f), \quad p_h^f, q_h^f \in \ker(\Pi_K^0),$$

respectively, where σ_1^K, σ_2^K and σ_0^K are positive multiplicative factors to take into account the magnitude of the physical parameters (independent of a mesh size).

Note that for all $\boldsymbol{v}_h^s \in \mathbf{V}_h(K)$, $q_h^f \in Q_h(K)$, these stabilizing terms satisfy the following relations (see, e.g., [29, 122])

$$\begin{aligned}
\alpha_* a_1^K(\boldsymbol{v}_h^s, \boldsymbol{v}_h^s) \le S_1^K(\boldsymbol{v}_h^s, \boldsymbol{v}_h^s) \le \alpha^* a_1^K(\boldsymbol{v}_h^s, \boldsymbol{v}_h^s),\\
\zeta_* a_2^K(q_h^f, q_h^f) \le S_2^K(q_h^f, q_h^f) \le \zeta^* a_2^K(q_h^f, q_h^f),\\
\tilde{\zeta}_* \tilde{a}_2^K(q_h^f, q_h^f) \le S_0^K(q_h^f, q_h^f) \le \tilde{\zeta}^* \tilde{a}_2^K(q_h^f, q_h^f),
\end{aligned} \tag{4.2.3}$$

where $\alpha_*, \alpha^*, \zeta_*, \zeta^*, \tilde{\zeta}_*, \tilde{\zeta}^*$ are positive constants independent of K and h_K. Now, for all $\boldsymbol{u}_h^s, \boldsymbol{v}_h^s \in \mathbf{V}_h$, $p_h^f, q_h^f \in Q_h$, the global discrete bilinear forms are specified as

$$\begin{aligned}
a_1^h(\boldsymbol{u}_h^s, \boldsymbol{v}_h^s) &:= \sum_{K\in\mathcal{T}_h} a_1^h(\boldsymbol{u}_h^s, \boldsymbol{v}_h^s)|_K, \quad a_2^h(p_h^f, q_h^f) := \sum_{K\in\mathcal{T}_h} a_2^h(p_h^f, q_h^f)|_K,\\
\tilde{a}_2^h(p_h^f, q_h^f) &:= \sum_{K\in\mathcal{T}_h} \tilde{a}_2^h(p_h^f, q_h^f)|_K, \quad b_1(\boldsymbol{v}_h^s, \phi_h) := \sum_{K\in\mathcal{T}_h} b_1^K(\boldsymbol{v}_h^s, \phi_h),\\
a_3(\psi_h, \phi_h) &:= \sum_{K\in\mathcal{T}_h} a_3^K(\psi_h, \phi_h), \quad b_2(q_h^f, \phi_h) := \sum_{K\in\mathcal{T}_h} b_2^K(q_h^f, \phi_h).
\end{aligned}$$

In addition, we observe that

$$b_2(p_h^f, \phi_h) = \frac{\alpha}{\lambda} \sum_{K\in\mathcal{T}_h} \int_K p_h^f \phi_h = \frac{\alpha}{\lambda} \sum_{K\in\mathcal{T}_h} \int_K \Pi_K^0 p_h^f \phi_h. \tag{4.2.4}$$

On the other hand, the discrete linear functionals, defined on each element K, are

$$F^h(\boldsymbol{v}_h^s)|_K := \rho \int_K \boldsymbol{b}_h(\cdot, t) \cdot \boldsymbol{v}_h^s, \quad \boldsymbol{v}_h^s \in \mathbf{V}_h; \quad G^h(q_h^f)|_K := \int_K \ell_h(\cdot, t) q_h^f, \quad q_h^f \in Q_h,$$

where the discrete load and volumetric source are given by:

$$\boldsymbol{b}_h(\cdot, t)|_K := \boldsymbol{\Pi}_K^{\mathbf{0}} \boldsymbol{b}(\cdot, t), \quad \ell_h(\cdot, t)|_K := \Pi_K^0 \ell(\cdot, t),$$

where $\mathbf{\Pi}_K^{\mathbf{0}}$ is projection onto piecewise constants on each K.

In view of (4.2.3), the discrete bilinear forms $a_1^h(\cdot,\cdot)$, $\tilde{a}_2^h(\cdot,\cdot)$ and $a_2^h(\cdot,\cdot)$ are coercive and bounded in the following manner [29, 18, 26]

$$
\begin{aligned}
a_1^h(\boldsymbol{v}_h^s,\boldsymbol{v}_h^s) &\geq \min\{1,\alpha_*\}\, 2\mu\, \|\boldsymbol{\varepsilon}(\boldsymbol{v}_h^s)\|_{0,\Omega}^2 && \text{for all } \boldsymbol{v}_h^s \in \mathbf{V}_h,\\
a_2^h(q_h^f,q_h^f) &\geq \min\{1,\zeta_*\}\, \frac{\kappa_{\min}}{\eta}\, \|\nabla q_h^f\|_{0,\Omega}^2 && \text{for all } q_h^f \in Q_h,\\
\tilde{a}_2^h(q_h^f,q_h^f) &\geq \min\{1,\tilde{\zeta}_*\}\left(c_0+\frac{\alpha^2}{\lambda}\right)\|q_h^f\|_{0,\Omega}^2 && \text{for all } q_h^f \in Q_h,\\
a_1^h(\boldsymbol{u}_h^s,\boldsymbol{v}_h^s) &\leq \max\{1,\alpha^*\}\, 2\mu\, \|\boldsymbol{\varepsilon}(\boldsymbol{u}_h^s)\|_{0,\Omega}\|\boldsymbol{\varepsilon}(\boldsymbol{v}_h^s)\|_{0,\Omega} && \text{for all } \boldsymbol{u}_h^s,\boldsymbol{v}_h^s \in \mathbf{V}_h,\\
a_2^h(p_h^f,q_h^f) &\leq \max\{1,\zeta^*\}\, \frac{\kappa_{\max}}{\eta}\, \|\nabla p_h^f\|_{0,\Omega}\|\nabla q_h^f\|_{0,\Omega} && \text{for all } p_h^f,q_h^f \in Q_h,\\
\tilde{a}_2^h(p_h^f,q_h^f) &\leq \max\{1,\tilde{\zeta}^*\}\left(c_0+\frac{\alpha^2}{\lambda}\right)\|p_h^f\|_{0,\Omega}\|q_h^f\|_{0,\Omega} && \text{for all } p_h^f,q_h^f \in Q_h.
\end{aligned}
$$

Moreover, by using definitions of the operators $\mathbf{\Pi}_K^{\mathbf{0}}$ and Π_K^0, we may deduce that the following bounds hold for the linear functionals:

$$
\begin{aligned}
F^h(\boldsymbol{v}_h^s) &\leq \rho\|\boldsymbol{b}\|_{0,\Omega}\|\boldsymbol{v}_h^s\|_{0,\Omega} && \text{for all } \boldsymbol{v}_h^s \in \mathbf{V}_h,\\
G^h(q_h^f) &\leq \|\ell\|_{0,\Omega}\|q_h^f\|_{0,\Omega} && \text{for all } q_h^f \in Q_h.
\end{aligned}
$$

We also recall that the bilinear form $b_1(\cdot,\cdot)$ satisfies the following discrete inf-sup condition on $\mathbf{V}_h \times Z_h$: there exists $\tilde{\beta} > 0$, independent of h, such that (see [29]),

$$
\sup_{\boldsymbol{v}_h \in \mathbf{V}_h \setminus\{0\}} \frac{b_1(\boldsymbol{v}_h^s,\phi_h)}{\|\boldsymbol{v}_h^s\|_{1,\Omega}} \geq \tilde{\beta}\|\phi_h\|_{0,\Omega} \quad \text{for all } \phi_h \in Z_h. \tag{4.2.5}
$$

The semidiscrete VE formulation is now defined as follows: For all $t > 0$, given $\boldsymbol{u}_h^s(0)$, $p_h(0)$, $\psi_h(0)$, find $\boldsymbol{u}_h^s \in \mathbf{L}^2((0,T],\mathbf{V}_h)$, $p_h^f \in L^2((0,T],Q_h)$, $\psi_h \in L^2((0,T],Z_h)$ with $\partial_t p_h^f \in L^2((0,T],Q_h)$, $\partial_t\psi_h \in L^2((0,T],Z_h)$ such that

$$
\begin{aligned}
a_1^h(\boldsymbol{u}_h^s,\boldsymbol{v}_h^s) \qquad\qquad + \quad b_1(\boldsymbol{v}_h^s,\psi_h) &= F^h(\boldsymbol{v}_h^s) \quad \forall \boldsymbol{v}_h^s \in \mathbf{V}_h, && \text{(4.2.6a)}\\
\tilde{a}_2^h(\partial_t p_h^f,q_h^f) + \qquad a_2^h(p_h^f,q_h^f) - b_2(q_h^f,\partial_t\psi_h) &= G^h(q_h^f) \quad \forall q_h^f \in Q_h, && \text{(4.2.6b)}\\
b_1(\boldsymbol{u}_h^s,\phi_h) + b_2(p_h^f,\phi_h) - \quad a_3(\psi_h,\phi_h) &= 0 \quad \forall \phi_h \in Z_h. && \text{(4.2.6c)}
\end{aligned}
$$

4.2.3 Stability of the semi-discrete scheme

The following result will be used for proving the stability and establishing the error estimates for the semi-discrete scheme without employing the Gronwall's inequality. For a detailed proof, we refer to [96, Lemma 3.2].

Lemma 4.1. *Let $X(t)$ be a continuous function, and consider the non-negative functions $F(t)$ and $D(t)$ satisfying, for constants $C_0 \geq 1$ and $C_1 > 0$, the bound*

$$X^2(t) \leq C_0 X^2(0) + C_1 X(0) + D(t) + \int_0^t F(s) X(s) \,\mathrm{d}s, \quad \forall\, t \in [0,T].$$

Then, for each $t \in [0,T]$, there holds

$$X(t) \lesssim X(0) + \max\left\{ C_1 + \int_0^t F(s)\,\mathrm{d}s,\ D(t)^{1/2} \right\}. \tag{4.2.7}$$

Note that squaring both sides of (4.2.7) and using Cauchy–Schwarz inequality, we can rewrite (4.2.7) in the following manner

$$X(t)^2 \lesssim X(0)^2 + \max\left\{ C_1^2 + \int_0^t F(s)^2\,\mathrm{d}s,\ D(t) \right\}. \tag{4.2.8}$$

Now we establish the stability of (4.2.6).

Theorem 4.1 (Stability of the semi-discrete problem)**.** *Let $(\boldsymbol{u}_h^s(t), p_h^f(t), \psi_h(t))$ be a solution of (4.2.6) for each $t \in (0,T]$. Then there exists a constant $C > 0$ independent of c_0, λ, and h, such that*

$$\begin{aligned}
&\mu\|\boldsymbol{\varepsilon}(\boldsymbol{u}_h^s(t))\|_{0,\Omega}^2 + c_0\|p_h^f(t)\|_{0,\Omega}^2 + \|\psi_h(t)\|_{0,\Omega}^2 + \frac{\kappa_{\min}}{\eta}\int_0^t \|\nabla p_h^f(s)\|_{0,\Omega}^2\,\mathrm{d}s \\
&\leq C\Bigg(\mu\|\boldsymbol{\varepsilon}(\boldsymbol{u}_h^s(0))\|_{0,\Omega}^2 + \left(c_0 + \frac{\alpha^2}{\lambda}\right)\|p_h^f(0)\|_{0,\Omega}^2 + \frac{1}{\lambda}\|\psi_h(0)\|_{0,\Omega}^2 \\
&\qquad + \int_0^t \|\partial_t \boldsymbol{b}(s)\|_{0,\Omega}^2\,\mathrm{d}s + \sup_{t\in[0,T]}\|\boldsymbol{b}(t)\|_{0,\Omega}^2 + \int_0^t \|\ell(s)\|_{0,\Omega}^2\,\mathrm{d}s \Bigg).
\end{aligned} \tag{4.2.9}$$

Proof. Following [96], we can differentiate equation (4.2.6c) with respect to time and choose as test function $\phi_h = -\psi_h$. We get

$$-b_1(\partial_t \boldsymbol{u}_h^s, \psi_h) - b_2(\partial_t p_h^f, \psi_h) + a_3(\partial_t \psi_h, \psi_h) = 0.$$

Then we take $q_h^f = p_h^f$ in (4.2.6b), $\boldsymbol{v}_h^s = \partial_t \boldsymbol{u}_h^s$ in (4.2.6a) and add the result to the previous relation to obtain

$$
\begin{aligned}
a_1^h(\boldsymbol{u}_h^s, \partial_t \boldsymbol{u}_h^s) + b_1(\partial_t \boldsymbol{u}_h^s, \psi_h) + \tilde{a}_2^h(\partial_t p_h^f, p_h^f) + a_2^h(p_h^f, p_h^f) - b_2(p_h^f, \partial_t \psi_h) \\
- b_1(\partial_t \boldsymbol{u}_h^s, \psi_h) - b_2(\partial_t p_h^f, \psi_h) + a_3(\partial_t \psi_h, \psi_h) = F^h(\partial_t \boldsymbol{u}_h^s) + G^h(p_h^f).
\end{aligned}
$$

Using the stability of the bilinear forms $a_1^h(\cdot,\cdot)$, $a_2^h(\cdot,\cdot)$, $S_0^K(\cdot,\cdot)$ as well as the definition of the discrete bilinear forms $b_1(\cdot,\cdot)$ (cf. (4.2.4)) and $\tilde{a}_2^h(\cdot,\cdot)$, we readily have

$$
\begin{aligned}
&\frac{\mu}{2}\frac{\mathrm{d}}{\mathrm{d}t}\|\boldsymbol{\varepsilon}(\boldsymbol{u}_h^s)\|_{0,\Omega}^2 + \frac{c_0}{2}\frac{\mathrm{d}}{\mathrm{d}t}\|p_h^f\|_{0,\Omega}^2 + \frac{\kappa_{\min}}{\eta}\|\nabla p_h^f\|_{0,\Omega}^2 + \frac{1}{\lambda}\|\psi_h\|_{0,\Omega}^2 \\
&+ \sum_K \left(\frac{\alpha^2}{\lambda}\Big(\big(\partial_t(\Pi_K^0 p_h^f), \Pi_K^0 p_h^f\big)_{0,K} + S_0^K\big((I-\Pi_K^0)\partial_t p_h^f, (I-\Pi_K^0)p_h^f\big)\Big) \right. \\
&\qquad\qquad \left. - \frac{\alpha}{\lambda}\Big((\Pi_K^0 p_h^f, \partial_t \psi_h)_{0,K} + \big(\partial_t(\Pi_K^0 p_h^f), \psi_h\big)_{0,K}\Big)\right) \qquad\qquad (4.2.10) \\
&\lesssim F^h(\partial_t \boldsymbol{u}_h^s) + G^h(p_h^f).
\end{aligned}
$$

Rearranging terms on the left-hand side gives

$$
\begin{aligned}
&\frac{\mu}{2}\frac{\mathrm{d}}{\mathrm{d}t}\|\boldsymbol{\varepsilon}(\boldsymbol{u}_h^s)\|_{0,\Omega}^2 + \frac{\kappa_{\min}}{\eta}\|\nabla p_h^f\|_{0,\Omega}^2 + \frac{c_0}{2}\frac{\mathrm{d}}{\mathrm{d}t}\|p_h^f\|_{0,\Omega}^2 \\
&+ \frac{1}{\lambda}\sum_K \left(\big(\partial_t(\alpha\Pi_K^0 p_h^f - \psi_h), (\alpha\Pi_K^0 p_h^f - \psi_h)\big)_{0,K} \right. \\
&\qquad\qquad \left. + \frac{\alpha^2}{2}\frac{\mathrm{d}}{\mathrm{d}t} S_0^K\big((I-\Pi_K^0)p_h^f, (I-\Pi_K^0)p_h^f\big)\right) \lesssim F^h(\partial_t \boldsymbol{u}_h^s) + G^h(p_h^f),
\end{aligned}
$$

and after exploiting the stability of $S_0^K(\cdot,\cdot)$ and integrating from 0 to t, we arrive at

$$
\begin{aligned}
&\mu\|\boldsymbol{\varepsilon}(\boldsymbol{u}_h^s(t))\|_{0,\Omega}^2 + c_0\|p_h^f(t)\|_{0,\Omega}^2 + \frac{\alpha^2}{\lambda}\sum_K \|(I-\Pi_K^0)p_h^f(t)\|_{0,K}^2 \\
&\qquad + \frac{1}{\lambda}\sum_K \|(\alpha\Pi_K^0 p_h^f - \psi_h)(t)\|_{0,K}^2 + \frac{\kappa_{\min}}{\eta}\int_0^t \|\nabla p_h^f(s)\|_{0,\Omega}^2\,\mathrm{d}s \\
&\le \mu\|\boldsymbol{\varepsilon}(\boldsymbol{u}_h^s(0))\|_{0,\Omega}^2 + c_0\|p_h^f(0)\|_{0,\Omega}^2 \\
&\qquad + \frac{\alpha^2}{\lambda}\sum_K \|(I-\Pi_K^0)p_h^f(0)\|_{0,K}^2 + \frac{1}{\lambda}\sum_K \|(\alpha\Pi_K^0 p_h^f - \psi_h)(0)\|_{0,K}^2
\end{aligned}
$$

$$+ C\Bigg(\underbrace{\rho\int_0^t \sum_K \big(\boldsymbol{b}(s), \boldsymbol{\Pi}_K^{\boldsymbol{0}}\partial_t \boldsymbol{u}_h^s(s)\big)_{0,K}\,\mathrm{d}s}_{=:T_1} + \underbrace{\int_0^t \sum_K \big(\ell(s), \Pi_K^0 p_h^f(s)\big)_{0,K}\,\mathrm{d}s}_{=:T_2} \Bigg).$$

Then, integrating by parts (with respect to time) and applying the Korn, Poincaré, and Young inequalities implies that

$$\begin{aligned}
T_1 &= \rho \sum_K \Big(\big(\boldsymbol{b}(t), \boldsymbol{\Pi}_K^{\boldsymbol{0}} \boldsymbol{u}_h^s(t)\big)_{0,K} - \big(\boldsymbol{b}(0), \boldsymbol{\Pi}_K^{\boldsymbol{0}} \boldsymbol{u}_h^s(0)\big)_{0,K} \Big) \\
&\qquad\qquad - \rho \int_0^t \sum_K \big(\partial_t \boldsymbol{b}(s), \boldsymbol{\Pi}_K^{\boldsymbol{0}} \boldsymbol{u}_h^s(s)\big)_{0,K}\,\mathrm{d}s \\
&\le \mu \|\boldsymbol{\varepsilon}(\boldsymbol{u}_h^s(t))\|_{0,\Omega}^2 + C_1\rho\Big(\frac{\rho}{\mu}\|\boldsymbol{b}(t)\|_{0,\Omega}^2 + \|\boldsymbol{b}(0)\|_{0,\Omega}\|\boldsymbol{\varepsilon}(\boldsymbol{u}_h^s(0))\|_{0,\Omega} \\
&\qquad\qquad\qquad + \int_0^t \|\partial_t \boldsymbol{b}(s)\|_{0,\Omega}\|\boldsymbol{\varepsilon}(\boldsymbol{u}_h^s(s))\|_{0,\Omega}\,\mathrm{d}s\Big).
\end{aligned}$$

In turn, the bound for T_2 follows from the Cauchy-Schwarz, Poincaré, and Young inequalities in the following manner:

$$\begin{aligned}
T_2 &= \int_0^t \sum_K (\ell(s), \Pi_K^0 p_h^f(s))_{0,K}\,\mathrm{d}s \\
&\le \int_0^t \|\ell(s)\|_{0,\Omega}\|p_h^f(s)\|_{0,\Omega}\,\mathrm{d}s \le C_2\frac{\eta}{\kappa_{\min}}\int_0^t \|\ell(s)\|_{0,\Omega}^2\,\mathrm{d}s + \frac{\kappa_{\min}}{2\eta}\int_0^t \|\nabla p_h^f(s)\|_{0,\Omega}^2\,\mathrm{d}s.
\end{aligned}$$

Thus, we achieve

$$\begin{aligned}
&\mu\|\boldsymbol{\varepsilon}(\boldsymbol{u}_h^s(t))\|_{0,\Omega}^2 + c_0\|p_h^f(t)\|_{0,\Omega}^2 + \frac{\alpha^2}{\lambda}\sum_K \|(I-\Pi_K^0)p_h^f(t)\|_{0,K}^2 \\
&\qquad + \frac{1}{\lambda}\sum_K \|(\alpha\Pi_K^0 p_h^f - \psi_h)(t)\|_{0,K}^2 + \frac{\kappa_{\min}}{2\eta}\int_0^t \|\nabla p_h^f(s)\|_{0,\Omega}^2\,\mathrm{d}s \\
&\le \mu\|\boldsymbol{\varepsilon}(\boldsymbol{u}_h^s(0))\|_{0,\Omega}^2 + c_0\|p_h^f(0)\|_{0,\Omega}^2 + \frac{\alpha^2}{\lambda}\sum_K \|(I-\Pi_K^0)p_h^f(0)\|_{0,K}^2 \\
&\qquad + \frac{1}{\lambda}\sum_K \|(\alpha\Pi_K^0 p_h^f - \psi_h)(0)\|_{0,K}^2 + C\Bigg(\int_0^t \|\ell(s)\|_{0,\Omega}^2\,\mathrm{d}s + \Big(\|\boldsymbol{b}(t)\|_{0,\Omega}^2 \\
&\qquad\qquad + \|\boldsymbol{b}(0)\|_{0,\Omega}\|\boldsymbol{\varepsilon}(\boldsymbol{u}_h^s(0))\|_{0,\Omega} + \int_0^t \|\partial_t \boldsymbol{b}(s)\|_{0,\Omega}\|\boldsymbol{\varepsilon}(\boldsymbol{u}_h^s(s))\|_{0,\Omega}\,\mathrm{d}s\Big)\Bigg).
\end{aligned} \tag{4.2.11}$$

Let $X^2(t)$ denote the lower bound in the inequality (4.2.11) and choose $C_0 = 1$, $C_1 = C\|\boldsymbol{b}(0)\|_0$, $F(t) = C\|\partial_t \boldsymbol{b}(t)\|_0$ and $D(t) = C(\|\boldsymbol{b}(t)\|_0^2 + \int_0^t \|\ell(s)\|_0^2\,\mathrm{d}s)$ in Lemma

4.1. Then (4.2.8) enables us to write

$$
\begin{aligned}
&\mu\|\boldsymbol{\varepsilon}(\boldsymbol{u}_h^s(t))\|_{0,\Omega}^2 + c_0\|p_h^f(t)\|_{0,\Omega}^2 + \frac{\alpha^2}{\lambda}\sum_K \|(I-\Pi_K^0)p_h^f(t)\|_{0,K}^2 \\
&\qquad + \frac{1}{\lambda}\sum_K \|(\alpha\Pi_K^0 p_h^f - \psi_h)(t)\|_{0,K}^2 + \frac{\kappa_{\min}}{2\eta}\int_0^t \|\nabla p_h^f(s)\|_{0,\Omega}^2\,\mathrm{d}s \\
&\lesssim \mu\|\boldsymbol{\varepsilon}(\boldsymbol{u}_h^s(0))\|_{0,\Omega}^2 + c_0\|p_h^f(0)\|_{0,\Omega}^2 + \frac{\alpha^2}{\lambda}\sum_K \|(I-\Pi_K^0)p_h^f(0)\|_{0,K}^2 \\
&\quad + \frac{1}{\lambda}\sum_K \|(\alpha\Pi_K^0 p_h^f - \psi_h)(0)\|_{0,K}^2 + \|\boldsymbol{b}(t)\|_{0,\Omega}^2 + \|\boldsymbol{b}(0)\|_{0,\Omega}^2 \\
&\quad + \int_0^t (\|\ell(s)\|_{0,\Omega}^2 + \|\partial_t \boldsymbol{b}(s)\|_{0,\Omega}^2)\,\mathrm{d}s.
\end{aligned}
\tag{4.2.12}
$$

On the other hand, the discrete inf-sup condition (4.2.5) along with (4.2.6a) gives

$$
\|\psi_h\|_{0,\Omega} \le \sup_{\boldsymbol{v}_h^s \in \mathbf{V}_h\setminus\{0\}} \frac{1}{\|\boldsymbol{v}_h^s\|_{1,\Omega}}\big(F^h(\boldsymbol{v}_h^s) - a_1^h(\boldsymbol{u}_h^s, \boldsymbol{v}_h^s)\big) \le C\big(\|\boldsymbol{b}\|_{0,\Omega} + \|\boldsymbol{\varepsilon}(\boldsymbol{u}_h^s)\|_{0,\Omega}\big).
\tag{4.2.13}
$$

And then note that inequality (4.2.12) together with (4.2.13) concludes the proof of (4.2.9). Moreover, we observe from (4.2.11) that the generic constant C appearing in (4.2.9) is independent of c_0, λ. Therefore the proved stability remains valid even with $c_0 \to 0$, $\lambda \to \infty$. □

The energy estimates (4.2.9) help us in obtaining the following result.

Corollary 4.1 (Solvability of the discrete problem)**.** *The problem* (4.2.6) *has a unique solution in* $\mathbf{V}_h \times Q_h \times Z_h$ *for each* $t \in (0,T]$.

Proof. Let $\boldsymbol{u}_h^s(t) := \sum_{i=1}^{N^{\mathbf{V}}} U_i(t)\xi_i$, $p_h^f(t) := \sum_{j=1}^{N^Q} P_j(t)\chi_j$, $\psi_h(t) := \sum_{l=1}^{N^Z} Z_l(t)\Phi_l$ where $\xi_i(1 \le i \le N^{\mathbf{V}})$, $\chi_j(1 \le j \le N^Q)$, $\Phi_l(1 \le l \le N^Z$, where N^Z coincides with the number of elements in $\mathcal{T}_h$) are the basis functions for the spaces $\mathbf{V}_h, Q_h, Z_h$ respectively. Then (4.2.6) can be written as the following system of first-order differential equations:

$$
\underbrace{\begin{pmatrix} \mathbf{0} & \mathbf{0} & \mathbf{0} \\ \mathbf{0} & \tilde{A}2 & -B2 \\ \mathbf{0} & \mathbf{0} & \mathbf{0} \end{pmatrix}}_{=:\mathcal{A}}
\begin{pmatrix} \dot{U}(t) \\ \dot{P}(t) \\ \dot{Z}(t) \end{pmatrix}
+
\underbrace{\begin{pmatrix} A1 & \mathbf{0} & B1 \\ \mathbf{0} & A2 & \mathbf{0} \\ B1 & B2 & -A3 \end{pmatrix}}_{=:\mathcal{B}}
\begin{pmatrix} U(t) \\ P(t) \\ Z(t) \end{pmatrix}
=
\begin{pmatrix} \boldsymbol{F}(t) \\ \boldsymbol{G}(t) \\ \mathbf{0} \end{pmatrix}.
\tag{4.2.14}
$$

In view of the classical theory of linear systems of differential equations, (4.2.14) possesses a unique solution if the matrix $\mathcal{A}+\mathcal{B}$ is invertible (see also [100]). To achieve this, we first rewrite the following problem corresponding to the matrix $\mathcal{A}+\mathcal{B}$: For $(L_1^h, L_2^h, L_3^h) \in \mathbf{V}'_h \times Q'_h \times Z'_h$, find $\boldsymbol{u}_h^s \in \mathbf{V}_h$, $p_h^f \in Q_h$, $q_h \in Z_h$ such that

$$
\begin{aligned}
a_1^h(\boldsymbol{u}_h^s, \boldsymbol{v}_h^s) \qquad\qquad\qquad\qquad &+ b_1(\boldsymbol{v}_h^s, \psi_h) = L_1^h(\boldsymbol{v}_h^s) \quad \forall \boldsymbol{v}_h^s \in \mathbf{V}_h, && (4.2.15a)\\
\tilde{a}_2^h(p_h^f, q_h^f) + \qquad\qquad a_2^h(p_h^f, q_h^f) &- b_2(q_h^f, \psi_h) = L_2^h(q_h^f) \quad \forall q_h^f \in Q_h, && (4.2.15b)\\
b_1(\boldsymbol{u}_h^s, \phi_h) + b_2(p_h^f, \phi_h) &- a_3(\psi_h, \phi_h) = L_3^h(\phi_h) \quad \forall \phi_h \in Z_h. && (4.2.15c)
\end{aligned}
$$

Now, the unique solvability of (4.2.15) (and the invertibility of the matrix $\mathcal{A}+\mathcal{B}$) can be established by showing that the homogeneous counterpart of system (4.2.15) has only the trivial solution. Setting the functionals defining the right-hand side of (4.2.15) to zero , i.e., $L_1^h(\boldsymbol{v}_h^s) = L_2^h(q_h) = L_3^h(\phi_h) = 0$, and choosing $\boldsymbol{v}_h^s = \boldsymbol{u}_h^s, \phi_h = \psi_h, q_h^f = p_h^f$ in (4.2.15), we readily obtain the following bounds by proceeding in the similar fashion (using the coercivity of $a_1^h(\cdot,\cdot)$, $a_2^h(\cdot,\cdot)$, Young's inequality and definition of $\tilde{a}_2^h(\cdot,\cdot)$, $b_2(\cdot,\cdot)$, $a_3^h(\cdot,\cdot)$) as in the proof of (4.2.9)

$$
\mu\|\boldsymbol{\varepsilon}(\boldsymbol{u}_h^s)\|_{0,\Omega}^2 + \frac{\kappa_{\min}}{\eta}\|\nabla p_h^f\|_{0,\Omega}^2 \le 0,
$$

and hence an application of the Poincaré and Korn inequalities together with the inf-sup condition of $b_1(\cdot,\cdot)$ yield $\boldsymbol{u}_h^s = \mathbf{0}$, $p_h^f = 0$ and $\psi_h = 0$. $\square$

Next, we discretize in time using the backward Euler method with the constant step size $\Delta t = T/N$ and denote any function f at $t = t_n$ by f^n. The fully discrete scheme reads: given initial conditions $\boldsymbol{u}_h^{s,0}$, $p_h^{f,0}$, ψ_h^0, and for $t_n = n\Delta t$, $n = 1, \ldots, N$, find $\boldsymbol{u}_h^{s,n} \in \mathbf{V}_h$, $p_h^{f,n} \in Q_h$ and $\psi_h^n \in Z_h$ such that for all $\boldsymbol{v}_h^s \in \mathbf{V}_h$, $q_h^f \in Q_h$ and $\phi_h \in Z_h$ such that

$$
\begin{aligned}
&a_1^h(\boldsymbol{u}_h^{s,n}, \boldsymbol{v}_h^s) && + b_1(\boldsymbol{v}_h^s, \psi_h^n) && = F^{h,n}(\boldsymbol{v}_h^s), && (4.2.16a)\\
&\tilde{a}_2^h\left(\delta_t p_h^{f,n}, q_h^f\right) + a_2^h(p_h^{f,n}, q_h^f) && - b_2\left(q_h^f, \delta_t \psi_h^n\right) && = G^{h,n}(q_h^f), && (4.2.16b)\\
&b_1(\boldsymbol{u}_h^{s,n}, \phi_h) \quad + b_2(p_h^{f,n}, \phi_h) && - a_3(\psi_h^n, \phi_h) && = 0, && (4.2.16c)
\end{aligned}
$$

where for all $\boldsymbol{v}_h^s \in \mathbf{V}_h$ and $q_h^f \in Q_h$ we define

$$
F^{h,n}(\boldsymbol{v}_h^s)|_K := \rho \int_K \boldsymbol{b}_h(t^n) \cdot \boldsymbol{v}_h^s, \quad G^{h,n}(q_h^f)|_K := \int_K \ell_h(t^n) q_h^f.
$$

With the aim of showing the stability and convergence of the fully-discrete scheme, we provide first the following auxiliary result. A proof, sketched below, follows similarly as in [98, Lemma 3.2].

Lemma 4.2. *Let $X_n,\ 1 \le n \le N$ be a finite sequence of functions with non-negative constants C_0, C_1 and finite sequences D_n and G_n such that*

$$X_n^2 \le C_0 X_0^2 + C_1 X_0 + D_n + \sum_{j=1}^{n} G_j X_j \quad \textit{for all } 1 \le n \le N.$$

Then there holds

$$X_n^2 \lesssim X_0^2 + \max\left\{ C_1^2 + \sum_{j=1}^{n} G_j^2,\ D_n \right\} \quad \textit{for all } 1 \le n \le N. \tag{4.2.17}$$

Proof. It is sufficient to show that the relation holds for n, which is the smallest integer such that $X_n = \max_{1\le i\le N} X_i$. There can be two possibilities, namely either (i) $C_1 X_0 + \sum_{j=1}^{n} G_j X_j \le D_n$, or (ii) $D_n > C_1 X_0 + \sum_{j=1}^{n} G_j X_j$. In case (i), the bound (4.2.17) trivially holds. In case (ii), using the upper bound X_n and Young's inequality yields

$$\begin{aligned} X_n^2 &\le C_0 X_0^2 + 2\left(C_1 X_0 + \sum_{j=1}^{n} G_j X_j\right) \lesssim \left(C_0 X_0 + 2\left(C_1 + \sum_{j=1}^{n} G_j\right)\right) X_n \\ &\le \frac{1}{2}\left(C_0 X_0 + 2\left(C_1 + \sum_{j=1}^{n} G_j\right)\right)^2 + \frac{1}{2} X_n^2. \end{aligned}$$

Now taking the common term of X_n^2 together and squaring the remaining terms on the right-hand side completes the proof. □

Theorem 4.2 (Stability of the fully-discrete problem)**.** *The unique solution to problem* (4.2.16) *depends continuously on data. More precisely, there exists a constant C*

independent of c_0, λ, h and Δt such that

$$\begin{aligned}
&\mu\|\boldsymbol{\varepsilon}(\boldsymbol{u}_h^{s,n})\|_{0,\Omega}^2 + c_0\|p_h^{f,n}\|_{0,\Omega}^2 + \|\psi_h^n\|_{0,\Omega}^2 + (\Delta t)\frac{\kappa_{\min}}{\eta}\sum_{j=1}^n \|\nabla p_h^{f,j}\|_{0,\Omega}^2 \\
&\leq C\Bigg(\mu\|\boldsymbol{\varepsilon}(\boldsymbol{u}_h^{s,0})\|_{0,\Omega}^2 + \Big(c_0 + \frac{\alpha^2}{\lambda}\Big)\|p_h^{f,0}\|_{0,\Omega}^2 + \frac{1}{\lambda}\|\psi_h^0\|_{0,\Omega}^2 + \max_{0\leq j\leq n}\|\boldsymbol{b}^j\|_{0,\Omega}^2 \qquad (4.2.18)\\
&\qquad + (\Delta t)\sum_{j=1}^n\Big(\|\partial_t \boldsymbol{b}^j\|_{0,\Omega}^2 + \|\ell^j\|_0^2\Big) + (\Delta t)^2\int_0^T \|\partial_{tt}\boldsymbol{b}(s)\|_{0,\Omega}^2\,\mathrm{d}s\Bigg),
\end{aligned}$$

with $\boldsymbol{b}^k := \boldsymbol{b}(\cdot, t^k)$ and $\ell^k := \ell(\cdot, t^k)$, for $k = 1, \dots, n$.

Proof. Taking $\boldsymbol{v}_h^s = \boldsymbol{u}_h^{s,n} - \boldsymbol{u}_h^{s,n-1}$ in (4.2.16a) gives

$$a_1^h(\boldsymbol{u}_h^{s,n}, \boldsymbol{u}_h^{s,n} - \boldsymbol{u}_h^{s,n-1}) + b_1(\boldsymbol{u}_h^{s,n} - \boldsymbol{u}_h^{s,n-1}, \psi_h^n) = F^{h,n}(\boldsymbol{u}_h^{s,n} - \boldsymbol{u}_h^{s,n-1}). \qquad (4.2.19)$$

A use of (4.2.6c) for the time step n, $n-1$ and setting $\phi_h = -\psi_h^n$, (4.2.16c) becomes

$$-b_1(\boldsymbol{u}_h^{s,n} - \boldsymbol{u}_h^{s,n-1}, \psi_h^n) - b_2(p_h^{f,n} - p_h^{f,n-1}, \psi_h^n) + a_3(\psi_h^n - \psi_h^{n-1}, \psi_h^n) = 0. \qquad (4.2.20)$$

Adding (4.2.20) and (4.2.19) readily gives

$$a_1^h(\boldsymbol{u}_h^{s,n}, \boldsymbol{u}_h^{s,n} - \boldsymbol{u}_h^{s,n-1}) + a_3(\psi_h^n - \psi_h^{n-1}, \psi_h^n) - b_2(p_h^{f,n} - p_h^{f,n-1}, \psi_h^n) = F^{h,n}(\boldsymbol{u}_h^{s,n} - \boldsymbol{u}_h^{s,n-1}), \qquad (4.2.21)$$

and choosing $q_h^f = p_h^{f,n}$ in (4.2.16b) implies the relation

$$\tilde{a}_2^h(p_h^{f,n} - p_h^{f,n-1}, p_h^{f,n}) + \Delta t\, a_2^h(p_h^{f,n}, p_h^{f,n}) - b_2(p_h^{f,n}, \psi_h^n - \psi_h^{n-1}) = \Delta t\, G^{h,n}(p_h^{f,n}). \qquad (4.2.22)$$

Next we proceed to adding (4.2.21) and (4.2.22), to get

$$\begin{aligned}
&a_1^h(\boldsymbol{u}_h^{s,n}, \boldsymbol{u}_h^{s,n} - \boldsymbol{u}_h^{s,n-1}) + \Delta t\, a_2^h(p_h^{f,n}, p_h^{f,n}) + a_3(\psi_h^n - \psi_h^{n-1}, \psi_h^n) \\
&\qquad + \tilde{a}_2^h(p_h^{f,n} - p_h^{f,n-1}, p_h^{f,n}) - b_2(p_h^{f,n} - p_h^{f,n-1}, \psi_h^n) - b_2(p_h^{f,n}, \psi_h^n - \psi_h^{n-1}) \\
&= F^{h,n}(\boldsymbol{u}_h^{s,n} - \boldsymbol{u}_h^{s,n-1}) + \Delta t\, G^{h,n}(p_h^{f,n}).
\end{aligned}$$

Repeating a similar argument as the one used to obtain (4.2.10), together with the inequality

$$(f_h^n - f_h^{n-1}, f_h^n) \geq \frac{1}{2}\big(\|f_h^n\|_{0,\Omega}^2 - \|f_h^{n-1}\|_{0,\Omega}^2\big), \tag{4.2.23}$$

for any discrete function f_h^j, $j = 1, \ldots, n$, we arrive at

$$\begin{aligned}
&\frac{\mu}{2}(\|\boldsymbol{\varepsilon}(\boldsymbol{u}_h^{s,n})\|_{0,\Omega}^2 - \|\boldsymbol{\varepsilon}(\boldsymbol{u}_h^{s,n-1})\|_{0,\Omega}^2) + (\Delta t)\frac{\kappa_{\min}}{\eta}\|\nabla p_h^{f,n}\|_{0,\Omega}^2 + \frac{1}{2}\sum_K c_0(\|\Pi_K^0 p_h^{f,n}\|_{0,K}^2 - \|\Pi_K^0 p_h^{f,n-1}\|_{0,K}^2) \\
&\qquad + \frac{1}{2}\Big(c_0 + \frac{\alpha^2}{\lambda}\Big)\sum_K(\|(I - \Pi_K^0)p_h^{f,n}\|_{0,K}^2 - \|(I - \Pi_K^0)p_h^{f,n-1}\|_{0,K}^2) \\
&\qquad + \frac{1}{2\lambda}\sum_K(\|\alpha\Pi_K^0 p_h^{f,n} - \psi_h^n\|_{0,K}^2 - \|\alpha\Pi_K^0 p_h^{f,n-1} - \psi_h^{n-1}\|_{0,K}^2) \\
&\lesssim (\Delta t)(\rho(\boldsymbol{b}_h^n, \delta_t\boldsymbol{u}_h^{s,n})_{0,\Omega} + (\ell_h^n, p_h^{f,n})_{0,\Omega}),
\end{aligned}$$

where we have denoted $\delta_t f_h(t_n) := \frac{f_h(t_n) - f_h(t_{n-1})}{\Delta t}$ for any time-space discrete function f_h. Summing over n we obtain

$$\begin{aligned}
&\frac{\mu}{2}(\|\boldsymbol{\varepsilon}(\boldsymbol{u}_h^{s,n})\|_{0,\Omega}^2 - \|\boldsymbol{\varepsilon}(\boldsymbol{u}_h^{s,0})\|_{0,\Omega}^2) + (\Delta t)\frac{\kappa_{\min}}{\eta}\sum_{j=1}^n\|\nabla p_h^{f,j}\|_{0,\Omega}^2 + \frac{1}{2}\sum_K c_0(\|\Pi_K^0 p_h^{f,n}\|_{0,K}^2 - \|\Pi_K^0 p_h^{f,0}\|_{0,K}^2) \\
&\qquad + \frac{1}{2}\Big(c_0 + \frac{\alpha^2}{\lambda}\Big)\sum_K(\|(I - \Pi_K^0)p_h^{f,n}\|_{0,K}^2 - \|(I - \Pi_K^0)p_h^{f,0}\|_{0,K}^2) \\
&\qquad + \frac{1}{2\lambda}\sum_K(\|\alpha\Pi_K^0 p_h^{f,n} - \psi_h^n\|_{0,K}^2 - \|\alpha\Pi_K^0 p_h^{f,0} - \psi_h^0\|_{0,K}^2) \\
&\lesssim \underbrace{\rho(\Delta t)\sum_{j=1}^n(\boldsymbol{b}_h^j, \delta_t\boldsymbol{u}_h^{s,j})_{0,\Omega}}_{=:J_1} + \underbrace{(\Delta t)\sum_{j=1}^n(\ell_h^j, p_h^{f,j})_{0,\Omega}}_{=:J_2}.
\end{aligned}$$

Using the equality

$$\sum_{j=1}^n(f_h^j - f_h^{j-1}, g_h^j) = (f_h^n, g_h^n) - (f_h^0, g_h^0) - \sum_{j=1}^n(f_h^{j-1}, g_h^j - g_h^{j-1}), \tag{4.2.24}$$

for any discrete functions f_h^j, g_h^j, $j = 1, \ldots, n$, along with Taylor expansion, Cauchy–Schwarz, Korn's inequality and generalized Young's inequality gives

$$J_1 = \rho\Big((\boldsymbol{b}_h^n, \boldsymbol{u}_h^{s,n})_{0,\Omega} - (\boldsymbol{b}_h^0, \boldsymbol{u}_h^{s,0})_{0,\Omega} - \sum_{j=1}^n(\boldsymbol{b}_h^j - \boldsymbol{b}_h^{j-1}, \boldsymbol{u}_h^{s,j-1})_{0,\Omega}\Big)$$

$$
\begin{aligned}
&= \rho\Big((\boldsymbol{b}_h^n, \boldsymbol{u}_h^{s,n})_{0,\Omega} - (\boldsymbol{b}_h^0, \boldsymbol{u}_h^{s,0})_{0,\Omega} - \Delta t \sum_{j=1}^{n} (\partial_t \boldsymbol{b}_h^j, \boldsymbol{u}_h^{s,j-1})_{0,\Omega} \\
&\qquad + \sum_{j=1}^{n} \Big(\int_{t_{j-1}}^{t_j} (s - t_{j-1}) \partial_{tt} \boldsymbol{b}_h(s) \, \mathrm{d}s, \boldsymbol{u}_h^{s,j-1} \Big)_{0,\Omega} \Big) \\
&\le \mu \|\boldsymbol{\varepsilon}(\boldsymbol{u}_h^{s,0})\|_{0,\Omega}^2 + \frac{\mu}{4} \|\boldsymbol{\varepsilon}(\boldsymbol{u}_h^{s,n})\|_{0,\Omega}^2 + C(\rho, \mu) \max_{0 \le j \le n} \|\boldsymbol{b}^j\|_{0,\Omega}^2 \\
&\qquad + C(\rho)(\Delta t) \sum_{j=1}^{n} \Big(\|\partial_t \boldsymbol{b}^j\|_{0,\Omega} + \Big((\Delta t) \int_{t_{j-1}}^{t_j} \|\partial_{tt} \boldsymbol{b}(s)\|_{0,\Omega}^2 \, \mathrm{d}s \Big)^{1/2} \Big) \|\boldsymbol{\varepsilon}(\boldsymbol{u}_h^{s,j-1})\|_{0,\Omega}.
\end{aligned}
$$

Another application of Young's inequality yields

$$
J_2 \le C_2(\eta, \kappa_{\min})(\Delta t) \sum_{j=1}^{n} \|\ell^j\|_{0,\Omega}^2 + (\Delta t) \frac{\kappa_{\min}}{2\eta} \sum_{j=1}^{n} \|p_h^{f,j}\|_{0,\Omega}^2.
$$

The bounds obtained for J_1, J_2, Π_K^0 and use of Lemma 4.2 imply

$$
\begin{aligned}
&\mu \|\boldsymbol{\varepsilon}(\boldsymbol{u}_h^{s,n})\|_{0,\Omega}^2 + c_0 \|p_h^{f,n}\|_{0,\Omega}^2 + (\Delta t) \frac{\kappa_{\min}}{\eta} \sum_{j=1}^{n} \|\nabla p_h^{f,j}\|_{0,\Omega}^2 \\
&\qquad + \Big(\frac{\alpha^2}{\lambda} \Big) \sum_K \|(I - \Pi_K^0) p_h^{f,n}\|_{0,K}^2 + \frac{1}{\lambda} \sum_K \|\alpha \Pi_K^0 p_h^{f,n} - \psi_h^n\|_{0,K}^2 \\
&\quad \lesssim \mu \|\boldsymbol{\varepsilon}(\boldsymbol{u}_h^{s,0})\|_{0,\Omega}^2 + \Big(c_0 + \frac{\alpha^2}{\lambda} \Big) \|p_h^{f,0}\|_{0,\Omega}^2 + \frac{1}{\lambda} \|\psi_h^0\|_{0,\Omega}^2 + \max_{0 \le j \le n} \|\boldsymbol{b}^j\|_{0,\Omega}^2 \\
&\qquad + (\Delta t) \sum_{j=1}^{n} \|\ell^j\|_{0,\Omega}^2 + (\Delta t)^2 \Big(\sum_{j=1}^{n} \|\partial_t \boldsymbol{b}^j\|_{0,\Omega}^2 + (\Delta t) \int_0^T \|\partial_{tt} \boldsymbol{b}(s)\|_{0,\Omega}^2 \, \mathrm{d}s \Big).
\end{aligned}
\tag{4.2.25}
$$

An application of (4.2.5) together with (4.2.16a) yields

$$
\|\psi_h^n\|_{0,\Omega} \le C(\|\boldsymbol{b}^n\|_{0,\Omega} + \|\boldsymbol{\varepsilon}(\boldsymbol{u}_h^{s,n})\|_{0,\Omega}). \tag{4.2.26}
$$

Finally, the bound (4.2.25) together with (4.2.26) concludes (4.2.18). □

It is worth pointing out that the proof is particularly delicate since the stabilisation term requires a careful treatment in order to guarantee that the bounds remain independent of the stability constants of the bilinear form $\tilde{a}_2(\cdot, \cdot)$.

Corollary 4.2 (Solvability of the fully discrete problem)**.** *The problem* (4.2.16) *has a unique solution in* $\mathbf{V}_h \times Q_h \times Z_h$.

Proof. It is sufficient to show that the homogeneous linear system corresponding to (4.2.16) has only a trivial solution, since $\mathbf{V}_h, Q_h$ and Z_h are finite dimensional spaces, and this can easily be shown by proceeding analogously to the proof of Corollary 4.1. $\square$

4.3 A priori error estimates

For the sake of error analysis, we require additional regularity: In particular, for any $t > 0$, we consider that the displacement is $\boldsymbol{u}^s(t) \in [H^2(\Omega)]^2$, the fluid pressure $p^f(t) \in H^2(\Omega)$, and the total pressure $\psi(t) \in H^1(\Omega)$. Furthermore, our subsequent analysis also requires the following regularity in time: $\partial_t \boldsymbol{u}^s \in \mathbf{L}^2(0,T;[H^2(\Omega)]^2)$, $\partial_t p^f \in L^2(0,T;H^2(\Omega))$, $\partial_t \psi \in L^2(0,T;H^1(\Omega))$, $\partial_{tt}\boldsymbol{u}^s \in \mathbf{L}^2(0,T;[L^2(\Omega)]^2)$ and $\partial_{tt}p^f, \partial_{tt}\psi \in L^2(0,T;L^2(\Omega))$.

We start by recalling an estimate for the interpolant $\boldsymbol{u}^s_I \in \mathbf{V}_h$ of $\boldsymbol{u}^s$ and $p^f_I \in Q_h$ of p^f (see [29]).

We now introduce the poroelastic projection operator: given $(\boldsymbol{u}^s, p^f, \psi) \in \mathbf{V} \times Q \times Z$, find $S^h := (S^{\boldsymbol{u}}_h \boldsymbol{u}^s, S^p_h p^f, S^\psi_h \psi) \in \mathbf{V}_h \times Q_h \times Z_h$ such that

$$\begin{aligned}
a_1^h(S^{\boldsymbol{u}}_h \boldsymbol{u}^s, \boldsymbol{v}^s_h) + \ b_1(\boldsymbol{v}^s_h, S^\psi_h \psi) &= a_1(\boldsymbol{u}^s, \boldsymbol{v}^s_h) + b_1(\boldsymbol{v}^s_h, \psi) && \text{for all } \boldsymbol{v}^s_h \in \mathbf{V}_h, && (4.3.1a)\\
b_1(S^{\boldsymbol{u}}_h \boldsymbol{u}^s, \phi_h) &= b_1(\boldsymbol{u}^s, \phi_h) && \text{for all } \phi_h \in Z_h, && (4.3.1b)\\
a_2^h(S^p_h p^f, q^f_h) &= a_2(p^f, q^f_h) && \text{for all } q^f_h \in Q_h, && (4.3.1c)
\end{aligned}$$

and we remark that S^h is defined by the combination of the saddle-point problem (4.3.1a), (4.3.1b) and the elliptic problem (4.3.1c); and hence, it is well-defined.

Theorem 4.3 (Estimates for the poroelastic projection)**.** *Let* $(\boldsymbol{u}^s, p^f, \psi)$ *and* $(S^{\boldsymbol{u}}_h \boldsymbol{u}^s, S^p_h p^f, S^\psi_h \psi)$ *be the unique solutions of* (4.2.6a)–(4.2.6c) *and* (4.3.1a), (4.3.1b)*, respectively. Then the following estimates hold:*

$$\|\boldsymbol{u}^s - S^{\boldsymbol{u}}_h \boldsymbol{u}^s\|_{1,\Omega} + \|\psi - S^\psi_h \psi\|_{0,\Omega} \le Ch(|\boldsymbol{u}^s|_{2,\Omega} + |\psi|_{1,\Omega}), \qquad (4.3.2a)$$

$$\|p^f - S^p_h p^f\|_{0,\Omega} + h\|p^f - S^p_h p^f\|_{1,\Omega} \le Ch^2 |p^f|_{2,\Omega}. \qquad (4.3.2b)$$

Proof. The estimates available for discretization of Stokes from Lemma 2.10 and elliptic problems [25] conclude the statement. $\square$

Remark 4.1. *Note that repeating the same arguments exploited in this and in the* *subsequent sections, it is possible to derive error estimates of order h^r. It suffices to assume that $\boldsymbol{u}^s(t) \in [H^{1+r}(\Omega)]^2$, $p^f(t) \in H^{1+r}(\Omega)$, and $\psi(t) \in H^r(\Omega)$, for $0 < r \leq 1$.*

Theorem 4.4 (Semi-discrete energy error estimates)**.** *Let the triplets $(\boldsymbol{u}^s(t), p^f(t), \psi(t)) \in \mathbf{V} \times Q \times Z$ and $(\boldsymbol{u}^s_h(t), p^f_h(t), \psi_h(t)) \in \mathbf{V}_h \times Q_h \times Z_h$ be the unique solutions to problems* (4.1.3a)–(4.1.3c) *and* (4.2.6a)–(4.2.6c)*, respectively. Then, the following bounds hold, with constants $C > 0$ independent of h, λ and c_0,*

$$\mu\|\boldsymbol{\varepsilon}((\boldsymbol{u}^s - \boldsymbol{u}^s_h)(t))\|^2_{0,\Omega} + \|(\psi - \psi_h)(t)\|^2_{0,\Omega} + \frac{\kappa_{\min}}{\eta}\int_0^t \|\nabla(p^f - p^f_h)(s)\|^2_{0,\Omega}\,\mathrm{d}s \;\leq\; C\,h^2.$$

Proof. Invoking the Scott-Dupont theory (see [113]) for the polynomial approximation: there exists a constant $C > 0$ such that for every r with $0 \leq r \leq 1$ and for every $\boldsymbol{u}^s \in [H^{1+r}(K)]^2$, there exists $\boldsymbol{u}^s_\pi \in [\mathbb{P}_k(K)]^2$, $k = 0, 1$, such that

$$\|\boldsymbol{u}^s - \boldsymbol{u}^s_\pi\|_{0,K} + h_K|\boldsymbol{u}^s - \boldsymbol{u}^s_\pi|_{1,K} \leq C h_K^{1+r}|\boldsymbol{u}^s|_{1+r,K} \quad \text{for all } K \in \mathcal{T}_h. \tag{4.3.3}$$

We can then write the displacement and total pressure error in terms of the poroelastic projector as follows

$$\begin{aligned}(\boldsymbol{u}^s - \boldsymbol{u}^s_h)(t) &= (\boldsymbol{u}^s - S^{\boldsymbol{u}}_h\boldsymbol{u}^s)(t) + (S^{\boldsymbol{u}}_h\boldsymbol{u}^s - \boldsymbol{u}^s_h)(t) := e^I_{\boldsymbol{u}}(t) + e^A_{\boldsymbol{u}}(t),\\ (\psi - \psi_h)(t) &= (\psi - S^\psi_h\psi)(t) + (S^\psi_h\psi - \psi_h)(t) := e^I_\psi(t) + e^A_\psi(t).\end{aligned}$$

Then, a combination of equations (4.3.1a), (4.2.6a) and (4.1.3a) gives

$$\begin{aligned}a^h_1(e^A_{\boldsymbol{u}}, \boldsymbol{v}^s_h) + b_1(\boldsymbol{v}^s_h, e^A_\psi) &= (a_1(\boldsymbol{u}, \boldsymbol{v}^s_h) - a^h_1(\boldsymbol{u}^s_h, \boldsymbol{v}^s_h)) + b_1(\boldsymbol{v}^s_h, \psi - \psi_h)\\ &= (F - F^h)(\boldsymbol{v}^s_h),\end{aligned}$$

and taking as test function $\boldsymbol{v}^s_h = \partial_t e^A_{\boldsymbol{u}}$, we can write the relation

$$a^h_1(e^A_{\boldsymbol{u}}, \partial_t e^A_{\boldsymbol{u}}) + b_1(\partial_t e^A_{\boldsymbol{u}}, e^A_\psi) = (F - F^h)(\partial_t e^A_{\boldsymbol{u}}). \tag{4.3.4}$$

Now, we write the pressure error in terms of the poroelastic projector as follows

$$(p^f - p^f_h)(t) = (p^f - S^p_h p^f)(t) + (S^p_h p^f - p^f_h)(t) := e^I_p(t) + e^A_p(t).$$

Using (4.3.1c), (4.2.6b) and (4.1.3b), we obtain

$$\begin{aligned}
&\tilde{a}_2^h(\partial_t e_p^A, q_h^f) + a_2^h(e_p^A, q_h^f) - b_2(q_h^f, \partial_t e_\psi^A) \\
&\quad = \tilde{a}_2^h(\partial_t S_h^p p^f, q_h^f) + a_2(p^f, q_h^f) - b_2(q_h^f, \partial_t S_h^\psi \psi) - G^h(q_h^f) \\
&\quad = (\tilde{a}_2^h(\partial_t S_h^p p^f, q_h^f) - \tilde{a}_2(\partial_t p^f, q_h^f)) + b_2(q_h^f, \partial_t e_\psi^I) + (G - G^h)(q_h^f).
\end{aligned}$$

We can take $q_h^f = e_p^A$, which leads to

$$\begin{aligned}
&\tilde{a}_2^h(\partial_t e_p^A, e_p^A) + a_2^h(e_p^A, e_p^A) - b_2(e_p^A, \partial_t e_\psi^A) \\
&\quad = (\tilde{a}_2^h(\partial_t S_h^p p^f, e_p^A) - \tilde{a}_2(\partial_t p^f, e_p^A)) + b_2(e_p^A, \partial_t e_\psi^I) + (G - G^h)(e_p^A).
\end{aligned} \tag{4.3.5}$$

Next we use (4.3.1b), (4.2.6c) and (4.1.3c), and this implies

$$\begin{aligned}
&b_1(e_{\boldsymbol{u}}^A, \phi_h) + b_2(e_p^A, \phi_h) - a_3(e_\psi^A, \phi_h) = b_1(S_h^{\boldsymbol{u}} \boldsymbol{u}^s, \phi_h) + b_2(S_h^p p^f, \phi_h) - a_3(S_h^\psi \psi, \phi_h) \\
&\quad = b_1(\boldsymbol{u}^s, \phi_h) + b_2(S_h^p p^f, \phi_h) - a_3(S_h^\psi \psi, \phi_h) = -b_2(e_p^I, \phi_h) + a_3(e_\psi^I, \phi_h).
\end{aligned}$$

Differentiating the above equation with respect to time and taking $\phi_h = -e_\psi^A$, we can assert that

$$-b_1(\partial_t e_{\boldsymbol{u}}^A, e_\psi^A) - b_2(\partial_t e_p^A, e_\psi^A) + a_3(\partial_t e_\psi^A, e_\psi^A) = b_2(\partial_t e_p^I, e_\psi^A) - a_3(\partial_t e_\psi^I, e_\psi^A). \tag{4.3.6}$$

Then we simply add (4.3.4), (4.3.5) and (4.3.6), to obtain

$$\begin{aligned}
&a_1^h(e_{\boldsymbol{u}}^A, \partial_t e_{\boldsymbol{u}}^A) + \tilde{a}_2^h(\partial_t e_p^A, e_p^A) + a_2^h(e_p^A, e_p^A) \\
&\qquad + a_3(\partial_t e_\psi^A, e_\psi^A) - b_2(e_p^A, \partial_t e_\psi^A) - b_2(\partial_t e_p^A, e_\psi^A) \\
&\quad = (F - F^h)(\partial_t e_{\boldsymbol{u}}^A) + (\tilde{a}_2^h(\partial_t S_h^p p, e_p^A) - \tilde{a}_2(\partial_t p, e_p^A)) \\
&\qquad + b_2(e_p^A, \partial_t e_\psi^I) + (G - G^h)(e_p^A) + b_2(\partial_t e_p^I, e_\psi^A) - a_3(\partial_t e_\psi^I, e_\psi^A).
\end{aligned} \tag{4.3.7}$$

Regarding the left-hand side of (4.3.7), repeating arguments to obtain alike to (4.2.10). That is,

$$\begin{aligned}
&a_1^h(e_{\boldsymbol{u}}^A, \partial_t e_{\boldsymbol{u}}^A) + \tilde{a}_2^h(\partial_t e_p^A, e_p^A) + a_2^h(e_p^A, e_p^A) + a_3(\partial_t e_\psi^A, e_\psi^A) - b_2(e_p^A, \partial_t e_\psi^A) - b_2(\partial_t e_p^A, e_\psi^A) \\
&\geq \frac{1}{2}\frac{\mathrm{d}}{\mathrm{d}t} a_1^h(e_{\boldsymbol{u}}^A, e_{\boldsymbol{u}}^A) + \frac{c_0}{2}\frac{\mathrm{d}}{\mathrm{d}t}\|e_p^A\|_{0,\Omega}^2 + a_2^h(e_p^A, e_p^A) \\
&\qquad + \frac{1}{\lambda}\sum_K \Big(\alpha^2 \big(\partial_t(\Pi_K^0 e_p^A), \Pi_K^0 e_p^A\big)_{0,K} + \alpha^2 S_0^K\big((I - \Pi_K^0)\partial_t e_p^A, (I - \Pi_K^0) e_p^A\big)
\end{aligned}$$

$$
\begin{aligned}
&\quad + (\partial_t e_\psi^A, e_\psi^A)_{0,K} - \alpha(\Pi_K^0 e_p^A, \partial_t e_\psi^A)_{0,K} - \alpha(\Pi_K^0 \partial_t e_p^A, e_\psi^A)_{0,K}\Big) \\
&\geq C\bigg(\mu \frac{\mathrm{d}}{\mathrm{d}t}\|\boldsymbol{\varepsilon}(e_{\boldsymbol{u}}^A)\|_{0,\Omega}^2 + c_0 \frac{\mathrm{d}}{\mathrm{d}t}\|e_p^A\|_{0,\Omega}^2 + \frac{2\kappa_{\min}}{\eta}\|\nabla e_p^A\|_{0,\Omega}^2 \\
&\quad + \frac{1}{\lambda}\sum_K \bigg(\alpha^2 \frac{\mathrm{d}}{\mathrm{d}t}\|(I - \Pi_K^0)e_p^A\|_{0,K}^2 + \frac{\mathrm{d}}{\mathrm{d}t}\|\alpha \Pi_K^0 e_p^A - e_\psi^A\|_{0,K}^2\bigg)\bigg).
\end{aligned}
$$

Then integrating equation (4.3.7) in time and consistency of the bilinear term $\tilde{a}_2(\cdot,\cdot)$ implies the bound

$$
\begin{aligned}
&\mu\|\boldsymbol{\varepsilon}(e_{\boldsymbol{u}}^A(t))\|_{0,\Omega}^2 + c_0\|e_p^A(t)\|_{0,\Omega}^2 + \frac{\kappa_{\min}}{\eta}\int_0^t \|\nabla e_p^A(s)\|_{0,\Omega}^2 \,\mathrm{d}s \\
&\quad + \frac{1}{\lambda}\sum_K \Big(\alpha^2\|(I - \Pi_K^0)e_p^A(t)\|_{0,K}^2 + \|(\alpha\Pi_K^0 e_p^A - e_\psi^A)(t)\|_{0,K}^2\Big) \\
&\lesssim \mu\|\boldsymbol{\varepsilon}(e_{\boldsymbol{u}}^A(0))\|_{0,\Omega}^2 + c_0\|e_p^A(0)\|_{0,\Omega}^2 \\
&\quad + \frac{1}{\lambda}\sum_K \Big(\alpha^2\|(I - \Pi_K^0)e_p^A(0)\|_{0,K}^2 + \|(\alpha\Pi_K^0 e_p^A - e_\psi^A)(0)\|_{0,K}^2\Big) \\
&\quad + \sum_{i=1}^4 D_i,
\end{aligned}
$$

where

$$
\begin{aligned}
D_1 &:= \rho\int_0^t \big((\boldsymbol{b} - \boldsymbol{b}^h)(s), \partial_t e_{\boldsymbol{u}}^A(s)\big)_{0,\Omega}\,\mathrm{d}s, \\
D_2 &:= \int_0^t \big((\ell - \ell^h)(s), e_p^A(s)\big)_{0,\Omega}\,\mathrm{d}s, \\
D_3 &:= \int_0^t \sum_K \Big(\tilde{a}_2^{h,K}\big(\partial_t(S_h^p p^f - p_\pi^f)(s), e_p^A(s)\big) - \tilde{a}_2^K\big(\partial_t(p^f - p_\pi^f)(s), e_p^A(s)\big)\Big)\,\mathrm{d}s, \\
\text{and } D_4 &:= \int_0^t \Big(b_2\big(e_p^A(s), \partial_t e_\psi^I(s)\big) + b_2\big(\partial_t e_p^I(s), e_\psi^A(s)\big) - a_3\big(\partial_t e_\psi^I(s), e_\psi^A(s)\big)\Big)\,\mathrm{d}s.
\end{aligned}
$$

Then we can integrate by parts (also in time), use Cauchy-Schwarz inequality and Young's inequality to arrive at

$$
\begin{aligned}
D_1 = \rho\bigg(&\big((\boldsymbol{b} - \boldsymbol{b}^h)(t), e_{\boldsymbol{u}}^A(t)\big)_{0,\Omega} - \big((\boldsymbol{b} - \boldsymbol{b}^h)(0), e_{\boldsymbol{u}}^A(0)\big)_{0,\Omega} \\
&- \int_0^t \big(\partial_t(\boldsymbol{b} - \boldsymbol{b}^h)(s), e_{\boldsymbol{u}}^A(s)\big)_{0,\Omega}\,\mathrm{d}s\bigg)
\end{aligned}
$$

$$\leq C_1(\rho,\mu)h\Big(h|\boldsymbol{b}(t)|_{1,\Omega}^2 + |\boldsymbol{b}(0)|_{1,\Omega}\|e_{\boldsymbol{u}}^A(0)\|_{0,\Omega} + \int_0^t |\partial_t\boldsymbol{b}(s)|_{1,\Omega}\|e_{\boldsymbol{u}}^A(s)\|_{0,\Omega}\,\mathrm{d}s\Big)$$
$$+\frac{\mu}{2}\|\boldsymbol{\varepsilon}(e_{\boldsymbol{u}}^A(t))\|_{0,\Omega}^2,$$

where we have used standard error estimate for the L^2-projection $\boldsymbol{\Pi}_K^{0,0}$ onto piecewise constant functions. Using also Cauchy-Schwarz inequality, standard error estimates for Π_K^0 on the term D_2, Young's and Poincaré inequality readily gives

$$D_2 \leq Ch\int_0^t |\ell(s)|_{1,\Omega}\|e_p^A(s)\|_{0,\Omega}\,\mathrm{d}s \leq C_2h^2\int_0^t |\ell(s)|_{1,\Omega}^2\,\mathrm{d}s + \frac{\kappa_{\min}}{6\eta}\int_0^t \|\nabla e_p^A(s)\|_{0,\Omega}^2\,\mathrm{d}s.$$

On the other hand, considering the polynomial approximation p_π^f (cf. (4.3.3)) of p^f, utilizing the triangle inequality, Young's and Poincaré inequality yield

$$\begin{aligned}
D_3 &\leq C\Big(c_0+\frac{\alpha^2}{\lambda}\Big)\int_0^t\sum_K\Big(\|\partial_t(S_h^p p^f - p_\pi^f)(s)\|_{0,K} + \|\partial_t(p^f - p_\pi^f)(s)\|_{0,K}\Big)\|e_p^A(s)\|_{0,K}\,\mathrm{d}s\\
&\leq Ch^2\Big(c_0+\frac{\alpha^2}{\lambda}\Big)\int_0^t |\partial_t p^f(s)|_{2,\Omega}\|e_p^A(s)\|_{0,\Omega}\,\mathrm{d}s\\
&\leq C_3h^4\Big(c_0+\frac{\alpha^2}{\lambda}\Big)^2\int_0^t |\partial_t p^f(s)|_{2,\Omega}^2\,\mathrm{d}s + \frac{\kappa_{\min}}{6\eta}\int_0^t\|\nabla e_p^A(s)\|_{0,\Omega}^2\,\mathrm{d}s.
\end{aligned}$$

Also,

$$\begin{aligned}
D_4 &= \int_0^t\Big(b_2\big(e_p^A(s),\partial_t e_\psi^I(s)\big) + b_2\big(\partial_t e_p^I(s), e_\psi^A(s)\big) - a_3\big(\partial_t e_\psi^I(s), e_\psi^A(s)\big)\Big)\,\mathrm{d}s\\
&\leq \frac{1}{\lambda}\int_0^t\Big(\alpha\|e_p^A(s)\|_{0,\Omega}\|\partial_t e_\psi^I(s)\|_{0,\Omega} + \big(\alpha\|\partial_t e_p^I(s)\|_{0,\Omega} + \|\partial_t e_\psi^I(s)\|_{0,\Omega}\big)\|e_\psi^A(s)\|_{0,\Omega}\Big)\,\mathrm{d}s\\
&\leq \frac{C}{\lambda}h\int_0^t\Big(\alpha\|e_p^A(s)\|_{0,\Omega}(|\partial_t\psi(s)|_{1,\Omega} + |\partial_t\boldsymbol{u}^s(s)|_{2,\Omega})\\
&\qquad + (\alpha h|\partial_t p^f(s)|_{2,\Omega} + |\partial_t\psi(s)|_{1,\Omega} + |\partial_t\boldsymbol{u}^s(s)|_{2,\Omega})\|e_\psi^A(s)\|_{0,\Omega}\Big)\,\mathrm{d}s.
\end{aligned}$$

Using (4.2.5) and a combination of equations (4.3.1a), (4.2.6a) and (4.1.3a), we get

$$\begin{aligned}
\|e_\psi^A(t)\|_{0,\Omega} &\leq \sup_{\boldsymbol{v}_h^s\in\mathbf{V}_h\setminus\{0\}}\frac{b_1(\boldsymbol{v}_h^s, e_\psi^A(t))}{\|\boldsymbol{v}_h^s\|_{1,\Omega}} \leq C\left(\rho\sum_K\|(\boldsymbol{b}-\boldsymbol{b}^h)(t)\|_{0,K} + \mu\|\boldsymbol{\varepsilon}(e_{\boldsymbol{u}}^A(t))\|_{0,\Omega}\right)\\
&\leq C\big(\rho\, h|\boldsymbol{b}(t)|_{1,\Omega} + \mu\|\boldsymbol{\varepsilon}(e_{\boldsymbol{u}}^A(t))\|_{0,\Omega}\big).
\end{aligned} \tag{4.3.8}$$

Then the bound of D_4 with the help of Young's and Poincaré inequality becomes

$$D_4 \leq \frac{C_6}{\lambda} h \int_0^t \Big((\alpha h |\partial_t p^f(s)|_{2,\Omega} + |\partial_t \psi(s)|_{1,\Omega} + |\partial_t \boldsymbol{u}^s(s)|_{2,\Omega})(\rho h |\boldsymbol{b}(s)|_{1,\Omega} + \mu \|\boldsymbol{\varepsilon}(e_{\boldsymbol{u}}^A(t))\|_{0,\Omega}) \\ + \alpha^2 \frac{h}{\lambda} (|\partial_t \psi(s)|_{1,\Omega} + |\partial_t \boldsymbol{u}^s(s)|_{2,\Omega})^2 \Big) \, \mathrm{d}s + \frac{\kappa_{\min}}{6\eta} \int_0^t \|\nabla e_p^A(s)\|_{0,\Omega}^2 \, \mathrm{d}s.$$

Combining the bounds of all $D_i, i = 1, 2, 3, 4$ and proceeding similar fashion as we obtained the bounds in (4.2.12) (using Lemma 4.1 and (4.2.8)), eventually allows us to conclude that

$$\begin{aligned} &\mu \|\boldsymbol{\varepsilon}(e_{\boldsymbol{u}}^A(t))\|_{0,\Omega}^2 + c_0 \|e_p^A(t)\|_{0,\Omega}^2 + \frac{\kappa_{\min}}{\eta} \int_0^t \|\nabla e_p^A(s)\|_{0,\Omega}^2 \, \mathrm{d}s \\ &\leq \mu \|\boldsymbol{\varepsilon}(e_{\boldsymbol{u}}^A(0))\|_{0,\Omega}^2 + \Big(c_0 + \frac{\alpha^2}{\lambda}\Big) \|e_p^A(0)\|_{0,\Omega}^2 + \frac{1}{\lambda} \|e_\psi^A(0)\|_{0,\Omega}^2 \\ &\quad + C\, h^2 \Bigg(\sup_{t \in [0,T]} |\boldsymbol{b}(t)|_{1,\Omega}^2 + \int_0^t \Bigg(|\boldsymbol{b}(s)|_{1,\Omega}^2 + |\partial_t \boldsymbol{b}(s)|_{1,\Omega}^2 + |\ell(s)|_{1,\Omega}^2 \\ &\qquad + \Big(\frac{1}{\lambda}\Big)^2 (|\partial_t \psi(s)|_{1,\Omega}^2 + |\partial_t \boldsymbol{u}^s(s)|_{2,\Omega}^2) + \Big(c_0 + \frac{\alpha^2}{\lambda}\Big)^2 h^2 |\partial_t p^f(s)|_{2,\Omega}^2 \Bigg) \, \mathrm{d}s \Bigg). \end{aligned}$$

Then choosing $\boldsymbol{u}_h^s(0) := S_h^{\boldsymbol{u}} \boldsymbol{u}^s(0)$, $\psi_h(0) := S_h^\psi \psi(0)$, $p_h^f(0) := S_h^p p^f(0)$ and applying the triangle inequality together with bound (4.3.8) completes the rest of the proof. $\square$

Following a similar structure to the proof of Theorem 4.4, we can establish error estimates for the fully-discrete problem. Details on the proof are postponed to the Appendix.

Theorem 4.5 (Fully-discrete error estimates)**.** *Let $(\boldsymbol{u}^s(t), p^f(t), \psi(t)) \in \mathbf{V} \times Q \times Z$ and $(\boldsymbol{u}_h^{s,n}, p_h^{f,n}, \psi_h^n) \in \mathbf{V}_h \times Q_h \times Z_h$ be the unique solutions to problems* (4.1.3a)-(4.1.3c) *and* (4.2.16a)-(4.2.16c)*, respectively. Then the following estimates hold for any $n = 1, \ldots, N$, with constants C independent of h, Δt, λ and c_0:*

$$\mu \|\boldsymbol{\varepsilon}(\boldsymbol{u}^s(t_n) - \boldsymbol{u}_h^{s,n})\|_{0,\Omega}^2 + \|\psi(t_n) - \psi_h^n\|_{0,\Omega}^2 \\ + (\Delta t) \frac{\kappa_{\min}}{\eta} \|\nabla (p^f(t_n) - p_h^{f,n})\|_{0,\Omega}^2 \leq C\,(h^2 + \Delta t^2). \tag{4.3.9}$$

Proof. As in the semidiscrete case we split the individual errors as

$$\begin{aligned} \boldsymbol{u}^s(t_n) - \boldsymbol{u}_h^{s,n} &= (\boldsymbol{u}^s(t_n) - S_h^{\boldsymbol{u}} \boldsymbol{u}^s(t_n)) + (S_h^{\boldsymbol{u}} \boldsymbol{u}^s(t_n) - \boldsymbol{u}_h^{s,n}) := E_{\boldsymbol{u}}^{I,n} + E_{\boldsymbol{u}}^{A,n}, \\ \psi(t_n) - \psi_h^n &= (\psi(t_n) - S_h^\psi \psi(t_n)) + (S_h^\psi \psi(t_n) - \psi_h^n) := E_\psi^{I,n} + E_\psi^{A,n}, \end{aligned}$$

$$p^f(t_n) - p_h^{f,n} = (p^f(t_n) - S_h^p p^f(t_n)) + (S_h^p p^f(t_n) - p_h^{f,n}) := E_p^{I,n} + E_p^{A,n}.$$

Then, from estimate (4.3.2a) and following the steps of the proof of Theorem 4.4 we get the bounds

$$\begin{aligned}
\|E_{\boldsymbol{u}}^{I,n}\|_{1,\Omega} &\leq Ch(|\boldsymbol{u}^s(t_n)|_{2,\Omega} + |\psi(t_n)|_{1,\Omega}) \\
&\leq Ch(|\boldsymbol{u}^s(0)|_{2,\Omega} + |\psi(0)|_{1,\Omega} \\
&\qquad + \|\partial_t \boldsymbol{u}^s\|_{\mathbf{L}^1([H^2(\Omega)]^2)} + \|\partial_t \psi\|_{L^1(H^1(\Omega))}), && (4.3.10a) \\
\|E_{\psi}^{I,n}\|_{0,\Omega} &\leq Ch(|\boldsymbol{u}^s(0)|_{2,\Omega} + |\psi(0)|_{1,\Omega} + \|\partial_t \boldsymbol{u}^s\|_{\mathbf{L}^1([H^2(\Omega)]^2)} \\
&\qquad + \|\partial_t \psi\|_{L^1(H^1(\Omega))}), && (4.3.10b) \\
\|E_p^{I,n}\|_{1,\Omega} &\leq Ch(|p^f(0)|_{2,\Omega} + \|\partial_t p^f\|_{L^1(H^2(\Omega))}). && (4.3.10c)
\end{aligned}$$

From equations (4.3.1a), (4.2.16a) and (4.1.3a), we readily get

$$a_1^h(E_{\boldsymbol{u}}^{A,n}, \boldsymbol{v}_h^s) + b_1(\boldsymbol{v}_h^s, E_\psi^{A,n}) = F^n(\boldsymbol{v}_h^s) - F^{h,n}(\boldsymbol{v}_h^s). \tag{4.3.11}$$

We then use (4.3.1b) and (4.2.20), and proceed to differentiate (4.1.3c) with respect to time. This implies

$$\begin{aligned}
&b_1(E_{\boldsymbol{u}}^{A,n} - E_{\boldsymbol{u}}^{A,n-1}, \phi_h) + b_2(E_p^{A,n} - E_p^{A,n-1}, \phi_h) - a_3(E_\psi^{A,n} - E_\psi^{A,n-1}, \phi_h) \\
&\quad = b_1((\boldsymbol{u}^s(t_n) - \boldsymbol{u}^s(t_{n-1})) - (\Delta t)\partial_t \boldsymbol{u}^s(t_n), \phi_h) \\
&\qquad + b_2((S_h^p p^f(t_n) - S_h^p p^f(t_{n-1})) - (\Delta t)\partial_t p^f(t_n), \phi_h) \\
&\qquad - a_3((S_h^\psi \psi(t_n) - S_h^\psi \psi(t_{n-1})) - (\Delta t)\partial_t \psi(t_n), \phi_h).
\end{aligned} \tag{4.3.12}$$

After choosing $\boldsymbol{v}_h^s = E_{\boldsymbol{u}}^{A,n} - E_{\boldsymbol{u}}^{A,n-1}$ in (4.3.11) and $\phi_h = -E_\psi^{A,n}$ in (4.3.12) and adding the outcomes, we readily get

$$\begin{aligned}
&a_1^h(E_{\boldsymbol{u}}^{A,n}, E_{\boldsymbol{u}}^{A,n} - E_{\boldsymbol{u}}^{A,n-1}) + a_3(E_\psi^{A,n} - E_\psi^{A,n-1}, E_\psi^{A,n}) - b_2(E_p^{A,n} - E_p^{A,n-1}, E_\psi^{A,n}) \\
&= \rho(\boldsymbol{b}(t_n) - \boldsymbol{b}_h^n, E_{\boldsymbol{u}}^{A,n} - E_{\boldsymbol{u}}^{A,n-1})_{0,\Omega} - b_1((\boldsymbol{u}^s(t_n) - \boldsymbol{u}^s(t_{n-1})) - (\Delta t)\partial_t \boldsymbol{u}^s(t_n), E_\psi^{A,n}) \\
&\qquad - b_2((S_h^p p^f(t_n) - S_h^p p^f(t_{n-1})) - (\Delta t)\partial_t p^f(t_n), E_\psi^{A,n}) \\
&\qquad + a_3((S_h^\psi \psi(t_n) - S_h^\psi \psi(t_{n-1})) - (\Delta t)\partial_t \psi(t_n), E_\psi^{A,n}).
\end{aligned} \tag{4.3.13}$$

Next, and as a consequence of using (4.3.1c), (4.2.6b) and (4.1.3b) with $q_h^f = E_p^{A,n}$, we are left with

$$\begin{aligned}
&\tilde{a}_2^h(E_p^{A,n}-E_p^{A,n-1},E_p^{A,n})+\Delta t a_2^h(E_p^{A,n},E_p^{A,n})-b_2(E_p^{A,n},E_\psi^{A,n}-E_\psi^{A,n-1})\\
&=\Delta t(\ell(t_n)-\ell_h^n,E_p^{A,n})_{0,\Omega}+\tilde{a}_2^h(S_h^p p^f(t_n)-S_h^p p^f(t_{n-1}),E_p^{A,n})\\
&\qquad-\tilde{a}_2((\Delta t)\partial_t p^f(t_n),E_p^{A,n})+b_2(E_p^{A,n},(\Delta t)\partial_t\psi-(S_h^\psi\psi(t_n))-S_h^\psi\psi(t_{n-1})).
\end{aligned}\tag{4.3.14}$$

If we then add the resulting equations (4.3.13)-(4.3.14) and repeat the same arguments used in deriving (4.2.10), we can assert that

$$\begin{aligned}
&a_3(E_\psi^{A,n}-E_\psi^{A,n-1},E_\psi^{A,n})-b_2(E_p^{A,n}-E_p^{A,n-1},E_\psi^{A,n})\\
&\qquad-b_2(E_p^{A,n},E_\psi^{A,n}-E_\psi^{A,n-1})+\tilde{a}_2^h(E_p^{A,n}-E_p^{A,n-1},E_p^{A,n})\\
&=(\Delta t)\Bigg(c_0(\delta_t E_p^{A,n},E_p^{A,n})_{0,\Omega}+\frac{1}{\lambda}\sum_K\big(\alpha^2(\delta_t(I-\Pi_K^0)E_p^{A,n},(I-\Pi_K^0)E_p^{A,n})_{0,K}\\
&\qquad-(\delta_t(\alpha\Pi_K^0E_p^{A,n}-E_\psi^{A,n}),\alpha\Pi_K^0E_p^{A,n}-E_\psi^{A,n})_{0,K}\big)\Bigg),
\end{aligned}$$

The left-hand side can be bounded by using the inequality (4.2.23) and then summing over n we get

$$\begin{aligned}
&\mu\|\boldsymbol{\varepsilon}(E_{\boldsymbol{u}}^{A,n})\|_{0,\Omega}^2+c_0\|E_p^{A,n}\|_{0,\Omega}^2+(\Delta t)\frac{\kappa_{\min}}{\eta}\sum_{j=1}^n\|\nabla E_p^{A,j}\|_{0,\Omega}^2\\
&\qquad+(1/\lambda)\sum_K\left(\alpha^2\|(I-\Pi_K^0)E_p^{A,n}\|_{0,K}^2+\|\alpha\Pi_K^0E_p^{A,n}-E_\psi^{A,n}\|_{0,K}^2\right)\\
&\le\mu\|\boldsymbol{\varepsilon}(E_{\boldsymbol{u}}^{A,0})\|_{0,\Omega}^2+c_0\|E_p^{A,0}\|_{0,\Omega}^2+(1/\lambda)\sum_K\left(\alpha^2\|(I-\Pi_K^0)E_p^{A,0}\|_{0,K}^2+\|\alpha\Pi_K^0E_p^{A,0}-E_\psi^{A,0}\|_{0,K}^2\right)\\
&\qquad+\underbrace{\sum_{j=1}^n\rho(\boldsymbol{b}(t_j)-\boldsymbol{b}_h^j,E_{\boldsymbol{u}}^{A,j}-E_{\boldsymbol{u}}^{A,j-1})_{0,\Omega}}_{=:L_1}+\underbrace{\sum_{j=1}^n\Delta t(\ell(t_j)-\ell_h^j,E_p^{A,j})_{0,\Omega}}_{=:L_2}\\
&\qquad\underbrace{-\sum_{j=1}^n b_1((\boldsymbol{u}^s(t_j)-\boldsymbol{u}^s(t_{j-1}))-(\Delta t)\partial_t\boldsymbol{u}^s(t_j),E_\psi^{A,j})}_{=:L_3}\\
&\qquad\underbrace{-\sum_{j=1}^n b_2((S_h^p p^f(t_j)-S_h^p p^f(t_{j-1}))-(\Delta t)\partial_t p^f(t_j),E_\psi^{A,j})}_{=:L_4}
\end{aligned}$$

$$
+ \underbrace{\sum_{j=1}^{n} a_3((S_h^{\psi}\psi(t_j) - S_h^{\psi}\psi(t_{j-1})) - (\Delta t)\partial_t\psi(t_j), E_{\psi}^{A,j})}_{:=L_5}
$$

$$
+ \underbrace{\sum_{j=1}^{n}(\tilde{a}_2^h(S_h^p p^f(t_j) - S_h^p p^f(t_{j-1}), E_p^{A,j}) - \tilde{a}_2((\Delta t)\partial_t p^f(t_j), E_p^{A,j}))}_{:=L_6}
$$

$$
+ \underbrace{\sum_{j=1}^{n} b_2(E_p^{A,j}, (\Delta t)\partial_t\psi - (S_h^{\psi}\psi(t_j) - S_h^{\psi}\psi(t_{j-1}))}_{:=L_7}.
$$

We bound the term L_1 with the help of formula (4.2.24), the estimates of projection $\mathbf{\Pi}_K^{\mathbf{0}}$, applying Taylor expansion, and using the generalized Young's inequality. This gives

$$
\begin{aligned}
L_1 &= \rho\Big(((\boldsymbol{b} - \boldsymbol{b}_h)(t_n), E_{\boldsymbol{u}}^{A,n})_{0,\Omega} - ((\boldsymbol{b} - \boldsymbol{b}_h)(0), E_{\boldsymbol{u}}^{A,0})_{0,\Omega} \\
&\qquad - \sum_{j=1}^{n}(\Delta t)(\delta_t(\boldsymbol{b} - \boldsymbol{b}_h)(t_j), E_{\boldsymbol{u}}^{A,j-1})_{0,\Omega})\Big) \\
&\le \frac{\mu}{2}\|\boldsymbol{\varepsilon}(E_{\boldsymbol{u}}^{A,n})\|_{0,\Omega}^2 + C_1\Big(\frac{\rho}{\mu}h|\boldsymbol{b}(0)|_{1,\Omega}\ \mu\|\boldsymbol{\varepsilon}(E_{\boldsymbol{u}}^{A,0})\|_{0,\Omega} + \frac{\rho^2}{\mu}h^2\max_{1\le j\le n}|\boldsymbol{b}(t_j)|_{1,\Omega}^2 \\
&\qquad + (\Delta t)\ h\sum_{j=1}^{n}\frac{\rho}{\mu}\Big(|\partial_t\boldsymbol{b}^j|_{1,\Omega} + \big(\Delta t\int_{t_{j-1}}^{t_j}|\partial_{tt}\boldsymbol{b}(s)|_{1,\Omega}^2\,\mathrm{d}s\big)^{1/2}\Big)\mu\|\boldsymbol{\varepsilon}(E_{\boldsymbol{u}}^{A,j-1})\|_{0,\Omega}\Big).
\end{aligned}
$$

Then the estimate satisfied by the projection Π_K^0 along with Poincaré and Young's inequalities, yield

$$
\begin{aligned}
L_2 &\le C_2\sum_{j=1}^{n}(\Delta t)h|\ell(t_j)|_{1,\Omega}\|\nabla E_p^{A,j}\|_{0,\Omega} \\
&\le C_2\sum_{j=1}^{n}(\Delta t)\frac{\eta}{\kappa_{\min}}h^2|\ell(t_j)|_{1,\Omega}^2 + (\Delta t)\frac{\kappa_{\min}}{6\eta}\sum_{j=1}^{n}\|\nabla E_p^{A,j}\|_{0,\Omega}^2.
\end{aligned}
$$

The discrete inf-sup condition (4.2.5) implies that

$$
\|E_{\psi}^{A,j}\|_{0,\Omega} \le C(h|\boldsymbol{b}(t_j)|_{1,\Omega} + \|\boldsymbol{\varepsilon}(E_{\boldsymbol{u}}^{A,j})\|_{0,\Omega}). \tag{4.3.15}
$$

Applying an expansion in Taylor series, together with (4.3.15), the Cauchy-Schwarz, and Young inequalities, enable us to write

$$L_3 \le C\sum_{j=1}^{n}\Big((\Delta t)^3\int_{t_{j-1}}^{t_j}\|\partial_{tt}\boldsymbol{u}^s(s)\|_{0,\Omega}^2\,\mathrm{d}s\Big)^{1/2}(h|\boldsymbol{b}(t_j)|_{1,\Omega}+\|\boldsymbol{\varepsilon}(E_{\boldsymbol{u}}^{A,j})\|_{0,\Omega}).$$

Then, after using the estimates of the projection S_h^p (4.3.2b), (4.3.15), and applying again Cauchy-Schwarz inequality, we get

$$\begin{aligned}L_4 &\le C\frac{\alpha}{\lambda}\sum_{j=1}^{n}\Big(\|S_h^p(p^f(t_j)-p^f(t_{j-1}))-(p^f(t_j)-p^f(t_{j-1}))\|_{0,\Omega}\\&\qquad+\|(p^f(t_j)-p^f(t_{j-1}))-(\Delta t)\partial_t p^f(t_j)\|_{0,\Omega}\Big)\|E_\psi^{A,j}\|_{0,\Omega}\\&\le C\frac{\alpha}{\lambda}\sum_{j=1}^{n}\Big(h^2\Big((\Delta t)\int_{t_{j-1}}^{t_j}|\partial_t p^f(s)|_{2,\Omega}^2\,\mathrm{d}s\Big)^{1/2}+\Big((\Delta t)^3\int_{t_{j-1}}^{t_j}\|\partial_{tt}p^f(s)\|_{0,\Omega}^2\,\mathrm{d}s\Big)^{1/2}\Big)\\&\qquad\times(\rho h|\boldsymbol{b}(t_j)|_{1,\Omega}+\|\boldsymbol{\varepsilon}(E_{\boldsymbol{u}}^{A,j})\|_{0,\Omega}).\end{aligned}$$

The stability of $a_3(\cdot,\cdot)$ and the proof for the bound of L_4 gives

$$\begin{aligned}L_5 &\le C(1/\lambda)\sum_{j=1}^{n}\|(S_h^\psi\psi(t_j)-S_h^\psi\psi(t_{j-1}))-(\Delta t)\partial_t\psi(t_j)\|_{0,\Omega}(\rho h|\boldsymbol{b}(t_j)|_{1,\Omega}+\|\boldsymbol{\varepsilon}(E_{\boldsymbol{u}}^{A,j})\|_{0,\Omega})\\&\le C(1/\lambda)\sum_{j=1}^{n}\Big(h^2\Big((\Delta t)\int_{t_{j-1}}^{t_j}(|\partial_t\boldsymbol{u}^s(s)|_{2,\Omega}^2+|\partial_t\psi(s)|_{1,\Omega}^2)\,\mathrm{d}s\Big)^{1/2}\\&\qquad+\Big((\Delta t)^3\int_{t_{j-1}}^{t_j}\|\partial_{tt}\psi(s)\|_{0,\Omega}^2\,\mathrm{d}s\Big)^{1/2}\Big)\times(\rho h|\boldsymbol{b}(t_j)|_{1,\Omega}+\|\boldsymbol{\varepsilon}(E_{\boldsymbol{u}}^{A,j})\|_{0,\Omega}).\end{aligned}$$

The polynomial approximation p_π for fluid pressure, consistency of the bilinear form $\tilde{a}_2^h(\cdot,\cdot)$, stability of the bilinear forms $\tilde{a}_2(\cdot,\cdot),\tilde{a}_2^h(\cdot,\cdot)$, the Cauchy-Schwarz, Poincaré and Young's inequalities gives

$$\begin{aligned}L_6 &= \sum_{j=1}^{n}\Big(\tilde{a}_2^h((S_h^p p^f(t_j)-S_h^p p^f(t_{j-1}))-(p_\pi^f(t_j)-p_\pi^f(t_{j-1})),E_p^{A,j})\\&\qquad+\tilde{a}_2((p_\pi^f(t_j)-p_\pi^f(t_{j-1}))-(p^f(t_j)-p^f(t_{j-1})),E_p^{A,j})\\&\qquad+\tilde{a}_2((p^f(t_j)-p^f(t_{j-1}))-(\Delta t)\partial_t p^f(t_j),E_p^{A,j})\Big)\\&\le C\Big(c_0+\frac{\alpha^2}{\lambda}\Big)^2\Big(h^4\|\partial_t p^f\|_{L^2(H^2(\Omega))}^2+(\Delta t)^2\|\partial_{tt}p^f\|_{L^2(L^2(\Omega))}^2\Big)\end{aligned}$$

$$+ \Delta t \frac{\kappa_{\min}}{6\eta} \sum_{j=1}^{n} \|\nabla E_p^{A,j}\|_{0,\Omega}^2.$$

The continuity of $b_2(\cdot,\cdot)$, the bound derived for the term L_5 and using the Young's inequality gives

$$\begin{aligned}
L_7 &\leq \frac{\alpha}{\lambda} \sum_{j=1}^{n} \|(\Delta t)\partial_t \psi(t_j) - (S_h^{\psi}\psi(t_j) - S_h^{\psi}\psi(t_{j-1}))\|_{0,\Omega} \|E_p^{A,j}\|_{0,\Omega} \\
&\leq C\Big(\frac{\alpha}{\lambda}\Big)^2 \Big(h^2 (\|\partial_t \psi\|^2_{L^2(H^1(\Omega))} + \|\partial_t \boldsymbol{u}^s\|^2_{\mathbf{L}^2([H^2(\Omega)]^2)}) + (\Delta t)^2 \|\partial_{tt}\psi\|^2_{L^2(L^2(\Omega))} \Big) \\
&\quad + (\Delta t) \frac{\kappa_{\min}}{6\eta} \sum_{j=1}^{n} \|\nabla E_p^{A,j}\|^2_{0,\Omega}.
\end{aligned}$$

In turn, putting together the bounds obtained for all L_i's, $i = 1, \ldots, 7$, using the Young's inequality and Lemma 4.2 concludes that

$$\begin{aligned}
&\mu \|\boldsymbol{\varepsilon}(E_{\boldsymbol{u}}^{A,n})\|^2_{0,\Omega} + c_0 \|E_p^{A,n}\|^2_{0,\Omega} + (\Delta t) \frac{\kappa_{\min}}{\eta} \sum_{j=1}^{n} \|\nabla E_p^{A,j}\|^2_{0,\Omega} \\
&\leq C \Big(\mu \|\boldsymbol{\varepsilon}(E_{\boldsymbol{u}}^{A,0})\|^2_{0,\Omega} + (c_0 + \alpha^2/\lambda) \|E_p^{A,0}\|^2_{0,\Omega} + (1/\lambda) \|E_{\psi}^{A,0}\|^2_{0,\Omega} + \Big(1 + \Delta t\Big) h^2 \max_{0 \leq j \leq n} |\boldsymbol{b}(t_j)|^2_{1,\Omega} \\
&\quad + h^2 \Delta t \sum_{j=1}^{n} (|\boldsymbol{b}(t_j)|^2_{1,\Omega} + (\Delta t)|\partial_t \boldsymbol{b}|^2_{1,\Omega} + |\ell(t_j)|^2_{1,\Omega}) + (\Delta t)^2 h^2 \|\partial_{tt} \boldsymbol{b}\|_{\mathbf{L}^2([H^1(\Omega)]^2)} \\
&\quad + (\Delta t)^2 \big((c_0 + \alpha^2/\lambda)^2 \|\partial_{tt} p^f\|^2_{L^2(L^2(\Omega))} + \|\partial_{tt} \boldsymbol{u}^s\|^2_{\mathbf{L}^2([L^2(\Omega)]^2)} + \frac{\alpha^2}{\lambda^2} \|\partial_{tt}\psi\|^2_{L^2(L^2(\Omega))} \big) \\
&\quad + h^2 \big(\frac{\alpha^2}{\lambda^2} \|\partial_t \psi\|^2_{L^2(H^1(\Omega))} + \frac{\alpha^2}{\lambda^2} \|\partial_t \boldsymbol{u}^s\|^2_{\mathbf{L}^2([H^2(\Omega)]^2)} + (c_0 + \alpha^2/\lambda)^2 h^2 \|\partial_t p^f\|^2_{L^2(H^2(\Omega))} \big) \Big).
\end{aligned}$$

And finally, the desired result (4.3.9) holds after choosing $\boldsymbol{u}_h^{s,0} := \boldsymbol{u}_I^s(0)$, $\psi_h^0 := \Pi^{0,0}\psi(0)$, $p_h^{f,0} := p_I^f(0)$ and applying triangle's inequality together with (4.3.10a)-(4.3.10c) and (4.3.15). □

Remark 4.2. *It is well known that an application of Grownwall's lemma implies an exponential dependency of the generic constant (appearing on the right-hand side) on the final time, and the resulting bounds are therefore not very useful for large time intervals. We stress that by following the approach used in [98, 96] we can establish convergence and stability for the semi- and fully discrete schemes circumventing the use of Gronwall's inequality. A different approach, employed in, e.g., [123] in the context of poroelasticity problems, is to integrate in time the mass conservation*

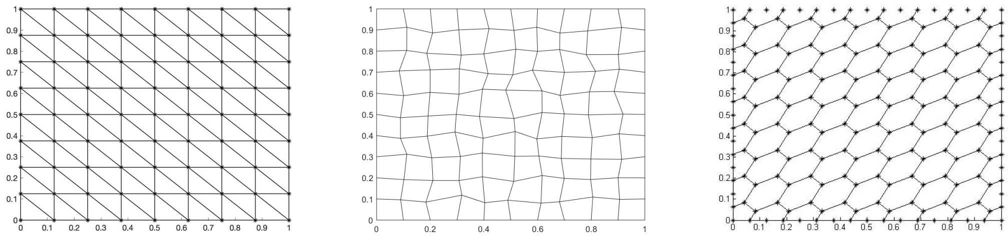

(a) (b) (c)

Figure 4.1: Samples of triangular (a), distorted quadrilateral (b), and hexagonal (c) meshes employed for the numerical tests in this section.

equation.

4.4 Numerical results

In this section conduct numerical tests to computationally reconfirm the convergence rates of the proposed VE scheme and present one test of applicative interest in poromechanics. All numerical results are produced by an in-house MATLAB code, using sparse factorization as linear solver.

4.4.1 Verification of spatial convergence

First we consider a steady version of the poroelasticity equations. An exact solution of the problem on a square domain $(0,1)^2$ is given by the smooth functions

$$\boldsymbol{u}^s(x,y) = \begin{pmatrix} -\cos(2\pi x)\ \sin(2\pi y) + \sin(2\pi y) + \sin^2(\pi x)\sin^2(\pi y) \\ \sin(2\pi x)\cos(2\pi y) - \sin(2\pi x) \end{pmatrix},$$
$$p^f(x,y) = \sin^2(\pi x)\sin^2(\pi y), \quad \psi(x,y) = \alpha p^f - \lambda \operatorname{div} \boldsymbol{u}^s.$$

The body load $\boldsymbol{f}$ and the fluid source ℓ are computed by evaluating these closed-form solutions and the problem is completely characterized after specifying the model constants

$$\nu = 0.3, \quad E_c = 100, \quad \kappa = 1, \quad \alpha = 1, \quad c_0 = 1, \quad \eta = 0.1,$$
$$\lambda = \frac{E_c \nu}{(1+\nu)(1-2\nu)}, \quad \mu = \frac{E_c}{(2+2\nu)}.$$

Ndof	h^{-1}	$e_1(\boldsymbol{u}^s)$	$r_1(\boldsymbol{u}^s)$	$e_0(\boldsymbol{u}^s)$	$r_0(\boldsymbol{u}^s)$	$e_0(\psi)$	$r_0(\psi)$	$e_1(p^f)$	$r_1(p^f)$	$e_0(p^f)$	$r_0(p^f)$
179	4	0.477968	-	0.271687	-	0.508386	-	0.444463	-	0.142539	-
819	8	0.204990	1.22	0.055766	2.28	0.198845	1.35	0.195632	1.18	0.029745	2.26
3419	16	0.097838	1.07	0.013083	2.09	0.091837	1.11	0.097854	1.00	0.007526	1.98
13819	32	0.049954	0.97	0.003322	1.98	0.043829	1.07	0.024456	1.02	0.001842	2.03
56067	64	0.024756	1.01	$8.2 \cdot 10^{-4}$	2.02	0.021704	1.01	0.024456	0.98	$4.7 \cdot 10^{-4}$	1.96

Table 4.1: Verification of space convergence for the method with $k = 1$. Errors and convergence rates r for solid displacement, total pressure and fluid pressure.

On a sequence of successively refined grids (we have employed for this particular case, uniform triangular meshes as depicted in Figure 4.1(a)) we compute errors and convergence rates according to the meshsize and tabulating also the total number of degrees of freedom (Ndof). The experimental error decay (with respect to mesh refinement) is measured using individual relative norms defined as follows:

$$e_1(\boldsymbol{u}^s) := \frac{\left(\sum_{K\in\mathcal{T}_h} |\boldsymbol{u}^s - \boldsymbol{\Pi}^{\boldsymbol{\varepsilon}}_K \boldsymbol{u}^s_h|^2_{1,K}\right)^{1/2}}{|\boldsymbol{u}^s|_{1,\Omega}}, \quad e_0(\boldsymbol{u}^s) := \frac{\left(\sum_{K\in\mathcal{T}_h} \|\boldsymbol{u}^s - \boldsymbol{\Pi}^{\boldsymbol{\varepsilon}}_K \boldsymbol{u}^s_h\|^2_{0,K}\right)^{1/2}}{\|\boldsymbol{u}^s\|_{0,\Omega}},$$
$$e_1(p^f) := \frac{\left(\sum_{K\in\mathcal{T}_h} |p^f - \Pi^{\nabla}_K p^f_h|^2_{1,K}\right)^{1/2}}{|p^f|_{1,\Omega}}, \quad e_0(p^f) := \frac{\left(\sum_{K\in\mathcal{T}_h} \|p^f - \Pi^{\nabla}_K p^f_h\|^2_{0,K}\right)^{1/2}}{\|p^f\|_{0,\Omega}},$$
$$e_0(\psi) := \frac{\left(\sum_{K\in\mathcal{T}_h} \|\psi - \psi_h\|^2_{0,K}\right)^{1/2}}{\|\psi\|_{0,\Omega}},$$

and Table 4.1 shows the convergence history, exhibiting optimal error decay.

4.4.2 Convergence with respect to the time advancing scheme

Regarding the convergence of the time discretization, we fix a relatively fine hexagonal mesh and construct successively refined partitions of the time interval $(0, 1]$. As in [109], and in order to avoid mixing errors coming from the spatial discretization, we modify the exact solutions to be

$$\boldsymbol{u}^s(x,y,t) = 100\sin(t)\begin{pmatrix} \frac{x}{\lambda} + y, \\ x + \frac{y}{\lambda} \end{pmatrix}, \; p^f(x,y,t) = \sin(t)(x+y), \; \psi(x,y,t) = \alpha p^f - \lambda \operatorname{div} \boldsymbol{u}^s,$$

Δt	$E_0(\boldsymbol{u}^s)$	$r_0(\boldsymbol{u}^s)$	$E_0(p^f)$	$r_0(p^f)$	$E_0(\psi)$	$r_0(\psi)$
0.5	0.002897	–	0.462768	–	0.398059	–
0.25	0.001362	1.09	0.218179	1.08	0.187834	1.08
0.125	$6.5173 \cdot 10^{-4}$	1.06	0.104546	1.06	0.090044	1.06
0.0625	$3.1756 \cdot 10^{-4}$	1.04	0.050955	1.04	0.043910	1.04
0.03125	$1.5664 \cdot 10^{-4}$	1.02	0.025123	1.02	0.021683	1.02
0.015625	$7.7950 \cdot 10^{-5}$	1.01	0.012469	1.01	0.010826	1.00

Table 4.2: Convergence of the time discretization for solid displacement, fluid pressure, and total pressure, using successive partitions of the time interval and a fixed hexagonal mesh.

and we use them to compute loads, sources, initial data, boundary values, and boundary fluxes. The model parameters assume the values

$$\kappa = 0.1, \quad \alpha = 1, \quad c_0 = 0, \quad \eta = 1, \quad \lambda = 1 \times 10^3 \quad \mu = 1. \tag{4.4.1}$$

The boundary definition is $\Gamma = [\{0\} \times (0,1)] \cup [(0,1) \times \{0\}]$ (bottom and left edges) and $\Sigma = \partial\Omega \setminus \Gamma$.

We recall that cumulative errors up to T associated with solid displacement, fluid pressure, and a generic pressure v (representing either fluid or total pressure), are defined as

$$\begin{aligned} E_0(\boldsymbol{u}^s) &= \left(\Delta t \sum_{n=1}^{N} \left(\sum_{K \in \mathcal{T}_h} \|\boldsymbol{u}^s(t_n) - \boldsymbol{\Pi}^{\boldsymbol{\varepsilon}}_K \boldsymbol{u}^{s,n}_h\|^2_{0,K} \right) \right)^{1/2}, \\ E_0(v) &= \left(\Delta t \sum_{n=1}^{N} \left(\sum_{K \in \mathcal{T}_h} \|v(t_n) - \Pi^{\nabla}_K v^n_h\|^2_{0,K} \right) \right)^{1/2}, \end{aligned} \tag{4.4.2}$$

respectively. From Table 4.2 we can readily observe that these errors decay with a rate of $O(\Delta t)$.

4.4.3 Verification of simultaneous space-time convergence for poroelasticity

Now we consider exact solid displacement and fluid pressure solving problem (4.1.1) on the square domain $\Omega = (0,1)^2$ and on the time interval $(0,1]$, given as

$$\boldsymbol{u}^s(x,y,t) = \begin{pmatrix} -\exp(-t)\sin(2\pi y)(1-\cos(2\pi x)) + \frac{\exp(-t)}{\mu+\lambda}\sin(\pi x)\sin(\pi y) \\ \exp(-t)\sin(2\pi x)(1-\cos(2\pi y)) + \frac{\exp(-t)}{\mu+\lambda}\sin(\pi x)\sin(\pi y) \end{pmatrix},$$
$$p^f(x,y,t) = \exp(-t)\sin(\pi x)\sin(\pi y), \quad \psi(x,y,t) = \alpha p^f - \lambda \operatorname{div} \boldsymbol{u}^s,$$

which satisfies $\operatorname{div} \boldsymbol{u}^s \to 0$ as $\lambda \to \infty$ (see similar tests in [93, 97]). The load functions, boundary values, and initial data can be obtained from these closed-form solutions, and alternatively to the dilation modulus and permeability specified in (4.4.1), we here choose larger values $\lambda = 1 \times 10^4$, and $\kappa = 1$.

In addition to the errors in (4.4.2), for displacement and for fluid pressure we will also compute

$$E_1(\boldsymbol{u}^s) = \left(\Delta t \sum_{n=1}^{N} \left(\sum_{K \in \mathcal{T}_h} |\boldsymbol{u}^s(t_n) - \boldsymbol{\Pi}_K^{\varepsilon} \boldsymbol{u}_h^{s,n}|_{1,K}^2 \right)\right)^{1/2},$$
$$E_1(p^f) = \left(\Delta t \sum_{n=1}^{N} \left(\sum_{K \in \mathcal{T}_h} |p^f(t_n) - \Pi_K^{\nabla} p_h^{f,n}|_{1,K}^2 \right)\right)^{1/2}.$$

We consider here pure Dirichlet boundary conditions for both displacement and fluid pressure. A backward Euler time discretization is used, and in this case, we are using successive refinements of the hexagonal partition of the domain as shown in Figure 4.1(c), simultaneously with a successive refinement of the time step. The cumulative errors are again computed until the final time $t = 1$, and the results are collected in Table 4.3. They show once more optimal convergence rates for the scheme in its lowest-order form.

Note from this and the previous test, that a zero constrained specific storage coefficient does not hinder the convergence properties.

4.4.4 Gradual compression of a poroelastic block

Finally we carry out a test involving the compression of a block occupying the region $\Omega = (0,1)^2$ by applying a sinusoidal-in-time traction on a small region on the top of

h^{-1}	$(\Delta t)^{-1}$	$E_1(\boldsymbol{u}^s)$	$r_1(\boldsymbol{u}^s)$	$E_0(\boldsymbol{u}^s)$	$r_0(\boldsymbol{u}^s)$	$E_1(p)$	$r_1(p)$	$E_0(p)$	$r_0(p)$	$E_0(\psi)$	$r_0(\psi)$
8	10	1.741116	-	0.101035	-	0.239518	-	0.009757	-	0.509493	-
16	20	0.892377	0.96	0.026166	1.95	0.123684	0.95	0.002528	1.95	0.251106	1.02
32	40	0.451402	0.98	0.006594	1.99	0.062743	0.98	0.000642	1.98	0.125025	1.01
64	80	0.227050	0.99	0.001650	2.00	0.031584	0.99	0.000161	1.99	0.062399	1.00
128	160	0.113876	1.00	0.000413	2.00	0.015844	1.00	0.000041	2.00	0.031165	1.00

Table 4.3: Convergence of the numerical method for displacement, fluid pressure, and total pressure, up to the final time $t = 1$, using simultaneous partitions of the time interval and of the spatial domain (using hexagonal meshes).

the box (see a similar test in [103]). The model parameters in this case are

$$\nu = 0.49995, \quad E_c = 3 \times 10^4, \quad \kappa = 1 \times 10^{-4}, \quad \alpha = 1, \quad c_0 = 1 \times 10^{-3},$$
$$\eta = 1, \quad \lambda = \frac{E_c \nu}{(1+\nu)(1-2\nu)}, \quad \mu = \frac{E_c}{(2+2\nu)}.$$

For this test, we have employed a mesh conformed by distorted quadrilaterals exemplified in Figure 4.1(b). The boundary conditions are of homogeneous Dirichlet type for fluid pressure on the whole boundary, and of mixed type for displacement, and the boundary is split as $\partial\Omega := \Gamma_1 \cup \Gamma_2 \cup \Gamma_3$. A traction $\boldsymbol{h}(t) = (0, -1.5 \times 10^4 \sin(\pi t))^T$ is applied on a segment of the top edge of the boundary $\Gamma_1 = (0.25, 0.75) \times \{1\}$, on the remainder of the top edge $\Gamma_2 = [0,1] \times \{1\} \backslash \Gamma_1$, we impose zero traction, and the body is clamped on the remainder of the boundary $\Gamma_3 = \partial\Omega \backslash (\Gamma_1 \cup \Gamma_2)$. No boundary conditions are prescribed for the total pressure. Initially the system is at rest $\boldsymbol{u}^s(0) = \mathbf{0}$, $\psi(0) = 0$, $p^f(0) = 0$, and we employ a backward Euler discretization of the time interval $(0, 0.5]$ with a constant time step $\Delta t = 0.1$. The numerical results obtained at the final time are depicted in Figure 4.2, where the profiles for fluid and total pressure present no spurious oscillations.

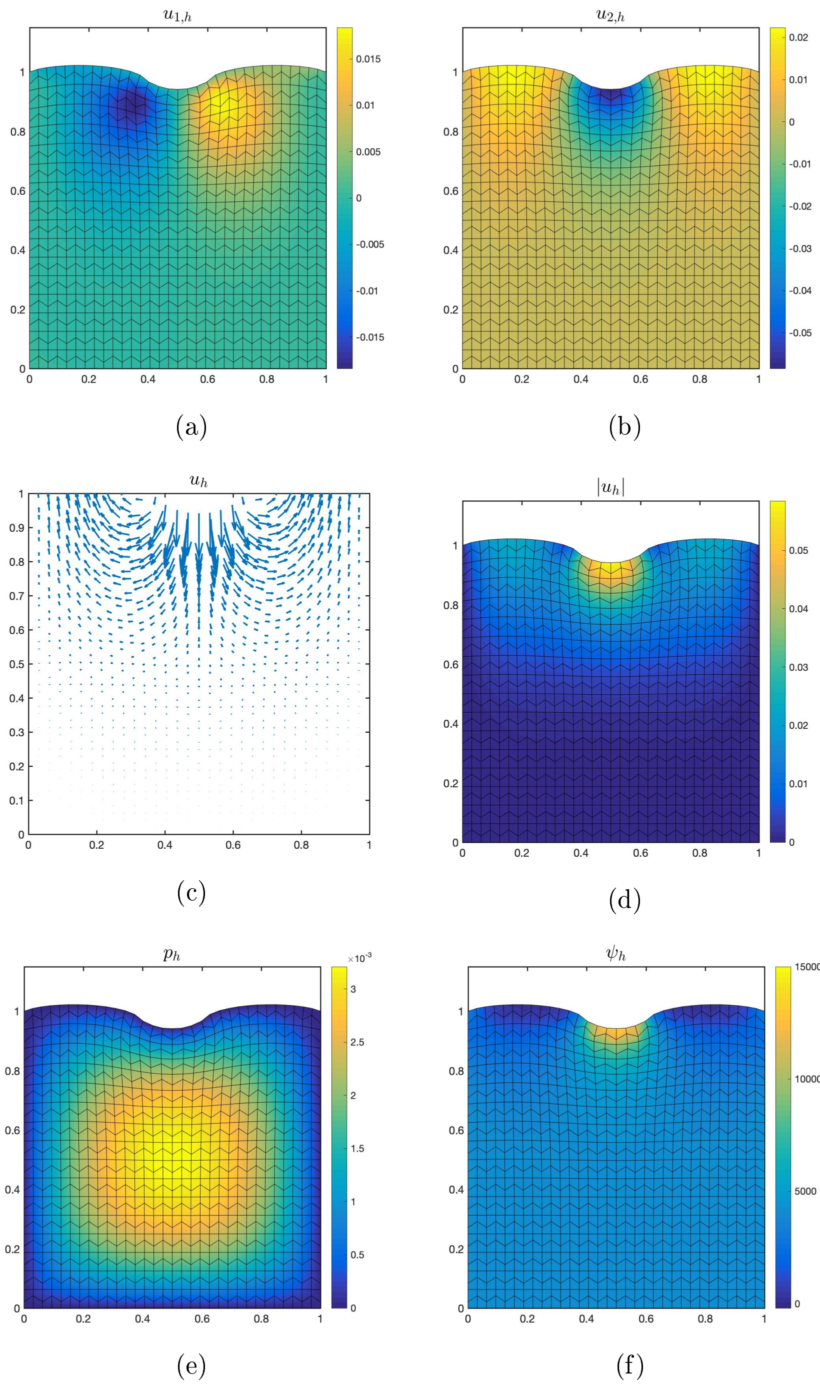

Figure 4.2: Compression of a poroelastic block after $t = 0.5$ adimensional units. Approximate displacement components (a,b), displacement vectors on the undeformed domain (c), displacement magnitude (d), fluid pressure (e), and total pressure (f), depicted on the deformed domain.

Chapter 5

Advection-Diffusion-Reaction equations in a Poroelastic media

This chapter focus on the development of VEMs for approximating the PDE system modelling poromechanical processes (formulated in mixed form using the solid deformation, fluid pressure, and total pressure) interacting with diffusing and reacting solutes in the medium. The space discretization relies on VE spaces containing piecewise linear polynomials as well as non-polynomial functions for displacement, pressure, and concentrations; and piecewise constants for total pressure. The Backward-Euler scheme is employed for the approximation of time derivatives. Using standard techniques of explicit schemes, we prove the well-posedness of the resultant fully discrete scheme, and *a priori* error estimates are established by introducing the suitable projection operators. Several numerical experiments are presented to validate the theoretical convergence rate and exhibit the performance of the proposed scheme.

This chapter is structured as follows. Section 5.1 is devoted to describing the governing equations that appear in the coupling of ADR and poroelasticity. In Section 5.2 we derive a weak formulation and include preliminary properties of the mathematical structure of the problem. The fully discretized scheme is presented and attained its well-posedness in Section 5.3. We established *a priori* error estimates in Section 5.4 with the help of Stokes and elliptic projection operators, and numerical experiments are conducted in Section 5.5.

5.1 Governing equations

Let us consider a piece of soft material as a porous medium composed of a mixture of incompressible grains and interstitial fluid, whose description can be placed in the context of the classical Biot problem. We recall here the three field formulation of the Biot's problem defined in Chapter 4 (referring [39]) as, one seeks for each time $t \in (0,T]$, the displacements of the porous skeleton, $\boldsymbol{u}^s(t) : \Omega \to \mathbb{R}^2$, the pore pressure of the fluid, $p^f(t) : \Omega \to \mathbb{R}$, and total pressure $\psi(t) : \Omega \to \mathbb{R}$, such that

$$\left(c_0 + \frac{\alpha^2}{\lambda}\right)\partial_t p^f - \frac{\alpha}{\lambda}\partial_t \psi - \frac{1}{\eta}\operatorname{div}(\kappa \nabla p^f) = \ell \qquad \text{in } \Omega \times (0,T], \quad (5.1.1a)$$

$$\boldsymbol{\sigma} = 2\mu\boldsymbol{\varepsilon}(\boldsymbol{u}^s) - \psi \mathbf{I}, \quad \text{in } \Omega \times (0,T], \quad (5.1.1b)$$

$$\psi = \alpha p^f - \lambda \operatorname{div} \boldsymbol{u}^s, \quad \text{in } \Omega \times (0,T], \quad (5.1.1c)$$

$$-\mathbf{div}\,\boldsymbol{\sigma} = \rho \boldsymbol{b} \qquad \text{in } \Omega \times (0,T]. \quad (5.1.1d)$$

We also consider the propagation of a generic species having concentration w_1, reacting with an additional species having concentration w_2. The problem can be written as follows

$$\partial_t w_1 + \boldsymbol{u}^s \cdot \nabla w_1 - \operatorname{div}\{D_1(\boldsymbol{x})\,\nabla w_1\} = f(w_1, w_2, \boldsymbol{u}^s) \quad \text{in } \Omega \times (0,T], \qquad (5.1.2a)$$

$$\partial_t w_2 + \boldsymbol{u}^s \cdot \nabla w_2 - \operatorname{div}\{D_2(\boldsymbol{x})\,\nabla w_2\} = g(w_1, w_2, \boldsymbol{u}^s) \quad \text{in } \Omega \times (0,T], \qquad (5.1.2b)$$

where D_1, D_2 are positive definite diffusion matrices (however we do not consider here cross-diffusion effects as in, e.g., [105, 124]). In the well-posedness analysis, the reaction kinetics are generic. Nevertheless, for sake of fixing ideas and in order to specify the coupling effects also through a stability analysis that will be conducted in [12], they will be chosen as a modification to the classical model from [125]

$$f(w_1, w_2, \boldsymbol{u}^s) = \beta_1(\beta_2 - w_1 + w_1^2 w_2) + \gamma\, w_1 \operatorname{div} \boldsymbol{u}^s,$$
$$g(w_1, w_2, \boldsymbol{u}^s) = \beta_1(\beta_3 - w_1^2 w_2) + \gamma\, w_2 \operatorname{div} \boldsymbol{u}^s,$$

where $\beta_1, \beta_2, \beta_3, \gamma$ are positive model constants. Note that the mechano-chemical feedback (the process where mechanical deformation modifies the reaction-diffusion effects) is here assumed only through advection and an additional reaction term depending on local dilation. The latter term is here modulated by $\gamma > 0$, thus representing a source for both species if the solid volume increases, otherwise the additional contribution is a sink for both chemicals [11].

The poromechanical deformations are also actively influenced by microscopic tension generation. A very simple description is given in terms of active stresses: we assume that the total Cauchy stress contains a passive and an active component, where the passive part is as in (5.1.1b) and

$$\boldsymbol{\sigma}_{\text{total}} = \boldsymbol{\sigma} + \boldsymbol{\sigma}_{\text{act}}, \tag{5.1.3}$$

where the active stress operates primarily on a given constant direction $\boldsymbol{k}$, and its intensity depends on a scalar field $r = r(w_1, w_2)$ and on a positive constant τ, to be specified later on (for example, see [126])

$$\boldsymbol{\sigma}_{\text{act}} = -\tau\, r \boldsymbol{k} \otimes \boldsymbol{k}. \tag{5.1.4}$$

In summary, the coupled system reads

$$\left.\begin{aligned} -\,\mathbf{div}(2\mu\boldsymbol{\varepsilon}(\boldsymbol{u}^s) - \psi\mathbf{I} + \boldsymbol{\sigma}_{\text{act}}) = \rho\boldsymbol{b}, \\ \left(c_0 + \frac{\alpha^2}{\lambda}\right)\partial_t p^f - \frac{\alpha}{\lambda}\partial_t\psi - \frac{1}{\eta}\operatorname{div}(\kappa\nabla p^f) = \ell, \\ \psi - \alpha p^f + \lambda \operatorname{div}\boldsymbol{u}^s = 0, \\ \partial_t w_1 + \boldsymbol{u}^s\cdot\nabla w_1 - \operatorname{div}(D_1(\boldsymbol{x})\,\nabla w_1) = f(w_1, w_2, \boldsymbol{u}^s), \\ \partial_t w_2 + \boldsymbol{u}^s\cdot\nabla w_2 - \operatorname{div}(D_2(\boldsymbol{x})\,\nabla w_2) = g(w_1, w_2, \boldsymbol{u}^s), \end{aligned}\right\} \text{ in } \Omega\times(0,T], \tag{5.1.5}$$

which we endow with appropriate initial data at rest

$$w_1(0) = w_{1,0},\ w_2(0) = w_{2,0},\ \boldsymbol{u}^s(0) = \mathbf{0},\ p^f(0) = 0,\ \psi(0) = 0 \quad \text{in } \Omega\times\{0\}, \tag{5.1.6}$$

and boundary conditions in the following manner

$$\boldsymbol{u}^s = \mathbf{0} \quad \text{and} \quad \frac{\kappa}{\eta}\nabla p^f\cdot\boldsymbol{n} = 0 \qquad \text{on } \Gamma\times(0,T], \tag{5.1.7a}$$

$$D_1(\boldsymbol{x})\nabla w_1\cdot\boldsymbol{n} = 0 \quad \text{and} \quad D_2(\boldsymbol{x})\nabla w_2\cdot\boldsymbol{n} = 0 \qquad \text{on } \Gamma\times(0,T], \tag{5.1.7b}$$

$$[2\mu\boldsymbol{\varepsilon}(\boldsymbol{u}^s) - \psi\,\mathbf{I} + \boldsymbol{\sigma}_{\text{act}}]\boldsymbol{n} = \mathbf{0} \quad \text{and} \quad p^f = 0 \qquad \text{on } \Sigma\times(0,T], \tag{5.1.7c}$$

$$w_1 = 0 \quad \text{and} \quad w_2 = 0 \qquad \text{on } \Sigma\times(0,T], \tag{5.1.7d}$$

where the boundary $\partial\Omega = \Gamma\cup\Sigma$ is disjointly split into Γ and Σ on which we prescribe clamped boundaries and zero fluid normal fluxes; and zero (total) traction together with constant fluid pressure, respectively. Moreover, zero concentrations normal fluxes are prescribed on $\partial\Omega$. We point out that, if we would like to start with a model in terms of the divergence ($\operatorname{div}(w_i\boldsymbol{u}^s)$ instead of $\boldsymbol{u}^s\cdot\nabla w_i$ in (5.1.2a)-(5.1.2b), $i\in\{1,2\}$), we need to assume zero total flux (including the advective term, see, e.g., [105]). Homogeneity of the boundary conditions is only assumed to simplify the exposition of the subsequent analysis.

5.2 Weak formulation

We will use the following notations for the Sobolev spaces in this chapter.

$$\mathbf{V} := [H^1_\Gamma(\Omega)]^2, \quad Q := H^1_\Sigma(\Omega), \quad Z := L^2(\Omega), \quad \text{and} \quad W := Q.$$

Say $\mathbb{V} := \mathbf{V} \times Q \times Z \times W \times W$. Let us multiply (5.1.5) by adequate test functions and integrate by parts (in space) whenever appropriate. Incorporating the boundary conditions (5.1.7a)-(5.1.7d) as well as the definition of the total stress (5.1.3), we end up with the following variational problem: For a given $t > 0$ and initial conditions (5.1.6), find $(\boldsymbol{u}^s(t), p^f(t), \psi(t),\ w_1(t), w_2(t)) \in \mathbb{V}$ such that

$$\begin{aligned}
a_1(\boldsymbol{u}^s, \boldsymbol{v}^s) \qquad\qquad &+ b_1(\boldsymbol{v}^s, \psi) = F_r(\boldsymbol{v}^s) && \forall \boldsymbol{v}^s \in \mathbf{V}, && (5.2.1a)\\
\tilde{a}_2(\partial_t p^f, q^f) \qquad\qquad &+ a_2(p^f, q^f) - b_2(q^f, \partial_t \psi) = G_\ell(q^f) && \forall q^f \in Q, && (5.2.1b)\\
b_1(\boldsymbol{u}^s, \phi) \quad &+ b_2(p^f, \phi) - a_3(\psi, \phi) = 0 && \forall \phi \in Z, && (5.2.1c)\\
m(\partial_t w_1, s) \qquad\qquad &+ a_4(w_1, s) + c(\boldsymbol{u}^s; w_1, s) = J_f(s) && \forall s \in W, && (5.2.1d)\\
m(\partial_t w_2, s) \qquad\qquad &+ a_5(w_2, s) + c(\boldsymbol{u}^s; w_2, s) = J_g(s) && \forall s \in W, && (5.2.1e)
\end{aligned}$$

where the formulation with the bilinear forms $a_1 : \mathbf{V} \times \mathbf{V} \to \mathbb{R}$, $a_2 : Q \times Q \to \mathbb{R}$, $a_3 : Z \times Z \to \mathbb{R}$, $a_4, a_5 : W \times W \to \mathbb{R}$, $b_1 : \mathbf{V} \times Q \to \mathbb{R}$, $b_2 : Q \times Z \to \mathbb{R}$, the trilinear form $c : \mathbf{V} \times W \times W \to \mathbb{R}$, and linear functionals $F_{\boldsymbol{b},r} : \mathbf{V} \to \mathbb{R}$ (for $\boldsymbol{b}$, r known), $G_\ell : Q \to \mathbb{R}$, $J_f, J_g : W \to \mathbb{R}$ (for known f and g), are defined as

$$\begin{gathered}
a_1(\boldsymbol{u}^s, \boldsymbol{v}^s) := 2\mu \int_\Omega \boldsymbol{\varepsilon}(\boldsymbol{u}^s) : \boldsymbol{\varepsilon}(\boldsymbol{v}^s), \quad b_1(\boldsymbol{v}^s, \phi) := -\int_\Omega \phi \operatorname{div} \boldsymbol{v}^s, \quad b_2(p^f, \phi) := \frac{\alpha}{\lambda} \int_\Omega p^f \phi,\\
\tilde{a}_2(p^f, q^f) := \left(c_0 + \frac{\alpha^2}{\lambda}\right) \int_\Omega p^f q^f, \quad a_2(p^f, q^f) := \frac{1}{\eta} \int_\Omega \kappa(\boldsymbol{x}) \nabla p^f \cdot \nabla q^f,\\
a_3(\psi, \phi) := \frac{1}{\lambda} \int_\Omega \psi\phi, \quad F_{\boldsymbol{b},r}(w_1, w_2; \boldsymbol{v}^s) := F_{\boldsymbol{b}}(\boldsymbol{v}^s) + F_r(w_1, w_2; \boldsymbol{v}^s),\\
\text{where } F_{\boldsymbol{b}}(\boldsymbol{v}^s) := \rho \int_\Omega \boldsymbol{b} \cdot \boldsymbol{v}^s, \quad F_r(w_1, w_2; \boldsymbol{v}^s) := \tau \int_\Omega r(w_1, w_2) \boldsymbol{k} \otimes \boldsymbol{k} : \boldsymbol{\varepsilon}(\boldsymbol{v}^s),\\
m(w_i, s) := \int_\Omega w_i\, s, \quad a_{3+i}(w_i, s) := \int_\Omega D_i(\boldsymbol{x}) \nabla w_i \cdot \nabla s, \text{ for } i = 1, 2,\\
c(\boldsymbol{u}^s; w, s) := \int_\Omega (\boldsymbol{u}^s \cdot \nabla w) s, \quad G_\ell(q^f) := \int_\Omega \ell\, q^f,
\end{gathered}$$

$$J_f(w_1, w_2, \boldsymbol{u}^s; s) := \int_\Omega f(w_1, w_2, \boldsymbol{u}^s)\, s, \quad J_g(w_1, w_2, \boldsymbol{u}^s; s) := \int_\Omega g(w_1, w_2, \boldsymbol{u}^s)\, s.$$

Preliminaries

We will consider that the initial data (5.1.6) are non-negative and regular enough. Moreover, throughout the chapter we will assume that the anisotropic permeability $\kappa(\boldsymbol{x})$ and the diffusion matrices $D_1(\boldsymbol{x}), D_2(\boldsymbol{x})$ are uniformly bounded and positive definite in Ω. The latter means that, there exist positive constants κ_1, κ_2, and D_i^a, D_i^b, $i \in \{1, 2\}$ such that $\forall \boldsymbol{w} \in \mathbb{R}^d$, $d = 1, 2$, $\forall \boldsymbol{x} \in \Omega$, we have

$$\kappa_1 |\boldsymbol{w}|^2 \leq \boldsymbol{w}^{\mathrm{t}} \kappa(\boldsymbol{x}) \boldsymbol{w} \leq \kappa_2 |\boldsymbol{w}|^2, \quad \text{and} \quad D_i^a |\boldsymbol{w}|^2 \leq \boldsymbol{w}^{\mathrm{t}} D_i(\boldsymbol{x}) \boldsymbol{w} \leq D_i^b |\boldsymbol{w}|^2.$$

Also, for a fixed $\boldsymbol{u}^s$, the reaction kinetics $f(w_1, w_2, \cdot), g(w_1, w_2, \cdot)$ satisfy the growth conditions, that is, for $z = f, g$

$$\begin{aligned} |z(w_1, w_2, \cdot)| &\leq C(1 + |w_1| + |w_2|), \\ \text{and } |z(w_1, w_2, \cdot) - z(\tilde{w}_1, \tilde{w}_2, \cdot)| &\leq C(|w_1 - \tilde{w}_1| + |w_2 - \tilde{w}_2|). \end{aligned} \tag{5.2.2}$$

Given w_1, $w_2 \in \mathbb{R}$, the scalar field $r(w_1, w_2)$ defined in (5.1.3) such that

$$\begin{aligned} |r(w_1, w_2)| &\leq |w_1| + |w_2|, \\ |r(w_1, w_2) - r(\tilde{w}_1, \tilde{w}_2)| &\leq C(|w_1 - \tilde{w}_1| + |w_2 - \tilde{w}_2|), \end{aligned} \tag{5.2.3}$$

and reaction kinetics $f(\cdot, \cdot, \boldsymbol{u}^s), g(\cdot, \cdot, \boldsymbol{u}^s)$ for fixed w_1, $w_2 \in \mathbb{R}$ holds

$$|z(\cdot, \cdot, \boldsymbol{u}^s) - z(\cdot, \cdot, \tilde{\boldsymbol{u}}^s)| \leq C |\operatorname{div} \boldsymbol{u}^s - \operatorname{div} \tilde{\boldsymbol{u}}^s|, \quad z = f, g.$$

In addition, the terms in (5.2.1) fulfill the following continuity bounds for all $\boldsymbol{u}^s, \boldsymbol{v}^s \in \mathbf{V}$, $p^f, q^f \in Q$, $w_1, w_2, s \in W$, $\psi, \phi \in Z$,

$$\begin{gathered} |a_1(\boldsymbol{u}^s, \boldsymbol{v}^s)| \leq 2\mu C_{k,2} \|\boldsymbol{u}^s\|_{1,\Omega} \|\boldsymbol{v}^s\|_{1,\Omega}, \quad |b_1(\boldsymbol{v}^s, \phi)| \leq \sqrt{d} \|\boldsymbol{v}^s\|_{1,\Omega} \|\phi\|_{0,\Omega}, \\ |a_2(p^f, q^f)| \leq \kappa_2\, \eta^{-1} \|p^f\|_{1,\Omega} \|q^f\|_{1,\Omega}, \quad |G_\ell(q^f)| \leq \|\ell\|_{0,\Omega} \|q^f\|_{0,\Omega}, \\ |a_3(\psi, \phi)| \leq \lambda^{-1} \|\psi\|_{0,\Omega} \|\phi\|_{0,\Omega}, \quad |b_2(q^f, \phi)| \leq \alpha \lambda^{-1} \|q^f\|_{1,\Omega} \|\phi\|_{0,\Omega}, \\ |F_{\boldsymbol{b},r}(w_1, w_2; \boldsymbol{v}^s)| \leq \rho \|\boldsymbol{b}\|_{0,\Omega} \|\boldsymbol{v}^s\|_{0,\Omega} + \tau \sqrt{C_{k,2}} \|r(w_1, w_2)\|_{0,\Omega} \|\boldsymbol{v}^s\|_{1,\Omega}, \\ |a_{3+i}(w_i, s)| \leq D_i^b \|w_i\|_{1,\Omega} \|s\|_{1,\Omega}, \quad \text{for } i = 1, 2, \\ |J_z(w_1, w_2, \boldsymbol{u}^s; s)| \leq \|z(w_1, w_2, \boldsymbol{u}^s)\|_{0,\Omega} \|s\|_{0,\Omega}, \ z = f, g, \end{gathered} \tag{5.2.4}$$

We also have the following coercivity and positivity bounds:

$$\begin{aligned} a_1(\boldsymbol{v}^s, \boldsymbol{v}^s) \geq 2\mu\, C_{k,1} \|\boldsymbol{v}^s\|_{1,\Omega}^2, \quad a_2(q^f, q^f)| \geq \frac{\kappa_1 c_p}{\eta} \|q^f\|_{1,\Omega}^2, \\ a_3(\phi, \phi) = \lambda^{-1} \|\phi\|_{0,\Omega}^2, \quad a_{3+i}(s, s) \geq c_p D_i^a \|s\|_{1,\Omega}^2 \text{ for } i = 1, 2, \end{aligned} \tag{5.2.5}$$

for all $\boldsymbol{v}^s \in \mathbf{V}$, $q^f \in Q$, $\phi \in Z$, $s \in W$, where $C_{k,1}$ and $C_{k,2}$ are the positive constants satisfying

$$C_{k,1} \|\boldsymbol{v}^s\|_{1,\Omega}^2 \leq \|\boldsymbol{\varepsilon}(\boldsymbol{v}^s)\|_{0,\Omega}^2 \leq C_{k,2} \|\boldsymbol{v}^s\|_{1,\Omega}^2,$$

and c_p is the Poincaré constant. Moreover, the bilinear form b_1 satisfies the inf-sup condition (see, e.g., [67]): For every $\phi \in Q$, there exists $\beta > 0$ such that

$$\sup_{\boldsymbol{v}^s \in \mathbf{V} \setminus \{0\}} \frac{b_1(\boldsymbol{v}^s, \phi)}{\|\boldsymbol{v}^s\|_{1,\Omega}} \geq \beta \|\phi\|_{0,\Omega}. \tag{5.2.6}$$

Remark 5.1. *The well-posedness of the weak formulation* (5.2.1) *of the fully coupled system* (5.1.5) *can be established through the semi-discretization in time technique (refer [127, 57]) using the compactness arguments, and thus the analysis for time discretization from [109] can be utilized for this strategy.*

5.3 Discrete formulations and wellposedness

In this section, by following VEMs for space discretization, we present a fully discrete scheme corresponding to (5.2.1). We also address the stability, existence, and uniqueness of the discrete VE solution. By introducing the adequate local and global discrete spaces associated with velocity, pressure, total volumetric stress, and concentrations, the VE formulation is described as follows.

5.3.1 Virtual element discretizations

Let the domain Ω be discretized into the family of the polygonal meshes $\mathcal{T}_h$ with mesh size h and element K, vertices on element K as V_i, $1 \leq i \leq N_K^v$ with N_K^v number of vertices in K, and any edge in the polygonal mesh is denoted by e. For any natural number k, let $\mathbb{P}_k(S)$ and $\mathcal{M}_k(S)$ represent the space of polynomials and monomials of degree less than or equal to k for any $S \subset \mathbb{R}^2$, respectively. We also suppose that the polygonal mesh satisfy the assumptions $(A1)$-$(A3)$ (see [18, 32]) presented in Chapter 2.

Before proceeding to define the VE spaces, we will recall few projections as follows.

The standard energy projection $\Pi_K^{\nabla} : H^1(K) \to \mathbb{P}_1(K)$ is defined as

$$(\nabla(\Pi_K^{\nabla} q - q), \nabla p_1)_{0,K} = 0 \qquad \text{for all } p_1 \in \mathbb{P}_1(K),$$

where the projection onto constants are maintained through another projection P_K^0 as

$$P_K^0(\Pi_K^{\nabla} q - q) = 0 \quad \text{where} \quad P_K^0 q := \frac{1}{N_K^v} \sum_{i=1}^{N_K^v} q(V_i).$$

The vectorial energy projection from the vector space $[H^1(K)]^2$ to $[\mathbb{P}_1(K)]^2$ denoted as $\boldsymbol{\Pi}_K^{\boldsymbol{\nabla}}$ defined exactly in same manner as scalar case shown above.

A variant of the vectorial projection $\boldsymbol{\Pi}_K^{\boldsymbol{\nabla}}$ and supported by the bilinear form $a_1^K(\cdot,\cdot)$, we define a projection $\boldsymbol{\Pi}_K^{\boldsymbol{\varepsilon}}$ as,

$$(\boldsymbol{\varepsilon}(\boldsymbol{\Pi}_K^{\boldsymbol{\varepsilon}} \boldsymbol{v} - \boldsymbol{v}), \boldsymbol{\varepsilon}(\boldsymbol{p}_1))_{0,K} = 0 \qquad \text{for all } \boldsymbol{p}_1 \in [\mathbb{P}_1(K)]^2,\ \boldsymbol{v} \in [H^1(K)]^2,$$

and the function $\boldsymbol{p}_1 \in \ker(a_1^K(\cdot,\cdot))$ are again taken care from $\mathbf{P}_K^0(\boldsymbol{\Pi}_K^{\boldsymbol{\varepsilon}} \boldsymbol{v} - \boldsymbol{v}, \boldsymbol{p}_1) = 0$, and $\mathbf{P}_K^0(\boldsymbol{v}, \boldsymbol{p}_1) = \frac{1}{N_K^v} \sum_{i=1}^{N_K^v} \boldsymbol{v}(V_i) \cdot \boldsymbol{p}_1(V_i)$.

The classical L^2-projection operator $\Pi_K^0 : L^2(K) \to \mathbb{P}_1(K)$ is expressed as

$$(\Pi_K^0 q - q, p_1)_{0,K} = 0 \qquad \text{for all } q \in L^2(K),\ p_1 \in \mathbb{P}_1(K).$$

Similar to the energy projections, the projections $\boldsymbol{\Pi}_K^{\mathbf{0},0} : [L^2(K)]^2 \to [\mathbb{P}_0(K)]^2$ and $\boldsymbol{\Pi}_K^{\mathbf{0}} : [L^2(K)]^2 \to [\mathbb{P}_1(K)]^2$ are identified as the vectorial L^2 projection onto constants and linear polynomials, respectively. We stress that these operators not only help us in deriving the optimal error estimates but also useful in the computation of discrete bilinear forms.

Then the local VE spaces are introduced as follows (refer [29, 24] and also defined earlier in (4.2.2)):

$$\mathbf{V}_h(K) := \left\{ \boldsymbol{v}_h \in [H^1(K)]^2 \cap \mathcal{B}(\partial K) : \begin{cases} (-\Delta \boldsymbol{v}_h - \nabla s)|_K = \mathbf{0}, \\ \operatorname{div} \boldsymbol{v}_h = c_d \in \mathbb{P}_0(K) \end{cases} \text{for some } s \in L^2(K) \right\},$$

$$\begin{aligned} Q_h(K) := \big\{ q_h \in H^1(K) \cap C^0(\partial K) :\ & q_h|_e \in \mathbb{P}_1(e)\ \forall e \in \partial K,\ \Delta q_h|_K \in \mathbb{P}_1(K), \\ & (\Pi_K^{\nabla} q_h - q_h, m_\alpha)_{0,K} = 0\ \forall m_\alpha \in \mathcal{M}_1(K) \big\}, \end{aligned}$$

$Z_h(K) := \mathbb{P}_0(K),$

where $c_d := \frac{1}{|K|}(\int_{\partial K} \boldsymbol{v} \cdot \boldsymbol{n}_K \, \mathrm{d}s)$ and

$$\mathcal{B}(\partial K) := \big\{ \boldsymbol{v}_h \in [C^0(\partial K)]^2 : \boldsymbol{v}_h|_e \cdot \boldsymbol{t}_K^e \in \mathbb{P}_1(e), \boldsymbol{v}_h|_e \cdot \boldsymbol{n}_K^e \in \mathbb{P}_2(e) \quad \forall e \in \partial K \big\}.$$

We have the following degrees of freedom depending on the corresponding spaces (refer [24, 29] and Chapter 2 for details on unisolvance):

For displacement:

- (D_v1) the values of $\boldsymbol{v}_h$ at all vertices of the element K,
- (D_v2) and value of $\boldsymbol{v}_h \cdot \boldsymbol{n}_K^e$ at mid point on each edge $e \in \partial K$;

for total volumetric stress:

- (D_z) value of ψ_h at any point in K;

and for pressure, or concentration:

- (D_q) the values of q_h at vertices of the element K.

Then the global spaces are given as

$$\mathbf{V}_h := \{v_h \in \mathbf{V} : v_h|_K \in \mathbf{V}_h(K) \; \forall K \in \mathcal{T}_h\}, \quad Z_h := \{\psi_h \in Z : \psi_h|_K \in Z_h(K) \; \forall K \in \mathcal{T}_h\},$$
$$Q_h := \{q_h \in Q : q_h|_K \in Q_h(K) \; \forall K \in \mathcal{T}_h\}, \quad W_h := \{s_h \in W : s_h|_K \in Q_h(K) \; \forall K \in \mathcal{T}_h\}.$$

Note from above that the local discrete spaces and their degrees of freedom for pressure and concentration are the same, and thus have the same local projection operators on each element $K \in \mathcal{T}_h$.

We define the local discrete bilinear forms by considering the computability, consistency, and stability, as:

$$a_1^{h,K}(\boldsymbol{u}_h^s, \boldsymbol{v}_h^s) := a_1^K(\boldsymbol{\Pi}_K^{\boldsymbol{\varepsilon}} \boldsymbol{u}_h^s, \boldsymbol{\Pi}_K^{\boldsymbol{\varepsilon}} \boldsymbol{v}_h^s) + 2\mu \; S^{\boldsymbol{\varepsilon},K}((\mathbf{I} - \boldsymbol{\Pi}_K^{\boldsymbol{\varepsilon}})\boldsymbol{u}_h^s, (\mathbf{I} - \boldsymbol{\Pi}_K^{\boldsymbol{\varepsilon}})\boldsymbol{v}_h^s),$$
$$b_1^K(\boldsymbol{v}_h^s, \phi_h) = (\operatorname{div} \boldsymbol{v}_h^s, \phi_h)_{0,K}, \quad b_2^K(q_h^f, \phi_h) := \alpha \, \lambda^{-1} (\Pi_K^0 q_h^f, \phi_h)_{0,K},$$
$$\tilde{a}_2^{h,K}(p_h^f, q_h^f) := \tilde{a}_2^K(\Pi_K^0 p_h^f, \Pi_K^0 q_h^f) + \big(c_0 + \alpha^2 \lambda^{-1}\big) \, S^{0,K}((I - \Pi_K^0)p_h^f, (I - \Pi_K^0)q_h^f),$$
$$a_2^{h,K}(p_h^f, q_h^f) := a_2^K(\Pi_K^\nabla p_h^f, \Pi_K^\nabla q_h^f) + \bar{\kappa} \, \eta^{-1} \; S^{\nabla,K}((I - \Pi_K^\nabla)p_h^f, (I - \Pi_K^\nabla)q_h^f),$$

$$a_3^K(\psi_h,\phi_h) := (\psi_h,\phi_h)_{0,K}, \quad c^{h,K}(\boldsymbol{v}_h^s; w_h, s_h) := \big((\boldsymbol{\Pi}_K^{\mathbf{0}}\boldsymbol{v}_h^s)\cdot(\boldsymbol{\Pi}_K^{\mathbf{0},0}\nabla w_h), \Pi_K^0 s_h\big)_{0,K},$$
$$a_i^{h,K}(w_h,s_h) := a_i^K(\Pi_K^\nabla w_h, \Pi_K^\nabla s_h) + \bar{D}_{i-3}\; S^{\nabla,K}((I-\Pi_K^\nabla)w_h, (I-\Pi_K^\nabla)s_h),\; i=4,5,$$
$$m^{h,K}(w_h,s_h) := m^K(\Pi_K^0 w_h, \Pi_K^0 s_h) + S^{0,K}((I-\Pi_K^0)w_h, (I-\Pi_K^0)s_h),$$

where $\bar{d}$ is average of function d over element K for parameters $d=\kappa, D_1, D_2$, and the stabilization terms on each K, with Ndof denoting the total number of degrees of freedom or dimension of the associated space to the variables (for instance, Ndof := dimension of $Q_h(K)$ in $S^{\nabla,K}(\cdot,\ \cdot)$ for pressure variables p_h, q_h), as

$$S^{\nabla,K}(w_h,\ s_h) := \sum_{r=1}^{\mathrm{Ndof}} \mathrm{dof}_r(w_h)\ \mathrm{dof}_r(s_h) \quad \text{with } \Pi_K^\nabla w_h, \Pi_K^\nabla s_h = 0,$$
$$S^{0,K}(w_h,\ s_h) := \mathrm{area}(K)\sum_{r=1}^{\mathrm{Ndof}} \mathrm{dof}_r(w_h)\ \mathrm{dof}_r(s_h) \quad \text{with } \Pi_K^0 w_h, \Pi_K^0 s_h = 0,$$
$$S^{\boldsymbol{\varepsilon},K}(\boldsymbol{u}_h^s, \boldsymbol{v}_h^s) := \sum_{r=1}^{\mathrm{Ndof}} \mathrm{dof}_r(\boldsymbol{u}_h^s)\ \mathrm{dof}_r(\boldsymbol{v}_h^s) \quad \text{with } \boldsymbol{\Pi}_K^{\boldsymbol{\varepsilon}}\boldsymbol{u}_h^s, \boldsymbol{\Pi}_K^{\boldsymbol{\varepsilon}}\boldsymbol{v}_h^s = 0.$$

Then the stabilization terms satisfies the stability condition with respect to the norm associated with the respective discrete bilinear forms as, for $s_h \in Q_h(K)$, $\boldsymbol{v}_h^s \in \mathbf{V}_h(K)$, we have

$$c_*|s_h|_{1,K}^2 \le S^{\nabla,K}(s_h,\ s_h) \le c^*|s_h|_{1,K}^2, \quad \tilde{c}_*\|s_h\|_{0,K}^2 \le S^{0,K}(s_h,\ s_h) \le \tilde{c}^*\|s_h\|_{0,K}^2,$$
$$\hat{c}_*\|\boldsymbol{\varepsilon}(\boldsymbol{v}_h^s)\|_{0,K}^2 \le S^{\boldsymbol{\varepsilon},K}(\boldsymbol{v}_h^s,\ \boldsymbol{v}_h^s) \le \hat{c}^*\|\boldsymbol{\varepsilon}(\boldsymbol{v}_h^s)\|_{0,K}^2,$$

where $c_*, c^*, \tilde{c}_*, \tilde{c}^*, \hat{c}_*, \hat{c}^*$ are constants independent of mesh size h_K and the given parameters.

The discrete functionals are defined in terms of L^2 projections as

$$G_l^h(q_h^f) := \sum_{K\in\mathcal{T}_h} \left\langle \ell_h, q_h^f \right\rangle_{0,K}, \; F_{\boldsymbol{b},r}^h(w_{1,h}, w_{2,h}; \boldsymbol{v}_h^s) := F_{\boldsymbol{b}}^h(\boldsymbol{v}_h^s) + F_r^h(w_{1,h}, w_{2,h}; \boldsymbol{v}_h^s),$$
$$\text{with} \quad F_{\boldsymbol{b}}^h(\boldsymbol{v}_h^s) := \sum_{K\in\mathcal{T}_h} \rho\,\langle \boldsymbol{b}_h, \boldsymbol{v}_h^s\rangle_{0,K},$$
$$F_r^h(w_{1,h}, w_{2,h}; \boldsymbol{v}_h^s) := \sum_{K\in\mathcal{T}_h} \tau\,\langle r_h(w_{1,h}, w_{2,h})(\boldsymbol{k}\otimes\boldsymbol{k}), \boldsymbol{\varepsilon}(\boldsymbol{v}_h^s)\rangle_{0,K},$$
$$J_z^h(w_{1,h}, w_{2,h}, \boldsymbol{u}_h^s; s_h) := \sum_{K\in\mathcal{T}_h} \langle z_h\,(w_{1,h}, w_{2,h}, \boldsymbol{u}_h^s)\,, s_h\rangle_{0,K}, \quad z=f,g,$$

where

$$\boldsymbol{b}_h|_K := \boldsymbol{\Pi}_K^{\mathbf{0},0}\boldsymbol{b}, \quad r_h\left(w_{1,h}, w_{2,h}\right)|_K := \Pi_K^{0,0} r\left(\Pi_K^0 w_{1,h}, \Pi_K^0 w_{2,h}\right), \quad \ell_h|_K := \Pi_K^0 \ell,$$
$$z_h\left(w_{1,h}, w_{2,h}, \boldsymbol{u}_h^s\right)|_K := \Pi_K^0 z\left(\Pi_K^0 w_{1,h}, \Pi_K^0 w_{2,h}, \boldsymbol{u}_h^s\right), \quad \text{for } z = f, g.$$

Note that $\Pi_K^0 z_h|_K = z_h|_K$ for functions $z_h = f_h, g_h$ and for each $K \in \mathcal{T}_h$.
Then, in general, the global discrete bilinear forms and discrete functional are defined naturally as

$$a^h(u_h, v_h) := \sum_{K \in \mathcal{T}_h} a^{h,K}(u_h, v_h), \quad F^h(v_h) := \sum_{K \in \mathcal{T}_h} F^{h,K}(v_h),$$

for any local discrete bilinear form $a^{h,K}(\cdot,\cdot)$ and discrete functional $F^{h,K}(\cdot)$. With the help of the stability of the projection operators and stabilization terms, we obtain the following continuity properties of bilinear and trilinear forms,

$$\begin{aligned}
a_1^h(\boldsymbol{u}_h^s, \boldsymbol{v}_h^s) &\leq 2\mu\hat{\alpha}^* \, \|\boldsymbol{\varepsilon}(\boldsymbol{u}_h^s)\|_{0,\Omega} \|\boldsymbol{\varepsilon}(\boldsymbol{v}_h^s)\|_{0,\Omega} \quad \forall \boldsymbol{u}_h^s, \boldsymbol{v}_h^s \in \mathbf{V}_h, \\
\tilde{a}_2^h(p_h^f, q_h^f) &\leq \tilde{\alpha}^* \left(c_0 + \alpha^2\lambda^{-1}\right) \|p_h^f\|_{0,\Omega} \|q_h^f\|_{0,\Omega} \quad \forall p_h^f, q_h^f \in Q_h, \\
a_2^h(p_h^f, q_h^f) &\leq \alpha^* \, \kappa_2 \eta^{-1} \, \|\nabla p_h^f\|_{0,\Omega} \|\nabla q_h^f\|_{0,\Omega} \quad \forall p_h^f, q_h^f \in Q_h, \\
m^h(w_h, s_h) &\leq \ \|w_h\|_{0,\Omega} \|s_h\|_{0,\Omega} \quad \forall w_h, s_h \in W_h, \\
a_{3+i}^h(w_h, s_h) &\leq \alpha^* D_i^b \|\nabla w_h\|_{0,\Omega} \|\nabla s_h\|_{0,\Omega} \quad \forall w_h, s_h \in W_h, \ i = 1, 2, \\
c^h(\boldsymbol{v}_h^s; w_h, s_h) &\leq C \ |\boldsymbol{v}_h^s|_{1,\Omega} \|w_h\|_{1,\Omega} \|s_h\|_{1,\Omega} \ \forall \boldsymbol{v}_h^s \in \mathbf{V}_h, w_h, s_h \in W_h,
\end{aligned} \tag{5.3.1}$$

bounds for the discrete functionals,

$$\begin{aligned}
G_\ell^h(q_h^f) &\leq \|\ell\|_{0,\Omega} \|q_h^f\|_{0,\Omega} \quad \forall q_h^f \in Q_h, \\
F_{\boldsymbol{b},r}^h(w_{1,h}, w_{2,h}; \boldsymbol{v}_h^s) &\leq C \ (\|\boldsymbol{b}\|_{0,\Omega} \|\boldsymbol{v}_h^s\|_{0,\Omega} + \|r_h\|_{0,\Omega} \|\boldsymbol{\varepsilon}(\boldsymbol{v}_h^s)\|_{0,\Omega}) \quad \forall \boldsymbol{v}_h^s \in \mathbf{V}_h, \\
J_z^h(w_{1,h}, w_{2,h}, \boldsymbol{u}_h^s; s_h) &\leq \ \|z_h\|_{0,\Omega} \|s_h\|_{0,\Omega} \ \forall s_h \in W_h, \ \text{for } z = f, g,
\end{aligned} \tag{5.3.2}$$

and coercivity properties, $\forall \boldsymbol{v}_h^s \in \mathbf{V}_h, q_h^f \in Q_h, s_h \in W_h$

$$\begin{aligned}
a_1^h(\boldsymbol{v}_h^s, \boldsymbol{v}_h^s) &\geq 2\mu\hat{\alpha}_* \|\boldsymbol{\varepsilon}(\boldsymbol{v}_h^s)\|_{0,\Omega}^2, \quad a_2^h(q_h^f, q_h^f) \geq \alpha_* \, \kappa_1 \, \eta^{-1} \, \|\nabla q_h^f\|_{0,\Omega}^2, \\
m^h(s_h, s_h) &\geq \ \tilde{\alpha}_* \|s_h\|_{0,\Omega}^2, \quad a_{3+i}^h(s_h, s_h) \geq \alpha_* D_i^a \|\nabla s_h\|_{0,\Omega}^2 \quad \text{for } i = 1, 2.
\end{aligned} \tag{5.3.3}$$

Also, the discrete inf-sup condition hold on $(\mathbf{V}_h, Z_h)$, that is, there exists $\tilde{\beta} > 0$

independent of h such that (refer [30, 32] and Chapter 2)

$$\sup_{\boldsymbol{v}_h^s \in \mathbf{V}_h \setminus \{0\}} \frac{b_1(\boldsymbol{v}_h^s, \phi_h)}{\|\boldsymbol{v}_h^s\|_{1,\Omega}} \geq \tilde{\beta} \|\phi_h\|_{0,\Omega} \quad \text{for all } \phi_h \in Z_h. \tag{5.3.4}$$

5.3.2 Fully discrete scheme

Let us discretize the time interval $(0, T]$ into N equispaced points and time step $\Delta t = \frac{T}{N}$ with n^{th} time step as $t^n = n\Delta t$, $n = 1, \ldots, N$, and use the following general notation for the first order backward difference $\Delta t\ \delta_t X^n := X^n - X^{n-1}$. In this way, we can write a discrete form of (5.2.1): From the given initial data $\boldsymbol{u}_h^{s,0}$, $p_h^{f,0}$, ψ_h^0, $w_{1,h}^0, w_{2,h}^0$ (which will be projections of the continuous initial conditions of each field) and starting with $n = 1$, we first solve for $\boldsymbol{u}_h^{s,n} \in \mathbf{V}_h$, $p_h^{f,n} \in Q_h$, $\psi_h^n \in Z_h$ such that, $\forall \boldsymbol{v}_h^s \in \mathbf{V}_h$, $q_h^f \in Q_h$, $\phi_h \in Z_h$,

$$a_1^h(\boldsymbol{u}_h^{s,n}, \boldsymbol{v}_h^s) + b_1(\boldsymbol{v}_h^s, \psi_h^n) = F_{\boldsymbol{b},r}^{h,n}(w_{1,h}^{n-1}, w_{2,h}^{n-1}; \boldsymbol{v}_h^s), \tag{5.3.5a}$$

$$\tilde{a}_2^h(\delta_t p_h^{f,n}, q_h^f) + a_2^h(p_h^{f,n}, q_h^f) - b_2(q_h^f, \delta_t \psi_h^n) = G_\ell^{h,n}(q_h^f), \tag{5.3.5b}$$

$$b_1(\boldsymbol{u}_h^{s,n}, \phi_h) + b_2(p_h^{f,n}, \phi_h) - a_3(\psi_h^n, \phi_h) = 0, \tag{5.3.5c}$$

And then we seek the concentrations $w_{1,h}^n, w_{2,h}^n \in W_h$ for given displacement $\boldsymbol{u}_h^{s,n} \in \mathbf{V}_h$ (solution of (5.3.5)) and known initial data $w_{1,h}^0, w_{2,h}^0$ such that, $\forall s_h \in W_h$

$$m^h(\delta_t w_{1,h}^n, s_h) + a_4^h(w_{1,h}^n, s_h) + c^h(\boldsymbol{u}_h^{s,n}; w_{1,h}^n, s_h) = J_f^{h,n}(w_{1,h}^{n-1}, w_{2,h}^{n-1}, \boldsymbol{u}_h^{s,n}; s_h), \tag{5.3.6a}$$

$$m^h(\delta_t w_{2,h}^n, s_h) + a_5^h(w_{2,h}^n, s_h) + c^h(\boldsymbol{u}_h^{s,n}; w_{2,h}^n, s_h) = J_g^{h,n}(w_{1,h}^{n-1}, w_{2,h}^{n-1}, \boldsymbol{u}_h^{s,n}; s_h). \tag{5.3.6b}$$

The above process of solving the problem continues iteratively for $n = 2, \ldots, N$. The discrete functionals on each $K \in \mathcal{T}_h$ and $1 \leq n \leq N$ involved in (5.3.5)-(5.3.6) are defined as

$$\begin{gathered}
G_\ell^{h,n}(q_h^f)|_K := (\ell_h^n|_K, q_h^f)_{0,K}, \\
J_z^{h,n}(w_{1,h}^{n-1}, w_{2,h}^{n-1}, \boldsymbol{u}_h^{s,n}; s_h)|_K := (z_h(w_{1,h}^{n-1}, w_{2,h}^{n-1}, \boldsymbol{u}_h^{s,n})|_K, s_h)_{0,K}, \text{ for } z = f, g, \\
F_{\boldsymbol{b},r}^{h,n}(w_{1,h}^{n-1}, w_{2,h}^{n-1}; \boldsymbol{v}_h^s)|_K := F_{\boldsymbol{b}}^{h,n}(\boldsymbol{v}_h^s)|_K + F_r^{h,n}(w_{1,h}^{n-1}, w_{2,h}^{n-1}; \boldsymbol{v}_h^s)|_K, \\
\text{with} \quad F_{\boldsymbol{b}}^{h,n}(\boldsymbol{v}_h^s)|_K := \rho(\boldsymbol{b}_h^n, \boldsymbol{v}_h^s)_{0,K}, \\
F_r^{h,n}(w_{1,h}^{n-1}, w_{2,h}^{n-1}; \boldsymbol{v}_h^s)|_K := \tau(r_h^{n-1}(w_{1,h}^{n-1}, w_{2,h}^{n-1})(\boldsymbol{k} \otimes \boldsymbol{k}), \boldsymbol{\varepsilon}(\boldsymbol{v}_h^s))_{0,K}.
\end{gathered}$$

We note that the above systems of equations are linear for each n since we have considered the explicit scheme in time discretization.

Existence and Uniqueness

We will show the well-posedness of the discrete scheme through stability and then the uniqueness of the linear system of equations. We start it by introducing the discrete-in-time l^2- norm as follows, for some Sobolev space V

$$\|X\|^2_{l^2(V)} := \|X\|^2_{l^2(0,t_n;V)} = \Delta t \sum_{j=0}^{n} \|X^j\|^2_V. \tag{5.3.7}$$

Now, we collect the following important results for the further analysis.

- Discrete Identity:

$$\int_\Omega X^n \delta_t X^n = \frac{1}{2}\delta_t \|X^n\|^2_{0,\Omega} + \frac{1}{2}\Delta t \|\delta_t X^n\|^2_{0,\Omega}.$$

- Integration by parts yields, for $\boldsymbol{v}^s \in \mathbf{V}$ and $w \in W$ (with the use of (5.1.7a) and (5.1.7d))

$$\int_\Omega (\boldsymbol{v}^s \cdot \nabla w) w \,\mathrm{d}x = \frac{1}{2}\int_\Omega \boldsymbol{v}^s \cdot \nabla w^2 \,\mathrm{d}x = -\frac{1}{2}\int_\Omega \operatorname{div}(\boldsymbol{v}^s) w^2 \,\mathrm{d}x.$$

In analysis, we will require next lemma which is referred from our previous work [39] (also in Chapter 4) and briefly explained here.

Lemma 5.1. *We have the following bound, for all $q_h^{f,n} \in Q_h$ and $\phi_h^n \in Z_h$ at each n,*

$$\begin{aligned}(\Delta t)\sum_{j=1}^{n} L_h^j \geq \frac{1}{2}\sum_{K\in\mathcal{T}_h} \Big(& c_0(\|\Pi_K^0 q_h^{f,n}\|^2_{0,K} - \|\Pi_K^0 q_h^{f,0}\|^2_{0,K}) \\ & +\lambda^{-1}\left(\|\alpha\Pi_K^0 q_h^{f,n} - \phi_h^n\|^2_{0,K} - \|\alpha\Pi_K^0 q_h^{f,0} - \phi_h^0\|^2_{0,K}\right) \\ & +\tilde{\alpha}_*\left(c_0 + \alpha^2\lambda^{-1}\right)\left(\|(I-\Pi_K^0)q_h^{f,n}\|^2_{0,K} - \|(I-\Pi_K^0)q_h^{f,0}\|^2_{0,K}\right)\Big),\end{aligned} \tag{5.3.8}$$

where

$$L_h^n := \tilde{a}_2^h(\delta_t q_h^{f,n}, q_h^{f,n}) - b_2(q_h^{f,n}, \delta_t \phi_h^n) - b_2(\delta_t q_h^{f,n}, q_h^{f,n}) + a_3(\delta_t \phi_h^n, \phi_h^n),$$

Proof. The commmutative property for the operators δ_t and Π_K^0 gives,

$$\tilde{a}_2^h(\delta_t q_h^{f,n}, q_h^{f,n}) = \sum_{K\in\mathcal{T}_h}\Big(\tilde{a}_2^K(\delta_t \Pi_K^0 q_h^{f,n}, \Pi_K^0 q_h^{f,n})$$

$$+\Big(c_0+\alpha^2\lambda^{-1}\Big)S^{0,K}(\delta_t(I-\Pi_K^0)q_h^{f,n},(I-\Pi_K^0)q_h^{f,n})\Big).$$

Then rewrite L_h^n as

$$\begin{aligned}L_h^n=\sum_{K\in\mathcal{T}_h}\Big(&\lambda^{-1}(\delta_t(\alpha\Pi_K^0q_h^{f,n}-\phi_h^n),\alpha\Pi_K^0q_h^{f,n}-\phi_h^n)_{0,K}\\&+\alpha^2\lambda^{-1}S^{0,K}(\delta_t(I-\Pi_K^0)q_h^{f,n},(I-\Pi_K^0)q_h^{f,n})\\&+c_0\Big((\delta_t\Pi_K^0q_h^{f,n},\Pi_K^0q_h^{f,n})_{0,K}+S^{0,K}(\delta_t(I-\Pi_K^0)q_h^{f,n},(I-\Pi_K^0)q_h^{f,n})\Big)\Big),\end{aligned}$$

then multiplying with Δt and using the equality (5.3.2), we obtain

$$\begin{aligned}(\Delta t)L_h^n\geq\frac{1}{2}\sum_{K\in\mathcal{T}_h}\delta_t\Big(&\lambda^{-1}\|\alpha\Pi_K^0q_h^{f,n}-\phi_h^n\|_{0,K}^2+c_0\|\Pi_K^0q_h^{f,n}\|_{0,K}^2\\&+\tilde{\alpha}_*\left(c_0+\alpha^2\lambda^{-1}\right)\|(I-\Pi_K^0)q_h^{f,n}\|_{0,K}^2\Big).\end{aligned}$$

Thus summing over n gives (5.3.8). □

Next, we recall a well-known lemma utilized to handle the analysis of the non-linear and time-dependent problems. Also, we consult the proof of the following lemma from [75, Lemma 5.1].

Lemma 5.2 (Generalized Discrete Gronwall lemma). *Let k, B, and a_j, b_j, c_j, γ_j, for integer $j\geq 0$, be non-negative numbers such that, for $n>0$, we have*

$$a_n+k\sum_{j=0}^n b_j\leq k\sum_{j=0}^n\gamma_j a_j+k\sum_{j=0}^n c_j+B.$$

If $k\gamma_j<1\ \forall j$ then

$$a_n+k\sum_{j=0}^n b_j\leq\exp\left(k\sum_{j=0}^n(1-k\gamma_j)^{-1}\gamma_j\right)\left\{k\sum_{j=0}^n c_j+B\right\}.\tag{5.3.9}$$

The next theorem establishes the existence and uniqueness result.

Theorem 5.1. *The fully-discrete formulation* (5.3.5)-(5.3.6) *of the coupled problem* (5.1.5) *has a unique solution* $(\boldsymbol{u}_h^{s,n},p_h^{f,n},\psi_h^n,w_{1,h}^n,w_{2,h}^n)\in\mathbb{V}_h:=\mathbf{V}_h\times Q_h\times Z_h\times W_h\times W_h$ *for each n.*

Proof. Referring to the previous chapter (Chapter 4), the linear problem (5.3.5) in the form of an uncoupled fully discrete scheme for poroelasticity problem is well-posed for a given data.

We will ensure the existence of a unique solution of linear uncoupled ADR equation (5.3.6) by virtue of the Lax-Milgram lemma. In order to proceed, we define the discrete bilinear form with given $\boldsymbol{u}_h^{s,n}$ as solution of the problem (5.3.5) as,

$$\mathcal{C}_i^h(w_{i,h}^n, s_h) := m^h(w_{i,h}^n, s_h) + \Delta t\Big(a_{3+i}^h(w_{i,h}^n, s_h) + c^h(\boldsymbol{u}_h^{s,n}; w_{i,h}^n, s_h)\Big) \quad \text{for} \quad i = 1, 2.$$

We can rewrite the uncoupled ADR problem (5.3.6) for all $s_h \in W_h$ as

$$\mathcal{C}_i^h(w_{i,h}^n, s_h) = \Delta t \; J_z^{h,n}(w_{1,h}^{n-1}, w_{2,h}^{n-1}, \boldsymbol{u}_h^{s,n}; s_h) + m^h(w_{i,h}^{n-1}, s_h),$$

for $z = f, g$ and $i = 1, 2$.
The continuity of right hand side obtained using the bounds of the discrete linear functionals $m^h(w_{1,h}^{n-1}, \cdot)$ and $J_z^{h,n}(w_{1,h}^{n-1}, w_{2,h}^{n-1}, \boldsymbol{u}_h^{s,n}; \cdot)$ with the help of bounds (5.3.1)-(5.3.2). Now, we will prove the coercivity of the discrete bilinear form $\mathcal{C}_i^h(\cdot,\cdot)$. For all $s_h \in W_h$, the usage of inverse inequality for polynomials leads to

$$\begin{aligned} c_h^K(\boldsymbol{u}_h^{s,n}; s_h, s_h) &\leq \|\boldsymbol{\Pi}_K^{\mathbf{0}} \boldsymbol{u}_h^{s,n}\|_{\infty,K} \|\boldsymbol{\Pi}_K^{\mathbf{0},0} \nabla s_h\|_{0,K} \|\Pi_K^0 s_h\|_{0,K} \\ &\leq C\|\boldsymbol{u}_h^{s,n}\|_{\infty,K} \|\nabla s_h\|_{0,K} \|s_h\|_{0,K}. \end{aligned}$$

Now, for any $s_h \in W_h$, the use of above bound for $c_h^K(\boldsymbol{u}_h^{s,n}; \cdot,\cdot)$, coercivity of the bilinear forms $m^h(\cdot,\cdot)$ and $a_{3+i}^h(\cdot,\cdot)$, and Young's inequality, we get

$$\begin{aligned} \mathcal{C}_i^h(s_h, s_h) &= m^h(s_h, s_h) + \Delta t\Big(a_{3+i}^h(s_h, s_h) + c^h(\boldsymbol{u}_h^{s,n}; s_h, s_h)\Big) \\ &\geq \Big(\tilde{\alpha}_* - \frac{C\Delta t}{2\alpha_* D_i^a}\|\boldsymbol{u}_h^{s,n}\|_{\infty,\Omega}^2\Big)\|s_h\|_{0,\Omega}^2 + \frac{\alpha_*}{2} D_i^a \Delta t \|\nabla s_h\|_{0,\Omega}^2. \end{aligned}$$

Choosing $\Delta t > 0$ small enough and require D_i^a so that

$$\tilde{\alpha}_* \geq \frac{C\|\boldsymbol{u}_h^{s,n}\|_{\infty,\Omega}^2}{2\alpha_* D_i^a}\Delta t,$$

we achieve the coercivity of $\mathcal{C}_i^h(\cdot,\cdot)$. Also, the continuity of discrete bilinear form $\mathcal{C}_i^h(\cdot,\cdot)$ is followed from the boundedness of the discrete bilinear forms (5.3.1). Thus, the Lax-Milgram lemma deduces the existence of a unique solution. $\square$

Now, we will establish the stability of fully discrete scheme by collecting the results from Lemmas 5.1 and 5.2.

Theorem 5.2. *Assume that* $(\boldsymbol{u}_h^{s,n}, p_h^{f,n}, \psi_h^n, w_{1,h}^n, w_{2,h}^n) \in \mathbb{V}_h$ *is solution of the fully discrete scheme* (5.3.5)-(5.3.6) *for the coupled problem* (5.1.5) *then it satisfies*

$$\begin{aligned}
&\|\boldsymbol{\varepsilon}(\boldsymbol{u}_h^{s,n})\|_{0,\Omega}^2 + \|p_h^f\|_{l^2(H^1(\Omega))}^2 + \|\psi_h^n\|_{0,\Omega}^2 + \sum_{i=1}^{2} \left(\|w_{i,h}^n\|_{0,\Omega}^2 + D_i^a \|w_{i,h}\|_{l^2(H^1(\Omega))}^2\right) \\
&\leq C\Bigg(\|\boldsymbol{\varepsilon}(\boldsymbol{u}_h^{s,0})\|_{0,\Omega}^2 + \|p_h^{f,0}\|_{0,\Omega}^2 + \|\psi_h^0\|_{0,\Omega}^2 + \sum_{i=1}^{2} \|w_{i,h}^0\|_{0,\Omega}^2 + \|\ell\|_{l^2(L^2(\Omega))}^2 \\
&\qquad + \sum_{j=1}^{n} \left(1 + \|\boldsymbol{b}^j\|_{0,\Omega}^2\right)\Bigg),
\end{aligned}$$

where $C > 0$ *is a constant independent of* h *and* Δt.

Proof. Taking $\boldsymbol{v}_h^{s,n} = \delta_t \boldsymbol{u}_h^{s,n}$ in (5.3.5a), $q_h^f = p_h^{f,n}$ in (5.3.5b), and for time step n and $n-1$ in equation (5.3.5c) with $\phi_h = \psi_h^n$ gives

$$\begin{aligned}
a_1^h(\boldsymbol{u}_h^{s,n}, \delta_t \boldsymbol{u}_h^{s,n}) + b_1(\delta_t \boldsymbol{u}_h^{s,n}, \psi_h^n) &= F_{\boldsymbol{b},r}^{h,n}(w_{1,h}^{n-1}, w_{2,h}^{n-1}; \delta_t \boldsymbol{u}_h^{s,n}), \\
\tilde{a}_2^h(\delta_t p_h^{f,n}, p_h^{f,n}) + a_2^h(p_h^{f,n}, p_h^{f,n}) - b_2(p_h^{f,n}, \delta_t \psi_h^n) &= G_\ell^{h,n}(p_h^{f,n}), \\
b_1(\delta_t \boldsymbol{u}_h^{s,n}, \psi_h^n) + b_2(\delta_t p_h^{f,n}, \psi_h^n) - a_3(\delta_t \psi_h^n, \psi_h^n) &= 0.
\end{aligned}$$

Adding these equations result into

$$\begin{aligned}
a_1^h(\boldsymbol{u}_h^{s,n}, \delta_t \boldsymbol{u}_h^{s,n}) + a_2^h(p_h^{f,n}, p_h^{f,n}) + \tilde{a}_2^h(\delta_t p_h^{f,n}, p_h^{f,n}) - b_2(p_h^{f,n}, \delta_t \psi_h^n) \\
-b_2(\delta_t p_h^{f,n}, \psi_h^n) + a_3(\delta_t \psi_h^n, \psi_h^n) \\
= F_{\boldsymbol{b},r}^{h,n}(w_{1,h}^{n-1}, w_{2,h}^{n-1}; \delta_t \boldsymbol{u}_h^{s,n}) + G_\ell^{h,n}(p_h^{f,n}).
\end{aligned}$$

Summing over n, and the use of (5.3.2) and bound of L_h^n from Lemma (5.1), we get

$$\begin{aligned}
&\frac{\mu}{2}\|\boldsymbol{\varepsilon}(\boldsymbol{u}_h^{s,n})\|_{0,\Omega}^2 + \mu\frac{\Delta t^2}{2}\sum_{j=1}^{n}\|\delta_t \boldsymbol{\varepsilon}(\boldsymbol{u}_h^{s,j})\|_{0,\Omega}^2 + \frac{\kappa_1}{\eta}\Delta t\sum_{j=1}^{n}\|\nabla p_h^{f,j}\|_{0,\Omega}^2 \\
&+ \frac{1}{2}\sum_{K\in\mathcal{T}_h}\Bigg(c_0\|\Pi_K^0 p_h^{f,n}\|_{0,K}^2 + \frac{1}{\lambda}\|\alpha\Pi_K^0 p_h^{f,n} - \psi_h^n\|_{0,K}^2 \\
&\qquad + \tilde{\alpha}_*\left(c_0 + \frac{\alpha^2}{\lambda}\right)\|(I - \Pi_K^0)p_h^{f,n}\|_{0,K}^2\Bigg) \\
&\leq \frac{\mu}{2}\|\boldsymbol{\varepsilon}(\boldsymbol{u}_h^{s,0})\|_{0,\Omega}^2 + C_{\tilde{\alpha}_*}\left(c_0 + \frac{\alpha^2}{\lambda}\right)\|p_h^{f,0}\|_{0,\Omega}^2 + \frac{1}{\lambda}\|\psi_h^0\|_{0,\Omega}^2
\end{aligned}$$

$$+ C\Delta t \sum_{j=1}^{n} \Big(F_{\boldsymbol{b},r}^{h,j}(w_{1,h}^{j-1}, w_{2,h}^{j-1}; \delta_t \boldsymbol{u}_h^{s,j}) + G_{\ell}^{h,j}(p_h^{f,j}) \Big).$$

The last second term on the right hand side can be bounded as

$$\begin{aligned}
&\Delta t \sum_{j=1}^{n} F_{\boldsymbol{b},r}^{h,j}(w_{1,h}^{j-1}, w_{2,h}^{j-1}; \delta_t \boldsymbol{u}_h^{s,j}) \\
&= \Delta t \sum_{j=1}^{n} \sum_{K\in\mathcal{T}_h} \Big(\rho \left\langle \boldsymbol{b}_h^j, \delta_t \boldsymbol{u}_h^{s,j} \right\rangle_{0,K} - \tau \left\langle r_h(w_{1,h}^{j-1}, w_{2,h}^{j-1})(\boldsymbol{k}\otimes\boldsymbol{k}), \delta_t \boldsymbol{\varepsilon}(\boldsymbol{u}_h^{s,j}) \right\rangle_{0,K} \Big) \\
&\leq \mu \frac{\Delta t^2}{4} \sum_{j=1}^{n} \|\delta_t \boldsymbol{\varepsilon}(\boldsymbol{u}_h^{s,j})\|_{0,\Omega}^2 + C \sum_{j=1}^{n} \Big(\|\boldsymbol{b}^j\|_{0,\Omega}^2 + \|w_{1,h}^{j-1}\|_{0,\Omega}^2 + \|w_{2,h}^{j-1}\|_{0,\Omega}^2 \Big).
\end{aligned}$$

Use of Young's inequality for the last term gives

$$\begin{aligned}
&\frac{\mu}{2}\|\boldsymbol{\varepsilon}(\boldsymbol{u}_h^{s,n})\|_{0,\Omega}^2 + \frac{\kappa_1}{\eta}\Delta t \sum_{j=1}^{n} \|\nabla p^{f,j}\|_{0,\Omega}^2 + \frac{1}{2}\sum_{K\in\mathcal{T}_h} \Bigg(\frac{1}{\lambda}\|\alpha \Pi_K^0 p_h^{f,n} - \psi_h^n\|_{0,K}^2 + c_0 \|\Pi_K^0 p_h^{f,n}\|_{0,K}^2 \\
&\quad + \tilde{\alpha}_* \left(c_0 + \frac{\alpha^2}{\lambda} \right) \left(\|(I - \Pi_K^0) p_h^{f,n}\|_{0,K}^2 \right) \Bigg) \\
&\leq \frac{\mu}{2}\|\boldsymbol{\varepsilon}(\boldsymbol{u}_h^{s,0})\|_{0,\Omega}^2 + C_{\tilde{\alpha}_*}\left(c_0 + \frac{\alpha^2}{\lambda} \right) \|p_h^{f,0}\|_{0,\Omega}^2 + \frac{1}{\lambda}\|\psi_h^0\|_{0,\Omega}^2 \\
&\quad + C \sum_{j=1}^{n} \Big(\|\boldsymbol{b}^j\|_{0,\Omega}^2 + \Delta t \|\ell^j\|_{0,\Omega}^2 + \|w_{1,h}^{j-1}\|_{0,\Omega}^2 + \|w_{2,h}^{j-1}\|_{0,\Omega}^2 \Big).
\end{aligned}$$

Using discrete inf-sup condition (5.3.4) and equation (5.3.5a), we obtain

$$\begin{aligned}
\tilde{\beta}\|\psi_h^n\|_{0,\Omega} &\leq \sup_{\boldsymbol{v}_h^s \in \mathbf{V}_h\setminus\{0\}} \frac{1}{\|\boldsymbol{v}_h^s\|_{1,\Omega}} \big(F_{\boldsymbol{b},r}^{h,n}(w_{1,h}^{n-1}, w_{2,h}^{n-1}; \boldsymbol{v}_h^s) - a_1^h(\boldsymbol{u}_h^{s,n}, \boldsymbol{v}_h^s) \big) \\
&\leq C\big(\|\boldsymbol{b}^n\|_{0,\Omega} + \|w_{1,h}^{n-1}\|_{0,\Omega} + \|w_{2,h}^{n-1}\|_{0,\Omega} + \mu \|\boldsymbol{\varepsilon}(\boldsymbol{u}_h^{s,n})\|_{0,\Omega} \big).
\end{aligned}$$

For given $\boldsymbol{u}_h^{s,n}$ as solution of the problem (5.3.5) and taking $s_h = w_{1,h}^n$ in (5.3.6a) then the use of Young's inequality with appropriate choice of ϵ and the bound of trilinear form $c_h(\cdot;\cdot,\cdot)$ implies

$$\begin{aligned}
&\frac{\Delta t}{2}\delta_t \|w_{1,h}^n\|_{0,\Omega}^2 + \Delta t\, D_1^a \|\nabla w_{1,h}^n\|_{0,\Omega}^2 \lesssim m^h(w_{1,h}^n - w_{1,h}^{n-1}, w_{1,h}^n) + \Delta t\, a_4^h(w_{1,h}^n, w_{1,h}^n) \\
&\quad = \Delta t \left(J_f^{h,n}(w_{1,h}^{n-1}, w_{2,h}^{n-1}, \boldsymbol{u}_h^{s,n}; w_{1,h}^n) - c^h(\boldsymbol{u}_h^{s,n}; w_{1,h}^n, w_{1,h}^n) \right) \\
&\quad \leq C\Delta t(1 + \|w_{1,h}^{n-1}\|_{0,\Omega}^2 + \|w_{2,h}^{n-1}\|_{0,\Omega}^2) + \Delta t(\epsilon + C_1 \|\boldsymbol{u}_h^{s,n}\|_{1,\infty,\Omega})\|w_{1,h}^n\|_{0,\Omega}^2.
\end{aligned}$$

Summing over n gives

$$\|w_{1,h}^n\|_{0,\Omega}^2 + \Delta t\, D_1^a \sum_{j=1}^n \|\nabla w_{1,h}^j\|_{0,\Omega}^2 \le \|w_{1,h}^0\|_{0,\Omega}^2 + C\Big(1 + \Delta t \sum_{j=1}^n \sum_{i=1}^2 \|w_{i,h}^{j-1}\|_{0,\Omega}^2\Big)$$
$$+ \Delta t \sum_{j=1}^n (\epsilon + C_1 \|\boldsymbol{u}_h^{s,j}\|_{1,\infty,\Omega}) \|w_{1,h}^j\|_{0,\Omega}^2.$$

Thus, again use of these arguments for equation (5.3.6b) with $s_h = w_{2,h}^n$, we get

$$\sum_{i=1}^2 \big(\|w_{i,h}^n\|_{0,\Omega}^2 + \Delta t\, D_i^a \sum_{j=1}^n \|\nabla w_{i,h}^j\|_{0,\Omega}^2\big)$$
$$\le \sum_{i=1}^2 \|w_{i,h}^0\|_{0,\Omega}^2 + C\Big(1 + \Delta t \sum_{j=1}^n \sum_{i=1}^2 \|w_{i,h}^{j-1}\|_{0,\Omega}^2\Big)$$
$$+ \Delta t \sum_{j=1}^n \big((\epsilon + C_1 \|\boldsymbol{u}_h^{s,j}\|_{1,\infty,\Omega}) \sum_{i=1}^2 \|w_{i,h}^j\|_{0,\Omega}^2\big).$$

Adding the resultant bounds gives

$$\mu \|\boldsymbol{\varepsilon}(\boldsymbol{u}_h^{s,n})\|_{0,\Omega}^2 + \frac{\kappa_1}{\eta} \Delta t \sum_{j=1}^n \|\nabla p^{f,j}\|_{0,\Omega}^2 + \|\psi_h^n\|_{0,\Omega}^2$$
$$+ \sum_{i=1}^2 \big(\|w_{i,h}^n\|_{0,\Omega}^2 + \Delta t\, D_i^a \sum_{j=1}^n \|\nabla w_{i,h}^j\|_{0,\Omega}^2\big)$$
$$\le \sum_{i=1}^2 \|w_{i,h}^0\|_{0,\Omega}^2 + \Delta t \sum_{j=1}^n \big((\epsilon + C_1 \|\boldsymbol{u}_h^{s,j}\|_{1,\infty,\Omega}) \sum_{i=1}^2 \|w_{i,h}^j\|_{0,\Omega}^2\big)$$
$$+ C\Big(\|\boldsymbol{\varepsilon}(\boldsymbol{u}_h^{s,0})\|_{0,\Omega}^2 + \|p_h^{f,0}\|_{0,\Omega}^2 + \|\psi_h^0\|_{0,\Omega}^2 + \sum_{j=1}^n \Big(1 + \|\boldsymbol{b}^j\|_{0,\Omega}^2 + \Delta t \|\ell^j\|_{0,\Omega}^2\Big)$$
$$+ \Delta t \sum_{j=1}^n \sum_{i=1}^2 \|w_{i,h}^{j-1}\|_{0,\Omega}^2\Big).$$

Assuming $M := \max\limits_{1 \le j \le n} \|\boldsymbol{u}_h^{s,j}\|_{1,\infty,\Omega} < \infty$ then choosing $\epsilon, \Delta t$ such that $\Delta t(\epsilon + C_1 M) < 1$. Thus, the use of discrete Gronwall lemma (Lemma 5.2) completes the stability of the discrete solution. $\square$

Therefore, we have the wellposedness of fully discrete scheme (5.3.5)-(5.3.6) from Theorem 5.1 and 5.2.

5.4 Error analysis

In order to see the rate of convergence of the proposed fully discrete scheme, we will derive the error estimates in suitable norms for each of the variables that appear in the formulation. For establishing the error estimates, we will be utilizing the well-known techniques/arguments used for time-dependent problems and imitating the steps used in showing the uniqueness and stability of the discrete scheme.

We will assume the following regularity assumptions to generate the convergence results: For all $t > 0$, the displacement of porous medium $\boldsymbol{u}^s(t) \in [H^2(\Omega)]^2$, the fluid pressure $p^f(t) \in H^2(\Omega)$, the total pressure $\psi(t) \in H^1(\Omega)$ and concentrations $w_1, w_2 \in H^2(\Omega)$. We also assume the regularity in time as,

$$\begin{gathered}\partial_t \boldsymbol{u}^s \in \mathbf{L}^2(0,T;[H^2(\Omega)]^2), \quad \partial_t p^f, \partial_t \psi \in L^2(0,T;H^1(\Omega)),\\ \partial_t w_1, \partial_t w_2 \in l^2(0,T;L^2(\Omega)), \quad \partial_{tt} \boldsymbol{u}^s \in \mathbf{L}^2(0,T;[L^2(\Omega)]^2),\\ \partial_{tt} p^f, \partial_{tt}\psi, \partial_{tt} w_1, \partial_{tt} w_2 \in L^2(0,T;L^2(\Omega)).\end{gathered}$$

Lemma 5.3. *For each $\boldsymbol{u}^s \in \mathbf{V} \cap [H^{1+r}(\Omega)]^2$ with $0 \leq r \leq 1$ under the assumptions on the polygonal mesh (mentioned in Section 5.3.1), there exists an interpolant $\boldsymbol{u}_I^s \in \mathbf{V}_h$ satisfying*

$$\|\boldsymbol{u}^s - \boldsymbol{u}_I^s\|_{0,\Omega} + h_K \ |\boldsymbol{u}^s - \boldsymbol{u}_I^s|_{1,\Omega} \leq C h^{1+r} |\boldsymbol{u}^s|_{1+r,\Omega}. \tag{5.4.1}$$

For given solution $(\boldsymbol{u}^s, p^f, \psi, w_1, w_2) \in \mathbb{V}$ of weak formulation (5.2.1), the projection $(S_h^{\boldsymbol{u}}\boldsymbol{u}^s, S_h^p p^f, S_h^{\psi}\psi, S_h^{w_1} w_1, S_h^{w_2} w_2) \in \mathbb{V}_h$ is defined for all $(\boldsymbol{v}_h^s, q_h^f, \phi_h, s_h, s_h) \in \mathbb{V}_h$ as

$$a_1(S_h^u \boldsymbol{u}^s, \boldsymbol{v}_h^s) + b_1(\boldsymbol{v}_h^s, S_h^{\psi}\psi) = a_1(\boldsymbol{u}^s, \boldsymbol{v}_h^s) + b_1(\boldsymbol{v}_h^s, \psi); \tag{5.4.2a}$$

$$b_1(S_h^u \boldsymbol{u}^s, \phi_h) = b_1(\boldsymbol{u}^s, \phi_h); \tag{5.4.2b}$$

$$a_2(S_h^p p^f, q_h^f) = a_2(p^f, q_h^f); \quad a_{3+i}^h(S_h^{w_i} w_i, s_h) = a_{3+i}(w_i, s_h). \tag{5.4.2c}$$

Note that $(S_h^{\boldsymbol{u}}, S_h^{\psi})$ and $S_h^p, S_h^{w_1}, S_h^{w_2}$ are standard Stokes and elliptic projection operators respectively. These operators also satisfy the following estimates (for instance [26] and also in Chapter 2):

Lemma 5.4. *Let $(\boldsymbol{u}^s, p^f, \psi, w_1, w_2) \in \mathbb{V}$ and $(S_h^{\boldsymbol{u}}\boldsymbol{u}^s, S_h^p p^f, S_h^{\psi}\psi, S_h^{w_1} w_1, S_h^{w_2} w_2) \in \mathbb{V}_h$ be the unique solutions to the system of equations* (5.2.1) *and* (5.4.2)*, respectively.*

Then,

$$
\begin{aligned}
\|\boldsymbol{u}^s - S_h^{\boldsymbol{u}}\boldsymbol{u}^s\|_{0,\Omega} + h(|\boldsymbol{u}^s - S_h^{\boldsymbol{u}}\boldsymbol{u}^s|_{1,\Omega} + \|\psi - S_h^{\psi}\psi\|_{0,\Omega}) \\
\leq Ch^2(|\boldsymbol{u}|_{2,\Omega} + |\psi|_{1,\Omega}),
\end{aligned} \tag{5.4.3a}
$$

$$
\|p^f - S_h^p p^f\|_{0,\Omega} + h|p^f - S_h^p p^f|_{1,\Omega} \leq Ch^2|p|_{2,\Omega}, \tag{5.4.3b}
$$

$$
\|w_i - S_h^{w_i} w_i\|_{0,\Omega} + h|w_i - S_h^{w_i} w_i|_{1,\Omega} \leq Ch^2|w_i|_{2,\Omega},\ i = 1, 2. \tag{5.4.3c}
$$

To derive the theoretical error estimates for fully discrete scheme, we decompose the error using the projection operator (defined in 5.4.2) as follows :

$$
\xi(t_n) - \xi_h^n = (\xi(t_n) - S_h^{\xi}\xi(t_n)) \ + \ (S_h^{\xi}\xi(t_n) - \xi_h^n) := \rho_\xi^n + \eta_\xi^n,
$$

for any $\xi(t_n) = \boldsymbol{u}^s(t_n), p^f(t_n), \psi(t_n), w_1(t_n), w_2(t_n),\ \xi_h^n = \boldsymbol{u}_h^{s,n}, p_h^{f,n}, \psi_h^n, w_{1,h}^n, w_{2,h}^n$ and for each n.

From the continuous problem (5.2.1) and fully discrete scheme (5.3.5)-(5.3.6), and an appeal to projection operator (5.4.2), the error equations for the fully discrete scheme in terms of η_ξ^n, where $\xi = \boldsymbol{u}^s, p^f, \psi, w_1, w_2$, are

$$
\begin{aligned}
a_1^h(\eta_{\boldsymbol{u}}^n, \boldsymbol{v}_h^s) + b_1(\boldsymbol{v}_h^s, \eta_\psi^n) &= F_{\boldsymbol{b},r}^n(w_1^n, w_2^n; \boldsymbol{v}_h^s) - F_{\boldsymbol{b},r}^{h,n}(w_{1,h}^{n-1}, w_{2,h}^{n-1}; \boldsymbol{v}_h^s), && (5.4.4a)\\
\tilde{a}_2^h(\delta_t\eta_p^n, q_h^f) + a_2^h(\eta_p^n, q_h^f) - b_2(q_h^f, \delta_t\eta_\psi^n) &= (G_\ell^n - G_\ell^{h,n})(q_h^f) + b_2(q_h^f, \delta_t S_h^{\psi}\psi^n - \partial_t\psi^n) && (5.4.4b)\\
&\quad + \left(\tilde{a}_2^h(\delta_t S_h^p p^n, q_h^f) - \tilde{a}_2(\partial_t p^n, q_h^f)\right),\\
b_1(\delta_t\eta_{\boldsymbol{u}}^n, \phi_h) + b_2(\delta_t\eta_p^n, \phi_h) - a_3(\delta_t\eta_\psi^n, \phi_h) &= -b_2(\delta_t\rho_p^n, \phi_h) + a_3(\delta_t\rho_\psi^n, \phi_h), && (5.4.4c)\\
m^h(\delta_t\eta_{w_1}^n, s_h) + a_4^h(\eta_{w_1}^n, s_h) &= \Big(\big(J_f^n(w_1^n, w_2^n, \boldsymbol{u}^{s,n}; s_h) - J_f^{h,n}(w_{1,h}^{n-1}, w_{2,h}^{n-1}, \boldsymbol{u}_h^{s,n}; s_h)\big)\\
&\quad - \big(m(\partial_t w_1^n, s_h) - m^h(\delta_t S_h^{w_1} w_1^n, s_h)\big) && (5.4.4d)\\
&\quad - \big(c(\boldsymbol{u}^{s,j}; w_1^j, s_h) - c^h(\boldsymbol{u}_h^{s,j}; w_{1,h}^j, s_h)\big)\Big),\\
m^h(\delta_t\eta_{w_2}^n, s_h) + a_5^h(\eta_{w_2}^n, s_h) &= \Big(\big(J_g^n(w_1^n, w_2^n, \boldsymbol{u}^{s,n}; s_h) - J_g^{h,n}(w_{1,h}^{n-1}, w_{2,h}^{n-1}, \boldsymbol{u}_h^{s,n}; s_h)\big)\\
&\quad - \big(m(\partial_t w_2^n, s_h) - m^h(\delta_t S_h^{w_2} w_2^n, s_h)\big) && (5.4.4e)\\
&\quad - \big(c(\boldsymbol{u}^{s,j}; w_2^j, s_h) - c^h(\boldsymbol{u}_h^{s,j}; w_{2,h}^j, s_h)\big)\Big),
\end{aligned}
$$

$\forall\ (\boldsymbol{v}_h^s, q_h^f, \phi_h, s_h, s_h) \in \mathbb{V}_h$.

Now, we will divide the derivation of error estimates for fully discrete scheme (5.3.5)-(5.3.6) into two lemmas: one containing the error bounds from the poroelasticity equations and the other-regarding ADR equations. We start here by recalling/mentioning the results to be used in succeeding lemmas.

The Taylor's expansion for any continuous function $f(t)$ gives at time $t = t_j,\ j = 1, \ldots, n$,

$$f(t_j) - f(t_{j-1}) = (\Delta t)\ \partial_t f(t_j) + \int_{t_{j-1}}^{t_j} (s - t_{j-1}) \partial_{tt} f(s)\, \mathrm{d}s. \tag{5.4.5}$$

This expansion imply the bounds in next corollary.

Corollary 5.1. *For any smooth enough function ξ, we have*

$$\sum_{j=1}^{n} \|\xi^j - \xi^{j-1}\|_{0,\Omega}^2 \leq C(\Delta t)^2 \Big(\sum_{j=1}^{n} \|\partial_t \xi^j\|_{0,\Omega}^2 + \|\partial_{tt}\xi(s)\|_{L^1(L^2(\Omega))}^2 \Big), \tag{5.4.6}$$

$$\Delta t \sum_{j=1}^{n} \|\partial_t \xi^j - \delta_t \xi^j\|_{0,\Omega}^2 \leq C(\Delta t)^3 \, \|\partial_{tt}\xi\|_{L^2(L^2(\Omega))}^2 \,, \tag{5.4.7}$$

Proof. Use of (5.4.5) gives

$$\begin{aligned}
\|\xi^j - \xi^{j-1}\|_{0,\Omega} &\leq (\Delta t) \|\partial_t \xi^j\|_{0,\Omega} + \int_{t_{j-1}}^{t_j} (s - t_{j-1}) \|\partial_{tt}\xi(s)\|_{0,\Omega}\, \mathrm{d}s \\
&\leq (\Delta t) \Big(\|\partial_t \xi^j\|_{0,\Omega} + \int_{t_{j-1}}^{t_j} \|\partial_{tt}\xi(s)\|_{0,\Omega}\, \mathrm{d}s \Big).
\end{aligned}$$

Squaring both sides and then summing over j conclude bound (5.4.6).

Again use of (5.4.5) followed with Cauchy-Schwarz inequality yield

$$\Delta t^2 \|\partial_t \xi^j - \delta_t \xi^j\|_{0,\Omega}^2 \leq \left\| \int_{t_{j-1}}^{t_j} (s - t_{j-1}) \partial_{tt}\xi(s)\, \mathrm{d}s \right\|_{0,\Omega}^2 \leq (\Delta t)^3 \, \|\partial_{tt}\xi\|_{L^2(t_{j-1}, t_j; L^2(\Omega))}^2 \,.$$

Summing over j from 1 to n deduce the bound (5.4.7). $\square$

Now, we derive the result below by using the Lipschitz condition of function $r(w_1^n, w_2^n)$ for each n, Corollary (5.1) and standard arguments.

Lemma 5.5 (Coupled poroelastic error bounds)**.** *Let* $(\boldsymbol{u}^{s,n}, p^{f,n}, \psi^n) \in \mathbf{V} \times Q \times Z$ *be the solution to the system* (5.2.1a)-(5.2.1c) *and* $(\boldsymbol{u}_h^{s,n}, p_h^{f,n}, \psi_h^n) \in \mathbf{V}_h \times Q_h \times Z_h$ *be the solution to the system* (5.3.5) *for each n. Then the following estimate holds, with* *constant C independent of h and Δt,*

$$\|\boldsymbol{\varepsilon}(\eta_{\boldsymbol{u}}^n)\|_{0,\Omega}^2 + \|\eta_\psi^n\|_{0,\Omega}^2 + \|\eta_p\|_{l^2(H^1(\Omega))}^2 \leq C\big(h^2 + \Delta t^2 + \sum_{j=1}^{n}\sum_{i=1}^{2}\|\eta_{w_i}^{j-1}\|_{0,\Omega}^2\big) \\ + 2\epsilon_3\Delta t\sum_{j=1}^{n}\|\eta_\psi^j\|_{0,\Omega}^2, \tag{5.4.8}$$

where $\epsilon_3 > 0$ chosen as needed in subsequent analysis.

Proof. Set $\boldsymbol{v}_h^s = \delta_t\eta_{\boldsymbol{u}}^n$ in (5.4.4a), $q_h^f = \eta_p^n$ in (5.4.4b), and $\phi_h = \eta_\psi^n$ in (5.4.4c) and adding them gives

$$\begin{aligned}
&a_1^h(\eta_{\boldsymbol{u}}^n, \delta_t\eta_{\boldsymbol{u}}^n) + a_2^h(\eta_p^n, \eta_p^n) + L_h^n \\
&= \big(F_{\boldsymbol{b},r}^n(w_1^n, w_2^n; \delta_t\eta_{\boldsymbol{u}}^n) - F_{\boldsymbol{b},r}^{h,j}(w_{1,h}^{n-1}, w_{2,h}^{n-1}; \delta_t\eta_{\boldsymbol{u}}^n)\big) + (G_\ell^n - G_\ell^{h,n})(\eta_p^n) \\
&\quad + \big(\tilde{a}_2^h(\delta_t S_h^p p^n, \eta_p^n) - \tilde{a}_2(\partial_t p^n, \eta_p^n)\big) + b_2(\eta_p^n, \delta_t S_h^\psi\psi^n - \partial_t\psi^n) \\
&\quad + b_2(\delta_t\rho_p^n, \eta_\psi^n) - a_3(\delta_t\rho_\psi^n, \eta_\psi^n).
\end{aligned}$$

Summing over each n then the use of Lemma 5.1 gives

$$\begin{aligned}
&\Delta t\sum_{j=1}^{n}\big(\delta_t a_1^h(\eta_{\boldsymbol{u}}^j, \eta_{\boldsymbol{u}}^j) + \Delta t\ a_1^h(\delta_t\eta_{\boldsymbol{u}}^j, \delta_t\eta_{\boldsymbol{u}}^j) + a_2^h(\eta_p^j, \eta_p^j) + L_h^j\big) \\
&= \Delta t\sum_{j=1}^{n}\Big(\big(F_{\boldsymbol{b},r}^j(w_1^j, w_2^j; \delta_t\eta_{\boldsymbol{u}}^j) - F_{\boldsymbol{b},r}^{h,j}(w_{1,h}^{j-1}, w_{2,h}^{j-1}; \delta_t\eta_{\boldsymbol{u}}^j)\big) + (G_\ell^j - G_\ell^{h,j})(\eta_p^j) \\
&\qquad + \big(\tilde{a}_2^h(\delta_t S_h^p p^j, \eta_p^j) - \tilde{a}_2(\partial_t p^j, \eta_p^j)\big) + b_2(\eta_p^j, \delta_t S_h^\psi\psi^j - \partial_t\psi^j) \\
&\qquad + b_2(\delta_t\rho_p^j, \eta_\psi^j) - a_3(\delta_t\rho_\psi^j, \eta_\psi^j)\Big) \\
&:= \sum_{i=1}^{6} R_i.
\end{aligned}$$

The error term R_1 can be written as

$$\begin{aligned}
R_1 = \Delta t\sum_{j=1}^{n}\sum_{K\in\mathcal{T}_h}&\Big(\rho\left((\mathbf{I} - \boldsymbol{\Pi}_K^{\mathbf{0},0})\boldsymbol{b}^j, \delta_t\eta_{\boldsymbol{u}}^j\right)_{0,K} \\
&\qquad + \big(F_r^j(w_1^j, w_2^j; \delta_t\eta_{\boldsymbol{u}}^j) - F_r^{h,j}(w_{1,h}^{j-1}, w_{2,h}^{j-1}; \delta_t\eta_{\boldsymbol{u}}^j)\big)\Big) \\
:= R_1^a + R_1^b.&
\end{aligned}$$

The Young's inequality with some constant $\epsilon_1 > 0$ gives

$$
\begin{aligned}
R_1^a &\leq \rho \frac{c_P}{\sqrt{C_{k,1}}} \Delta t \sum_{j=1}^{n} \sum_{K \in \mathcal{T}_h} \|(\mathbf{I} - \mathbf{\Pi}_K^{\mathbf{0},0}) \boldsymbol{b}^j\|_{0,K} \|\boldsymbol{\varepsilon}(\delta_t \eta_{\boldsymbol{u}}^j)\|_{0,K} \\
&\leq C h^2 \sum_{j=1}^{n} |\boldsymbol{b}^j|_{1,\Omega}^2 + \epsilon_1 \Delta t^2 \sum_{j=1}^{n} \|\boldsymbol{\varepsilon}(\delta_t \eta_{\boldsymbol{u}}^j)\|_{0,\Omega}^2.
\end{aligned}
$$

The bound of R_1^b is through the property of function $r(w_1, w_2)$ and triangle's inequality as follows

$$
\begin{aligned}
R_1^b &\leq \tau \Delta t \sum_{j=1}^{n} \|(r(w_1^j, w_2^j) - r_h(w_{1,h}^{j-1}, w_{2,h}^{j-1}))\|_{0,\Omega} \|\delta_t \boldsymbol{\varepsilon}(\eta_{\boldsymbol{u}}^j)\|_{0,\Omega} \\
&\leq \epsilon_1 \Delta t^2 \sum_{j=1}^{n} \left\|\boldsymbol{\varepsilon}(\delta_t \eta_{\boldsymbol{u}}^j)\right\|_{0,\Omega}^2 + C\tau \sum_{j=1}^{n} \|(r(w_1^j, w_2^j) - r_h(w_{1,h}^{j-1}, w_{2,h}^{j-1}))\|_{0,\Omega}^2.
\end{aligned}
$$

The last term on right hand side for each $K \in \mathcal{T}_h$ can be bounded as

$$
\begin{aligned}
&\|(r(w_1^j, w_2^j) - r_h(w_{1,h}^{j-1}, w_{2,h}^{j-1}))\|_{0,K} \\
&\leq \|r(w_1^j, w_2^j) - r(w_1^{j-1}, w_2^{j-1})\|_{0,K} + \|(I - \Pi_K^0) r(w_1^{j-1}, w_2^{j-1})\|_{0,K} \\
&\quad + \|\Pi_K^0 r(w_1^{j-1}, w_2^{j-1}) - r_h(w_1^{j-1}, w_2^{j-1})\|_{0,K} + \|r_h(w_1^{j-1}, w_2^{j-1}) - r_h(w_{1,h}^{j-1}, w_{2,h}^{j-1})\|_{0,K} \\
&\leq Ch \left(|r(w_1^{j-1}, w_2^{j-1})|_{1,\Omega} + |w_1^{j-1}|_{1,\Omega} + |w_2^{j-1}|_{1,\Omega}\right) + \sum_{i=1}^{2} \left(\|w_i^j - w_i^{j-1}\|_{0,\Omega} + \|\eta_{w_i}^{j-1}\|_{0,\Omega}\right).
\end{aligned}
$$

The bound (5.4.6) gives

$$
\begin{aligned}
R_1^b &\leq \epsilon_1 \Delta t^2 \sum_{j=0}^{n} \|\boldsymbol{\varepsilon}(\delta_t \eta_{\boldsymbol{u}}^j)\|_{0,\Omega}^2 + C\tau^2 \sum_{j=1}^{n} \sum_{i=1}^{2} \|\eta_{w_i}^{j-1}\|_{0,\Omega}^2 \\
&\quad + C\tau^2 \sum_{i=1}^{2} \Big(h^2 \sum_{j=0}^{n-1} |w_i^j|_{1,\Omega}^2 + (\Delta t)^2 \big(\sum_{j=1}^{n} \|\partial_t w_i^j\|_{0,\Omega}^2 + \|\partial_{tt} w_i(s)\|_{L^1(L^2(\Omega))}^2\big)\Big).
\end{aligned}
$$

Use of Cauchy-Schwarz, Poincaré and Young's inequalities with constant $\epsilon_2 > 0$ implies

$$
R_2 \leq C\ h(\Delta t) \sum_{j=1}^{n} |\ell^j|_{1,\Omega} \|\eta_p^j\|_{0,\Omega} \leq \epsilon_2 \Delta t \sum_{j=1}^{n} \|\nabla \eta_p^j\|_{0,\Omega}^2 + C h^2 \|\ell\|_{l^2(H^1(\Omega))}^2.
$$

Use of polynomial approximation and consistency of discrete bilinear form $\tilde{a}_2^{h,K}(\cdot,\cdot)$ gives

$$
\begin{aligned}
R_3 \leq (\Delta t)(c_0 + \alpha^2\lambda^{-1}) \sum_{j=1}^{n} \sum_{K\in\mathcal{T}_h} \Big(&\|\delta_t(S_h^p p^{f,j} - \Pi_K^0 p^{f,j})\|_{0,K} + \|\delta_t(\Pi_K^0 p^{f,j} - p^{f,j})\|_{0,K} \\
&+ \|\delta_t p^{f,j} - \partial_t p^{f,j}\|_{0,K}\Big) \|\eta_p^j\|_{0,K} \\
:= R_3^a + R_3^b + R_3^c.&
\end{aligned}
$$

The term R_3^a can be bounded using Cauchy-Schwarz and Young's inequality as

$$
\begin{aligned}
R_3^a &\leq (c_0 + \alpha^2\lambda^{-1}) \sum_{j=1}^{n} \sum_{K\in\mathcal{T}_h} \Big(\int_{t_{j-1}}^{t_j} \left\|\partial_t(S_h^p p^f - \Pi_K^0 p^f)(s)\right\|_{0,K} \,\mathrm{d}s \Big) \left\|\eta_p^j\right\|_{0,K} \\
&\leq (c_0 + \alpha^2\lambda^{-1})\ h \sum_{j=1}^{n} \Big(\Delta t \int_{t_{j-1}}^{t_j} |\partial_t p^f(s)|_{1,\Omega}^2 \,\mathrm{d}s\Big)^{1/2} \left\|\eta_p^j\right\|_{0,\Omega} \\
&\leq C\ h^2 \|\partial_t p^f\|_{L^2(H^1(\Omega))}^2 + \epsilon_2 \Delta t \sum_{j=1}^{n} \|\nabla \eta_p^j\|_{0,\Omega}^2.
\end{aligned}
$$

Now the same steps leads to

$$
\begin{aligned}
R_3^b &\leq (c_0 + \alpha^2\lambda^{-1}) \sum_{j=1}^{n} \sum_{K\in\mathcal{T}_h} \|(I - \Pi_K^0)(p^{f,j} - p^{f,j-1})\|_{0,K} \|\eta_p^j\|_{0,K} \\
&\leq C\ h^2 \|\partial_t p^f\|_{L^2(H^1(\Omega))}^2 + \epsilon_2 \Delta t \sum_{j=1}^{n} \|\nabla \eta_p^j\|_{0,\Omega}^2.
\end{aligned}
$$

The bound of R_3^c is followed from (5.4.7) using Taylor's expansion as

$$
\begin{aligned}
R_3^c &= (\Delta t)(c_0 + \alpha^2\lambda^{-1}) \sum_{j=1}^{n} \|\delta_t p^{f,j} - \partial_t p^{f,j}\|_{0,\Omega}\|_{0,\Omega} \|\eta_p^j\|_{0,\Omega} \\
&\leq C(\Delta t)^3 \left\|\partial_{tt} p^f\right\|_{L^2(L^2(\Omega))}^2 + \epsilon_2 \Delta t \sum_{j=1}^{n} \|\nabla \eta_p^j\|_{0,\Omega}^2.
\end{aligned}
$$

An application of Lemma 5.1 and Young's inequality implies

$$
R_4 = (\Delta t)\alpha\lambda^{-1} \sum_{j=1}^{n} \|\delta_t S_h^{\psi} \psi^j - \partial_t \psi^j\|_{0,\Omega} \|\eta_p^j\|_{0,\Omega}
$$

$$\leq C\left(h^2\int_0^{t_n}\|\partial_t\psi(s)\|_{1,\Omega}^2\,\mathrm{d}s+(\Delta t)^3\,\|\partial_{tt}\psi\|^2_{L^2(L^2(\Omega))}\right)+\epsilon_2\Delta t\sum_{j=1}^n\|\nabla\eta_p^j\|^2_{0,\Omega}.$$

Use of the estimates (5.4.3a) and Lemma 5.1 as seen in bound of R_3^a with constant $\epsilon_3>0$ gives

$$\begin{aligned}R_5&\leq C\alpha\lambda^{-1}\Delta t\sum_{j=1}^n\left\|\int_{t_{j-1}}^{t_j}\partial_t\rho_p(s)\,\mathrm{d}s\right\|_{0,\Omega}\|\eta_\psi^j\|_{0,\Omega}\\&\leq C\ h^2\|\partial_t p^f\|^2_{L^2(H^1(\Omega))}+\epsilon_3\Delta t\sum_{j=1}^n\|\eta_\psi^j\|^2_{0,\Omega}.\end{aligned}$$

Similar to bound of term R_5, we get

$$R_6=-\sum_{j=1}^n a_3(\rho_\psi^j-\rho_\psi^{j-1},\eta_\psi^j)\leq C\ h^2\|\partial_t\psi\|^2_{L^2(H^1(\Omega))}\,\mathrm{d}s+\epsilon_3\Delta t\sum_{j=1}^n\|\eta_\psi^j\|^2_{0,\Omega}.$$

Combining the bounds of R_i's, we get

$$\begin{aligned}&\mu(\|\boldsymbol{\varepsilon}(\eta_{\boldsymbol{u}}^n)\|^2_{0,\Omega}-\|\boldsymbol{\varepsilon}(\eta_{\boldsymbol{u}}^0)\|^2_{0,\Omega})+\kappa_1\eta^{-1}\Delta t\sum_{j=1}^n\|\nabla\eta_p^n\|^2_{0,\Omega}\\&+\frac{1}{2}\sum_{K\in\mathcal{T}_h}\Bigg(\lambda^{-1}\left(\|\alpha\Pi_K^0\eta_p^n-\eta_\psi^n\|^2_{0,K}-\|\alpha\Pi_K^0\eta_p^0-\eta_\psi^0\|^2_{0,K}\right)+c_0(\|\Pi_K^0\eta_p^n\|^2_{0,K}-\|\Pi_K^0\eta_p^0\|^2_{0,K})\\&\qquad+\left(c_0+\alpha^2\lambda^{-1}\right)\left(\|(I-\Pi_K^0)\eta_p^n\|^2_{0,K}-\|(I-\Pi_K^0)\eta_p^0\|^2_{0,K}\right)\Bigg)\\&\leq C(h^2+\Delta t^2)+2\epsilon_3\Delta t\sum_{j=1}^n\|\eta_\psi^j\|^2_{0,\Omega}+C\sum_{j=1}^n\sum_{i=1}^2\|\eta_{w_i}^{j-1}\|^2_{0,\Omega}\\&\quad+2\epsilon_1\|\boldsymbol{\varepsilon}(\eta_{\boldsymbol{u}}^n)\|^2_{0,\Omega}+5\epsilon_2\Delta t\sum_{j=1}^n\|\nabla\eta_p^j\|^2_{0,\Omega}.\end{aligned}$$

Using inf-sup condition of $b_1(\cdot,\cdot)$ and error equation (5.4.4a), we obtain

$$\begin{aligned}\|\eta_\psi^n\|_{0,\Omega}&\leq\sup_{\boldsymbol{v}_h^s\in\mathbf{V}_h\setminus\{0\}}\frac{C}{\|\boldsymbol{v}_h^s\|_{1,\Omega}}\left(F^n_{\boldsymbol{b},r}(w_1^n,w_2^n;\boldsymbol{v}_h^s)-F^{h,n}_{\boldsymbol{b},r}(w_{1,h}^{n-1},w_{2,h}^{n-1};\boldsymbol{v}_h^s)-a_1^h(\eta_{\boldsymbol{u}}^n,\boldsymbol{v}_h^s)\right)\\&\leq C\Big(h\big(|\boldsymbol{b}^n|_{1,\Omega}+\sum_{i=1}^2|w_i^{n-1}|_{1,\Omega}\big)+(\Delta t)\sum_{i=1}^2\left(\|\partial_t w_i^n\|_{0,\Omega}+\|\partial_{tt}w_i(s)\|_{L^1(t_{n-1},t_n;L^2(\Omega))}\right)\end{aligned}$$

$$+\sum_{i=1}^{2}\|\eta_{w_i}^{n-1}\|_{0,\Omega}+\mu\|\boldsymbol{\varepsilon}(\eta_{\boldsymbol{u}}^{n})\|_{0,\Omega}\Big).$$

Therefore, the adequate choices of ϵ's and choosing the initial conditions using projections as

$$\boldsymbol{u}_h^{s,0}:=\boldsymbol{u}_I^s(0) \text{ and } \ p_h^{f,0}:=p_I^f(0)$$

conclude the error bounds (5.4.8). $\square$

Note that the initial conditions are chosen so that the estimates of $\eta_{\boldsymbol{u}}^n, \eta_p^n$ and η_ψ^n are known, and can consider another such choice for analysis and computations.

Next, we approach the remaining error equations corresponding to ADR equations to avail the following lemma.

Lemma 5.6 (Coupled ADR error bounds)**.** *Let* $(w_1^n, w_2^n)\in[W]^2$ *be the solution to the continuous problem* (5.2.1d)-(5.2.1e) *and* $(w_{1,h}^n, w_{2,h}^n)\in[W_h]^2$ *be the solution of the fully discrete problem* (5.3.6) *for each* n*. Then the following estimate holds, with constant* C *independent of* h *and* Δt*,*

$$\begin{aligned}
&\sum_{i=1}^{2}\Big(\|\eta_{w_i}^{n}\|_{0,\Omega}^2+D_1^a(\Delta t)\sum_{j=1}^{n}|\eta_{w_i}^{j}|_{1,\Omega}^2\Big)\\
&\leq \Delta t^2\sum_{j=1}^{n}(2\epsilon_1\|\boldsymbol{\varepsilon}(\eta_{\boldsymbol{u}}^{j})\|_{0,\Omega}^2+6\epsilon_4|\eta_{w_1}^{j}|_{1,\Omega}^2)\\
&\qquad +C\Big(h^2+\Delta t^2+\sum_{j=1}^{n}(\|\eta_{\boldsymbol{u}}^{j-1}\|_{0,\Omega}^2+\sum_{i=1}^{2}\|\eta_{w_i}^{j-1}\|_{0,\Omega}^2)\Big).
\end{aligned}\tag{5.4.9}$$

Proof. Taking $s_h=\eta_{w_1}^n$ in (5.4.4d), then multiplying with Δt and summing over n enable us to get

$$\begin{aligned}
&(\|\eta_{w_1}^{n}\|_{0,\Omega}^2-\|\eta_{w_1}^{0}\|_{0,\Omega}^2)+D_1^a\Delta t\sum_{j=1}^{n}\|\nabla\eta_{w_1}^{j}\|_{0,\Omega}^2\\
&\leq C\Delta t\sum_{j=1}^{n}\Big(\big(J_f^j(w_1^j,w_2^j,\boldsymbol{u}^{s,j};\eta_{w_1}^j)-J_f^{h,j}(w_{1,h}^{j-1},w_{2,h}^{j-1},\boldsymbol{u}_h^{s,j};\eta_{w_1}^j)\big)\\
&\qquad\qquad -\big(m(\partial_t w_1^j,\eta_{w_1}^j)-m^h(\delta_t S_h^{w_1}w_1^j,\eta_{w_1}^j)\big)\\
&\qquad\qquad -\big(c(\boldsymbol{u}^{s,j};w_1^j,\eta_{w_1}^j)-c^h(\boldsymbol{u}_h^{s,j};w_{1,h}^j,\eta_{w_1}^j)\big)\Big),\\
&:=A_1+A_2+A_3.
\end{aligned}$$

Use of estimates for projection Π_K^0, use of (5.4.3) and (5.4.6), and Young's inequality with $\epsilon_1\epsilon_4 = C^2/4$ with $\epsilon_1, \epsilon_4 > 0$ gives

$$\begin{aligned}
A_1 \le C\Delta t \sum_{j=1}^{n} \sum_{K\in\mathcal{T}_h} \Big(&\big\| f_h(w_{1,h}^{j-1}, w_{2,h}^{j-1}, \boldsymbol{u}^{s,j}) - f_h(w_{1,h}^{j-1}, w_{2,h}^{j-1}, \boldsymbol{u}_h^{s,j}) \big\|_{0,K} \\
&+ \big\| f_h(w_1^{j-1}, w_2^{j-1}, \boldsymbol{u}^{s,j}) - f_h(w_{1,h}^{j-1}, w_{2,h}^{j-1}, \boldsymbol{u}^{s,j}) \big\|_{0,K} \\
&+ \big\| \Pi_K^0 f(w_1^{j-1}, w_2^{j-1}, \boldsymbol{u}^{s,j}) - f_h(w_1^{j-1}, w_2^{j-1}, \boldsymbol{u}^{s,j}) \big\|_{0,K} \\
&+ \big\| (I - \Pi_K^0) f(w_1^{j-1}, w_2^{j-1}, \boldsymbol{u}^{s,j}) \big\|_{0,K} \Big) \big\| \eta_{w_1}^j \big\|_{0,K} \\
\le C\Delta t \sum_{j=1}^{n} \Big(&\|\rho_{\boldsymbol{u}}^j\|_{0,\Omega} + \|\eta_{\boldsymbol{u}}^j\|_{0,\Omega} + h|f(w_1^{j-1}, w_2^{j-1}, \boldsymbol{u}^{s,j})|_{1,\Omega} \\
&+ \sum_{i=1}^{2} \big(\|\rho_{w_i}^{j-1}\|_{0,\Omega} + \|\eta_{w_i}^{j-1}\|_{0,\Omega} + \|w_i^j - w_i^{j-1}\|_{0,\Omega} \big) \Big) \big\| \eta_{w_1}^j \big\|_{0,\Omega} \\
\le C \sum_{j=1}^{n} \sum_{i=1}^{2} &\|\eta_{w_i}^{j-1}\|_{0,\Omega}^2 + \epsilon_1 \ \Delta t \|\eta_{\boldsymbol{u}}^j\|_{0,\Omega}^2 + \epsilon_4 \ \Delta t \sum_{j=1}^{n} \big\| \eta_{w_1}^j \big\|_{0,\Omega}^2 \\
+ C \sum_{j=1}^{n} \Big(&h^2 \Big(|\boldsymbol{u}^{s,j}|_{2,\Omega}^2 + |f(w_1^{j-1}, w_2^{j-1}, \boldsymbol{u}^{s,j})|_{1,\Omega}^2 + \sum_{i=1}^{2} |w_i^{j-1}|_{2,\Omega}^2 \Big) \\
&+ (\Delta t)^2 \sum_{i=1}^{2} \Big(\|\partial_t w_i^j\|_{0,\Omega} + \int_{t_{j-1}}^{t_j} \|\partial_{tt} w_i(s)\|_{0,\Omega} \,\mathrm{d}s \Big)^2 \Big).
\end{aligned}$$

The use of consistency for bilinear form $m^h(\cdot,\cdot)$ and bounds (5.4.6)-(5.4.7) with Young's inequality for $\epsilon_4 > 0$ gives

$$\begin{aligned}
A_2 &= C\Delta t \sum_{j=1}^{n} \sum_{K\in\mathcal{T}_h} \big(m^K(\partial_t w_1^j - \delta_t \Pi_K^0 w_1^j, \eta_{w_1}^j) - m^{h,K}(\delta_t(S_h^{w_1} w_1^j - \Pi_K^0 w_1^j), \eta_{w_1}^j) \big) \\
&\le C\Delta t \sum_{j=1}^{n} \sum_{K\in\mathcal{T}_h} \Big(\|\partial_t w_1^j - \delta_t \Pi_K^0 w_1^j\|_{0,K} + \|\delta_t (w_1^j - S_h^{w_1} w_1^j)\|_{0,K} \Big) \|\eta_{w_1}^j\|_{0,K} \\
&\le \epsilon_4 \Delta t \sum_{j=1}^{n} \|\nabla \eta_{w_1}^j\|_{0,\Omega}^2 + C\Big(h^2 \int_0^{t_n} |\partial_t w_1(s)|_{1,\Omega}^2 \,\mathrm{d}s + (\Delta t)^2 \int_0^{t_n} \|\partial_{tt} w_1(s)\|_{0,\Omega}^2 \,\mathrm{d}s \Big).
\end{aligned}$$

Assume that ∇w_1^j and $\boldsymbol{u}_h^{s,j}$ are bounded for each j then the values of $\|\nabla w_1^j\|_{\infty,K}$ and $\|\Pi_K^0 \boldsymbol{u}_h^{s,j}\|_{\infty,K}$ (by use of inverse estimate) are finite respectively. Thus, by applying the Cauchy-Schwarz and Young's inequalities implies

$$
\begin{aligned}
A_3 = C\Delta t \sum_{j=1}^{n} \sum_{K\in\mathcal{T}_h} \Big(& \big(\boldsymbol{u}^{s,j}\cdot\nabla w_1^j, (I-\Pi_K^0)\eta_{w_1}^j\big)_{0,K} \\
& + \big((\boldsymbol{u}^{s,j}-\boldsymbol{\Pi}_K^{\mathbf{0}}\boldsymbol{u}_h^{s,j})\cdot\nabla w_1^j, \Pi_K^0\eta_{w_1}^j\big)_{0,K} \\
& + \big(\boldsymbol{\Pi}_K^{\mathbf{0}}\boldsymbol{u}_h^{s,j}\cdot(\nabla w_1^j - \boldsymbol{\Pi}_K^{\mathbf{0},0}\nabla w_{1,h}^j), \Pi_K^0\eta_{w_1}^j\big)_{0,K}\Big) \\
\leq C\Delta t \sum_{j=1}^{n} \sum_{K\in\mathcal{T}_h} \Big(& \|(\mathbf{I}-\boldsymbol{\Pi}_K^{\mathbf{0}})(\boldsymbol{u}^{s,j}\cdot\nabla w_1^j)\|_{0,K} + \|(\mathbf{I}-\boldsymbol{\Pi}_K^{\mathbf{0}})\boldsymbol{u}^{s,j}\|_{0,K}\|\nabla w_1^j\|_{\infty,K} \\
& + \|\boldsymbol{\Pi}_K^{\mathbf{0}}(\boldsymbol{u}^{s,j}-\boldsymbol{u}_h^{s,j})\|_{0,K}\|\nabla w_1^j\|_{\infty,K} \\
& + \|\boldsymbol{\Pi}_K^{\mathbf{0}}\boldsymbol{u}_h^{s,j}\|_{\infty,K}\|\nabla w_1^j - \boldsymbol{\Pi}_K^{\mathbf{0},0}\nabla w_{1,h}^j)\|_{0,K}\Big)\|\eta_{w_1}^j\|_{0,K} \\
\leq C\, h^2 \sum_{j=1}^{n} \Big(& \|(\boldsymbol{u}^{s,j}\cdot\nabla w_1^j)\|_{1,\Omega}^2 + |\boldsymbol{u}^{s,j}|_{1,\Omega}^2 + |\nabla w_1^j|_{1,\Omega}^2\Big) \\
+ \Delta t^2 \sum_{j=1}^{n} & (\epsilon_1\|\eta_{\boldsymbol{u}}^j\|_{0,\Omega}^2 + \epsilon_4|\eta_{w_1}^j|_{1,\Omega}^2).
\end{aligned}
$$

Thus, the bounds of A_i's gives

$$
\begin{aligned}
\|\eta_{w_1}^n\|_{0,\Omega}^2 + \Delta t \sum_{j=1}^{n} \|\nabla\eta_{w_1}^j\|_{0,\Omega}^2 \leq C\Big(& h^2 + \Delta t^2 + \|\eta_{w_1}^0\|_{0,\Omega}^2 + \sum_{j=1}^{n}\sum_{i=1}^{2} \|\eta_{w_i}^{j-1}\|_{0,\Omega}^2\Big) \\
& + \Delta t \sum_{j=1}^{n} (\epsilon_1\|\eta_{\boldsymbol{u}}^j\|_{0,\Omega}^2 + 3\epsilon_4|\eta_{w_1}^j|_{1,\Omega}^2).
\end{aligned}
$$

Similar to the above bounds, taking $s_h = \eta_{w_2}^n$ in (5.4.4e), we get the error bounds in the terms of η_{w_2}. Thus, the addition of the bounds for w_1 and w_2 concludes the proof. $\square$

We proceed to apply the discrete Gronwall's inequality in Lemma 5.3.9 with the combination of results from Lemma 5.5 and 5.6 yield

$$
\|\boldsymbol{\varepsilon}(\eta_{\boldsymbol{u}}^n)\|_{0,\Omega}^2 + \|\eta_\psi^n\|_{0,\Omega}^2 + \|\eta_p\|_{l^2(H^1(\Omega))}^2 + \|\eta_{w_1}\|_{l^2(H^1(\Omega))}^2 + \|\eta_{w_2}\|_{l^2(H^1(\Omega))}^2 \leq C(h^2 + \Delta t^2).
$$

Finally, usage of triangle's inequality with the estimates (5.4.3a)-(5.4.3c) give rise to the final result:

Theorem 5.3 (Fully-discrete error estimates)**.** *Let* $(\boldsymbol{u}^s(t_n), p^f(t_n), \psi(t_n), w_1(t_n), w_2(t_n)) \in \mathbb{V}$ *be the solution to the system* (5.2.1)*, and* $(\boldsymbol{u}_h^{s,n}, p_h^{f,n}, \psi_h^n, w_{1,h}^n, w_{2,h}^n) \in \mathbb{V}_h$ *be the solu-*

tion to the system (5.3.5)-(5.3.6) *for each* $n = 1, \ldots, N$. *Then the following estimate holds, with constant* C *independent of* h *and* Δt,

$$\|\boldsymbol{\varepsilon}(\boldsymbol{u}^s(t_n) - \boldsymbol{u}_h^{s,n})\|_{0,\Omega}^2 + \|\psi(t_n) - \psi_h^n\|_{0,\Omega}^2 + \|p^f - p_h^f\|_{l^2(H^1(\Omega))}^2 + \sum_{i=1}^{2} \|w_i - w_{i,h}\|_{l^2(H^1(\Omega))}^2 \leq C(\Delta t^2 + h^2).$$

Remark 5.2. *The lowest order case is considered throughout the thesis, and the analysis for higher-order approximation can be derived in a similar manner by carefully handling the discrete trilinear form* $c_h(\cdot;\cdot,\cdot)$ *and also considering the stable pair of VE spaces for displacement and total pressure. In addition, the VE spaces corresponding to displacement and pressure variables are required to have the same approximation order, to obtain the optimal error estimates.*

5.5 Numerical investigations

The algorithm for the numerical scheme (5.3.5)-(5.3.6) can be described as: For given initial conditions of displacement and pressure with solution of problem (5.3.6) at previous time step t_{n-1}, we solve the fully discrete poroelastic problem (5.3.5) to get $\boldsymbol{u}_h^{s,n}, p_h^{f,n}, \psi_h^n$ for any $n = 1, \ldots, N$. Now, we further use the solution $\boldsymbol{u}_h^{s,n}$ as well as the initial conditions of concentration variables to look for the solution of the linear system of equations (5.3.6). We repeat the process till the solution of (5.3.5)-(5.3.6) at the final time T is obtained.

We define the L^2 and H^1 errors for the approximation spaces as

$$E_0(v) := \sum_{K \in \mathcal{T}_h} \|v - \Pi_K^0 v_h\|_{0,K} \quad \text{and} \quad E_1(v) := \sum_{K \in \mathcal{T}_h} \|\nabla v - \boldsymbol{\Pi}_K^{\mathbf{0},0} \nabla v_h\|_{0,K},$$

where v can be global displacement $\boldsymbol{u}^s$, fluid pressure p^f, total pressure ψ and concentrations w_1, w_2. The convergence rates of the errors $E_k(v)$ and $E_k'(v)$ with $k = 0, 1$ for the corresponding mesh sizes h and h' respectively, are calculated as

$$r_k(v) = \frac{\log(E_k(v)/E_k'(v))}{\log(h/h')}.$$

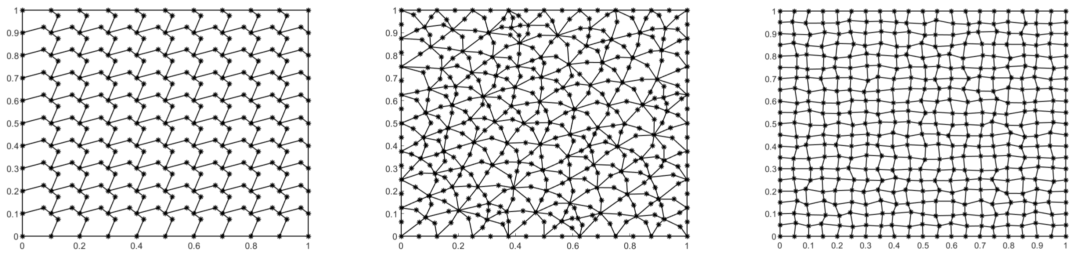

(a) (b) (c)

Figure 5.1: Samples of meshes employed for the numerical tests: (a) Concave mesh $\mathcal{N}_h$, (b) Distorted triangular mesh $\mathcal{H}_h$, and (c) Distorted square mesh $\mathcal{D}_h$.

5.5.1 Space and time convergence

We initiate the tests in the domain $\Omega := (0,1)^2$ and verify the spatial convergence rate of the VEM for given exact solutions by discretizing the domain into elements containing non-convex polygons seen in Figure 5.1(a). For this, we consider the following exact solutions for global displacement and fluid pressure,

$$\boldsymbol{u}^s(x,y,t) = \begin{pmatrix} t\left(-\cos(2\pi x)\sin(2\pi y) + sin(2\pi y) + \sin^2(\pi x)\sin^2(\pi y)\right) \\ t\left(\sin(2\pi x)\cos(2\pi y) - \sin(2\pi x)\right); \end{pmatrix},$$
$$p^f(x,y,t) = t\,\sin^2\pi x \sin^2\pi y,$$

together with the parametric values

$$\nu = 0.3, \quad E = 100, \quad \kappa = 1, \quad \alpha = 1, \quad c_0 = 1, \quad \eta = 0.1,$$

$$\lambda = \frac{\nu\ E}{(1+\nu)(1-2\nu)}, \quad \mu = \frac{E}{2(1+\nu)},$$

and scalar function $r(w_1, w_2) := w_1 + w_2$. Also, the exact concentration solutions are given as

$$w_1(x,y,t) = w_2(x,y,t) = t\ \sin\pi x\ \sin\pi y,$$

and the reaction kinematics with unit value of $D_1, D_2, \beta_1, \beta_2, \beta_3$, and $\gamma = 0.1$ making the concentration equations with different load functions. However, the load functions $\boldsymbol{b}$, ℓ, and the exact global pressure ψ is obtained from the respective equations (5.1.1) in domain Ω with $\tau = 1, \rho = 1$. We show the computed rate of convergence for meshes in Figure 5.1 with $h = \Delta t$ in the Figure 5.2, supporting the theoretical results in Section 5.4.

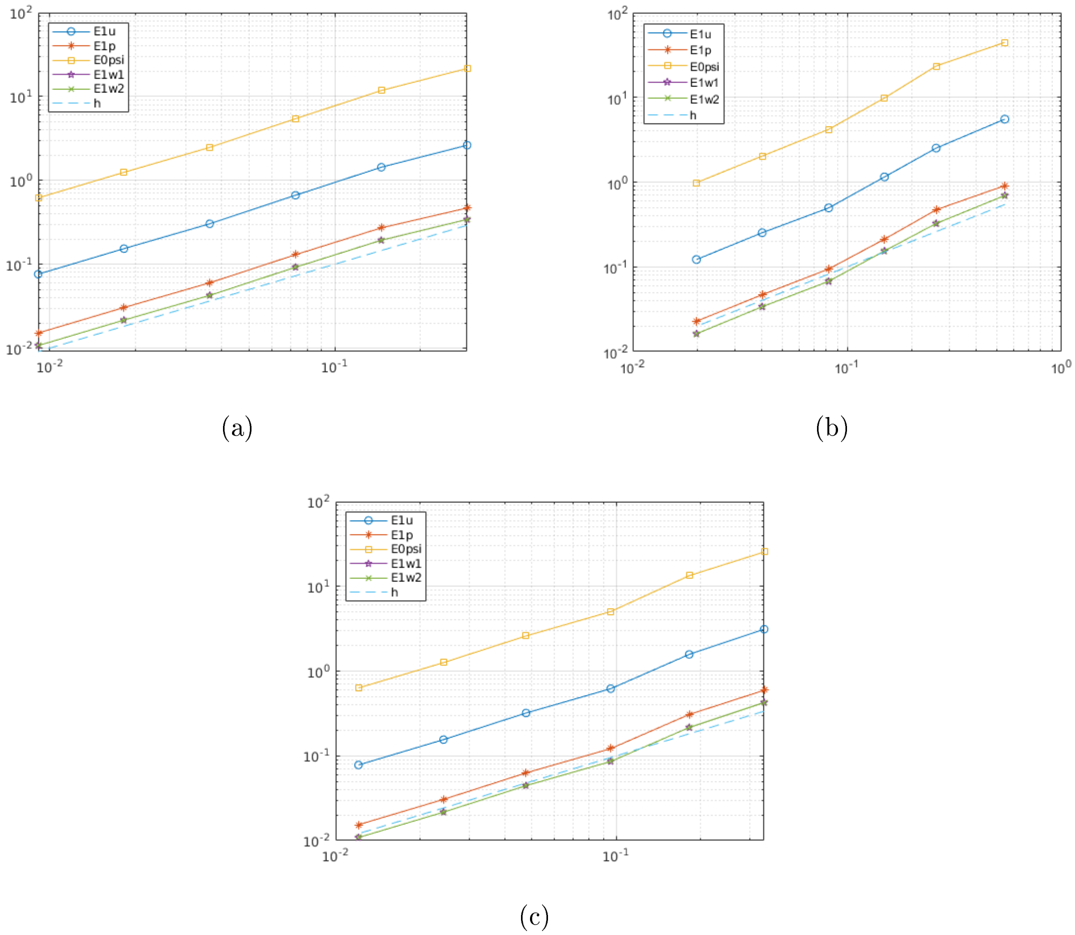

Figure 5.2: Computed errors with varying mesh size h and Δt for three meshes: (a) $\mathcal{N}_h$, (b) $\mathcal{H}_h$, and (c) $\mathcal{D}_h$.

5.5.2 Space convergence with mixed boundary conditions

For this, we consider the following exact solutions for global displacement and fluid pressure in domain Ω,

$$\boldsymbol{u}^s(x,y,t) = \begin{pmatrix} \exp(-t)\sin\pi x\,\sin\pi y \\ \exp(-t)\sin\pi x\,\sin\pi y \end{pmatrix}, \quad p^f(x,y,t) = \exp(-t)\sin\pi x\,(1+\cos\pi y),$$

together with the parametric values

$$\nu = 0.495, \quad E = 100, \quad \kappa = 0.5, \quad \alpha = 0.1, \quad c_0 = 1e-03, \quad \eta = 0.1,$$
$$\lambda = \frac{\nu\, E}{(1+\nu)(1-2\nu)}, \quad \mu = \frac{E}{2(1+\nu)},$$

and scalar function $r(w_1, w_2) := w_1 + w_2$. Also, the exact concentration solutions are given as

$$w_1(x,y,t) = \exp(-t)(-\cos 2\pi x\, \sin 2\pi y + \sin 2\pi y + \sin^2 \pi x\, \sin^2 \pi y),$$
$$w_2(x,y,t) = \exp(-t)(\sin 2\pi x\, \cos 2\pi y - \sin 2\pi x),$$

taking the diffusion constants $D_1 = 0.01$, $D_2 = 1$, and the reaction kinematics with smaller values $\gamma = 0.0001$, $\beta_3 = 0.80$, β_1, $\beta_2 = 0.15$. Taking $\tau = 10, \rho = 1$, the load functions $\boldsymbol{b}, \ell$ and the exact global pressure ψ are obtained from the respective problem (5.1.1) in domain Ω. We can note that we have considered the parametric values to check the extend of method with small c_0 and D_1 as well as large values of λ.

We display the computed rate of convergence in the Table 5.1 with $\Delta t = 0.005$ and varying mesh sizes h on a distorted triangular meshes (shown in figure 5.1(b)).

h^{-1}	$E_1(\boldsymbol{u})$	$r_1(\boldsymbol{u})$	$E_1(p)$	$r_1(p)$	$E_0(\psi)$	$r_0(\psi)$	$E_1(w_1)$	$r_1(w_1)$	$E_1(w_2)$	$r_1(w_2)$
10	9.5977	–	0.7165	–	$1.722e03$	–	3.20087	–	2.4415	–
20	6.363	0.60	0.3882	0.88	$0.986e03$	0.81	1.71905	0.90	1.4639	0.74
40	3.3798	0.91	0.1816	1.10	$0.494e03$	1.00	0.75061	1.20	0.71354	1.04
80	1.7046	0.99	0.0903	1.01	$0.243e03$	1.02	0.36788	1.03	0.3543	1.01
160	0.8712	0.97	0.04501	1.00	$0.123e03$	0.99	0.18661	0.98	0.17916	0.98
320	0.4327	1.01	0.02245	1.00	$0.061e03$	1.02	0.09323	1.00	0.08955	1.00

Table 5.1: Computed errors and its rate of convergence with mesh size h

The computed error in the total pressure is seeming high due to the high value of the exact solution, and the computed convergence rate shows the decrease in error.

Chapter 6

Conclusions

In this dissertation, we have proposed new VEMs for the approximation of non-stationary incompressible fluid flow problems, linear poroelasticity equations, and coupled poroelasticity advection-diffusion-reaction equations. We have contributed to introducing new VE spaces suitable for this type of problem, and we have developed the well-posedness analysis of the associated discrete formulations. Moreover, we have established optimal error estimates in natural norms for all the unknown variables that appeared in the formulations. We emphasize that the classical lowest order VE space from, e.g. [29] does not compute the L^2 projection onto piecewise linear polynomials, which is necessary for defining the discrete bilinear form corresponding to reaction terms. Therefore, we have modified the spaces accordingly. The VE spaces proposed here contribute to the satisfaction of the inf-sup condition, and therefore, the resulting schemes for poroelasticity are locking-free [97]. Apart from the theoretical aspects, we have addressed computational aspects of the proposed family of discretizations for each of the problems under investigation. We have generated numerical implementations targeting the experimental validation of the theoretical convergence rates, and we have also tested the proposed methods in problems of more applicative character.

In what follows we summarize the main findings obtained in each chapter of the thesis in Section 6.1 and the general conclusions based on these findings in Section 6.2. Furthermore, we present the possible extensions of this thesis in Section 6.3.

6.1 Summary

Chapter 1 dealt with the review and applications of fluid flow problems governed by a class of time-dependent PDEs and an extensive literature survey of VEMs with their advancement during the last decade. This chapter also highlighted the related work and specific contribution of the thesis as far as VE approximations of non-stationary fluid flow problems are concerned. Moreover, we addressed the suitability and advantages of the proposed method in comparison with other existing numerical schemes, such as finite element methods, finite volume methods, and discontinuous Galerkin methods in the context of fluid flow problems.

In Chapter 2, we have proposed a VEM for approximating the transient Stokes problem defined over polygonal domains. The semi-discrete formulation is based on the lowest order VE spaces associated with pressure and velocity, and they have been constructed in such a fashion that they satisfy the inf-sup condition and are also locally divergence-free. We stress that considering the regularity (in the context of non-stationary Stokes equations), the choice of stable higher-order VEMs ($k \geq 2$) given in [30, 36] may not be appropriate, since in that case, one would require the higher regularity assumptions on the continuous solutions which may not be realistic (see [68]). The fully discrete scheme obtained by employing the backward Euler method is also discussed and analyzed. With the help of L^2 and Stokes projection operator, we established the optimal error estimates under minimum regularity assumptions on the continuous solutions. Numerical experiments are also conducted to support the theoretical findings.

In Chapter 3, we have extended the analysis of Chapter 2 to nonstationary Navier-Stokes equation. Establishment of optimal *a priori* error estimates and the well-posedness for both semi and fully discrete schemes can be considered as novelty and major contributions of this work. Newton's method has been exploited to solve the resulting nonlinear system of equations, and several numerical tests have been performed to validate the theoretical rate of convergence.

In Chapter 4, we have proposed a new VEM for Biot's equation of linear poroelasticity. The finite-dimensional formulation is based on the VE spaces introduced in [29], which can be regarded as low-order and stable VEs, hence being computationally competitive compared to other existing stable pairs for incompressible flow problems. Both semi and fully discrete formulations are discussed and analyzed, and they constitute the first fully VEM discretization for poroelasticity problems. Optimal and Lamé-robust error estimates have been established for solid displacement, fluid pressure, and total pressure, in natural norms without weights. This has been achieved with the help of appropriate poroelastic projection operators. Numerical experiments have been performed using different polygonal meshes, and they not only put evidence to computational verification for convergence of scheme (where rates of error decay in space and time are in excellent agreement with the theoretically derived error bounds) but also its performance in simple poromechanical tests.

By extending the analysis of [39, 83], we have discussed and analyzed the lowest order conforming VEMs for the approximation of coupled poroelasticity and ADR equations in Chapter 5. The major contributions of this chapter are: well-posedness of fully discrete schemes and establishing the optimal *a priori* error estimates for all the variables that naturally appeared in the weak formulation. A set of numerical experiments have been also provided for justifying convergence analysis of the proposed scheme. The possible extensions of this work include the study of general flow-transport problems and the coupling with other phenomena such as diffusion of solutes in multilayer poromechanics or multiple-network consolidation models [96].

6.2 Concluding remarks

We would like to make the following remarks/comments on theoretical and computational aspects of VE approximations applied to the problems listed in Chapters 2–5.

- Considering computational advantages, in this thesis, we have constructed the lowest order, i.e., $k = 1$ virtual spaces, such that they satisfy the required LBB condition and the discrete velocities are locally divergence-free for Stokes and Navier-Stokes equations, which are essential in view of the physical nature of the problems. Nonetheless, the present analysis can easily be extended to higher-order spaces that satisfy the LBB condition. We emphasize that the other lowest order spaces that contain $\mathbb{P}_1 - \mathbb{P}_1$ type elements can also be employed for the approximation of these problems. Of course, as these pairs are not inf-sup stable, suitable stabilization is required. Depending on the type of stabilization, some drawbacks could include issues related to small-time steps producing unstable solutions, but including consistently stabilized methods (see [82] for transient Stokes and Navier-Stokes equations) should suffice.

- For the VE schemes proposed to approximate poroelastic and coupled poroelastic-ADR equations, we have derived error estimates only in energy norms for displacement by utilizing the properties of L^2-projection onto the piecewise constant functions. We can also establish optimal L^2- error estimates for displacement by taking the L^2-projection onto the piecewise linear functions, choosing appropriate approximation of the right-hand side, and exploiting the idea of enhanced spaces introduced in [83]. However, in that case, a more sophisticated analysis has to be carried out to accomplish this purpose, as standard duality arguments cannot be readily used due to the fact that we have an overall unsymmetric discrete formulation.

- For the time-dependent incompressible fluid flow problem, we mention that there has been a series of studies regarding the unrealistic regularity assumptions near initial time $t \to 0$ (for more details, we refer to, e.g., [68, 75]). The analysis in these works cannot be extended from the parabolic problem to unsteady Stokes equations in a usual way since we do not have the required regularity requirements of the solution. And imposing such conditions would lead to unrealistic compatibility conditions. In view of these regularity constraints, we have proposed divergence-free lowest order stable VE schemes and have established optimal error estimates in natural norms. We stress that this analysis can be extended to higher-order provided the continuous solution has enough regularity.

- For the poroelasticity problem, we derive stability for semi-discrete and fully-discrete schemes and establish the optimal convergence of the VE scheme in the natural norms. These bounds turn to be robust with respect to the dilation modulus of the deformable porous structure (which tends to infinity as the Poisson ratio approaches 0.5) and of the specific storage coefficient (reaching very small values in some regimes), and therefore the method is considered as locking-free. A further advantage of the proposed virtual discretization is that it combines primal and mixed VE spaces. We would like to mention that the present analysis can be extended for general k and variable parametric data, which may be the case while dealing with more realistic problems such as interface problems, by following the analysis of [25, 32, 120].

- The fully discrete scheme proposed for approximating the coupled ADR-poroelastic problem is a decoupled linear explicit scheme at each time level, and therefore, it is relatively cheap. We could have opted for other implicit schemes such as those proposed in [109, 127, 105]. However, the fully discrete formulation of these schemes will turn out to be a system of coupled nonlinear equations. In that case, the fixed-point theory along with Gronwall's inequality can be utilized to show the well-posedness of the resultant system. We stress that the convergence analysis will be more involved in this case, and a modification of the techniques is required for deriving optimal convergence rates.

6.3 Future work

Possible extensions emanating from this thesis are manifold. In particular, we aim at applying and generalizing the VE approximation developed so far, in the solution of a wider class of coupled transport fluid flow problems. A unified VE analysis would help in the study of such problems. From these milestone problems, we mention the following two concrete examples to be studied in forthcoming contributions.

6.3.1 Coupled sedimentation-consolidation.

Consider an incompressible mixture of fluid and solid particles flowing through a porous medium occupying the domain $\Omega \subset \mathbb{R}^d$, $d = 2$ or $d = 3$ in [128, 129]. We assume that the suspended solid particles do not attach to the porous skeleton. Then the motion of the mixture and the evolution of the solids concentration within it can be described by the initial-boundary value problem (here confined, for the sake of simplicity of the presentation, to the so-called batch case, where fluid velocity is simply zero everywhere on the boundary): we seek the volume-averaged flow velocity of the mixture $\boldsymbol{u}$, the solids concentration c, and the pressure field p such that

$$
\begin{aligned}
\phi\,\partial_t c + \boldsymbol{u}\cdot\nabla c - \operatorname{div}(\vartheta(c)\nabla c - f_{\boldsymbol{b}}(c)\boldsymbol{k}) &= 0 \qquad \text{in } \Omega\times(0,T],\\
\partial_t \boldsymbol{u} + (\nabla\boldsymbol{u})\boldsymbol{u} - \mathbf{div}\big(\mu(c)\boldsymbol{\varepsilon}(\boldsymbol{u}) - p\mathbf{I}\big) - \rho_{\mathrm{s}} c\boldsymbol{g} &= \mathbf{0} \qquad \text{in } \Omega\times(0,T],\\
\operatorname{div}\boldsymbol{u} &= s \qquad \text{in } \Omega\times(0,T],
\end{aligned}
$$

with given initial and boundary conditions, where $\mu = \mu(c)$ is the concentration-dependent viscosity, ϕ is the porosity of the underlying porous structure, $\mu(c)\boldsymbol{\varepsilon}(\boldsymbol{u}) - p\boldsymbol{I}$ is the Cauchy stress tensor, $\boldsymbol{\varepsilon}(\boldsymbol{u}) = \frac{1}{2}(\nabla\boldsymbol{u} + \nabla\boldsymbol{u}^{\mathrm{T}})$ is the infinitesimal rate of strain, and $\boldsymbol{g}$ is the gravity acceleration. The material specific diffusion function $\vartheta = \vartheta(c)$ and the flux density vector $f_{\mathrm{b}}(c)\boldsymbol{k}$ describes the effect of hindered settling aligned with gravity, and where $\boldsymbol{k}$ is the upwards-pointing unit vector and f_{b} denotes the

Kynch batch flux density function.

For this problem, we would like to analyze higher-order VE approximation by following the ideas given in [83, 39, 32] with emphasis on both implementation and convergence analysis. We also show the well-posedness of the discrete formulation and establish optimal error estimates under suitable assumptions on the mesh.

6.3.2 Coupled poroelasticity and elasticity problem

Let us consider a bounded Lipschitz domain $\Omega \subset \mathbb{R}^d$, $d \in \{2, 3\}$, together with a partition into non-overlapping and connected subdomains Ω^E, Ω^P representing zones of non-pay rock (where we will set the equations of linear elasticity) and a reservoir (where we aim at solving the poroelasticity equations), respectively [120, 106]. We also assume that the reservoir is completely immersed in the overall domain: $\overline{\Omega^P} \subset \Omega$, such that the interface between the two subdomains, denoted as $\Sigma = \partial\Omega^P \cap \partial\Omega^E$, coincides with the boundary of the pay zone. Note that on the interface we consider that the normal unit vector $\boldsymbol{n}$ is pointing from Ω^P to Ω^E. The boundary of the domain Ω is separated in terms of the boundaries of two individual subdomains, that is $\partial\Omega := \Gamma^{\mathrm{P}} \cup \Gamma^{\mathrm{E}}$, and then subdivided as the disjoint Dirichlet and Neumann type condition as $\Gamma^{\mathrm{P}} := \Gamma^{\mathrm{P}}_D \cup \Gamma^{\mathrm{P}}_N$ and $\Gamma^{\mathrm{E}} := \Gamma^{\mathrm{E}}_D \cup \Gamma^{\mathrm{E}}_N$ respectively.

In the overall domain, our problem stated as: for given body loads $\boldsymbol{b}^{\mathrm{P}}(t) : \Omega^P \to \mathbb{R}^d$, $\boldsymbol{b}^{\mathrm{E}} : \Omega^E \to \mathbb{R}^d$, and a volumetric source or sink $\ell^{\mathrm{P}}(t) : \Omega^P \to \mathbb{R}$, one seeks for each time $t \in (0, T]$, the vector of solid displacements $\boldsymbol{u}^{\mathrm{E}} : \Omega^E \to \mathbb{R}^d$ of the non-pay zone, the elastic pressure $\psi^{\mathrm{E}} : \Omega^E \to \mathbb{R}$, the displacement $\boldsymbol{u}^{\mathrm{P}}(t) : \Omega^P \to \mathbb{R}^d$, the pore fluid pressure $p^{\mathrm{P}}(t) : \Omega^P \to \mathbb{R}$, and the total pressure $\psi^{\mathrm{P}}(t) : \Omega^P \to \mathbb{R}$ of the reservoir, satisfying:

$$
\begin{aligned}
-\mathbf{div}(2\mu^{\mathrm{P}}\boldsymbol{\varepsilon}(\boldsymbol{u}^{\mathrm{P}}) - \psi^{\mathrm{P}}\mathbf{I}) &= \boldsymbol{b}^{\mathrm{P}} && \text{in } \Omega^P \times (0, T], \\
\left(c_0 + \frac{\alpha^2}{\lambda^{\mathrm{P}}}\right)\partial_t p^{\mathrm{P}} - \frac{\alpha}{\lambda^{\mathrm{P}}}\partial_t\psi^{\mathrm{P}} - \frac{1}{\eta}\operatorname{div}(\kappa\nabla p^{\mathrm{P}}) &= \ell^{\mathrm{P}} && \text{in } \Omega^P \times (0, T], \\
\psi^{\mathrm{P}} - \alpha p^{\mathrm{P}} + \lambda^{\mathrm{P}} \operatorname{div} \boldsymbol{u}^{\mathrm{P}} &= 0 && \text{in } \Omega^P \times (0, T], \\
-\mathbf{div}(2\mu^{\mathrm{E}}\boldsymbol{\varepsilon}(\boldsymbol{u}^{\mathrm{E}}) - \psi^{\mathrm{E}}\mathbf{I}) &= \boldsymbol{b}^{\mathrm{E}} && \text{in } \Omega^E \times (0, T], \\
\psi^{\mathrm{E}} + \lambda^{\mathrm{E}} \operatorname{div} \boldsymbol{u}^{\mathrm{E}} &= 0 && \text{in } \Omega^E \times (0, T].
\end{aligned}
$$

Here $\kappa(\boldsymbol{x})$ is the hydraulic conductivity of the porous medium η is the constant viscosity of the interstitial fluid, c_0 is the storativity coefficient, α is the Biot-Willis consolidation parameter, and $\mu^{\mathrm{E}}, \lambda^{\mathrm{E}}$ and $\mu^{\mathrm{P}}, \lambda^{\mathrm{P}}$ are the Lamé parameters associated with the constitutive law of the solid on the elastic and on the poroelastic subdomain, respectively. The poroelastic stress $\widetilde{\boldsymbol{\sigma}} = \boldsymbol{\sigma} - \alpha p^{\mathrm{P}}\mathbf{I}$ is composed by the effective mechanical stress $\lambda^{\mathrm{P}}(\operatorname{div} \boldsymbol{u}^{\mathrm{P}})\mathbf{I} + 2\mu^{\mathrm{P}}\boldsymbol{\varepsilon}(\boldsymbol{u}^{\mathrm{P}})$ plus the non-viscous fluid stress (the fluid pressure scaled with α).

This system must be complemented by mixed boundary conditions, a set of transmission conditions, representing the continuity of the medium, the balance of total tractions, and no-flux of fluid at the interface, respectively; and initial conditions $p^{\mathrm{P}}(0)$ and $\boldsymbol{u}^{\mathrm{P}}(0)$ in $\Omega^{\mathrm{P}} \times \{0\}$.

As far as VE approximations are concerned, here, we would like to employ the virtual spaces introduced in [39] by admitting the polynomial of degree $k \geq 1$. We plan to propose the mixed discrete formulation in a way that the corresponding VE scheme does not require Lagrange multipliers to impose the transmission conditions (continuity of displacement and total traction, and no-flux for the fluid) on the interface. In the implementation procedure, arbitrary small edges will be allowed in the process of mesh generation, and theoretical convergence analysis will be carried out by borrowing the ideas from [54] in which small edges are considered for the approximation of elliptic problems.

Bibliography

[1] G. P. Galdi, *An introduction to the mathematical theory of the Navier-Stokes equations*, 2nd ed., ser. Springer Monographs in Mathematics. Springer, New York, 2011, steady-state problems. [Online]. Available: https://doi.org/10.1007/978-0-387-09620-9

[2] O. A. Ladyzhenskaya, *The mathematical theory of viscous incompressible flow*, ser. Mathematics and its Applications, Vol. 2, revised and enlarged, Translated from the Russian by Richard A. Silverman and John Chu. Gordon and Breach, Science Publishers, New York-London-Paris, 1969.

[3] A. N. Gorban and I. V. Karlin, "Beyond navier–stokes equations: capillarity of ideal gas," *Contemporary Physics*, vol. 58, no. 1, pp. 70–90, 2017. [Online]. Available: https://doi.org/10.1080/00107514.2016.1256123

[4] J.-F. Gerbeau and C. Le Bris, "A coupled system arising in magnetohydrodynamics," *Appl. Math. Lett.*, vol. 12, no. 3, pp. 53–57, 1999. [Online]. Available: https://doi.org/10.1016/S0893-9659(98)00172-4

[5] V. Gitis, G. Rothenberg, V. Gitis, G. Rothenberg, A. A. Kiss, and D. Eisenberg, *Handbook of Porous Materials*. WORLD SCIENTIFIC, 2021. [Online]. Available: https://www.worldscientific.com/doi/abs/10.1142/11909

[6] K. Terzaghi, *Theoretical Soil Mechanics*. John Wiley and Sons, 1943. [Online]. Available: https://doi.org/10.1002/9780470172766

[7] B. M. Das, *Principles of Geotechnical Engineering, 7th Edition*. Boston, MA : Cengage Learning, 1997.

[8] M. A. Biot, "General theory of three-dimensional consolidation," *J. Appl. Phys.*, vol. 12, 1941. [Online]. Available: https://doi.org/10.1063/1.1712886

[9] Y. Fung, *Biomechanics, Mechanical Properties of Living Tissues*, 2nd ed. Springer-Verlag, 1993.

[10] A. Ehret, K. Bircher, A. Stracuzzi, V. Marina, M. Zündel, and E. Mazza, "Inverse poroelasticity as a fundamental mechanism in biomechanics and mechanobiology," *Nat Commun.*, vol. 8, no. 1, 2017. [Online]. Available: https://doi.org/10.1038/s41467-017-00801-3

[11] A. A. Neville, P. C. Matthews, and H. M. Byrne, "Interactions between pattern formation and domain growth," *Bull. Math. Biol.*, vol. 68, no. 8, pp. 1975–2003, 2006. [Online]. Available: https://doi.org/10.1007/s11538-006-9060-5

[12] L. Miguel De Oliveira Vilaca, B. Gómez-Vargas, S. Kumar, R. Ruiz-Baier, and N. Verma, "Stability analysis for a new model of multi-species convection-diffusion-reaction in poroelastic tissue," *Appl. Math. Model.*, vol. 84, pp. 425–446, 2020. [Online]. Available: https://doi.org/10.1016/j.apm.2020.04.014

[13] C. Talischi, G. H. Paulino, A. Pereira, and I. F. M. Menezes, "`PolyMesher`: a general-purpose mesh generator for polygonal elements written in Matlab," *Struct. Multidiscip. Optim.*, vol. 45, no. 3, pp. 309–328, 2012. [Online]. Available: https://doi.org/10.1007/s00158-011-0706-z

[14] E. L. Wachspress, *A rational finite element basis*, ser. Mathematics in Science and Engineering, Vol. 114. Academic Press, Inc. [Harcourt Brace Jovanovich, Publishers], New York-London, 1975.

[15] N. Sukumar and A. Tabarraei, "Conforming polygonal finite elements," *Internat. J. Numer. Methods Engrg.*, vol. 61, no. 12, pp. 2045–2066, 2004. [Online]. Available: https://doi.org/10.1002/nme.1141

[16] M. Berndt, K. Lipnikov, D. Moulton, and M. Shashkov, "Convergence of mimetic finite difference discretizations of the diffusion equation," *East-West J. Numer. Math.*, vol. 9, no. 4, pp. 265–284, 2001.

[17] J. Droniou, R. Eymard, T. Gallouët, C. Guichard, and R. Herbin, "An error estimate for the approximation of linear parabolic equations by the gradient discretization method," in *Finite volumes for complex applications VIII—methods and theoretical aspects*, ser. Springer Proc. Math.

Stat. Springer, Cham, 2017, vol. 199, pp. 371–379. [Online]. Available: https://doi.org/10.1007/978-3-319-57397-7_3

[18] L. Beirão da Veiga, F. Brezzi, A. Cangiani, G. Manzini, L. D. Marini, and A. Russo, "Basic principles of virtual element methods," *Math. Models Methods Appl. Sci.*, vol. 23, no. 1, pp. 199–214, 2013. [Online]. Available: https://doi.org/10.1142/S0218202512500492

[19] J. Wang and X. Ye, "A weak Galerkin finite element method for second-order elliptic problems," *J. Comput. Appl. Math.*, vol. 241, pp. 103–115, 2013. [Online]. Available: https://doi.org/10.1016/j.cam.2012.10.003

[20] D. A. Di Pietro and A. Ern, "A hybrid high-order locking-free method for linear elasticity on general meshes," *Comput. Methods Appl. Mech. Engrg.*, vol. 283, pp. 1–21, 2015. [Online]. Available: https://doi.org/10.1016/j.cma.2014.09.009

[21] L. Beirão da Veiga, F. Brezzi, L. D. Marini, and A. Russo, "The hitchhiker's guide to the virtual element method," *Math. Models Methods Appl. Sci.*, vol. 24, no. 8, pp. 1541–1573, 2014. [Online]. Available: https://doi.org/10.1142/S021820251440003X

[22] L. Beirão da Veiga, K. Lipnikov, and G. Manzini, *The mimetic finite difference method for elliptic problems*, ser. MS&A. Modeling, Simulation and Applications. Springer, Cham, 2014, vol. 11. [Online]. Available: https://doi.org/10.1007/978-3-319-02663-3

[23] S. C. Brenner, Q. Guan, and L.-Y. Sung, "Some estimates for virtual element methods," *Comput. Methods Appl. Math.*, vol. 17, no. 4, pp. 553–574, 2017. [Online]. Available: https://doi.org/10.1515/cmam-2017-0008

[24] B. Ahmad, A. Alsaedi, F. Brezzi, L. D. Marini, and A. Russo, "Equivalent projectors for virtual element methods," *Comput. Math. Appl.*, vol. 66, no. 3, pp. 376–391, 2013. [Online]. Available: https://doi.org/10.1016/j.camwa.2013.05.015

[25] L. Beirão da Veiga, F. Brezzi, L. D. Marini, and A. Russo, "Virtual element method for general second-order elliptic problems on polygonal meshes," *Math. Models Methods Appl. Sci.*, vol. 26, no. 4, pp. 729–750, 2016. [Online]. Available: https://doi.org/10.1142/S0218202516500160

[26] G. Vacca and L. Beirão da Veiga, "Virtual element methods for parabolic problems on polygonal meshes," *Numer. Methods Partial Differential Equations*, vol. 31, no. 6, pp. 2110–2134, 2015. [Online]. Available: https://doi.org/10.1002/num.21982

[27] D. Adak, E. Natarajan, and S. Kumar, "Convergence analysis of virtual element methods for semilinear parabolic problems on polygonal meshes," *Numer. Methods Partial Differential Equations*, vol. 35, no. 1, pp. 222–245, 2019. [Online]. Available: https://doi.org/10.1002/num.22298

[28] ——, "Virtual element method for semilinear hyperbolic problems on polygonal meshes," *Int. J. Comput. Math.*, vol. 96, no. 5, pp. 971–991, 2019. [Online]. Available: https://doi.org/10.1080/00207160.2018.1475651

[29] P. F. Antonietti, L. Beirão da Veiga, D. Mora, and M. Verani, "A stream virtual element formulation of the Stokes problem on polygonal meshes," *SIAM J. Numer. Anal.*, vol. 52, no. 1, pp. 386–404, 2014. [Online]. Available: https://doi.org/10.1137/13091141X

[30] L. Beirão da Veiga, C. Lovadina, and G. Vacca, "Divergence free virtual elements for the Stokes problem on polygonal meshes," *ESAIM Math. Model. Numer. Anal.*, vol. 51, no. 2, pp. 509–535, 2017. [Online]. Available: https://doi.org/10.1051/m2an/2016032

[31] D. Frerichs and C. Merdon, "Divergence-preserving reconstructions on polygons and a really pressure-robust virtual element method for the stokes problem," *IMA J. Numer. Anal.*, 2020. [Online]. Available: https://doi.org/10.1093/imanum/draa073

[32] L. Beirão da Veiga, C. Lovadina, and G. Vacca, "Virtual elements for the Navier-Stokes problem on polygonal meshes," *SIAM J. Numer. Anal.*, vol. 56, no. 3, pp. 1210–1242, 2018. [Online]. Available: https://doi.org/10.1137/17M1132811

[33] X. Liu and Z. Chen, "The nonconforming virtual element method for the Navier-Stokes equations," *Adv. Comput. Math.*, vol. 45, no. 1, pp. 51–74, 2019. [Online]. Available: https://doi.org/10.1007/s10444-018-9602-z

[34] G. N. Gatica, B. Gomez-Vargas, and R. Ruiz-Baier, "Analysis and mixed-primal finite element discretisations for stress-assisted diffusion problems,"

Comput. Methods Appl. Mech. Engrg., vol. 337, pp. 411–438, 2018. [Online]. Available: https://doi.org/10.1016/j.cma.2018.03.043

[35] L. Beirão da Veiga, D. Mora, and G. Vacca, "The Stokes complex for virtual elements with application to Navier-Stokes flows," *J. Sci. Comput.*, vol. 81, no. 2, pp. 990–1018, 2019. [Online]. Available: https://doi.org/10.1007/s10915-019-01049-3

[36] G. Vacca, "An H^1-conforming virtual element for Darcy and Brinkman equations," *Math. Models Methods Appl. Sci.*, vol. 28, no. 1, pp. 159–194, 2018. [Online]. Available: https://doi.org/10.1142/S0218202518500057

[37] J. Coulet, I. Faille, V. Girault, N. Guy, and F. Nataf, "A fully coupled scheme using virtual element method and finite volume for poroelasticity," *Comput. Geosci.*, vol. 24, no. 2, pp. 381–403, 2020. [Online]. Available: https://doi.org/10.1007/s10596-019-09831-w

[38] X. Tang, Z. Liu, B. Zhang, and M. Feng, "A low-order locking-free virtual element for linear elasticity problems," *Comput. Math. Appl.*, vol. 80, no. 5, pp. 1260–1274, 2020. [Online]. Available: https://doi.org/10.1016/j.camwa.2020.04.032

[39] D. M. R. R.-B. Raimund Bürger, Sarvesh Kumar and N. Verma, "Virtual element methods for the three-field formulation of time-dependent linear poroelasticity," *Adv. Comput. Math.*, vol. 47, no. 2, 2021. [Online]. Available: https://doi.org/10.1007/s10444-020-09826-7

[40] G. Vacca, "Virtual element methods for hyperbolic problems on polygonal meshes," *Comput. Math. Appl.*, vol. 74, no. 5, pp. 882–898, 2017. [Online]. Available: https://doi.org/10.1016/j.camwa.2016.04.029

[41] F. Brezzi, R. S. Falk, and L. D. Marini, "Basic principles of mixed virtual element methods," *ESAIM Math. Model. Numer. Anal.*, vol. 48, no. 4, pp. 1227–1240, 2014. [Online]. Available: https://doi.org/10.1051/m2an/2013138

[42] L. Beirão da Veiga, F. Brezzi, L. D. Marini, and A. Russo, "Mixed virtual element methods for general second order elliptic problems on polygonal meshes," *ESAIM Math. Model. Numer. Anal.*, vol. 50, no. 3, pp. 727–747, 2016. [Online]. Available: https://doi.org/10.1051/m2an/2015067

[43] L. Beirão da Veiga, F. Brezzi, and L. D. Marini, “Virtual elements for linear elasticity problems,” *SIAM J. Numer. Anal.*, vol. 51, no. 2, pp. 794–812, 2013. [Online]. Available: https://doi.org/10.1137/120874746

[44] A. Cangiani, G. Manzini, and O. J. Sutton, “Conforming and nonconforming virtual element methods for elliptic problems,” *IMA J. Numer. Anal.*, vol. 37, no. 3, pp. 1317–1354, 2017. [Online]. Available: https://doi.org/10.1093/imanum/drw036

[45] A. Cangiani, P. Chatzipantelidis, G. Diwan, and E. H. Georgoulis, “Virtual element method for quasilinear elliptic problems,” *IMA J. Numer. Anal.*, vol. 40, no. 4, pp. 2450–2472, 2020. [Online]. Available: https://doi.org/10.1093/imanum/drz035

[46] L. Beirão da Veiga, A. Pichler, and G. Vacca, “A virtual element method for the miscible displacement of incompressible fluids in porous media,” *Comput. Methods Appl. Mech. Engrg.*, vol. 375, pp. Paper No. 113 649, 35, 2021. [Online]. Available: https://doi.org/10.1016/j.cma.2020.113649

[47] L. Beirão da Veiga, F. Dassi, and G. Vacca, “The Stokes complex for virtual elements in three dimensions,” *Math. Models Methods Appl. Sci.*, vol. 30, no. 3, pp. 477–512, 2020. [Online]. Available: https://doi.org/10.1142/S0218202520500128

[48] L. Beirão Da Veiga, F. Brezzi, F. Dassi, L. D. Marini, and A. Russo, “Serendipity virtual elements for general elliptic equations in three dimensions,” *Chin. Ann. Math. Ser. B*, vol. 39, no. 2, pp. 315–334, 2018. [Online]. Available: https://doi.org/10.1007/s11401-018-1066-4

[49] L. Beirão da Veiga, F. Brezzi, F. Dassi, L. D. Marini, and A. Russo, “A family of three-dimensional virtual elements with applications to magnetostatics,” *SIAM J. Numer. Anal.*, vol. 56, no. 5, pp. 2940–2962, 2018. [Online]. Available: https://doi.org/10.1137/18M1169886

[50] F. Dassi, C. Lovadina, and M. Visinoni, “A three-dimensional Hellinger-Reissner virtual element method for linear elasticity problems,” *Comput. Methods Appl. Mech. Engrg.*, vol. 364, pp. 112 910, 17, 2020. [Online]. Available: https://doi.org/10.1016/j.cma.2020.112910

[51] X. Liu, R. Li, and Z. Chen, “A virtual element method for the coupled Stokes-Darcy problem with the Beaver-Joseph-Saffman interface condition,” *Calcolo*, vol. 56, no. 4, pp. Paper No. 48, 28, 2019. [Online]. Available: https://doi.org/10.1007/s10092-019-0345-0

[52] F. Aldakheel, B. Hudobivnik, and P. Wriggers, “Virtual elements for finite thermo-plasticity problems,” *Comput. Mech.*, vol. 64, no. 5, pp. 1347–1360, 2019. [Online]. Available: https://doi.org/10.1007/s00466-019-01714-2

[53] L. Beirão da Veiga, C. Lovadina, and A. Russo, “Stability analysis for the virtual element method,” *Math. Models Methods Appl. Sci.*, vol. 27, no. 13, pp. 2557–2594, 2017. [Online]. Available: https://doi.org/10.1142/S021820251750052X

[54] S. C. Brenner and L.-Y. Sung, “Virtual element methods on meshes with small edges or faces,” *Math. Models Methods Appl. Sci.*, vol. 28, no. 7, pp. 1291–1336, 2018. [Online]. Available: https://doi.org/10.1142/S0218202518500355

[55] D. Irisarri and G. Hauke, “Stabilized virtual element methods for the unsteady incompressible Navier-Stokes equations,” *Calcolo*, vol. 56, no. 4, pp. Paper No. 38, 21, 2019. [Online]. Available: https://doi.org/10.1007/s10092-019-0332-5

[56] J. Guo and M. Feng, “A new projection-based stabilized virtual element method for the Stokes problem,” *J. Sci. Comput.*, vol. 85, no. 1, pp. Paper No. 16, 28, 2020. [Online]. Available: https://doi.org/10.1007/s10915-020-01301-1

[57] R. Temam, *Navier-Stokes equations. Theory and numerical analysis.* North-Holland Publishing Co., Amsterdam-New York-Oxford, 1977, studies in Mathematics and its Applications, Vol. 2.

[58] B. Rivière, J. Tan, and T. Thompson, “Error analysis of primal discontinuous Galerkin methods for a mixed formulation of the Biot equations,” *Comput. Math. Appl.*, vol. 73, no. 4, pp. 666–683, 2017. [Online]. Available: https://doi.org/10.1016/j.camwa.2016.12.030

[59] X. Chen, Y. Li, C. Drapaca, and J. Cimbala, “A unified framework of continuous and discontinuous Galerkin methods for solving the incompressible Navier-Stokes equation,” *J. Comput. Phys.*, vol. 422, p. 109799, 2020. [Online]. Available: https://doi.org/10.1016/j.jcp.2020.109799

[60] J. Li, Y. He, and Z. Chen, "A new stabilized finite element method for the transient Navier-Stokes equations," *Comput. Methods Appl. Mech. Engrg.*, vol. 197, no. 1-4, pp. 22–35, 2007. [Online]. Available: https://doi.org/10.1016/j.cma.2007.06.029

[61] S. Kumar and R. Ruiz-Baier, "Equal order discontinuous finite volume element methods for the Stokes problem," *J. Sci. Comput.*, vol. 65, no. 3, pp. 956–978, 2015. [Online]. Available: https://doi.org/10.1007/s10915-015-9993-7

[62] A. Cangiani, V. Gyrya, and G. Manzini, "The nonconforming virtual element method for the Stokes equations," *SIAM J. Numer. Anal.*, vol. 54, no. 6, pp. 3411–3435, 2016. [Online]. Available: https://doi.org/10.1137/15M1049531

[63] F. Brezzi and M. Fortin, *Mixed and hybrid finite element methods*, ser. Springer Series in Computational Mathematics. Springer-Verlag, New York, 1991, vol. 15. [Online]. Available: https://doi.org/10.1007/978-1-4612-3172-1

[64] L. Mu and X. Ye, "A finite volume method for solving Navier-Stokes problems," *Nonlinear Anal.*, vol. 74, no. 17, pp. 6686–6695, 2011. [Online]. Available: https://doi.org/10.1016/j.na.2011.06.048

[65] S. Kumar, R. Oyarzúa, R. Ruiz-Baier, and R. Sandilya, "Conservative discontinuous finite volume and mixed schemes for a new four-field formulation in poroelasticity," *ESAIM Math. Model. Numer. Anal.*, vol. 54, no. 1, pp. 273–299, 2020. [Online]. Available: https://doi.org/10.1051/m2an/2019063

[66] N. Ahmed, A. Linke, and C. Merdon, "On really locking-free mixed finite element methods for the transient incompressible Stokes equations," *SIAM J. Numer. Anal.*, vol. 56, no. 1, pp. 185–209, 2018. [Online]. Available: https://doi.org/10.1137/17M1112017

[67] V. Girault and P.-A. Raviart, *Finite element methods for Navier-Stokes equations*, ser. Springer Series in Computational Mathematics. Springer-Verlag, Berlin, 1986, vol. 5, theory and algorithms. [Online]. Available: https://doi.org/10.1007/978-3-642-61623-5

[68] J. G. Heywood and R. Rannacher, "Finite element approximation of the nonstationary Navier-Stokes problem. I. Regularity of solutions and second-

order error estimates for spatial discretization," *SIAM J. Numer. Anal.*, vol. 19, no. 2, pp. 275–311, 1982. [Online]. Available: https://doi.org/10.1137/0719018

[69] G. He, Y. He, and Z. Chen, "A penalty finite volume method for the transient Navier-Stokes equations," *Appl. Numer. Math.*, vol. 58, no. 11, pp. 1583–1613, 2008. [Online]. Available: https://doi.org/10.1016/j.apnum.2007.09.006

[70] C.-m. Xie and M.-f. Feng, "New nonconforming finite element method for solving transient Naiver-Stokes equations," *Appl. Math. Mech. (English Ed.)*, vol. 35, no. 2, pp. 237–258, 2014. [Online]. Available: https://doi.org/10.1007/s10483-014-1787-6

[71] C. Xu, D. Shi, and X. Liao, "Low order nonconforming mixed finite element method for nonstationary incompressible Navier-Stokes equations," *Appl. Math. Mech. (English Ed.)*, vol. 37, no. 8, pp. 1095–1112, 2016. [Online]. Available: https://doi.org/10.1007/s10483-016-2120-8

[72] E. Burman and M. A. Fernández, "Continuous interior penalty finite element method for the time-dependent Navier-Stokes equations: space discretization and convergence," *Numer. Math.*, vol. 107, no. 1, pp. 39–77, 2007. [Online]. Available: https://doi.org/10.1007/s00211-007-0070-5

[73] J. G. Heywood and R. Rannacher, "Finite element approximation of the nonstationary Navier-Stokes problem. II. Stability of solutions and error estimates uniform in time," *SIAM J. Numer. Anal.*, vol. 23, no. 4, pp. 750–777, 1986. [Online]. Available: https://doi.org/10.1137/0723049

[74] ——, "Finite element approximation of the nonstationary Navier-Stokes problem. III. Smoothing property and higher order error estimates for spatial discretization," *SIAM J. Numer. Anal.*, vol. 25, no. 3, pp. 489–512, 1988. [Online]. Available: https://doi.org/10.1137/0725032

[75] ——, "Finite-element approximation of the nonstationary Navier-Stokes problem. IV. Error analysis for second-order time discretization," *SIAM J. Numer. Anal.*, vol. 27, no. 2, pp. 353–384, 1990. [Online]. Available: https://doi.org/10.1137/0727022

[76] Y. He, "A fully discrete stabilized finite-element method for the time-dependent Navier-Stokes problem," *IMA J. Numer. Anal.*, vol. 23, no. 4, pp. 665–691, 2003. [Online]. Available: https://doi.org/10.1093/imanum/23.4.665

[77] Y. He and W. Sun, "Stabilized finite element method based on the Crank-Nicolson extrapolation scheme for the time-dependent Navier-Stokes equations," *Math. Comp.*, vol. 76, no. 257, pp. 115–136, 2007. [Online]. Available: https://doi.org/10.1090/S0025-5718-06-01886-2

[78] Y. Jiang, L. Mei, and H. Wei, "A stabilized finite element method for transient Navier-Stokes equations based on two local Gauss integrations," *Internat. J. Numer. Methods Fluids*, vol. 70, no. 6, pp. 713–723, 2012. [Online]. Available: https://doi.org/10.1002/fld.2708

[79] X. Lu and P. Lin, "Error estimate of the P_1 nonconforming finite element method for the penalized unsteady Navier-Stokes equations," *Numer. Math.*, vol. 115, no. 2, pp. 261–287, 2010. [Online]. Available: https://doi.org/10.1007/s00211-009-0277-8

[80] H. Qiu, C. Xue, and L. Xue, "Low-order stabilized finite element methods for the unsteady Stokes/Navier-Stokes equations with friction boundary conditions," *Math. Methods Appl. Sci.*, vol. 41, no. 5, pp. 2119–2139, 2018. [Online]. Available: https://doi.org/10.1002/mma.4738

[81] Y. Shang, "New stabilized finite element method for time-dependent incompressible flow problems," *Internat. J. Numer. Methods Fluids*, vol. 62, no. 2, pp. 166–187, 2010. [Online]. Available: https://doi.org/10.1002/fld.2010

[82] P. B. Bochev, M. D. Gunzburger, and J. N. Shadid, "On inf-sup stabilized finite element methods for transient problems," *Comput. Methods Appl. Mech. Engrg.*, vol. 193, no. 15-16, pp. 1471–1489, 2004. [Online]. Available: https://doi.org/10.1016/j.cma.2003.12.034

[83] N. Verma and S. Kumar, "Lowest order virtual element approximations for transient stokes problem on polygonal meshes," *Calcolo*, vol. 58, 2021. [Online]. Available: https://doi.org/10.1007/s10092-021-00440-7

[84] F. J. Gaspar, F. J. Lisbona, and P. N. Vabishchevich, “Finite difference schemes for poro-elastic problems,” *Comput. Methods Appl. Math.*, vol. 2, no. 2, pp. 132–142, 2002. [Online]. Available: https://doi.org/10.2478/cmam-2002-0008

[85] P. J. Phillips and M. F. Wheeler, “A coupling of mixed and continuous Galerkin finite element methods for poroelasticity. I. The continuous in time case,” *Comput. Geosci.*, vol. 11, no. 2, pp. 131–144, 2007. [Online]. Available: https://doi.org/10.1007/s10596-007-9045-y

[86] ——, “A coupling of mixed and continuous Galerkin finite element methods for poroelasticity. II. The discrete-in-time case,” *Comput. Geosci.*, vol. 11, no. 2, pp. 145–158, 2007. [Online]. Available: https://doi.org/10.1007/s10596-007-9044-z

[87] X. Hu, C. Rodrigo, F. J. Gaspar, and L. T. Zikatanov, “A nonconforming finite element method for the Biot’s consolidation model in poroelasticity,” *J. Comput. Appl. Math.*, vol. 310, pp. 143–154, 2017. [Online]. Available: https://doi.org/10.1016/j.cam.2016.06.003

[88] D. Boffi, M. Botti, and D. A. Di Pietro, “A nonconforming high-order method for the Biot problem on general meshes,” *SIAM J. Sci. Comput.*, vol. 38, no. 3, pp. A1508–A1537, 2016. [Online]. Available: https://doi.org/10.1137/15M1025505

[89] P. J. Phillips and M. F. Wheeler, “A coupling of mixed and discontinuous Galerkin finite-element methods for poroelasticity,” *Comput. Geosci.*, vol. 12, no. 4, pp. 417–435, 2008. [Online]. Available: https://doi.org/10.1007/s10596-008-9082-1

[90] R. Wang, X. Wang, and R. Zhang, “A modified weak Galerkin finite element method for the poroelasticity problems,” *Numer. Math. Theory Methods Appl.*, vol. 11, no. 3, pp. 518–539, 2018.

[91] M. Sun and H. Rui, “A coupling of weak Galerkin and mixed finite element methods for poroelasticity,” *Comput. Math. Appl.*, vol. 73, no. 5, pp. 804–823, 2017. [Online]. Available: https://doi.org/10.1016/j.camwa.2017.01.007

[92] C. Niu, H. Rui, and M. Sun, “A coupling of hybrid mixed and continuous Galerkin finite element methods for poroelasticity,” *Appl.*

Math. Comput., vol. 347, pp. 767–784, 2019. [Online]. Available: https://doi.org/10.1016/j.amc.2018.11.021

[93] G. Fu, "A high-order HDG method for the Biot's consolidation model," *Comput. Math. Appl.*, vol. 77, no. 1, pp. 237–252, 2019. [Online]. Available: https://doi.org/10.1016/j.camwa.2018.09.029

[94] M. Botti, D. A. Di Pietro, and P. Sochala, "A hybrid high-order discretization method for nonlinear poroelasticity," *Comput. Methods Appl. Math.*, vol. 20, no. 2, pp. 227–249, 2020. [Online]. Available: https://doi.org/10.1515/cmam-2018-0142

[95] J. J. Lee, K.-A. Mardal, and R. Winther, "Parameter-robust discretization and preconditioning of Biot's consolidation model," *SIAM J. Sci. Comput.*, vol. 39, no. 1, pp. A1–A24, 2017. [Online]. Available: https://doi.org/10.1137/15M1029473

[96] J. J. Lee, E. Piersanti, K.-A. Mardal, and M. E. Rognes, "A mixed finite element method for nearly incompressible multiple-network poroelasticity," *SIAM J. Sci. Comput.*, vol. 41, no. 2, pp. A722–A747, 2019. [Online]. Available: https://doi.org/10.1137/18M1182395

[97] S.-Y. Yi, "A study of two modes of locking in poroelasticity," *SIAM J. Numer. Anal.*, vol. 55, no. 4, pp. 1915–1936, 2017. [Online]. Available: https://doi.org/10.1137/16M1056109

[98] J. J. Lee, "Robust three-field finite element methods for Biot's consolidation model in poroelasticity," *BIT*, vol. 58, no. 2, pp. 347–372, 2018. [Online]. Available: https://doi.org/10.1007/s10543-017-0688-3

[99] X. Tang, Z. Liu, B. Zhang, and M. Feng, "On the locking-free three-field virtual element methods for Biot's consolidation model in poroelasticity," *ESAIM Math. Model. Numer. Anal.*, vol. 55, no. suppl., pp. S909–S939, 2021. [Online]. Available: https://doi.org/10.1051/m2an/2020064

[100] S.-Y. Yi, "A coupling of nonconforming and mixed finite element methods for Biot's consolidation model," *Numer. Methods Partial Differential Equations*, vol. 29, no. 5, pp. 1749–1777, 2013. [Online]. Available: https://doi.org/10.1002/num.21775

[101] Z. Ge, Y. He, and Y. He, "A lowest equal-order stabilized mixed finite element method based on multiphysics approach for a poroelasticity model," *Appl. Numer. Math.*, vol. 153, pp. 1–14, 2020. [Online]. Available: https://doi.org/10.1016/j.apnum.2020.01.024

[102] C. Rodrigo, X. Hu, P. Ohm, J. H. Adler, F. J. Gaspar, and L. T. Zikatanov, "New stabilized discretizations for poroelasticity and the Stokes' equations," *Comput. Methods Appl. Mech. Engrg.*, vol. 341, pp. 467–484, 2018. [Online]. Available: https://doi.org/10.1016/j.cma.2018.07.003

[103] R. Oyarzúa and R. Ruiz-Baier, "Locking-free finite element methods for poroelasticity," *SIAM J. Numer. Anal.*, vol. 54, no. 5, pp. 2951–2973, 2016. [Online]. Available: https://doi.org/10.1137/15M1050082

[104] M. Alvarez, G. N. Gatica, and R. Ruiz-Baier, "An augmented mixed-primal finite element method for a coupled flow-transport problem," *ESAIM Math. Model. Numer. Anal.*, vol. 49, no. 5, pp. 1399–1427, 2015. [Online]. Available: https://doi.org/10.1051/m2an/2015015

[105] V. Anaya, M. Bendahmane, D. Mora, and R. Ruiz Baier, "On a vorticity-based formulation for reaction-diffusion-Brinkman systems," *Netw. Heterog. Media*, vol. 13, no. 1, pp. 69–94, 2018. [Online]. Available: https://doi.org/10.3934/nhm.2018004

[106] V. Anaya, Z. de Wijn, B. Gómez-Vargas, D. Mora, and R. Ruiz-Baier, "Rotation-based mixed formulations for an elasticity-poroelasticity interface problem," *SIAM J. Sci. Comput.*, vol. 42, no. 1, pp. B225–B249, 2020. [Online]. Available: https://doi.org/10.1137/19M1268343

[107] G. N. Gatica, A. Márquez, and S. Meddahi, "Analysis of the coupling of primal and dual-mixed finite element methods for a two-dimensional fluid-solid interaction problem," *SIAM J. Numer. Anal.*, vol. 45, no. 5, pp. 2072–2097, 2007. [Online]. Available: https://doi.org/10.1137/060660370

[108] O. A. Ladyženskaja, V. A. Solonnikov, and N. N. Uralćeva, *Linear and quasi-linear equations of parabolic type*, ser. Translated from the Russian by S. Smith. Translations of Mathematical Monographs, Vol. 23. American Mathematical Society, Providence, R.I., 1968.

[109] N. Verma, B. Gómez-Vargas, L. Miguel De Oliveira Vilaca, S. Kumar, and R. Ruiz-Baier, "Well-posedness and discrete analysis for advection-diffusion-reaction in poroelastic media," *Applic. Anal.*, vol. 28, 2020. [Online]. Available: https://doi.org/10.1080/00036811.2021.1877677

[110] M. K. Brun, I. Berre, J. M. Nordbotten, and F. A. Radu, "Upscaling of the coupling of hydromechanical and thermal processes in a quasi-static poroelastic medium," *Transp. Porous Media*, vol. 124, no. 1, pp. 137–158, 2018. [Online]. Available: https://doi.org/10.1007/s11242-018-1056-8

[111] M. K. Brun, E. Ahmed, J. M. Nordbotten, and F. A. Radu, "Well-posedness of the fully coupled quasi-static thermo-poroelastic equations with nonlinear convective transport," *J. Math. Anal. Appl.*, vol. 471, no. 1-2, pp. 239–266, 2019. [Online]. Available: https://doi.org/10.1016/j.jmaa.2018.10.074

[112] A. T. Hill and E. Süli, "Approximation of the global attractor for the incompressible Navier-Stokes equations," *IMA J. Numer. Anal.*, vol. 20, no. 4, pp. 633–667, 2000. [Online]. Available: https://doi.org/10.1093/imanum/20.4.633

[113] S. C. Brenner and L. R. Scott, *The mathematical theory of finite element methods*, 3rd ed., ser. Texts in Applied Mathematics. Springer, New York, 2008, vol. 15. [Online]. Available: https://doi.org/10.1007/978-0-387-75934-0

[114] Y. Shang, "Error analysis of a fully discrete finite element variational multiscale method for time-dependent incompressible Navier-Stokes equations," *Numer. Methods Partial Differential Equations*, vol. 29, no. 6, pp. 2025–2046, 2013. [Online]. Available: https://doi.org/10.1002/num.21787

[115] V. John, *Finite element methods for incompressible flow problems*, ser. Springer Series in Computational Mathematics. Springer, Cham, 2016, vol. 51. [Online]. Available: https://doi.org/10.1007/978-3-319-45750-5

[116] R. A. Adams, *Sobolev spaces.* Academic Press [A subsidiary of Harcourt Brace Jovanovich, Publishers], New York-London, 1975, pure and Applied Mathematics, Vol. 65.

[117] H. Abboud, V. Girault, and T. Sayah, "A second order accuracy for a full discretized time-dependent Navier-Stokes equations by a two-grid scheme,"

Numer. Math., vol. 114, no. 2, pp. 189–231, 2009. [Online]. Available: https://doi.org/10.1007/s00211-009-0251-5

[118] V. Anaya, M. Bendahmane, D. Mora, and M. Sepúlveda, "A virtual element method for a nonlocal FitzHugh-Nagumo model of cardiac electrophysiology," *IMA J. Numer. Anal.*, vol. 40, no. 2, pp. 1544–1576, 2020. [Online]. Available: https://doi.org/10.1093/imanum/drz001

[119] V. Anaya, Z. de Wijn, B. Gómez-Vargas, D. Mora, and R. Ruiz-Baier, "Rotation-based mixed formulations for an elasticity-poroelasticity interface problem," *SIAM J. Sci. Comput.*, vol. 42, no. 1, pp. B225–B249, 2020. [Online]. Available: https://doi.org/10.1137/19M1268343

[120] V. Girault, G. Pencheva, M. F. Wheeler, and T. Wildey, "Domain decomposition for poroelasticity and elasticity with DG jumps and mortars," *Math. Models Methods Appl. Sci.*, vol. 21, no. 1, pp. 169–213, 2011. [Online]. Available: https://doi.org/10.1142/S0218202511005039

[121] R. E. Showalter, "Diffusion in poro-elastic media," *J. Math. Anal. Appl.*, vol. 251, no. 1, pp. 310–340, 2000. [Online]. Available: https://doi.org/10.1006/jmaa.2000.7048

[122] L. Beirão da Veiga and D. Mora, "A mimetic discretization of the Reissner-Mindlin plate bending problem," *Numer. Math.*, vol. 117, no. 3, pp. 425–462, 2011. [Online]. Available: https://doi.org/10.1007/s00211-010-0358-8

[123] L. Botti, M. . Botti, and D. . A. Pietro, "An abstract analysis framework for monolithic discretisations of poroelasticity with application to hybrid high-order methods," *Comput. Math. Appl.*, 2020. [Online]. Available: https://doi.org/10.1016/j.camwa.2020.06.004

[124] P. Recho, A. Hallou, and E. Hannezo, "Theory of mechano-chemical pattering in biphasic biological tissues," *PNAS.*, vol. 116, no. 12, pp. 5344–5349, 2019. [Online]. Available: https://doi.org/10.1073/pnas.1813255116

[125] J. Schnakenberg, "Simple chemical reaction systems with limit cycle behaviour," *J. Theoret. Biol.*, vol. 81, no. 3, pp. 389–400, 1979. [Online]. Available: https://doi.org/10.1016/0022-5193(79)90042-0

[126] G. W. Jones and S. J. Chapman, "Modeling growth in biological materials," *SIAM Rev.*, vol. 54, no. 1, pp. 52–118, 2012. [Online]. Available: https://doi.org/10.1137/080731785

[127] G. Chamoun, M. Saad, and R. Talhouk, "A coupled anisotropic chemotaxis-fluid model: the case of two-sidedly degenerate diffusion," *Comput. Math. Appl.*, vol. 68, no. 9, pp. 1052–1070, 2014. [Online]. Available: https://doi.org/10.1016/j.camwa.2014.04.010

[128] R. Bürger, R. Ruiz-Baier, and H. Torres, "A stabilized finite volume element formulation for sedimentation-consolidation processes," *SIAM J. Sci. Comput.*, vol. 34, no. 3, pp. B265–B289, 2012. [Online]. Available: https://doi.org/10.1137/110836559

[129] R. Bürger, S. Kumar, and R. Ruiz-Baier, "Discontinuous finite volume element discretization for coupled flow-transport problems arising in models of sedimentation," *J. Comput. Phys.*, vol. 299, pp. 446–471, 2015. [Online]. Available: https://doi.org/10.1016/j.jcp.2015.07.020

List of Publications

Papers published in Refereed Journals

1. N. Verma and S. Kumar, *Lowest order virtual element approximations for transient Stokes problem on polygonal meshes.* Calcolo **58** (2021), Available online: https://doi.org/10.1007/s10092-021-00440-7.

2. R. Bürger, S. Kumar, D. Mora, R. Ruiz-Baier and N. Verma *Virtual element methods for the three-field formulation of time-dependent linear poroelasticity.* Advances in Computational Mathematics **47**(2) (2021), Available online: https://doi.org/10.1007/s10444-020-09826-7.

3. N. Verma, B. Gómez-Vargas, L.M. De Oliveira Vilaca, S. Kumar, and R. Ruiz-Baier, *Well-posedness and discrete analysis for advection-diffusion-reaction in poroelastic media.* Applicable Analysis, (2020), Available online: https://doi.org/10.1080/00036811.2021.1877677.

4. L.M. De Oliveira Vilaca, B. Gómez-Vargas, S. Kumar, R. Ruiz-Baier, and N. Verma, *Stability analysis for a new model of multi-species convection-diffusion-reaction in poroelastic tissue.* Applied Mathematical Modelling, **84** (2020) 425–446.
   Available online: https://doi.org/10.1016/j.apm.2020.04.014.

Papers submitted to Refereed Journals

1. N. Verma and S. Kumar, *Virtual element approximations for non-stationary Navier-Stokes equations on polygonal meshes.*

2. N. Verma and S. Kumar, *Virtual element approximations for two species model of the advection-diffusion-reaction in a poroelastic media.*

Talks in reputed Conferences

1. "Virtual element methods for the three-field formulation of linear poroelasticity problem" in "SIAM Conference on Mathematical Computational Issues in the Geosciences, GS21", Virtual Conference (Milan, Italy) on June 21-24, 2021. (Funded by *SIAM Student Travel Award*)

2. Presented "Virtual element method for nonstationary Stokes problem" and recieved *Best paper presentation award* in "International conference and 22nd Annual Convention of VPI" on AOSM-2019 held at BITS Pilani, Rajasthan, India on December 28-30, 2019.